

**Microhabitat Effects on Nitrous Oxide Emissions, Production  
Pathways, and Reduction in Floodplain Soils**

**Inauguraldissertation**

zur Erlangung der Würde eines Doktors der Philosophie

vorgelegt der

Philosophisch-Naturwissenschaftlichen Fakultät

der Universität Basel

von

Martin Ley  
aus Basel, Schweiz

2022

Genehmigt von der Philosophisch-Naturwissenschaftlichen Fakultät

auf Antrag von

Prof. Dr. Moritz F. Lehmann

Dr. Jörg Luster

Dr. Martin Maier

Basel, den 14. Dezember 2021

Prof. Dr. Marcel Mayor

Dekan

# Table of contents

Summary.....	v
List of Abbreviations.....	viii
Acknowledgements.....	xi
<i>Chapter 1</i> .....	<i>1</i>
1.1 Rationale.....	1
1.2 Microbial pathways and genetic markers involved in N <sub>2</sub> O production and consumption ...	3
1.3 Semiterrestrial soils as important sources of nitrous oxide .....	6
1.4 Environmental controls on N <sub>2</sub> O emissions from floodplain soils .....	7
1.5 Stable isotope biogeochemistry of N <sub>2</sub> O .....	11
1.6 Study site .....	14
1.7 Project objectives and relevance .....	16
<i>Chapter 2</i> .....	<i>27</i>
Graphical Abstract.....	27
Abstract.....	28
2.1 Introduction .....	29
2.2 Material and Methods .....	32
2.2.1 Model soils.....	32
2.2.2 Mesocosms.....	34
2.2.3 Experimental setup.....	35
2.2.4 Sampling and analyses .....	36
2.2.5 Data analyses.....	37
2.3 Results.....	38
2.3.1 Soil moisture and redox potential.....	38
2.3.2 Hydrochemistry of soil solutions .....	40
2.3.3 Nitrous oxide emissions .....	41

<b>2.4 Discussion</b>	<b>42</b>
2.4.1 Effect of aggregate size on N <sub>2</sub> O emissions	43
2.4.2 Litter effect on N <sub>2</sub> O emissions	46
2.4.3 Effects of <i>Salix viminalis</i>	46
<b>2.5 Conclusion</b>	<b>48</b>
<b>Acknowledgements</b>	<b>49</b>
<b>References</b>	<b>50</b>
<b>Chapter 3</b>	<b>55</b>
<b>Abstract</b>	<b>55</b>
<b>3.1 Introduction</b>	<b>56</b>
<b>3.2 Material and methods</b>	<b>59</b>
3.2.1 Experimental setup	59
3.2.2 Air, soil water and soil sampling	60
3.2.3 Microbiological analyses	61
3.2.3.1 Soil DNA extraction, PCR and amplicon sequencing	61
3.2.3.2 Quantitative PCR of nitrogen cycling genes	62
3.2.4 Natural abundance stable isotope analyses	62
3.2.4.1 Soil-emitted N <sub>2</sub> O	62
3.2.4.2 Soil-solution NO <sub>x</sub> and soil water	64
3.2.5 N <sub>2</sub> O source partitioning and N <sub>2</sub> O reduction	64
3.2.6 Statistical analysis	67
<b>3.3 Results</b>	<b>68</b>
3.3.1 Prokaryotic and fungal communities	68
3.3.2 Abundance of key N-cycling genes	71
3.3.3 <sup>15</sup> N enrichment of NO <sub>x</sub> in the soil solution	74
3.3.4 Source partitioning and reduction of soil emitted N <sub>2</sub> O	75
<b>3.4 Discussion</b>	<b>79</b>
3.4.1 Treatment-specific, flood-resilient soil microbiomes with a similar potential to produce N <sub>2</sub> O	79
3.4.2 Flood-induced changes in the abundance of functional genes related to N <sub>2</sub> O production pathways	81
3.4.3 N <sub>2</sub> O production by bacterial denitrification during flooding	83
3.4.4 N <sub>2</sub> O production pathways in the post-flood phase	83
3.4.5 N <sub>2</sub> O reduction during the drying phase	86
<b>3.5 Conclusion</b>	<b>87</b>

<b>Acknowledgements</b> .....	<b>89</b>
<b>References</b> .....	<b>90</b>
<b>Chapter 4</b> .....	<b>101</b>
<b>Abstract</b> .....	<b>101</b>
<b>4.1 Introduction</b> .....	<b>102</b>
<b>4.2 Methods</b> .....	<b>105</b>
4.2.1 Site description and experimental design .....	105
4.2.2 Stable isotope analyses and isotopic mass balances .....	107
4.2.3 N <sub>2</sub> O source partitioning and fractional N <sub>2</sub> O reduction.....	108
4.2.4 Nucleic acid extraction, quality control and reverse transcription .....	109
4.2.5 Quantitative PCR of nitrogen cycling gene transcripts .....	110
4.2.6 Statistical analyses .....	110
<b>4.3 Results</b> .....	<b>111</b>
4.3.1 Physicochemical parameters of pore water .....	111
4.3.2 N <sub>2</sub> O fluxes and soil concentrations .....	113
4.3.3 Stable isotope ratios of soil-emitted N <sub>2</sub> O .....	115
4.3.4 N <sub>2</sub> O source partitioning and estimates of partial N <sub>2</sub> O reduction.....	117
4.3.5 Abundance of key functional gene transcripts .....	120
<b>4.4 Discussion</b> .....	<b>123</b>
4.4.1 Pioneer vegetation shapes N <sub>2</sub> O emission patterns in the riparian zone.....	123
4.4.2 Simultaneous activity of oxidative and reductive processes causes prolonged N <sub>2</sub> O emissions from soils under <i>P. arundinacea</i> stands .....	126
<b>4.5 Conclusion</b> .....	<b>128</b>
<b>Acknowledgements</b> .....	<b>130</b>
<b>References</b> .....	<b>131</b>
<b>Chapter 5</b> .....	<b>139</b>
<b>5.1 Overview of main findings</b> .....	<b>139</b>
5.1.1 Mesocosm Experiment.....	139
5.1.2 Field Manipulation Experiment .....	141
<b>5.2 Flood frequency – a reliable predictor of periods of enhanced N<sub>2</sub>O emissions</b> .....	<b>141</b>

<b>5.3</b>	<b>Soil aggregates – functional base units of N<sub>2</sub>O emissions.....</b>	<b>142</b>
<b>5.4</b>	<b>Litter accumulation – Soil-structuring microhabitat, nutrient source and promoter of reductive N transformation processes .....</b>	<b>143</b>
<b>5.5</b>	<b>Plant-soil interactions – Determinants of N<sub>2</sub>O production and consumption from floodplain vegetation stands.....</b>	<b>145</b>
<b>5.6</b>	<b>Towards improved interpretation methods of natural abundance stable isotopes .....</b>	<b>147</b>
<b>5.7</b>	<b>Outlook .....</b>	<b>148</b>
	<b>References .....</b>	<b>151</b>
	<i>Supplementary Material Chapter 2 .....</i>	<i>154</i>
	<i>Supplementary Material Chapter 3 .....</i>	<i>156</i>
	<i>Supplementary Material Chapter 4 .....</i>	<i>166</i>

---

## Summary

The potential of river floodplains to emit nitrous oxide (N<sub>2</sub>O), a powerful greenhouse gas and ozone-depleting compound, considerably reduces the climate regulation function of these dynamic transition zones between aquatic and terrestrial ecosystems. However, the assessment of N<sub>2</sub>O emissions from floodplain soils is challenging, due to the inherently high spatial heterogeneity and the characteristic occurrence of sporadic inundation phases. Such short-term flood events can temporarily alter the conditions for nitrogen (N) transformation processes taking place within distinct microhabitats, which can lead to the local formation of transient hot spots of enhanced N<sub>2</sub>O emissions. This situation emphasizes the urgent need to understand how characteristic factors of microhabitat formation in river floodplains control the balance between major microbial N<sub>2</sub>O source processes and N<sub>2</sub>O reduction to N<sub>2</sub> that determine the magnitude and duration of N<sub>2</sub>O emissions. Therefore, the main objective of this thesis project was to systematically assess the relative importance of microhabitat effects related to soil aggregate size, organic matter accumulation, and plant-soil interactions on the microbial N<sub>2</sub>O production and consumption processes controlling the spatiotemporal emission patterns of N<sub>2</sub>O under changing pore water saturation. To achieve this objective, a mesocosm experiment under controlled climatic conditions, and a study within the framework of a field manipulation experiment were conducted.

In the mesocosm experiment, presented in chapters 2 and 3, two model soils with equivalent structure and texture, comprising macroaggregates (4000–250 µm) or microaggregates (< 250 µm) from a N-rich floodplain soil were used. These model soils were planted either with basket willow (*Salix viminalis* L.), mixed with leaf litter, or left unamended. The resulting six aggregate size / amendment factor combinations were exposed to a flood of 48 hours and then left to dry. Emission rates of N<sub>2</sub>O during the experiment were determined using the closed-chamber method. The relative contributions of different N transformation processes to the production of N<sub>2</sub>O and the degree of N<sub>2</sub>O reduction to N<sub>2</sub> were assessed using a novel approach based on the isotopic and isotopomeric composition of the emitted N<sub>2</sub>O. In addition, the prokaryotic and fungal soil microbiomes were characterized by sequencing of DNA and qPCR of functional genes related to potentially N<sub>2</sub>O producing and consuming processes. N<sub>2</sub>O production during the 48-hour flood phase originated almost entirely from heterotrophic bacterial denitrification and/or nitrifier-denitrification in all experimental treatments, yet most of the produced N<sub>2</sub>O was further reduced to N<sub>2</sub> resulting in low N<sub>2</sub>O flux rates. In the drying phase, a period of enhanced N<sub>2</sub>O emissions occurred in all treatments, however with the

---

unamended and litter added model soils with macroaggregates emitting significantly more N<sub>2</sub>O than in all other treatments. During this period, most of the N<sub>2</sub>O production continued to derive from bacterial denitrification in anoxic micro-sites. However, the aeration of the inter-aggregate pore space led to additional contributions by oxidative N<sub>2</sub>O production, the magnitude of which depended on treatment and time point within the drying phase. Also here, aggregate size emerged as a key parameter. Unamended macroaggregates seemed to prolong anoxia within microsites when compared to microaggregates. Litter addition further enhanced soil anoxia but also altered soil structure and nutrient availability. This increased soil heterogeneity modulated the temporal pattern of the N<sub>2</sub>O emission, leading to short-term peaks of high N<sub>2</sub>O fluxes at the beginning of the period of enhanced N<sub>2</sub>O emissions. These maximum N<sub>2</sub>O emissions were the result of rapid changes in N<sub>2</sub>O source partitioning of nitrifying and denitrifying processes in combination with a temporary partial disruption of N<sub>2</sub>O reduction. By contrast, the presence of *S. viminalis* prevented the occurrence of strong N<sub>2</sub>O emissions from both model soils, attenuating any effect of flooding and aggregate size on N<sub>2</sub>O production pathways and the degree of N<sub>2</sub>O reduction. Root respiration and the decomposition of root exudates likely promoted the formation of anoxic microsites that support complete denitrification, resulting in the low emission rates observed in the planted model soils. Irrespective of treatment and throughout the experiment, nitrogen-cycling gene abundances revealed a higher potential for bacterial denitrification and for N<sub>2</sub>O reduction than for ammonia oxidation, thus supporting the implications of the isotopic data on the dominance of denitrification in N<sub>2</sub>O production and on the generally high degree of N<sub>2</sub>O reduction. DNA sequencing data and functional gene abundances further revealed that large and small soil aggregates represent distinct microhabitats with a different potential for both denitrifying and nitrifying processes, thus suggesting that in addition to structure-related physical effects, differences in the microbial community composition contribute to aggregate size effects on N<sub>2</sub>O emission rates and N<sub>2</sub>O production pathways. Litter accumulations strongly altered the soil microbial community composition of the aggregate size fractions, whereas the presence of willow had little respective effects. Both soil amendments affected the abundance of ammonia-oxidizing bacteria and archaea, but not the one of denitrifying microorganisms.

The field study, presented in chapter 4, took place in the hydrologically most dynamic floodplain zone of a re-naturalized section of the Thur River in NE Switzerland. In a randomized complete block design, experimental plots where the dominant vegetation, the pioneer plant canary ryegrass (*Phalaris arundinacea* L.), was constantly removed were compared to unmanipulated plots. During a three-week drying-phase after a major flood, the



---

dynamics of efflux, source partitioning and reduction of N<sub>2</sub>O were assessed using the same methods as in the mesocosm experiment. In addition, temporal changes in the activity of specific groups of N transforming soil microorganisms were analyzed using extracted RNA. It became evident, that young, sandy sediments under a dense plant cover experienced longer periods of elevated N<sub>2</sub>O emissions, whereas emissions from bare sediments gradually decreased after initial peak rates. Nitrification and/or fungal denitrification contributed consistently about 20-30 % to gross N<sub>2</sub>O production in plots covered by *P. arundinacea*, whereas this process group contributed only to the beginning of the post-flood phase to N<sub>2</sub>O emissions from bare plots. N<sub>2</sub>O reduction was temporarily interrupted at the beginning of the post-flood phase in bare plots, whereas N<sub>2</sub>O reduction in the *Phalaris* plots was stable during the entire drying phase. The detection of denitrifying and nitrite oxidizing microorganisms as the most active N transforming microorganisms in this part of the river floodplain further supported the results from source partitioning and reflected the adaptation of the microbial community to fluctuating redox conditions.

Overall, the results of this thesis (i) demonstrate the importance of soil aggregation, litter accumulation and plant-soil interactions in floodplain soils in governing the production, consumption, and emission of N<sub>2</sub>O during flood-induced hot moments, (ii) present evidence for the formation of related specific microhabitats and indications of explanatory physical effects, (iii) highlighted the role of microbial N<sub>2</sub>O reduction as a major controlling factor of N<sub>2</sub>O emissions (iv) and confirm the dominance of denitrifying processes as source processes. Our findings thus should help to predict the location of temporary hotspots of N<sub>2</sub>O emissions, and to improve the estimations of local N<sub>2</sub>O budgets of river floodplains in a world of global climate change.

---

## List of Abbreviations

N <sup>α</sup>	Central position of nitrogen in the linear, asymmetric N <sub>2</sub> O molecule
N <sup>β</sup>	Outer position of nitrogen in the linear, asymmetric N <sub>2</sub> O molecule
<sup>14</sup> N	Nitrogen with a core consisting of 7 protons and 7 neutrons (light nitrogen)
<sup>15</sup> N	Nitrogen with a core consisting of 7 protons and 8 neutrons (heavy nitrogen)
16S	Small-subunit rRNA
AMO	Ammonia monooxygenase
ANAMMOX	Anaerobic ammonia oxidation
AOA	Ammonia oxidizing archaea
AOB	Ammonia oxidizing bacteria
BaSIEL	University of Basel Stable Isotope Ecology Laboratory
BNF	Biological nitrogen fixation
C	Carbon
CaCO <sub>3</sub>	Calcium carbonate
cd <sub>1</sub> -NIR	Heme-containing nitrite reductase
cDNA	Complementary DNA
CH <sub>4</sub>	Methane
CO <sub>2</sub>	Carbon dioxide
Comammox	Complete ammonia oxidation
C <sub>org</sub>	Organic carbon
Cu-NIR	Copper-containing nitrite reductase
DNRA	Dissimilatory nitrate reduction to ammonium
DOC	Dissolved organic carbon
EEA	European Environment Agency
E <sub>h</sub>	Redox potential
EMPA	Swiss Federal Laboratories for Materials Science and Technology
ESVs	Exact sequence variants
EtOH	Ethanol
E <sub>var</sub>	Smith and Wilson's evenness index
FD	Fungal denitrification
GHG	Greenhouse gas
<sup>H/L</sup> R	Heavy to light isotope ratio
HAO	Hydroxylamine oxidoreductase

---

HD	Heterotrophic denitrification
HSD	Tukey's honestly significant difference
IRMS	Isotope ratio mass spectrometer
ITS2	Internal transcribed spacer region 2
$k^h$	Reaction rate of heavier isotopologues
$k^l$	Reaction rate of lighter isotopologues
LAL	Large aggregates, litter
LAP	Large aggregates, plant
LAU	Large aggregates, unamended
$Mg(ClO_4)_2$	Magnesium perchlorate
MMO	Methane monooxygenase
M-R	Mixing-reduction
MS	Mean sum of squares
N	Nitrogen
$N_2$	Dinitrogen
$N_2O$	Nitrous oxide
ND	Nitrifier denitrification
$NH_2OH$	Hydroxylamine
$NH_3$	Ammonia
$NH_4^+$	Ammonium
NI	Nitrification
NMDS	Non-metrical multidimensional scaling
NO	Nitric oxide
$NO_2^-$	Nitrite
$NO_2$	Nitrogen dioxide
$NO_3^-$	Nitrate
NOB	Nitrite oxidizing bacteria
NOR	Nitric oxide reductase
NOS	Nitrous oxide reductase
$N_r$	Reactive forms of nitrogen
ns	Not statistically significant
O	Oxygen
$O_2$	Elemental oxygen
OTUs	Operational taxonomic units

---

---

P	Phosphorus
PMMA	Polymethyl methacrylate
Prok.	Prokaryote
PVC	Polyvinyl chloride
qPCR	Quantitative polymerase chain reaction
RDP	Ribosomal Database Project
RIN	RNA Integrity number
R-M	Reduction-mixing
rN <sub>2</sub> O	Residual N <sub>2</sub> O
S	Sulfur
SAL	Small aggregates, litter
SAP	Small aggregates, plant
SAU	Small aggregates, unamended
SD	Standard deviation
SE	Standard error
SNSF	Swiss National Science Foundation
SOM	Soil organic matter
SP	Site preference
SS	Sum of squares
TN	Total nitrogen
VSMOW	Vienna Standard Mean Ocean Water
VWC	Volumetric water content
WFPS	Water-filled pore space
WSL	Swiss Federal Institute for Forest, Snow and Landscape Research

---

## Acknowledgements

Many people have supported me in my PhD project, and I would like to take this opportunity to express my gratitude.

First, I would like to thank my supervisors, Dr. Jörg Luster and Prof. Moritz Lehmann, for providing me with an opportunity to work in this project and for their great support throughout my PhD. The stimulating discussions and constructive criticisms were very motivating and extended my understanding of the subject matter beyond my expectations. It has been a great experience that has helped me to grow personally and scientifically. My sincere thanks also go to Dr. Pascal Niklaus for measuring the concentrations of our N<sub>2</sub>O samples, for allowing me to use his laboratory for DEA measurements, for his invaluable suggestions on the manuscripts, and, above all, for his extensive expertise regarding the statistical analysis of our data. Furthermore, I am extremely grateful to Dr. Beat Frey for introducing me to the field of microbiology, which was new to me at the time. With his and Beat Stierli's help, I was able to acquire a good methodological foundation in molecular biological working procedures within a short period of time. I am grateful to Beat for always being available with advice to discuss experimental outcomes or a manuscript. I would also like to thank Dr. Martin Hartmann for his willingness to help me with the analysis of microbial sequencing data and giving me the opportunity to learn the way of processing raw sequencing data. His advice substantially extended my knowledge of bioinformatics, for which I am very grateful.

Further, I am immensely thankful to the members of the aquatic and isotope biogeochemistry research group at the University of Basel. I want to express my gratitude to Dr. Jakob Zopfi for the interesting discussions about microbial community analysis and interpretation. I am grateful for the inspiring discussions with Paul and Claudia about the twists and turns in N<sub>2</sub>O natural abundance isotope geochemistry and Maciej for his encouraging consultations. I would also like to thank the current and former doctoral students Adeline, Jana, Guangyi, Lea, Yuki for their collegiality. I also want to express my gratitude to Dr. Franz Conen in the environmental geosciences group for the inspiring talks and keeping me informed about relevant literature. A special thank you goes to our returning guest researcher Anna-Neva for our long, not always scientific, talks in front of the IRMS. See you hopefully soon in Israel.

I am very happy to have had the opportunity to meet and work with my colleagues at WSL. I thank Ivano Brunner for his help with the interpretation of fungal community patterns. I also wish to thank our technicians Daniel, Roger, Noureddine and Marco for their invaluable help in the laboratory and the field. Special thanks go to the PhD students and PostDocs in the forest soil and biogeochemistry research unit Sia, Dominik, Sonia, Thomas, Claude, Jasmin, Maggie,

---

Carla, and Johanna, as well as Anil, Manuel, Emily Solly, Emily Oliveira and Aline. I am grateful for sharing a great time, for fruitful discussions, exciting excursions and conferences, and wonderful barbecues after a hard day's work.

I am deeply grateful to my family and friends for their unconditional love and relentless support in all situations and their confidence in me. I am thankful for the loving support from my mother and in-laws and their help in taking care of our son, when mommy and daddy needed a breather or had to work.

The most important persons whom I must thank is my wife Svenja and my beloved son Benjamin. Without her caring love I would not have made it through the PhD. During the last couple of years, Svenja always had my back. She supported me not only morally, but also actively in the laboratory during the molecular biological analyses. In addition, she lovingly took care of our son when Daddy once again had no time to play. My son was a source of joy for me during the hard times of writing this PhD thesis. I look forward to spending more of these wonderful hours together with him in the future and showing him the world.

I am moreover thankful to my friends Simon and Fredy as well as their families contributing to maintain the life-work balance through organizing game nights, having dinner together and supporting me as friends.

I hope I did not forget anyone whose contribution to this thesis should have been mentioned here. I am very grateful for all the encounters I had during the time of my PhD project, and I do hope that I could be as much of a support to others as I was supported by them.

# Chapter 1

## Introduction

### 1.1 Rationale

Nitrogen (N) belongs to the most important elements sustaining all life on our planet. It is most abundant in rocks and sediments bound as ammonia ( $\text{NH}_3$ ) at an estimated  $1.8 \times 10^{10}$  Tg N, but its geological release via weathering and erosion is of minor importance for the shorter-term biogeochemical nitrogen cycle. By far the most important N pool within the geosphere is atmospheric dinitrogen gas ( $\text{N}_2$ ) with  $3.9 \times 10^9$  Tg N (Canfield et al., 2005; Kuypers et al., 2018). To become available for metabolic processes of organisms, the relatively inert  $\text{N}_2$  needs to be transformed by biological or abiotic processes into more reactive forms of nitrogen ( $\text{N}_r$ ). Only a small fraction of  $\text{N}_2$  is abiotically converted to reactive nitric oxide (NO) and nitrogen dioxide ( $\text{NO}_2$ ) by lightning, releasing about 4 Tg of fixed N annually (Hill et al., 1980; Ciais et al., 2013). In contrast, biological nitrogen fixation (BNF) conducted by highly diverse but relatively rare bacteria and archaea in natural ecosystems provides today on average about 220 Tg N per year of bioavailable N in form of  $\text{NH}_3$  (Codispoti, 2007; Vitousek et al., 2013; Voss et al., 2013; Kuypers et al., 2018).

Prior to the industrialization of agriculture, the anthropogenic impact on the N cycle was negligible. The sources of  $\text{N}_r$  were in relative equilibrium with natural  $\text{N}_r$  sinks, like sedimentation of particulate N compounds, atmospheric decomposition of NO and nitrous oxide ( $\text{N}_2\text{O}$ ), and, most importantly, the bacterial process of denitrification, returning  $\text{N}_r$  to the atmospheric  $\text{N}_2$  pool. With the advent of artificial fertilizers produced via the Haber-Bosch process ( $\text{N}_2 + 3 \text{H}_2 \rightarrow 2 \text{NH}_3$ ), this balance has become increasingly perturbed in favor of the source term. With the use of artificial fertilizers and the cultivation of legumes, which live in symbiosis with N fixing microorganisms, agriculture has been intensified to meet the food demand of an ever-growing human population, nearly doubling the availability of  $\text{N}_r$  (Galloway et al., 2008). In combination with an increased application of manure, agricultural practices involving artificial fertilizer became the largest anthropogenic source for  $\text{N}_r$ , but also inputs from fossil fuel combustion and industrial activities contribute to the strong human impact on the N cycle. Since croplands are open systems, the consequences of human interference with the N cycle are not limited to agricultural fields, but also affect natural aquatic and terrestrial ecosystems. Nitrogenous compounds can leave agricultural sites either by leaching or runoff

into ground and surface waters or volatilization, followed by partial deposition in adjacent riparian zones. These compounds can participate in a broad spectrum of N transformation processes, which are often intertwined with other elemental cycles, such as carbon (C), sulfur (S) and phosphorus (P), changing not only the availability but also the demand for the other elements (Gruber and Galloway, 2008). This can have several detrimental effects on the affected ecosystem in terms of structure and functioning, ranging from decline in water quality, aquatic eutrophication, and loss of biodiversity, with implications for the health of natural aquatic environments and their ecosystem functioning (Erismann et al., 2013). Moreover, if these ecosystems are used for drinking water supply, high concentrations of nitrogenous oxides can have severe health consequences for the affected population.

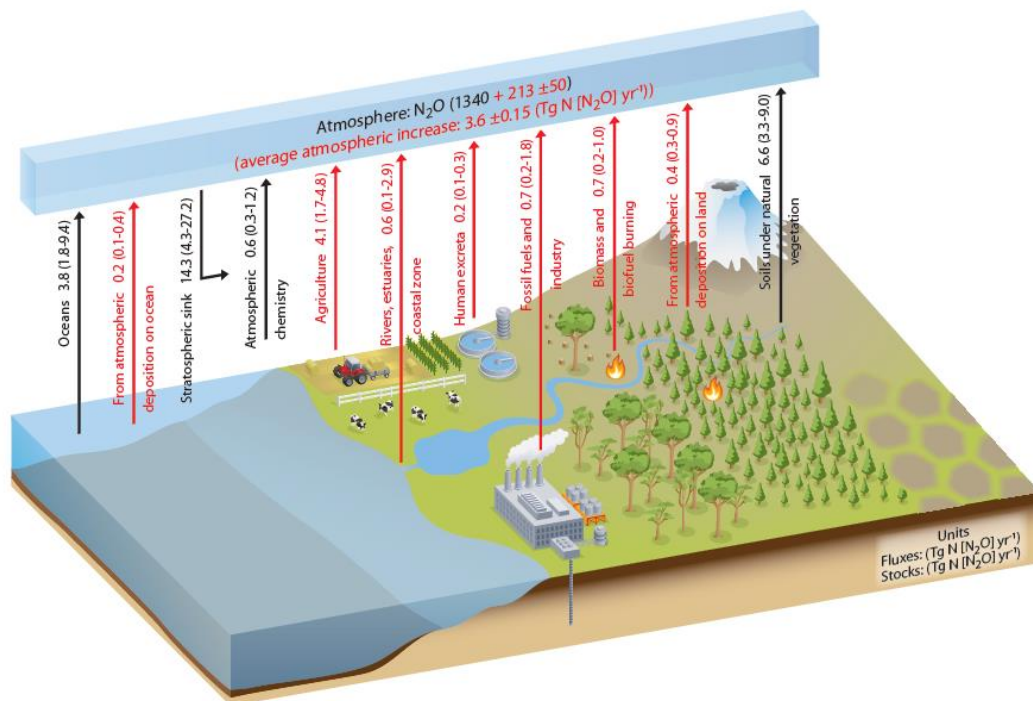


**Figure 1.1.** Estimated global annual fluxes of  $\text{N}_2\text{O}$  taken from Ciais et al. (2013). The stratospheric sink of  $\text{N}_2\text{O}$  is the sum of losses via photolysis and reaction with oxygen radicals in the  $^1\text{D}$  excited state. The global magnitude of this sink is adjusted here to be equal to the difference between the total sources and the observed growth rate. The atmospheric inventories have been calculated using a conversion factor of 4.79 TgN ( $\text{N}_2\text{O}$ ) per ppb (Prather et al., 2012)

Another negative effect in natural ecosystems linked to elevated  $\text{N}_r$  deposition and stimulated N transformation/turnover, that directly contributes to global climate change, is the increased formation of  $\text{N}_2\text{O}$ . Its global warming potential over a time horizon of 100 years is about 300 times higher than that of carbon dioxide ( $\text{CO}_2$ ) and has an atmospheric lifetime of  $131 \pm 10$



years, making it a potent greenhouse gas (GHG; Forster et al., 2007; Prather et al., 2012). In addition, N<sub>2</sub>O emerges to be the dominant agent depleting the ozone layer by its photolytic destruction and photo-oxidation reaction with oxygen radicals in the <sup>1</sup>D state (Ravishankara et al., 2009; Fleming et al., 2011). The continuous increase of N<sub>2</sub>O in the atmosphere by more than 20 % from pre-industrial (1750) concentrations of 270 ppb to 331 ppb in 2019 makes this GHG an increasingly important component of total GHG budgets (Tian et al., 2020). However, due to spatiotemporal heterogeneity in the overall emissions of N<sub>2</sub>O in both aquatic and terrestrial environments, N<sub>2</sub>O budgets are challenging to assess, and are subject to great uncertainties, especially with regards to emissions from soils under natural vegetation (Ciais et al., 2013). On a more local scale, this holds particularly true for the interface between aquatic and terrestrial ecosystems, such as floodplains. Floodplains are typically characterized by complex spatial patterns of diverse habitats with different properties that are important modulators of N transformation processes, and which can be temporarily altered by periodic flood events. Since most of N<sub>2</sub>O is produced by microbial processes, there is an urgent need to understand the effects of microhabitat formation on the mechanisms underlying the microbial transformation of N in such dynamic ecosystems. With a deeper understanding of the controlling factors of microbial N<sub>2</sub>O production and consumption, it will not only be possible to improve our predictions of N<sub>2</sub>O emission hotspots, but also to further refine local N<sub>2</sub>O budgets. For these reasons, the work presented in this thesis project focuses on the systematical assessment of microhabitat effects characteristic for river floodplains on N<sub>2</sub>O emissions under various water regimes, in the laboratory and the field.

The following five sections will provide a brief overview of the current state of knowledge on the most common microbial N transformation processes and microorganisms involved in the formation of N<sub>2</sub>O (Chapter 1.2.), whereas determining factors of N<sub>2</sub>O emissions from floodplain soils will be introduced in chapter 1.3. Chapter 1.4. provides basic information about the analysis of natural abundance stable isotopes of N<sub>2</sub>O, since these methods will be central tools to elucidate the dynamics of major N<sub>2</sub>O source processes and N<sub>2</sub>O reduction in this thesis project. In chapter 1.5. a general description of the study site follows. The last introductory section describes the general objectives of this thesis project (Chapter 1.6.).

## **1.2 Microbial pathways and genetic markers involved in N<sub>2</sub>O production and consumption**

The N cycle comprises a broad range of microbial transformation reactions, in which N-containing molecules as inert and harmless as N<sub>2</sub> can be converted into highly reactive and toxic

---

N compounds like NO or climate-relevant compounds such as N<sub>2</sub>O (Kuypers et al., 2018). These transformation reactions occur under environmental conditions spanning from fully oxic to anoxic and are performed by microorganisms either to build up biomass (assimilation) or to conserve energy (dissimilation). Nitrogenous compounds can thereby take on oxidation states ranging from -III to +V, serving either as electron donors or acceptors. Many of these reactive N compounds are produced during several of these enzymatically mediated transformation processes. This results in a complex network of interconnected processes, which can be carried out by a diverse spectrum of microorganisms from all three domains of life, including some microorganisms normally associated with other biogeochemical cycles, such as methane- or sulfur-oxidizing bacteria. N<sub>2</sub>O can be formed in association with many of the microbial oxidative or reductive N transformation processes, either as a mandatory intermediate, as a by-product of detoxification reactions, or by abiotic decomposition of an extracellular intermediate. Exceptions are the biological fixation of elemental nitrogen, ammonification, e.g., the conversion of organic N compounds to NH<sub>3</sub>, and assimilation of inorganic nitrogen molecules into microbial or plant biomass. Among all other, different forms of nitrification and denitrification account for about 70 % of globally emitted N<sub>2</sub>O from natural ecosystems (Butterbach-Bahl et al., 2013). Several other biotic and abiotic N transforming processes, like dissimilatory nitrate reduction to ammonium (DNRA; Burgin and Hamilton, 2007; Rütting et al., 2011; Giles et al., 2012), anaerobic ammonia oxidation (ANAMMOX; Ali et al., 2016), fungal co-denitrification (Spott et al., 2011; Shoun et al., 2012) and abiotic chemodenitrification (Jones et al., 2015; Stanton et al., 2018) have also been reported to produce N<sub>2</sub>O, at least to a minor extent. Although the latter processes fulfill important functions as sources and sinks of reactive nitrogenous compounds, their environmental relevance in the production and consumption of N<sub>2</sub>O remains ambiguous (Kuypers et al., 2018). Therefore, in the following section of this paragraph, the focus will be on the processes of bacterial and archaeal nitrification, nitrifier denitrification as well as bacterial and fungal denitrification, the key processes with regards to the production and emission of N<sub>2</sub>O.

The aerobic process of **Nitrification** comprises two main steps, ammonia oxidation and nitrite oxidation. Ammonia oxidation itself can be subdivided into two sub-steps: ammonia oxidation to hydroxylamine (NH<sub>2</sub>OH), and NH<sub>2</sub>OH oxidation to NO, and further to nitrite (NO<sub>2</sub><sup>-</sup>). NH<sub>3</sub> oxidation to NH<sub>2</sub>OH is carried out by chemolithoautotrophic bacteria (AOB) found in the β- and γ- classes of the proteobacteria phylum, and by archaea (AOA) of the *Thaumarchaeota* phylum, both of which convert NH<sub>3</sub> using characteristic ammonia monooxygenase enzymes (AMO) (Schleper and Nicol, 2010). The genes encoding the alpha subunit of AMO (*amoA*) in

bacteria or archaea can be used as marker genes for this group of organisms. This first conversion step can also be carried out by some methanotrophic bacteria in the  $\gamma$ -proteobacteria class, using methane monooxygenase (MMO), although very inefficiently (Stein and Klotz, 2011). AOB oxidize the produced hydroxylamine further to NO, using the hydroxylamine oxidoreductase (HAO) enzyme followed by a proposed reverse-operating copper-containing nitrite reductase (unknown Cu-NIR) producing  $\text{NO}_2^-$  (Caranto and Lancaster, 2017). By contrast, the enzyme(s) used to oxidize  $\text{NH}_2\text{OH}$  and convert it further to  $\text{NO}_2^-$  in AOA are still unknown (Simon and Klotz, 2013). Nitrite oxidation, the second main step in the nitrification process, is carried out by nitrite oxidizing bacteria (NOB) that can be found amongst all classes of the Phylum *Proteobacteria*, *Chloroflexi*, *Nitrospinae* and *Nitrospirae*. These bacteria carry the membrane-bound NXR enzyme encoded in the powerful functional and phylogenetic marker gene, *nxrB*, to catalyze the oxidation of  $\text{NO}_2^-$  to nitrate (Daims et al., 2016). Recently, the complete oxidation of  $\text{NH}_3$  all the way to  $\text{NO}_3^-$  by a single microorganism (*nitrospira inopinata*) from the genus *Nitrospira* was discovered in a process termed complete ammonia oxidation (comammox), demonstrating that nitrification is not necessarily carried out by two distinct groups of microorganisms (Daims et al., 2015; van Kessel et al., 2015; Kits et al., 2019). In the nitrification process,  $\text{N}_2\text{O}$  is mainly produced during abiotic reactions of the two extracellular intermediates hydroxylamine and nitric oxide during bacterial and archaeal ammonia oxidation and the comammox process (Kozłowski et al., 2016; Liu et al., 2017). However, under anoxic conditions it has been recently demonstrated that some AOB (e.g., *Nitrosomonas europaea*) are capable to reduce  $\text{NH}_2\text{OH}$  directly to  $\text{N}_2\text{O}$  using the cytochrome P460 enzyme (Caranto et al., 2016). Furthermore, under anoxic conditions, some ammonia-oxidizing bacteria can produce  $\text{N}_2\text{O}$  using enzymes commonly found in denitrifying microorganisms in a process called **nitrifier-denitrification**, where nitric oxide gets reduced to  $\text{N}_2\text{O}$  upon nitrite reduction (Arp and Stein, 2003). **Denitrification** is the four-step dissimilatory reduction process of  $\text{NO}_3^-$  to  $\text{N}_2$  occurring under suboxic to anoxic conditions. The entire process (complete denitrification) or in parts (partial denitrification) is widespread among mostly heterotrophic bacteria, many of them are facultative anaerobes, mostly belonging to the genera *Pseudomonas*, *Alcaligenes*, *Bacillus*, *Agribacterium*, and *Flavibacterium* (Zumft, 1997). In the first step,  $\text{NO}_3^-$  is converted to  $\text{NO}_2^-$  either by the membrane-bound and/or the periplasmatic NAR enzyme. The produced  $\text{NO}_2^-$  is subsequently reduced to the toxic gas NO by either a heme-containing nitrite reductase ( $\text{cd}_1$ -NIR) or the copper-containing Cu-NIR encoded by the process marker genes *nirS* and the *nirK* gene, respectively. A diverse group of nitric oxide reductase enzymes (NOR) is responsible for the conversion of NO to  $\text{N}_2\text{O}$  and

serves either for detoxification or respiration. The final step in the bacterial denitrification process, the reduction of  $\text{N}_2\text{O}$  to  $\text{N}_2$ , is the only biological sink of  $\text{N}_2\text{O}$  discovered so far and is catalyzed by the periplasmatic enzyme nitrous oxide reductase (NOS), encoded in the marker gene *nosZ* (Kuypers et al., 2018). Moreover, it has been demonstrated that many fungi of the orders *Hypocerales* (e.g., *Fusarium oxysporum*), *Eurotiales*, *Sordariales*, and *Cheatosphaeriales* are capable to perform a form of incomplete denitrification (**fungal denitrification**) under oxygen-limited conditions using enzymes that are specific for fungi (e.g., cytochrome  $\text{P}_{450}\text{NOR}$ ). All denitrifying fungi assessed so far lack a *nosZ* gene, making  $\text{N}_2\text{O}$  the end-product of fungal denitrification. This highlights the role of this process in context of  $\text{N}_2\text{O}$  accumulation as a pure source of  $\text{N}_2\text{O}$  (Laughlin and Stevens, 2002; Shoun et al., 2012; Maeda et al., 2015).

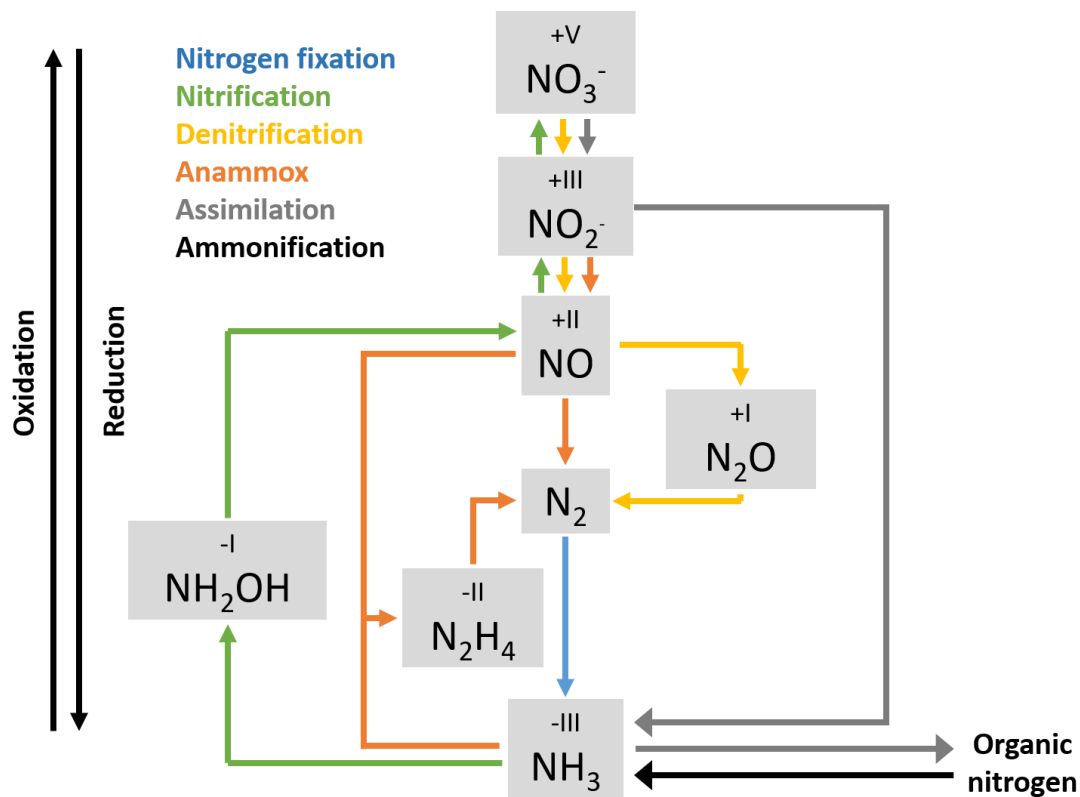


**Figure 1.2.** Microbial transformation processes of nitrogen compounds adapted from Kuypers et al., (2018). The oxidation state of the nitrogen atom is indicated above the respective compound.

### 1.3 Semiterrestrial soils as important sources of nitrous oxide

The potential to emit greenhouse gases, such as carbon dioxide ( $\text{CO}_2$ ), methane ( $\text{CH}_4$ ) and  $\text{N}_2\text{O}$ , affects the climate-regulation function of ecosystems (Anderson- Teixeira and DeLucia 2011). River floodplain soils develop mainly from sediments deposited during regular phases of inundation by river overflow, groundwater rises and/or surface run-off. With increasing

distance from the average discharge shoreline, the influence of flood disturbance diminishes, resulting in a heterogeneous pattern of habitats with different soil development stages and vegetation succession. Within these distinct habitats, biogeochemical processes are closely linked to the river discharge dynamics. Flood events, for example, lead to temporary fluctuations in pore water saturation, causing transient changes in the soil redox state between oxic, suboxic and anoxic conditions. In addition, flooding also can lead to a sudden input of allochthonous carbon sources, nitrogen substrates and other nutrients, stimulating microbial transformation processes, as well as microorganisms. The retention of reactive nitrogen compounds in combination with an enhanced biogeochemical cycling is thereby a much-desired ecosystem service of river floodplains to remove water pollutants, and to ensure water quality and biodiversity in the river system. However, such a dynamic and heterogeneous environment is also conducive to N<sub>2</sub>O production, and has, in fact, been demonstrated to be a potential hotspot of N<sub>2</sub>O emissions (van den Heuvel et al., 2009; Jungkunst et al., 2004). The flood-pulse driven increase in emissions of a potent ozone-depleting greenhouse gas is of particular concern in the context of the predicted increase in extreme precipitation events (Madsen et al., 2014; Kovats et al., 2015). A higher frequency of heavy rainfalls could lead to more flash flood events in floodplains, when located in river catchments without any natural or artificial reservoirs that would act to buffer any sudden increase in discharge. Considering more frequent and longer flood-related periods of enhanced N<sub>2</sub>O emissions (“hot moments”) in the future, these floodplains are likely to gain importance as terrestrial N<sub>2</sub>O sources. This prospect of a potential increase in the relevance of floodplains in the global greenhouse gas budget demands a better understanding of site-specific factors determining the temporal patterns and magnitudes of enhanced post-flood N<sub>2</sub>O emissions. The latter is needed to develop appropriate mitigation strategies for riparian ecosystems.

#### **1.4 Environmental controls on N<sub>2</sub>O emissions from floodplain soils**

Soil emissions of N<sub>2</sub>O can undergo a high spatiotemporal variability in natural ecosystems (Jacinthe et al., 2012; Poblador et al., 2017; de Carlo et al., 2019). Each of the main production and consumption processes of N<sub>2</sub>O described in paragraph 1.2. functions within specific biogeochemical optimum ranges regarding water availability, oxygen partial pressure, N substrate concentrations, and biodegradable carbon compounds. However, little is known about the environmental factors providing optimal conditions for different N-transforming processes and the resilience of these microhabitats to disturbance. A deviation from these optimal environmental conditions could alter the balance between N<sub>2</sub>O production and consumption in

confined areas or even the entire soil column, and thus modulate net N<sub>2</sub>O emissions (Vieten et al., 2009). In addition, the exchange of N<sub>2</sub>O and other gases between soils and the atmosphere mainly occurs through molecular diffusion, which is modulated by *soil structure*, pore water saturation as well as the solubility of N<sub>2</sub>O in soil water (Heincke and Kaupenjohann, 1999; Böttcher et al., 2011). Diffusion and gas solubility, but also microbial reaction rates, depend strongly on *soil temperature*. Within the mesophilic temperature range of 20 – 45 °C, the rate of many biochemical reactions in soils, like soil respiration, increases by a factor of about two upon an increase of temperature by 10 °C, even though the optimal temperature for specific microorganisms might differ. Soil *pH* is another important property with a strong effect on net N<sub>2</sub>O production. In riparian soils, as well as in laboratory studies, it has been shown that below pH 5.4, denitrification rates are strongly reduced, shifts in the community structure of denitrifying microorganisms occur, and the ability to reduce N<sub>2</sub>O to N<sub>2</sub> is lowered. This results in higher net N<sub>2</sub>O production rates, which can be attributed to the differential pH sensitivities of specific denitrification enzymes (van den Heuvel et al., 2011; Brenzinger et al., 2015).

*Soil water content* can be considered as one of the chief environmental variables governing the main N transforming reactions in soils and modulating the net N<sub>2</sub>O fluxes from soils to the atmosphere. High water content, for example, can produce temporary diffusion barriers, which impede the exchange of gaseous compounds like oxygen, promoting anoxic conditions. On the other hand, a minimum amount of free water is required in all N transforming microbial processes, and soil water content can therefore also directly or indirectly affect microbial rates (Thorbjørn et al., 2008; Neira et al., 2015). For example, microbial activity during the strictly aerobic nitrification process has been found to peak when 60 % of the total pore space of the soil is filled with water (WFPS), whereas denitrifying microorganisms begin to use alternative electron acceptors, i.e., NO<sub>3</sub><sup>-</sup>, when oxygen becomes limiting at 80 % WFPS (Robertson and Groffman, 2015). The distribution of pore water in unsaturated soils, in turn, depends on *soil texture*, bulk density, and tortuosity of the pore space, which can lead to an uneven spatial arrangement of differentially diffusion-limited soil volumes, allowing oxic and suboxic, or even anoxic microhabitats to occur simultaneously in close vicinity to each other (Maag and Vinther 1996; Bateman and Baggs 2005). In addition, highest N<sub>2</sub>O emissions are often observed at intermediate soil water contents, since N<sub>2</sub>O reduction to N<sub>2</sub> and limitation of N<sub>2</sub>O transport often becomes more important under full, or almost complete pore water saturation (Christiansen et al., 2012).

Depending on the sequential order of wetting and drying, different processes may be responsible for enhanced N<sub>2</sub>O emissions. Although not a subject of this thesis project, the effect

of *drying/re-wetting* will be briefly addressed here for the sake of completeness. After periods of drying, occasionally strong N<sub>2</sub>O emissions have been observed upon *re-wetting*, and related to an initial flush in N mineralization, which subsequently increases the activity of nitrifying microorganisms, in turn providing the substrates for denitrification during anoxic phases of the flood event (Baldwin and Mitchell, 2000). However, the magnitude of the resulting N<sub>2</sub>O fluxes of this temporal coupling of processes seems to depend on the residual moisture during the dry phase and on the degree of wetting (Machado dos Santos Pinto et al., 2020; Pinto et al., 2021). High N<sub>2</sub>O emissions observed in the drying phase after inundation of river sediments and floodplain soils are suggested to be the result of an accelerated N turnover caused by spatially *coupled nitrification-denitrification* (Baldwin and Mitchell, 2000; Koschorreck and Darwich, 2003; Shrestha et al., 2014). This coupling of aerobic and anaerobic processes is promoted, when oxic and anoxic microsites develop in close vicinity of each other. Such strong gradients of oxygen concentrations can occur during soil pore space desaturation when the surface of soil aggregates already experience oxic conditions, but intra-aggregate pore structure and internal diffusion barriers preserve anoxic microhabitats within the aggregate (Ebrahimi and Or, 2016). The effect of aggregate structure on the distribution of redox conditions mentioned above highlights the relevance of aggregate-related microhabitats, which are biogeochemically distinct from the surrounding soil matrix. *Soil aggregates* are the basic units of soil structure and consist of mineral particles and dead organic material bound together by organic and mineral agents, fungal hyphae, and plant roots (Tisdall and Oades, 1982; Six et al., 2004). These differently sized organo-mineral clusters create a complex network of soil pores, regulating the transport of water, dissolved substrates, and gases in the inter-aggregate pore space, as well as within themselves (Or et al., 2007). This tortuous internal pore space in combination with an uneven distribution of organic substances creates various microhabitats suitable for distinct microbial consortia using a multitude of metabolic processes. Microbial communities and their activities can vary amongst different sizes of soil aggregates (Bach et al., 2018; Wilpiseski et al., 2019). In terms of N transformation, a positive relation between aggregate size and net N<sub>2</sub>O production has been observed in N-rich soils (Jahangir et al., 2011). Furthermore, the predominant N-transforming process responsible for N<sub>2</sub>O production can differ between small and large aggregates (Sey et al., 2008).

The interaction of vascular *plants* with their soil environment creates also specific microhabitats, which can modulate N<sub>2</sub>O producing processes (Philippot 2009). For example, the development of a root network increases the porosity of the soil system, thus facilitating pore water movement and gas exchange (Vergani and Graf, 2015; Swanson et al., 2017). The

exudation of easily degradable organic compounds by plant roots can stimulate microbial N mineralization activity, but can also enhance respiration, which in turn leads to local oxygen limitation and denitrification in some areas of the rhizosphere (Luster et al., 2009; Koranda et al., 2011; Fender et al., 2013). However, specific inhibiting agents released from the plant roots can also decrease nitrification activity (Philippot et al., 2009). In addition, the competition of plants with microorganisms for nutrients and water in the rhizosphere affects the availability of N substrates, ultimately shaping the community structure of the rhizosphere microbiome (Dennis et al., 2010; Koranda et al., 2011; Bender et al., 2014). Many plants occurring in environments with sporadically water-logged soils developed internal physiological traits in the roots to cope with periodical O<sub>2</sub> limitations in the rhizosphere (Colmer, 2003). The most common adaptation is the development of voluminous canals in the root capable of gas transport from the shoot to the root apex, called aerenchyma (Sorrell and Brix, 2015). By radial oxygen loss, these porous roots can create oxic conditions in the vicinity of the root tip allowing root penetration even into anoxic soil zones. Consequently, within this oxic zone created by the plant, oxidative N transformations can take place in close distance to otherwise anoxic areas in the soil (Philippot et al. 2009). Furthermore, it has been shown that soil gases such as CO<sub>2</sub>, CH<sub>4</sub>, and N<sub>2</sub>O can bypass the soil matrix via aerenchyma, but the significance of this process for gas emissions from soils or wetlands to the atmosphere is still unresolved (Marushchak et al., 2016). In soils, the decomposition of *leaf or root litter* is an important source for C and N compounds which can create local hot spots of microbial activity. This depends on the chemical properties and therefore degradability of the organic material and the composition of the associated microbial community (Chèneby et al., 2010; Myrold and Bottomley, 2015). The release of labile C compounds and nutrients from accumulated plant residues has been found to stimulate N-transforming processes, promoting the emission of N<sub>2</sub>O from soils (Loecke and Robertson, 2009; Li et al., 2016). Riparian zones are no exception in this regard, since buried organic-rich horizons in sediments deposited during flooding are known to be hotspots of N mineralization and nitrification during unsaturated conditions (Hill, 2011).



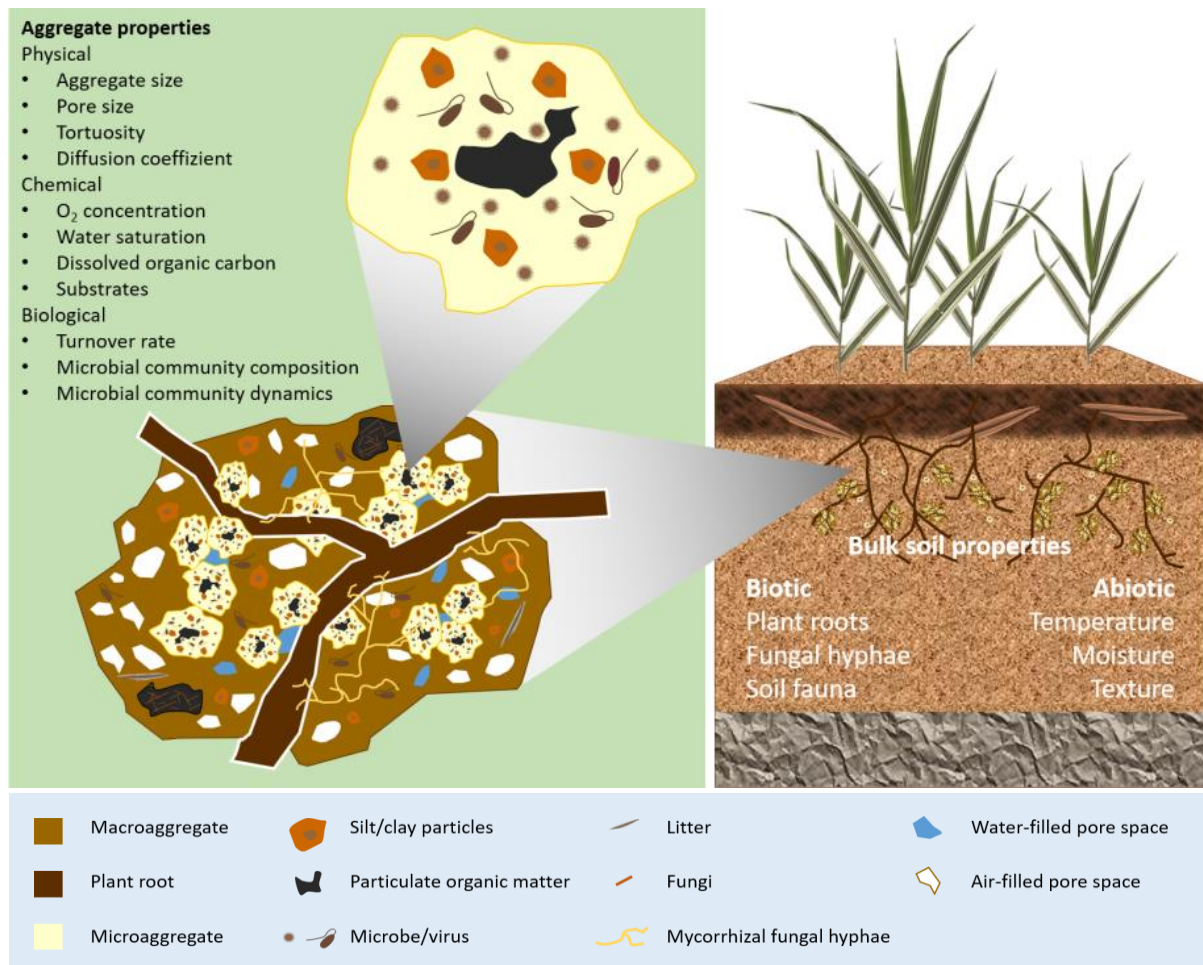


**Figure 1.3.** Schematic depiction of the spatial relationship between micro- and macroaggregates in a soil profile. The determining physicochemical and biological factors shaping the N transforming reactivity in soil aggregates as well as the external reaction environment in the bulk soil are listed next to the illustrations. Anthropogenic disturbances of these factors related to global climate change or soil management are not illustrated here (modified after Wang et al., 2019; Wilpieszski et al., 2019).

### 1.5 Stable isotope biogeochemistry of N<sub>2</sub>O

Natural abundance stable isotope ratio measurements (see Box 1) can provide important information on the sources and transformation of various N compounds like N<sub>2</sub>O. This is because microbial conversion of N compounds is often associated with a reaction-specific isotope fractionation caused by the preferential use of substrate compounds comprising the lighter isotopes over molecules composed of the heavier isotopes. Such isotope effects are related to the higher strength of the molecular bonds of the heavier isotopes and the higher energy necessary to break these bonds, which leads to slightly slower reaction rates for the heavier isotopologues ( $k^h$ ) compared to rates for the lighter isotopologues ( $k^l$ ). Consequently,

during the consumption of the substrate in a specific reaction becomes enriched in heavier isotopes, whereas the product is relatively depleted in the heavier isotopes (Sharp, 2007). This enrichment of the substrate pool in the heavy isotopes is more pronounced in closed systems, where the substrate is consumed without replenishment, than in open systems with a steady re-supply of new substrate (Fry, 2006; Denk et al., 2017). If the reaction rates follow first-order kinetics depending on the substrate concentration, the fractionation factor  $\alpha$  equals  $k^l/k^h$ . The fractionation factor  $\alpha$  corresponds to the isotope effect  $\epsilon$  (in the permil notation), where  $\epsilon$  (‰) =  $(\alpha - 1) \times 1000$  (Sharp, 2007). Since enzymatic reaction rates are sensitive to ambient physicochemical conditions like temperature, pH, enzyme, and substrate availability, as well as the presence of any activators or inhibitors, a certain range of  $\epsilon$  can apply to a given reaction.

#### Box 1 | Stable Isotope Terminology and Standards

In the analysis of the isotopic composition of N<sub>2</sub>O, the focus is on the stable isotopes of N and oxygen (O). N has two stable isotopes, <sup>14</sup>N and <sup>15</sup>N. While <sup>14</sup>N accounts for 99.64 %, <sup>15</sup>N accounts just for 0.36 % of the total N abundance. O has three stable isotopes: <sup>16</sup>O, <sup>17</sup>O and <sup>18</sup>O representing 99.76 %, 0.04 % and 0.2 %, of all O atoms, respectively (Fry, 2006; Sharp, 2007). These differences in abundances can be used to calculate ratios of heavy vs. light isotopes (R), e.g., <sup>15</sup>N/<sup>14</sup>N or <sup>18</sup>O/<sup>16</sup>O. These ratios can be used in the  $\delta$ -notation, in which sample isotope ratios are put in relation to an internationally recognized standard to identify relative differences between sample and standard.

$$\delta_{sample}(\text{‰}) = \left( \frac{R_{sample} - R_{standard}}{R_{standard}} \right) \times 1000$$

Where  $R_{sample}$  and  $R_{standard}$  represent the abundance ratio of the heavy versus the light isotope in the sample and the standard, respectively, and  $\delta_{sample}$  the delta value of the sample in per mil (Sharp, 2007). The international standard for N is atmospheric N<sub>2</sub> and for O the Vienna Standard Mean Ocean Water (VSMOW).

To characterize different isotopic forms of molecules containing several elements with more than one stable isotope, two terms are commonly used: **isotopologues** and **isotopomers**. Isotopologues are molecules that differ in isotopic composition and can have the same or different molecular masses. By contrast, isotopomers are molecules of the same mass that differ only in the relative position of the isotopic elements within the molecule. For N<sub>2</sub>O, there are four main isotopologues, <sup>14</sup>N<sup>14</sup>N<sup>16</sup>O, <sup>14</sup>N<sup>14</sup>N<sup>18</sup>O, <sup>14</sup>N<sup>15</sup>N<sup>16</sup>O and <sup>15</sup>N<sup>14</sup>N<sup>16</sup>O, where the last two molecules are the isotopomers of N<sub>2</sub>O. The site specificity is termed **site preference** (SP), which is calculated by using the intramolecular distribution of the heavy (<sup>15</sup>N) and light N (<sup>14</sup>N) atoms between the central ( $\alpha$ ) and outer ( $\beta$ ) positions in the linear, asymmetric N<sub>2</sub>O molecule ( $^{15}N\ SP = \delta^{15}N^{\alpha} - \delta^{15}N^{\beta}$ ). Both bulk and site-specific isotopic composition of the N<sub>2</sub>O molecule can provide information on the source and fate of N<sub>2</sub>O in natural environments.

The assessment of source contribution and N<sub>2</sub>O reduction in floodplain soils requires analytical methods suitable for a natural, hydrologically dynamic, and spatially heterogeneous ecosystem.

Under such conditions, where the application of isotopically enriched (labeled) substrates would be less suitable to trace biogeochemical N transforming processes, the analysis of natural abundance stable isotopes of soil-emitted N<sub>2</sub>O could represent a promising, non-invasive alternative method in these natural and near-natural systems. The three simultaneously determined isotopic signatures,  $\delta^{15}\text{N}_{\text{bulk}}$ ,  $\delta^{18}\text{O}_{\text{N}_2\text{O}}$  and  $^{15}\text{N}$  SP of N<sub>2</sub>O (see definition in box 1) provide information about the source contribution, as well as the extent of partial N<sub>2</sub>O reduction at the time of emission. When interpreting N<sub>2</sub>O stable isotope ratios, it must be considered that  $\delta^{15}\text{N}_{\text{bulk}}$  and  $\delta^{18}\text{O}_{\text{N}_2\text{O}}$  in emitted N<sub>2</sub>O are dependent on the isotopic composition of the initial substrates, e.g., NO<sub>3</sub><sup>-</sup>, NH<sub>4</sub><sup>+</sup> and H<sub>2</sub>O (Park et al., 2011; Lewicka-Szczebak et al., 2014, 2020). However, due to the almost complete O exchange between nitrogen oxides and water during N<sub>2</sub>O production processes, the  $\delta^{18}\text{O}_{\text{N}_2\text{O}}$  value has been shown to be a less variable parameter than  $\delta^{15}\text{N}_{\text{bulk}}$  when used as a tracer for distinguishing N<sub>2</sub>O production processes (Kool et al., 2007; Snider et al., 2012; Lewicka-Szczebak et al., 2016). Similarly,  $^{15}\text{N}$  SP is an excellent indicator of N<sub>2</sub>O production due to the distinct ranges for nitrification or denitrification (Fig. 4), and it is assumed to be independent of substrate isotopic signatures (Toyoda and Yoshida, 1999; Ostrom and Ostrom, 2017). Therefore, the symmetry of the intermediate species and site specificity in N–O bond rupture of the intermediate solely, apart from the reduction of N<sub>2</sub>O to N<sub>2</sub>, determines  $^{15}\text{N}$  SP during the elementary reaction step that leads to N<sub>2</sub>O formation, like the reduction of two NO molecules with NOR and two electrons during denitrification (Toyoda et al., 2005). In addition, N<sub>2</sub>O reduction to N<sub>2</sub> results in the simultaneous increase of all isotopic signatures of the residual N<sub>2</sub>O and therefore the associated isotope effect must be considered to obtain accurate estimations for the original  $\delta^{18}\text{O}_{\text{N}_2\text{O}}$  and  $^{15}\text{N}$  SP values of unreduced N<sub>2</sub>O (Decock and Six, 2013). The wealth of biogeochemical information within one single molecule inspired an increasing use of the isotopic parameters mentioned above in dual-isotope mapping ( $^{15}\text{N}$  SP vs.  $\delta^{18}\text{O}_{\text{N}_2\text{O}}$  or  $^{15}\text{N}$  SP vs.  $\delta^{15}\text{N}_{\text{bulk}}$ ) and mixing model approaches to determine source partitioning and N<sub>2</sub>O reduction simultaneously (Toyoda et al., 2011; Lewicka-Szczebak et al., 2017, 2020; Buchen et al., 2018; Verhoeven et al., 2019). In this thesis project the dual-isotope mapping approach originally proposed by Lewicka-Szczebak et al. (2017) and improved by the insights from Yu et al. (2020) and Lewicka-Szczebak et al. (2020) will be applied not only under controlled conditions (Chapter 3) but also for the first time in a near-natural ecosystem of a restored river floodplain (Chapter 4).

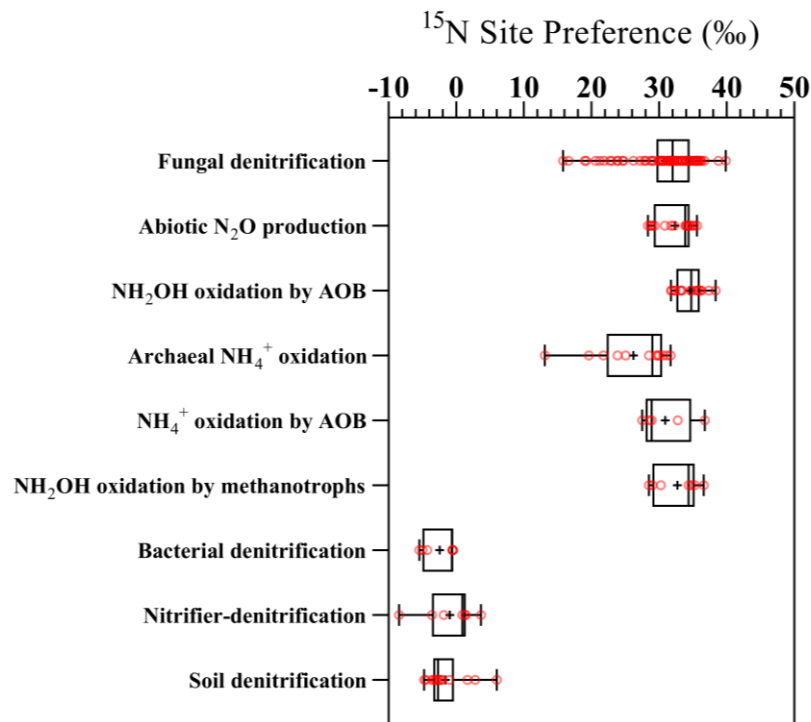


**Figure 1.4.** Reported ranges of <sup>15</sup>N SP values for distinct N<sub>2</sub>O producing processes. The individual values were taken from Denk et al. (2017) and the literature cited therein. In the soil incubation study of Lewicka-Szczebak et al. (2014), no distinction was made between the isotopic signatures of N<sub>2</sub>O produced by nitrifier-denitrification and heterotrophic bacterial denitrification. Therefore, this data is presented separately as ‘soil denitrification’.

## 1.6 Study site

A 2-km long, restored section of the Thur River at Niederneunforn (NE Switzerland; 47°35'28" N, 8°46'26" E) was selected as study site for this project. In this area, the mean annual temperature was 9.1 °C and the mean annual precipitation was 1015 mm. The perialpine river Thur itself originates in the limestone formations of the Mount Säntis region (2500 m.a.s.l.) and crosses the Swiss Plateau prior its confluence with the Rhine River. With a catchment covering an area of 1750 km<sup>2</sup> (Samaritani et al., 2011), the Thur River is the largest river in Switzerland without natural or artificial retention basins, which promotes the occurrence of flash floods (Schirmer et al., 2014). The nivo-pluvial hydrological regime of the river indeed causes frequent inundation of the investigated floodplain in spring during the period of snow melt, and after intense precipitation events (Fournier et al., 2013). This is reflected by the high variability of the average daily discharge, which can range from 2 to 1130 m<sup>3</sup> s<sup>-1</sup>. The average annual discharge at the field site is 50 m<sup>3</sup> s<sup>-1</sup> (Shrestha et al., 2014). The restoration of the previously

channelized river section led to the formation of various gravel bars colonized by pioneer vegetation, and an increased hydrological connectivity (e.g., increased flood dynamics) between the river and the floodplain (Schirmer et al., 2014). During severe flood events, even the old alluvial forest is reconnected with the river by breaches in the former levees. Consequently, areas with different succession stages of soil and vegetation development emerged along a decreasing hydrodynamic intensity gradient perpendicular to the flow direction of the river. All soils in the floodplain are buffered by calcium carbonate (mean  $\text{CaCO}_3$ : 38.5 %; pH: 7.5) and are rich in N ( $N_{\text{total}}$ :  $1.2 \pm 0.3 \text{ g kg}^{-1}$ ; mean  $\pm$  SD) with an average C:N ratio of 15. The soil material used in the mesocosm experiment (Chapter 2 and 3) was collected from a location within the floodplain, which experiences between one to two flooding events per year and is comprised of older alluvial sediments from the riverbanks. The riparian willow forest growing at this location is dominated by mature white willow (*Salix alba* L.) (Samaritani et al., 2011; Fig 1.5). The field manipulation experiment (Chapter 4) was conducted on a large gravel bar, covered with thick layers of young alluvial overbank sediments, which get inundated more than ten times per year (Samaritani et al., 2011). This area is covered by dense patches of the canary ryegrass *Phalaris arundinacea* (Schirmer et al., 2014; Fig. 1.5).

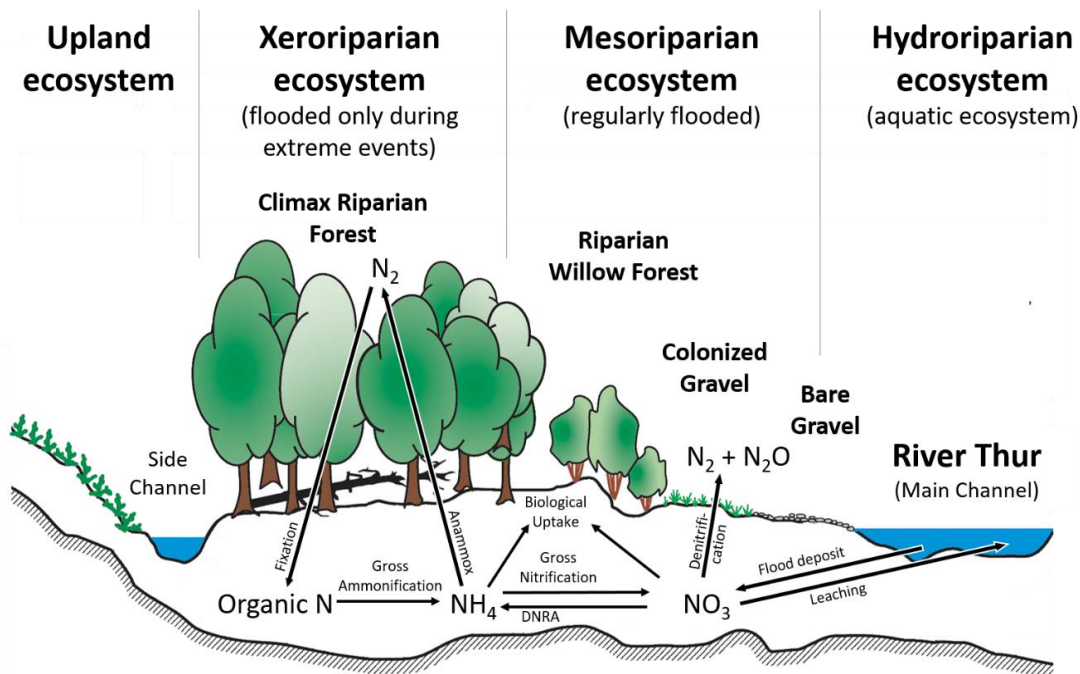


**Figure 1.5.** Classification of the riparian ecosystems, including their characteristic flood dynamics, along a lateral transect through the research site in the Thur River floodplain at Niederneunforn (TG, Switzerland). Further, a schematic representation of the nitrogen cycle in river floodplains was added (modified after Bertrand et al., 2012; Pinay et al., 2018; Schirmer et al., 2014)

## 1.7 Project objectives and relevance

The overarching objective of this thesis project was to systematically assess the relative importance of microhabitat effects related to soil aggregate size, organic matter accumulation, and plant-soil interactions on the microbial N<sub>2</sub>O production and consumption processes controlling the spatiotemporal emission patterns of N<sub>2</sub>O from river floodplains under changing pore water saturation. To approach this task, we combined trace gas, isotopic, and molecular analyses to gain comprehensive information on the pathways and modes of N<sub>2</sub>O production versus consumption during hot moments of N<sub>2</sub>O production in association with flooding, as well as on the key microbial players involved, as assessed through the analysis of specific marker genes. Two comprehensive experiments were conducted: A mesocosm experiment with soils from the study site under controlled conditions, the results of which are presented in Chapters 2 and 3 of this thesis, and an investigation within the framework of a field-manipulation experiment at the study site, the outcomes of which forming the basis for Chapter 4.

In Chapter 2, we examined how single or combined factors of microhabitat formation affect the magnitude and temporal pattern of N<sub>2</sub>O emissions during and after a short-term flood event. Here, special attention was paid to the preservation of the soil structure, as this aspect is often not considered in studies of aggregate size effects on N<sub>2</sub>O emissions. The effects of different unamended aggregate size fractions and combinations with buried plant litter or growing basket willow clones (*Salix viminalis* L.) on net N<sub>2</sub>O production were studied. This part of the study was intended to test the potential of the above-mentioned factors of microhabitat formation to promote or reduce N<sub>2</sub>O emissions, an important aspect when attempting to identify potential hot spots of N<sub>2</sub>O emissions.

Chapter 3 builds on the insights gained in Chapter 2 but extends the investigation to how specific factor combinations of microhabitat formation determine the dynamics of the various microbial N<sub>2</sub>O source processes, and the extent of N<sub>2</sub>O reduction, which lead to enhanced N<sub>2</sub>O emissions in a flooding-drying situation. In addition, the impact of these specific microhabitat effects on the development of the soil microbiome in general, and on the N transforming microbial community, was assessed. For this purpose, a combination of stable isotope analyses at a relatively high temporal resolution and molecular biological techniques was applied.

The field experiment described in Chapter 4 extends our knowledge of microhabitat effects and advanced analytical techniques from the mesocosm experiment to field conditions in a floodplain. It was conducted in the hydrologically most active section of the study site since flooding is most likely to have the strongest impact on N transformation processes in this area.

Knowledge of microhabitat effects, linked to the emerging colonization of this area with patches of pioneer vegetation (*Phalaris arundinacea* L.), on the intensity and duration of post-flood periods of enhanced N<sub>2</sub>O emissions is still limited. Thus, the main objective was to assess microhabitat effects associated with the presence/absence of pioneer plants on the dynamics of the N transforming microorganisms and the consequences for the source partitioning of major microbial N<sub>2</sub>O production pathways and N<sub>2</sub>O reduction.

This thesis project extends our knowledge of how small-scale environmental heterogeneity controls the exchange of the ozone-depleting greenhouse gas N<sub>2</sub>O between soils and atmosphere. In combination with a deeper understanding of the spatiotemporal dynamics of microbial N<sub>2</sub>O production and consumption processes, this project also provides the means necessary to improve model predictions on N<sub>2</sub>O emissions from natural and near-natural floodplain ecosystems in context of a changing climate. Further, the insights gained in this project will advance the development of indicators of N<sub>2</sub>O emission potential, and therefore help to improve ecosystem management practices to mitigate the severe impact of N<sub>2</sub>O emissions on the climate regulation function of floodplain ecosystems.

## References

- Ali, M., Rathnayake, R.M.L.D., Zhang, L., Ishii, S., Kindaichi, T., Satoh, H., Toyoda, S., Yoshida, N., Okabe, S., 2016. Source identification of nitrous oxide emission pathways from a single-stage nitrification-anammox granular reactor. *Water Research* 102, 147–157. doi:10.1016/j.watres.2016.06.034
- Arah, J.R.M., 1992. New Formulae for Mass Spectrometric Analysis of Nitrous Oxide and Dinitrogen Emissions. *Soil Science Society of America Journal* 56, 795–800. doi:10.2136/sssaj1992.03615995005600030020x
- Arp, D.J., Stein, L.Y., 2003. Metabolism of Inorganic N Compounds by Ammonia-Oxidizing Bacteria. *Critical Reviews in Biochemistry and Molecular Biology* 38, 471–495. doi:10.1080/10409230390267446
- Bach, E.M., Williams, R.J., Hargreaves, S.K., Yang, F., Hofmockel, K.S., 2018. Greatest soil microbial diversity found in micro-habitats. *Soil Biology and Biochemistry* 118, 217–226. doi:10.1016/j.soilbio.2017.12.018
- Baldwin, D.S., Mitchell, A.M., 2000. The effects of drying and re-flooding on the sediment and soil nutrient dynamics of lowland river–floodplain systems: a synthesis. *Regulated Rivers: Research & Management* 16, 457–467. doi:10.1002/1099-1646(200009/10)16:5<457::AID-RRR597>3.3.CO;2-2
- Bender, S.F., Plantenga, F., Neftel, A., Jocher, M., Oberholzer, H.-R., Köhl, L., Giles, M., Daniell, T.J., van der Heijden, M.G., 2014. Symbiotic relationships between soil fungi and plants reduce N<sub>2</sub>O emissions from soil. *The ISME Journal* 8, 1336–1345. doi:10.1038/ismej.2013.224
- Bertrand, G., Goldscheider, N., Gobat, J.-M., & Hunkeler, D. (2012). Review: From multi-scale conceptualization to a classification system for inland groundwater-dependent ecosystems. *Hydrogeology Journal*, 20(1), 5–25. <https://doi.org/10.1007/s10040-011-0791-5>
- Boast, C.W., Mulvaney, R.L., Baveye, P., 1988. Evaluation of Nitrogen-15 Tracer Techniques for Direct Measurement of Denitrification in Soil: I. Theory. *Soil Science Society of America Journal* 52, 1317–1322. doi:10.2136/sssaj1988.03615995005200050020x
- Böttcher, J., Weymann, D., Well, R., von der Heide, C., Schwen, A., Flessa, H., Duijnisveld, W.H.M., 2011. Emission of groundwater-derived nitrous oxide into the atmosphere: model simulations based on a <sup>15</sup>N field experiment. *European Journal of Soil Science* 62, 216–225. doi:10.1111/j.1365-2389.2010.01311.x
- Brenzinger, K., Dörsch, P., Braker, G., 2015. pH-driven shifts in overall and transcriptionally active denitrifiers control gaseous product stoichiometry in growth experiments with extracted bacteria from soil. *Frontiers in Microbiology* 6, 1–11. doi:10.3389/fmicb.2015.00961
- Buchen, C., Lewicka-Szczepak, D., Flessa, H., Well, R., 2018. Estimating N<sub>2</sub>O processes during grassland renewal and grassland conversion to maize cropping using N<sub>2</sub>O isotopocules. *Rapid Communications in Mass Spectrometry* 32, 1053–1067. doi:10.1002/rcm.8132
- Burgin, A.J., Hamilton, S.K., 2007. Have we overemphasized the role of denitrification in aquatic ecosystems? A review of nitrate removal pathways. *Frontiers in Ecology and the Environment* 5, 89–96. doi:10.1890/1540-9295(2007)5[89:HWOTRO]2.0.CO;2 [https://doi.org/10.1890/1540-9295\(2007\)5\[89:HWOTRO\]2.0.CO;2](https://doi.org/10.1890/1540-9295(2007)5[89:HWOTRO]2.0.CO;2)
- Butterbach-Bahl, K., Baggs, E.M., Dannenmann, M., Kiese, R., Zechmeister-Boltenstern, S., 2013. Nitrous oxide emissions from soils: how well do we understand the processes and their controls? *Philosophical*



- Transactions of the Royal Society of London. Series B, Biological Sciences 368, 20130122.  
doi:10.1098/rstb.2013.0122
- Canfield, D.E., Kristensen, E., Thamdrup, B., 2005. Aquatic geomicrobiology. *Advances in Marine Biology* 48, 1–599. doi:10.1016/S0065-2881(05)48017-7
- Caranto, J.D., Lancaster, K.M., 2017. Nitric oxide is an obligate bacterial nitrification intermediate produced by hydroxylamine oxidoreductase. *Proceedings of the National Academy of Sciences* 114, 8217–8222. doi:10.1073/pnas.1704504114
- Caranto, J.D., Vilbert, A.C., Lancaster, K.M., 2016. *Nitrosomonas europaea* cytochrome P460 is a direct link between nitrification and nitrous oxide emission. *Proceedings of the National Academy of Sciences* 113, 14704–14709. doi:10.1073/pnas.1611051113
- Chèneby, D., Bru, D., Pascault, N., Maron, P.A., Ranjard, L., Philippot, L., 2010. Role of Plant Residues in Determining Temporal Patterns of the Activity, Size, and Structure of Nitrate Reducer Communities in Soil. *Applied and Environmental Microbiology* 76, 7136–7143. doi:10.1128/AEM.01497-10
- Christiansen, J.R., Vesterdal, L., Gundersen, P., 2012. Nitrous oxide and methane exchange in two small temperate forest catchments—effects of hydrological gradients and implications for global warming potentials of forest soils. *Biogeochemistry* 107, 437–454. doi:10.1007/s10533-010-9563-x
- Ciais, P., Sabine, C., Bala, G., Bopp, L., Brovkin, V., Canadell, J., Chhabra, A., DeFries, R., Galloway, J., Heimann, M., Jones, C., Quéré, C. le, Myneni, R.B., Piao, S., Thornton, P., 2013. Carbon and Other Biogeochemical Cycles, in: *Intergovernmental Panel on Climate Change (Ed.), Climate Change 2013 - The Physical Science Basis*. Cambridge University Press, Cambridge, pp. 465–570. doi:10.1017/CBO9781107415324.015
- Codispoti, L.A., 2007. An oceanic fixed nitrogen sink exceeding 400 Tg N a<sup>&lt;sup>−1</sup></sup> vs the concept of homeostasis in the fixed-nitrogen inventory. *Biogeosciences* 4, 233–253. doi:10.5194/bg-4-233-2007
- Colmer, T.D., 2003. Long-distance transport of gases in plants: a perspective on internal aeration and radial oxygen loss from roots. *Plant, Cell & Environment* 26, 17–36. doi:10.1046/j.1365-3040.2003.00846.x
- Daims, H., Lebedeva, E. v., Pjevac, P., Han, P., Herbold, C., Albertsen, M., Jehmlich, N., Palatinszky, M., Vierheilig, J., Bulaev, A., Kirkegaard, R.H., von Bergen, M., Rattei, T., Bendinger, B., Nielsen, P.H., Wagner, M., 2015. Complete nitrification by *Nitrospira* bacteria. *Nature* 528, 504–509. doi:10.1038/nature16461
- Daims, H., Lücker, S., Wagner, M., 2016. A New Perspective on Microbes Formerly Known as Nitrite-Oxidizing Bacteria. *Trends in Microbiology* 24, 699–712. doi:10.1016/j.tim.2016.05.004
- de Carlo, N.D., Oelbermann, M., Gordon, A.M., 2019. Spatial and Temporal Variation in Soil Nitrous Oxide Emissions from a Rehabilitated and Undisturbed Riparian Forest. *Journal of Environmental Quality* 48, 624–633. doi:10.2134/jeq2018.10.0357
- Decock, C., Six, J., 2013. On the potential of  $\delta^{18}\text{O}$  and  $\delta^{15}\text{N}$  to assess  $\text{N}_2\text{O}$  reduction to  $\text{N}_2$  in soil. *European Journal of Soil Science* 64, 610–620. doi:10.1111/ejss.12068
- Denk, T.R.A., Mohn, J., Decock, C., Lewicka-Szczebak, D., Harris, E., Butterbach-Bahl, K., Kiese, R., Wolf, B., 2017. The nitrogen cycle: A review of isotope effects and isotope modeling approaches. *Soil Biology and Biochemistry* 105, 121–137. doi:10.1016/j.soilbio.2016.11.015

- Dennis, P.G., Miller, A.J., Hirsch, P.R., 2010. Are root exudates more important than other sources of rhizodeposits in structuring rhizosphere bacterial communities? *FEMS Microbiology Ecology* 72, 313–327. doi:10.1111/j.1574-6941.2010.00860.x
- Ebrahimi, A., Or, D., 2016. Microbial community dynamics in soil aggregates shape biogeochemical gas fluxes from soil profiles – upscaling an aggregate biophysical model. *Global Change Biology* 22, 3141–3156. doi:10.1111/gcb.13345
- Erismann, J.W., Galloway, J.N., Seitzinger, S., Bleeker, A., Dise, N.B., Petrescu, A.M.R., Leach, A.M., de Vries, W., 2013. Consequences of human modification of the global nitrogen cycle. *Philosophical Transactions of the Royal Society B: Biological Sciences* 368, 20130116. doi:10.1098/rstb.2013.0116
- Fender, A.-C., Leuschner, C., Schützenmeister, K., Gansert, D., Jungkunst, H.F., 2013. Rhizosphere effects of tree species – Large reduction of N<sub>2</sub>O emission by saplings of ash, but not of beech, in temperate forest soil. *European Journal of Soil Biology* 54, 7–15. doi:10.1016/j.ejsobi.2012.10.010
- Fleming, E.L., Jackman, C.H., Stolarski, R.S., Douglass, A.R., 2011. A model study of the impact of source gas changes on the stratosphere for 1850–2100. *Atmospheric Chemistry and Physics* 11, 8515–8541. doi:10.5194/acp-11-8515-2011
- Forster, P., Ramaswamy, V., Artaxo, P., Bernsten, T., Betts, R., Fahey, D.W., Haywood, J., Lean, J., Lowe, D.C., Myhre, G., Nganga, J., Prinn, R., Raga, G., Schulz, M., van Dorland, R., 2007. Changes in Atmospheric Constituents and in Radiative Forcing, in: Solomon, S., Qin, D., Manning, M., Chen, Z., Marquis, M., Averyt, K.B., Tignor, M., Miller, H.L. (Eds.), *Climate Change 2007: The Physical Science Basis*. Cambridge University Press, Cambridge, United Kingdom and New York, NY, USA, pp. 129–234.
- Fournier, B., Guenat, C., Bullinger-Weber, G., Mitchell, E.A.D., 2013. Spatio-temporal heterogeneity of riparian soil morphology in a restored floodplain. *Hydrology and Earth System Sciences* 17, 4031–4042. doi:10.5194/hess-17-4031-2013
- Fry, B., 2006. *Stable Isotope Ecology*. Springer New York, New York, NY. doi:10.1007/0-387-33745-8
- Galloway, J.N., Townsend, A.R., Erismann, J.W., Bekunda, M., Cai, Z., Freney, J.R., Martinelli, L.A., Seitzinger, S.P., Sutton, M.A., 2008. Transformation of the Nitrogen Cycle: Recent Trends, Questions, and Potential Solutions. *Science* 320, 889–892. doi:10.1126/science.1136674
- Giles, M., Morley, N., Baggs, E.M., Daniell, T.J., 2012. Soil nitrate reducing processes - Drivers, mechanisms for spatial variation, and significance for nitrous oxide production. *Frontiers in Microbiology* 3, 1–16. doi:10.3389/fmicb.2012.00407
- Groffman, P.M., Altabet, M. a., Böhlke, J.K., Butterbach-Bahl, K., David, M.B., Firestone, M.K., Giblin, A.E., Kana, T.M., Nielsen, L.P., Voytek, M.A., 2006. Methods for measuring denitrification: diverse approaches to a difficult problem. *Ecological Applications : A Publication of the Ecological Society of America* 16, 2091–122. doi:10.1890/1051-0761(2006)016[2091:mfmdda]2.0.co;2
- Gruber, N., Galloway, J.N., 2008. An Earth-system perspective of the global nitrogen cycle. *Nature* 451, 293–296. doi:10.1038/nature06592
- Heincke, M., Kaupenjohann, M., 1999. Effects of soil solution on the dynamics of N<sub>2</sub>O emissions: a review. *Nutrient Cycling in Agroecosystems* 55, 133–157. doi:10.1023/A:1009842011599
- Hill, A.R., 2011. Buried organic-rich horizons: their role as nitrogen sources in stream riparian zones. *Biogeochemistry* 104, 347–363. doi:10.1007/s10533-010-9507-5

- Hill, R.D., Rinker, R.G., Wilson, H.D., 1980. Atmospheric Nitrogen Fixation by Lightning. *Journal of the Atmospheric Sciences* 37, 179–192. doi:10.1175/1520-0469(1980)037<0179:ANFBL>2.0.CO;2
- Jacinthe, P.A., Bills, J.S., Tedesco, L.P., Barr, R.C., 2012. Nitrous Oxide Emission from Riparian Buffers in Relation to Vegetation and Flood Frequency. *Journal of Environmental Quality* 41, 95–105. doi:10.2134/jeq2011.0308
- Jahangir, M.M.R., Roobroeck, D., van Cleemput, O., Boeckx, P., 2011. Spatial variability and biophysicochemical controls on N<sub>2</sub>O emissions from differently tilled arable soils. *Biology and Fertility of Soils* 47, 753–766. doi:10.1007/s00374-011-0580-2
- Jones, L.C., Peters, B., Lezama Pacheco, J.S., Casciotti, K.L., Fendorf, S., 2015. Stable isotopes and iron oxide mineral products as markers of chemodenitrification. *Environmental Science and Technology* 49, 3444–3452. doi:10.1021/es504862x
- Jungkunst, H.F., Fiedler, S., Stahr, K., 2004. N<sub>2</sub>O emissions of a mature Norway spruce (*Picea abies*) stand in the Black Forest (southwest Germany) as differentiated by the soil pattern. *Journal of Geophysical Research* 109, D07302. doi:10.1029/2003JD004344
- Kits, K.D., Jung, M., Vierheilig, J., Pjevac, P., Sedlacek, C.J., Liu, S., Herbold, C., Stein, L.Y., Richter, A., Wissel, H., Brüggemann, N., Wagner, M., Daims, H., 2019. Low yield and abiotic origin of N<sub>2</sub>O formed by the complete nitrifier *Nitrospira inopinata*. *Nature Communications* 10, 1–12. doi:10.1038/s41467-019-09790-x
- Kool, D.M., Wrage, N., Oenema, O., Dolfig, J., van Groenigen, J.W., 2007. Oxygen exchange between (de)nitrification intermediates and H<sub>2</sub>O and its implications for source determination of NO<sub>3</sub><sup>-</sup> and N<sub>2</sub>O: a review. *Rapid Communications in Mass Spectrometry* 21, 3569–3578. doi:10.1002/rcm.3249
- Koranda, M., Schneckler, J., Kaiser, C., Fuchslueger, L., Kitzler, B., Stange, C.F., Sessitsch, A., Zechmeister-Boltenstern, S., Richter, A., 2011. Microbial processes and community composition in the rhizosphere of European beech – The influence of plant C exudates. *Soil Biology and Biochemistry* 43, 551–558. doi:10.1016/j.soilbio.2010.11.022
- Koschorreck, M., Darwich, A., 2003. Nitrogen dynamics in seasonally flooded soils in the Amazon floodplain. *Wetlands Ecology and Management* 11, 317–330. doi:10.1023/B:WETL.0000005536.39074.72
- Kovats, R.S., Valentini, R., Bouwer, L.M., Georgopoulou, E., Jacob, D., Martin, E., Rounsevell, M., Soussana, J.F., 2015. Europe, in: Barros, V.R., Field, C.B., Dokken, D.J., Mastrandrea, M.D., Mach, K.J. (Eds.), *Climate Change 2014: Impacts, Adaptation and Vulnerability*. Cambridge University Press, Cambridge, pp. 1267–1326. doi:10.1017/CBO9781107415386.003
- Kozłowski, J.A., Stieglmeier, M., Schleper, C., Klotz, M.G., Stein, L.Y., 2016. Pathways and key intermediates required for obligate aerobic ammonia-dependent chemolithotrophy in bacteria and Thaumarchaeota. *The ISME Journal* 10, 1836–1845. doi:10.1038/ismej.2016.2
- Kuypers, M.M.M., Marchant, H.K., Kartal, B., 2018. The microbial nitrogen-cycling network. *Nature Reviews Microbiology* 16, 263–276. doi:10.1038/nrmicro.2018.9
- Laughlin, R.J., Stevens, R.J., 2002. Evidence for Fungal Dominance of Denitrification and Codenitrification in a Grassland Soil. *Soil Science Society of America Journal* 66, 1540. doi:10.2136/sssaj2002.1540
- Lewicka-Szczebak, D., Augustin, J., Giesemann, A., Well, R., 2017. Quantifying N<sub>2</sub>O reduction to N<sub>2</sub> based on N<sub>2</sub>O isotopocules – validation with independent methods (helium incubation and <sup>15</sup>N gas flux method). *Biogeosciences* 14, 711–732. doi:10.5194/bg-14-711-2017

- Lewicka-Szczebak, D., Dyckmans, J., Kaiser, J., Marca, A., Augustin, J., Well, R., 2016. Oxygen isotope fractionation during N<sub>2</sub>O production by soil denitrification. *Biogeosciences* 13, 1129–1144. doi:10.5194/bg-13-1129-2016
- Lewicka-Szczebak, D., Piotr Lewicki, M., Well, R., 2020. N<sub>2</sub>O isotope approaches for source partitioning of N<sub>2</sub>O production and estimation of N<sub>2</sub>O reduction-validation with the <sup>15</sup>N gas-flux method in laboratory and field studies. *Biogeosciences* 17, 5513–5537. doi:10.5194/bg-17-5513-2020
- Lewicka-Szczebak, D., Well, R., Köster, J.R., Fuß, R., Senbayram, M., Dittert, K., Flessa, H., 2014. Experimental determinations of isotopic fractionation factors associated with N<sub>2</sub>O production and reduction during denitrification in soils. *Geochimica et Cosmochimica Acta* 134, 55–73. doi:10.1016/j.gca.2014.03.010
- Li, X., Sørensen, P., Olesen, J.E., Petersen, S.O., 2016. Evidence for denitrification as main source of N<sub>2</sub>O emission from residue-amended soil. *Soil Biology and Biochemistry* 92, 153–160. doi:10.1016/j.soilbio.2015.10.008
- Liu, S., Han, P., Hink, L., Prosser, J.I., Wagner, M., Brüggemann, N., 2017. Abiotic Conversion of Extracellular NH<sub>2</sub>OH Contributes to N<sub>2</sub>O Emission during Ammonia Oxidation. *Environmental Science and Technology* 51, 13122–13132. doi:10.1021/acs.est.7b02360
- Loecke, T.D., Robertson, G.P., 2009. Soil resource heterogeneity in terms of litter aggregation promotes nitrous oxide fluxes and slows decomposition. *Soil Biology and Biochemistry* 41, 228–235. doi:10.1016/j.soilbio.2008.10.017
- Luster, J., Göttlein, A., Nowack, B., Sarret, G., 2009. Sampling, defining, characterising and modeling the rhizosphere—the soil science tool box. *Plant and Soil* 321, 457–482. doi:10.1007/s11104-008-9781-3
- Machado dos Santos Pinto, R., Weigelhofer, G., Diaz-Pines, E., Guerreiro Brito, A., Zechmeister-Boltenstern, S., Hein, T., 2020. River-floodplain restoration and hydrological effects on GHG emissions: Biogeochemical dynamics in the parafluvial zone. *Science of The Total Environment* 715, 136980. doi:10.1016/j.scitotenv.2020.136980
- Madsen, H., Lawrence, D., Lang, M., Martinkova, M., Kjeldsen, T.R., 2014. Review of trend analysis and climate change projections of extreme precipitation and floods in Europe. *Journal of Hydrology* 519, 3634–3650. doi:10.1016/j.jhydrol.2014.11.003
- Maeda, K., Spor, A., Edel-Hermann, V., Heraud, C., Breuil, M.C., Bizouard, F., Toyoda, S., Yoshida, N., Steinberg, C., Philippot, L., 2015. N<sub>2</sub>O production, a widespread trait in fungi. *Scientific Reports* 5, 9697. doi:10.1038/srep09697
- Marushchak, M.E., Friborg, T., Biasi, C., Herbst, M., Johansson, T., Kiepe, I., Liimatainen, M., Lind, S.E., Martikainen, P.J., Virtanen, T., Soegaard, H., Shurpali, N.J., 2016. Methane dynamics in the subarctic tundra: Combining stable isotope analyses, plot-And ecosystem-scale flux measurements. *Biogeosciences* 13, 597–608. doi:10.5194/bg-13-597-2016
- Myrold, D.D., Bottomley, P.J., 2015. Nitrogen Mineralization and Immobilization, in: *Methods in Soil Biology*. pp. 157–172. doi:10.2134/agronmonogr49.c5
- Neira, J., Ortiz, M., Morales, L., Acevedo, E., 2015. Oxygen diffusion in soils: Understanding the factors and processes needed for modeling. *Chilean Journal of Agricultural Research* 75, 35–44. doi:10.4067/S0718-58392015000300005

- Or, D., Smets, B.F., Wraith, J.M., Dechesne, A., Friedman, S.P., 2007. Physical constraints affecting bacterial habitats and activity in unsaturated porous media – a review. *Advances in Water Resources* 30, 1505–1527. doi:10.1016/j.advwatres.2006.05.025
- Ostrom, N.E., Ostrom, P.H., 2017. Mining the isotopic complexity of nitrous oxide: a review of challenges and opportunities. *Biogeochemistry* 132, 359–372. doi:10.1007/s10533-017-0301-5
- Park, S., Pérez, T., Boering, K.A., Trumbore, S.E., Gil, J., Marquina, S., Tyler, S.C., 2011. Can N<sub>2</sub>O stable isotopes and isotopomers be useful tools to characterize sources and microbial pathways of N<sub>2</sub>O production and consumption in tropical soils? *Global Biogeochemical Cycles* 25, 1–16. doi:10.1029/2009GB003615
- Philippot, L., Hallin, S., Börjesson, G., Baggs, E.M., 2009. Biochemical cycling in the rhizosphere having an impact on global change. *Plant and Soil* 321, 61–81. doi:10.1007/s11104-008-9796-9
- Pinay, G., Bernal, S., Abbott, B. W., Lupon, A., Marti, E., Sabater, F., & Krause, S. (2018). Riparian Corridors: A New Conceptual Framework for Assessing Nitrogen Buffering Across Biomes. *Frontiers in Environmental Science*, 6(JUN), 1–11. <https://doi.org/10.3389/fenvs.2018.00047>
- Pinto, R., Weigelhofer, G., Brito, A.G., Hein, T., 2021. Effects of dry-wet cycles on nitrous oxide emissions in freshwater sediments: a synthesis. *PeerJ* 9, e10767. doi:10.7717/peerj.10767
- Poblador, S., Lupon, A., Sabaté, S., Sabater, F., 2017. Soil water content drives spatiotemporal patterns of CO<sub>2</sub> and N<sub>2</sub>O emissions from a Mediterranean riparian forest soil. *Biogeosciences* 14, 4195–4208. doi:10.5194/bg-14-4195-2017
- Prather, M.J., Holmes, C.D., Hsu, J., 2012. Reactive greenhouse gas scenarios: Systematic exploration of uncertainties and the role of atmospheric chemistry. *Geophysical Research Letters* 39, 1–5. doi:10.1029/2012GL051440
- Ravishankara, A.R., Daniel, J.S., Portmann, R.W., 2009. Nitrous Oxide (N<sub>2</sub>O): The Dominant Ozone-Depleting Substance Emitted in the 21st Century. *Science* 326, 123–125. doi:10.1126/science.1176985
- Robertson, G.P., Groffman, P.M., 2015. Nitrogen Transformations, in: *Soil Microbiology, Ecology and Biochemistry*. Elsevier, pp. 421–446. doi:10.1016/B978-0-12-415955-6.00014-1
- Rütting, T., Boeckx, P., Müller, C., Klemetsson, L., 2011. Assessment of the importance of dissimilatory nitrate reduction to ammonium for the terrestrial nitrogen cycle. *Biogeosciences* 8, 1779–1791. doi:10.5194/bg-8-1779-2011
- Samaritani, E., Shrestha, J., Fournier, B., Frossard, E., Gillet, F., Guenat, C., Niklaus, P.A., Pasquale, N., Tockner, K., Mitchell, E.A.D., Luster, J., 2011. Heterogeneity of soil carbon pools and fluxes in a channelized and a restored floodplain section (Thur River, Switzerland). *Hydrology and Earth System Sciences* 15, 1757–1769. doi:10.5194/hess-15-1757-2011
- Schirmer, M., Luster, J., Linde, N., Perona, P., Mitchell, E.A.D., Barry, D.A., Hollender, J., Cirpka, O.A., Schneider, P., Vogt, T., Radny, D., Durisch-Kaiser, E., 2014. Morphological, hydrological, biogeochemical and ecological changes and challenges in river restoration the Thur River case study. *Hydrology and Earth System Sciences* 18, 2449–2462. doi:10.5194/hess-18-2449-2014
- Schleper, C., Nicol, G.W., 2010. Ammonia-Oxidising Archaea – Physiology, Ecology and Evolution, in: *Advances in Microbial Physiology*. Elsevier Ltd, pp. 1–41. doi:10.1016/B978-0-12-381045-8.00001-1

- Sey, B.K., Manceur, A.M., Whalen, J.K., Gregorich, E.G., Rochette, P., 2008. Small-scale heterogeneity in carbon dioxide, nitrous oxide and methane production from aggregates of a cultivated sandy-loam soil. *Soil Biology and Biochemistry* 40, 2468–2473. doi:10.1016/j.soilbio.2008.05.012
- Sharp, Z., 2007. Principles of stable isotope geochemistry, *Choice Reviews Online*. doi:10.5860/choice.44-6251
- Shoun, H., Fushinobu, S., Jiang, L., Kim, S.W., Wakagi, T., 2012. Fungal denitrification and nitric oxide reductase cytochrome P450nor. *Philosophical Transactions of the Royal Society B: Biological Sciences* 367, 1186–1194. doi:10.1098/rstb.2011.0335
- Shrestha, J., Niklaus, P.A., Pasquale, N., Huber, B., Barnard, R.L., Frossard, E., Schleppei, P., Tockner, K., Luster, J., 2014. Flood pulses control soil nitrogen cycling in a dynamic river floodplain. *Geoderma* 228–229, 14–24. doi:10.1016/j.geoderma.2013.09.018
- Simon, J., Klotz, M.G., 2013. Diversity and evolution of bioenergetic systems involved in microbial nitrogen compound transformations. *Biochimica et Biophysica Acta (BBA) - Bioenergetics* 1827, 114–135. doi:10.1016/j.bbabi.2012.07.005
- Six, J., Bossuyt, H., Degryze, S., Denef, K., 2004. A history of research on the link between (micro)aggregates, soil biota, and soil organic matter dynamics. *Soil and Tillage Research* 79, 7–31. doi:10.1016/j.still.2004.03.008
- Snider, D.M., Venkiteswaran, J.J., Schiff, S.L., Spoelstra, J., 2012. Deciphering the oxygen isotope composition of nitrous oxide produced by nitrification. *Global Change Biology* 18, 356–370. doi:10.1111/j.1365-2486.2011.02547.x
- Sorrell, B.K., Brix, H., 2015. Gas Transport and Exchange through Wetland Plant Aerenchyma, in: *Methods in Biogeochemistry of Wetlands*. pp. 177–196. doi:10.2136/sssabookser10.c11
- Spott, O., Russow, R., Stange, C.F., 2011. Formation of hybrid N<sub>2</sub>O and hybrid N<sub>2</sub> due to codenitrification: First review of a barely considered process of microbially mediated N-nitrosation. *Soil Biology and Biochemistry* 43, 1995–2011. doi:10.1016/j.soilbio.2011.06.014
- Stanton, C.L., Reinhard, C.T., Kasting, J.F., Ostrom, N.E., Haslun, J.A., Lyons, T.W., Glass, J.B., 2018. Nitrous oxide from chemodenitrification: A possible missing link in the Proterozoic greenhouse and the evolution of aerobic respiration. *Geobiology* 16, 597–609. doi:10.1111/gbi.12311
- Stein, L.Y., Klotz, M.G., 2011. Nitrifying and denitrifying pathways of methanotrophic bacteria. *Biochemical Society Transactions* 39, 1826–1831. doi:10.1042/BST20110712
- Swanson, W., de Jager, N.R., Strauss, E., Thomsen, M., 2017. Effects of flood inundation and invasion by *Phalaris arundinacea* on nitrogen cycling in an Upper Mississippi River floodplain forest. *Ecohydrology* 10, 1–12. doi:10.1002/eco.1877
- Thorbjørn, A., Moldrup, P., Blendstrup, H., Komatsu, T., Rolston, D.E., 2008. A Gas Diffusivity Model Based on Air-, Solid-, and Water-Phase Resistance in Variably Saturated Soil. *Vadose Zone Journal* 7, 1276. doi:10.2136/vzj2008.0023
- Tian, H., Xu, R., Canadell, J.G., Thompson, R.L., Winiwarter, W., Suntharalingam, P., Davidson, E.A., Ciais, P., Jackson, R.B., Janssens-Maenhout, G., Prather, M.J., Regnier, P., Pan, N., Pan, S., Peters, G.P., Shi, H., Tubiello, F.N., Zaehle, S., Zhou, F., Arneeth, A., Battaglia, G., Berthet, S., Bopp, L., Bouwman, A.F., Buitenhuis, E.T., Chang, J., Chipperfield, M.P., Dangal, S.R.S., Dlugokencky, E., Elkins, J.W., Eyre, B.D., Fu, B., Hall, B., Ito, A., Joos, F., Krummel, P.B., Landolfi, A., Laruelle, G.G., Lauerwald, R., Li, W., Lienert, S., Maavara, T., MacLeod, M., Millet, D.B., Olin, S., Patra, P.K., Prinn, R.G., Raymond,

- P.A., Ruiz, D.J., van der Werf, G.R., Vuichard, N., Wang, J., Weiss, R.F., Wells, K.C., Wilson, C., Yang, J., Yao, Y., 2020. A comprehensive quantification of global nitrous oxide sources and sinks. *Nature* 586, 248–256. doi:10.1038/s41586-020-2780-0
- Tisdall, J.M., Oades, J.M., 1982. Organic matter and water-stable aggregates in soils. *Journal of Soil Science* 33, 141–163. doi:10.1111/j.1365-2389.1982.tb01755.x
- Toyoda, S., Mutobe, H., Yamagishi, H., Yoshida, N., Tanji, Y., 2005. Fractionation of N<sub>2</sub>O isotopomers during production by denitrifier. *Soil Biology and Biochemistry* 37, 1535–1545. doi:10.1016/j.soilbio.2005.01.009
- Toyoda, S., Yano, M., Nishimura, S., Akiyama, H., Hayakawa, A., Koba, K., Sudo, S., Yagi, K., Makabe, A., Tobari, Y., Ogawa, N.O., Ohkouchi, N., Yamada, K., Yoshida, N., 2011. Characterization and production and consumption processes of N<sub>2</sub>O emitted from temperate agricultural soils determined via isotopomer ratio analysis. *Global Biogeochemical Cycles* 25, 1–17. doi:10.1029/2009GB003769
- Toyoda, S., Yoshida, N., 1999. Determination of nitrogen isotopomers of nitrous oxide on a modified isotope ratio mass spectrometer. *Analytical Chemistry* 71, 4711–4718. doi:10.1021/ac9904563
- van den Heuvel, R.N., Bakker, S.E., Jetten, M.S.M., Hefting, M.M., 2011. Decreased N<sub>2</sub>O reduction by low soil pH causes high N<sub>2</sub>O emissions in a riparian ecosystem. *Geobiology* 9, 294–300. doi:10.1111/j.1472-4669.2011.00276.x
- van den Heuvel, R.N., Hefting, M.M., Tan, N.C.G., Jetten, M.S.M., Verhoeven, J.T.A., 2009. N<sub>2</sub>O emission hotspots at different spatial scales and governing factors for small scale hotspots. *Science of the Total Environment* 407, 2325–2332. doi:10.1016/j.scitotenv.2008.11.010
- van Kessel, M.A.H.J., Speth, D.R., Albertsen, M., Nielsen, P.H., Op Den Camp, H.J.M., Kartal, B., Jetten, M.S.M., Lüscher, S., 2015. Complete nitrification by a single microorganism. *Nature* 528, 555–559. doi:10.1038/nature16459
- Vergani, C., Graf, F., 2015. Soil permeability, aggregate stability and root growth: a pot experiment from a soil bioengineering perspective. *Ecohydrology* 9, 830–842. doi:10.1002/eco.1686
- Verhoeven, E., Barthel, M., Yu, L., Celi, L., Said-Pullicino, D., Sleutel, S., Lewicka-Szczebak, D., Six, J., Decock, C., 2019. Early season N<sub>2</sub>O emissions under variable water management in rice systems: Source-partitioning emissions using isotope ratios along a depth profile. *Biogeosciences* 16, 383–408. doi:10.5194/bg-16-383-2019
- Vieten, B., Conen, F., Neftel, A., Alewell, C., 2009. Respiration of nitrous oxide in suboxic soil. *European Journal of Soil Science* 60, 332–337. doi:10.1111/j.1365-2389.2009.01125.x
- Vitousek, P.M., Menge, D.N.L., Reed, S.C., Cleveland, C.C., 2013. Biological nitrogen fixation: rates, patterns and ecological controls in terrestrial ecosystems. *Philosophical Transactions of the Royal Society B: Biological Sciences* 368, 20130119. doi:10.1098/rstb.2013.0119
- Voss, M., Bange, H.W., Dippner, J.W., Middelburg, J.J., Montoya, J.P., Ward, B., 2013. The marine nitrogen cycle: recent discoveries, uncertainties and the potential relevance of climate change. *Philosophical Transactions of the Royal Society B: Biological Sciences* 368, 20130121. doi:10.1098/rstb.2013.0121
- Wang, B., Brewer, P. E., Shugart, H. H., Lerdau, M. T., & Allison, S. D. (2019). Soil aggregates as biogeochemical reactors and implications for soil–atmosphere exchange of greenhouse gases—A concept. *Global Change Biology*, 25(2), 373–385. <https://doi.org/10.1111/gcb.14515>

- Wilpiseski, R.L., Aufrecht, J.A., Retterer, S.T., Sullivan, M.B., Graham, D.E., Pierce, E.M., Zablocki, O.D., Palumbo, A. v., Elias, D.A., 2019. Soil Aggregate Microbial Communities: Towards Understanding Microbiome Interactions at Biologically Relevant Scales. *Applied and Environmental Microbiology* 85, 1–18. doi:10.1128/AEM.00324-19
- Yu, L., Harris, E., Lewicka-Szczebak, D., Barthel, M., Blomberg, M.R.A., Harris, S.J., Johnson, M.S., Lehmann, M.F., Liisberg, J., Müller, C., Ostrom, N.E., Six, J., Toyoda, S., Yoshida, N., Mohn, J., 2020. What can we learn from N<sub>2</sub>O isotope data? – Analytics, processes and modelling. *Rapid Communications in Mass Spectrometry* 34, 1–14. doi:10.1002/rcm.8858
- Zumft, W.G., 1997. Cell biology and molecular basis of denitrification. *Microbiology and Molecular Biology Reviews* 61, 533–616. doi:10.1128/mubr.61.4.533-616.1997



## Chapter 2

# Alteration of nitrous oxide emissions from floodplain soils by aggregate size, litter accumulation and plant–soil interactions

Martin Ley<sup>1,2</sup>, Moritz F. Lehmann<sup>2</sup>, Pascal A. Niklaus<sup>3</sup>, and Jörg Luster<sup>1</sup>

<sup>1</sup>Swiss Federal Institute for Forest, Snow and Landscape Research WSL, Zürcherstrasse 111, 8903 Birmensdorf, Switzerland

<sup>2</sup>Department of Environmental Sciences, University of Basel, Bernoullistrasse 30, 4056 Basel, Switzerland

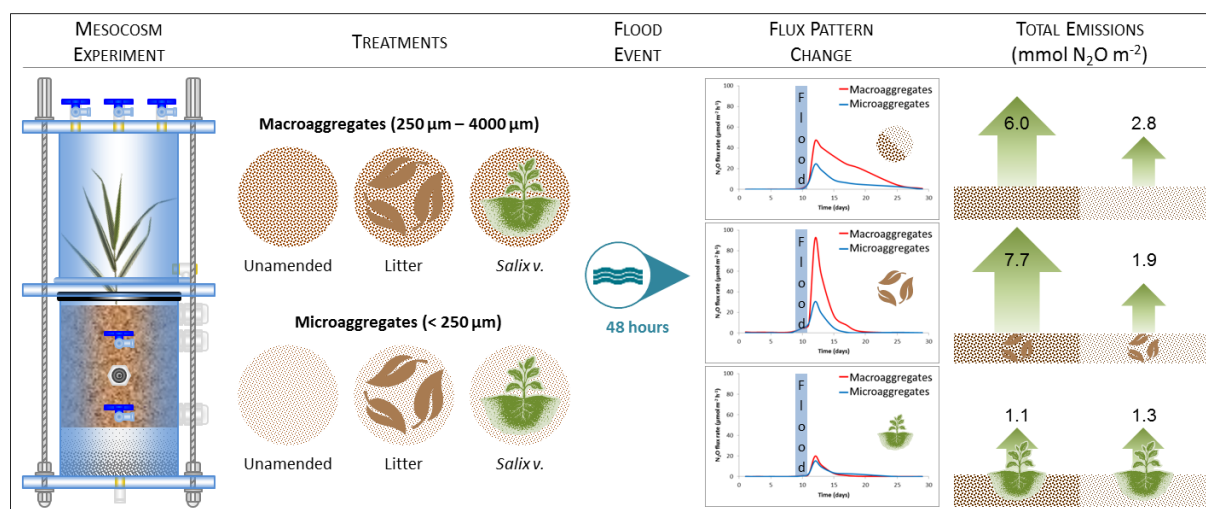
<sup>3</sup>Department of Evolutionary Biology and Environmental Studies, University of Zürich, Winterthurerstrasse 190, 8057 Zurich, Switzerland

Correspondence to: Martin Ley (martin.ley@wsl.ch)

Received: 11 Jun 2018 – Discussion started: 02 Jul 2018 – Revised: 15 Oct 2018 – Accepted: 13 Nov 2018 – Published: 27 Nov 2018

Published in: Biogeosciences, 15, 7043–7057, 2018

## Graphical Abstract



**Abstract**

Semi-terrestrial soils such as floodplain soils are considered potential hotspots of nitrous oxide (N<sub>2</sub>O) emissions. Microhabitats in the soil, such as within and outside of aggregates, in the detritusphere, and/or in the rhizosphere, are considered to promote and preserve specific redox conditions. Yet, our understanding of the relative effects of such microhabitats and their interactions on N<sub>2</sub>O production and consumption in soils is still incomplete. Therefore, we assessed the effect of aggregate size, buried leaf litter, and plant-soil interactions on the occurrence of enhanced N<sub>2</sub>O emissions under simulated flooding/drying conditions in a mesocosm experiment. We used two model soils with equivalent structure and texture, comprising macroaggregates (4000–250 μm) or microaggregates (< 250 μm) from a N-rich floodplain soil. These model soils were planted either with basket willow (*Salix viminalis* L.), mixed with leaf litter, or left unamended. After 48 hours of flooding, a period of enhanced N<sub>2</sub>O emissions occurred in all treatments. The unamended model soils with macroaggregates emitted significantly more N<sub>2</sub>O during this period than those with microaggregates. Litter addition modulated the temporal pattern of the N<sub>2</sub>O emission, leading to short-term peaks of high N<sub>2</sub>O fluxes at the beginning of the period of enhanced N<sub>2</sub>O emissions. The presence of *S. viminalis* strongly suppressed the N<sub>2</sub>O emission from the macroaggregated model soil, masking any aggregate-size effect. Integration of the flux data with data on soil bulk density, moisture, redox potential and soil solution composition suggest that macroaggregates provided more favorable conditions for spatially coupled nitrification–denitrification, which are particularly conducive to net N<sub>2</sub>O production, than microaggregates. The local increase in organic carbon in the detritusphere appears to first stimulate N<sub>2</sub>O emissions, but ultimately, respiration of the surplus organic matter shifts the system towards redox conditions where N<sub>2</sub>O reduction to N<sub>2</sub> dominates. Similarly, the low emission rates in the planted soils can be best explained by root exudation of low-molecular weight organic substances supporting complete denitrification in the anoxic zones, but also by the inhibition of denitrification in the zone, where rhizosphere aeration takes place. Together, our experiments highlight the importance of microhabitat formation in regulating oxygen (O<sub>2</sub>) content and the completeness of denitrification in soils during drying after saturation. Moreover, they will help to better predict the conditions under which hotspots, and moments, of enhanced N<sub>2</sub>O emissions are most likely to occur in hydrologically dynamic soil systems like floodplain soils.

---

## 2.1 Introduction

Nitrous oxide ( $\text{N}_2\text{O}$ ) is a potent greenhouse gas with a global warming potential over a 100 year time horizon 298 times higher than the one of carbon dioxide (Forster et al., 2007). Given its role as climate-relevant gas and in the depletion of stratospheric ozone (Ravishankara et al., 2009), the steady increase of its average atmospheric concentration of  $0.75\text{ppb yr}^{-1}$  (Hartmann et al., 2013) asks for a quantitative understanding of its sources and the factors that control its production. On a global scale, vegetated soils are the main natural terrestrial sources of  $\text{N}_2\text{O}$ . Agriculture is the main anthropogenic source and the main driver of increasing atmosphere  $\text{N}_2\text{O}$  concentrations (Ciais et al., 2013).

In soils, several biological nitrogen (N) transformation processes produce  $\text{N}_2\text{O}$  either as a mandatory intermediate or as a by-product (Spott et al., 2011). Under oxic conditions, the most important process is obligate aerobic nitrification that yields  $\text{N}_2\text{O}$  as by-product when hydroxylamine decomposes (Zhu et al., 2013). Under low oxygen availability, nitrifier denitrification and heterotrophic denitrification with  $\text{N}_2\text{O}$  as intermediate become more relevant (Philippot et al., 2009). At stably anoxic conditions and low concentrations of nitrate ( $\text{NO}_3^-$ ), complete denitrification consumes substantial amounts of previously produced  $\text{N}_2\text{O}$  by further reduction to  $\text{N}_2$  (Baggs, 2008; Vieten et al., 2009). In environments that do not sustain stable anoxia, but undergo sporadic transitions between oxic and anoxic conditions, the activity of certain  $\text{N}_2\text{O}$  reductases can be suppressed by transiently elevated  $\text{O}_2$  concentration and thus can lead to the accumulation of  $\text{N}_2\text{O}$  (Morley et al., 2008).

Nitrous oxide emissions from soils depend on the availability of carbon (C) and N substrates that fuel the involved microbial processes. On the other hand, given its dependency on  $\text{O}_2$ ,  $\text{N}_2\text{O}$  production is also governed by the diffusive supply of  $\text{O}_2$  through soils. Similarly, soil  $\text{N}_2\text{O}$  emissions are modulated by diffusive  $\text{N}_2\text{O}$  transport from the site of production to the soil surface (e.g., Böttcher et al., 2011; Heincke and Kaupenjohann, 1999). Substrate availability, gas diffusivity, and the distribution of soil organisms are highly heterogeneous in soils at a small scale, with micro-niches in particular within soil aggregates, within the detritosphere, and within the rhizosphere. These can result in “hot spots” with high denitrification activity (Kuzyakov and Blagodatskaya, 2015).

Soil aggregate formation is a key process in building soil structure and pore space. Soil aggregates undergo different stages in their development, depending on the degradability of the main binding agent (Tisdall and Oades, 1982). Initially, highly persistent primary organo–mineral clusters (20–250  $\mu\text{m}$ ) are held together by root hairs and hyphae, thus forming macroaggregates (> 250  $\mu\text{m}$ ). Upon decomposition of these temporary binding agents and the

---

subsequent disruption of the macroaggregates, microaggregates (< 250  $\mu\text{m}$ ) are released (Elliott and Coleman, 1988; Oades, 1984; Six et al., 2004). These consist of clay-encrusted fragments of organic debris coated with polysaccharides and proteins. This multi-stage development leads to a complex relationship between aggregate size, intra-aggregate structure and soil structure (Ball, 2013; Totsche et al., 2017), which influences soil aeration, substrate distribution and pore water dynamics (Six et al., 2004). Often, micro-site heterogeneity increases with aggregate size, thus fostering the simultaneous activity of different  $\text{N}_2\text{O}$  producing microbial communities with distinct functional traits (Bateman and Baggs, 2005). Aggregate size effects on  $\text{N}_2\text{O}$  production and consumption have generally been studied in static batch incubation experiments with a comparatively small number of isolated aggregates of uniform size, at constant levels of water saturation (Diba et al., 2011; Drury et al., 2004; Jahangir et al., 2011; Khalil et al., 2005; Sey et al., 2008), and through modelling approaches (Renault and Stengel, 1994; Stolk et al., 2011). Previous work provided partially inconsistent results, which led to an ongoing discourse about the interplay of physicochemical properties and different aggregate sizes in controlling  $\text{N}_2\text{O}$  emission. Such inconsistencies may in parts be attributed to the use of different aggregate size classes, changes in soil structure by aggregate separation, other methodological constraints (water saturation, redox potential), and differences in microbial communities. The effects of specific aggregate sizes within a simulated soil structure, in combination with fluctuating water saturation, on soil  $\text{N}_2\text{O}$  emissions have, to our knowledge, not been addressed specifically.

Similar to soil aggregates, the detritosphere and the rhizosphere (the zone of the soil that is affected by root activity) (Baggs, 2011; Luster et al., 2009), can be considered biogeochemical hot spots (Kuzyakov and Blagodatskaya, 2015; Myrold et al., 2011). Here, carbon availability is much higher than in the bulk soil and thus rarely limiting microbial process rates. The detritosphere consists of dead organic material, which spans a wide range of recalcitrance to microbial decomposition. Spatially confined accumulations of variably labile soil litter form microhabitats that are often colonized by highly active microbial communities (Parkin, 1987). Aggregation of litter particles has been shown to affect  $\text{N}_2\text{O}$  emissions (Loecke and Robertson, 2009). Hill (2011) identified buried organic-rich litter horizons in a stream riparian zone as hot spots of N cycling. Similarly, in the rhizosphere, root exudates and exfoliated root cells provide ample degradable organic substrate for soil microbes (Robertson and Groffman, 2015). Yet, plant growth may also affect soil microbial communities through competition for water and nutrients (e.g., fixed N) (Bender et al., 2014; Myrold et al., 2011). The combined effects of these plant–soil interactions on  $\text{N}_2\text{O}$  production have been reviewed by Philippot et al. (2009). Root-derived bioavailable organic compounds can stimulate heterotrophic microbial activity,

specifically N mineralization and denitrification. Nitrification in turn can be enhanced by the elevated N turnover and mineralization rates, but may also be negatively affected by specific inhibitors released from the root or through plant-driven ammonium depletion. The ability of some plants adapted to water-saturated conditions to „pump“ air into the rhizosphere via aerenchyma (gas conductive channels in the root) leads to an improved oxygenation of the rhizosphere and a stimulation of nitrification (Philippot et al., 2009). Surrounded by otherwise anoxic sediments, such aerated micro-environments may create optimal conditions for coupled nitrification–denitrification (Baldwin and Mitchell, 2000; Koschorreck and Darwich, 1998). On the other hand, transport of N<sub>2</sub>O produced in the soil to the atmosphere is may be facilitated via these plant-internal channels, bypassing diffusive transport barriers and enhancing soil–atmosphere gas fluxes (Jørgensen et al., 2012).

The dynamics of N<sub>2</sub>O emissions are strongly coupled to the dynamics of pore water. Re-wetting of previously dried soil can lead to strong N<sub>2</sub>O emissions (Goldberg et al., 2010; Ruser et al., 2006), likely fostered by a wetting-induced flush in N mineralization (Baldwin and Mitchell, 2000). On the other hand, the drying-phase after water saturation of sediments and soils can lead to a period of enhanced N<sub>2</sub>O emissions (e.g., Baldwin and Mitchell, 2000; Groffman and Tiedje, 1988; Rabot et al., 2014; Shrestha et al., 2012) when water-filled pore space (WFPS) exceeds 60% (Beare et al., 2009; Rabot et al., 2014). The increased N<sub>2</sub>O production has been attributed to enhanced coupled nitrification–denitrification (Baldwin and Mitchell, 2000). Depending on the spatial distribution of water films around soil particles and tortuosity (which is a function of aggregate size and soil structure), the uneven drying of the soil after full saturation may generate conditions that are conducive to the formation of anaerobic zones in otherwise oxic environments (Young and Ritz, 2000). Pore water thereby acts as a diffusion barrier for gas exchange, limiting the O<sub>2</sub> availability in the soil pore space (Butterbach-Bahl et al., 2013). Moreover, pore water serves as a medium for the diffusive dispersal of dissolved C and N substrates, e.g., from the site of litter decomposition to spatially separated N<sub>2</sub>O producing microbial communities (Hu et al., 2015). Therefore, fluctuations in water saturation efficiently promote the development of hot spots and hot moments of N<sub>2</sub>O emissions in floodplain soils and other semi-terrestrial soils (Hefting et al., 2004; Shrestha et al., 2012).

The main objective of the present experimental study was to assess both the relative and combined effects of soil microhabitats associated with soil aggregates, the detritusphere and plant–soil interactions on N<sub>2</sub>O emissions from floodplain soils under changing pore-space saturation. We simulated a flooding event in mesocosm experiments with main focus on the dynamics of N<sub>2</sub>O emissions during hot moments in the drying phase after flooding. To isolate

the effect of aggregate-size and to minimize confounding effects of differences in soil structure, we prepared model soils by mixing aggregate size fractions of a floodplain soil with suitable inert material. The combined effects of soil aggregate size and plant detritus or plant-soil interactions were addressed by mixing the model soils with leaf litter or by planting them with willow cuttings (*Salix viminalis* L.).

We demonstrate that the level of soil aggregation significantly affects N<sub>2</sub>O emission rates from floodplain soils through its modulating control on the model soil's physicochemical properties. We further show that these effects can be modified by the presence of a detritosphere and by root–soil interactions, changing carbon and N substrate availability and redox conditions.

## 2.2 Material and Methods

### 2.2.1 Model soils

In February 2014, material from the uppermost 20 cm of a N-rich gleyic Fluvisol (calcaric, humic siltic) with 20% sand and 18% clay (Samaritani et al., 2011) was collected in the restored Thur River floodplain near Niederneunforn (NE Switzerland 47°35' N, 8°46' E, 453 m.a.s.l.; MAT 9.1 °C; MAP 1015 mm). After removing plant residues such as roots, twigs and leaves, the soil was mixed and air-dried to a gravimetric water content of  $24.7 \pm 0.4$  %. In the next step, the original floodplain soil material, consisting of  $18.5 \pm 4.6$  % aggregates smaller than 250  $\mu\text{m}$  and  $81.5 \pm 4.6$  % macroaggregates (mean  $\pm$  SD; n = 10), was separated into a macroaggregate fraction (250–4000  $\mu\text{m}$ ) and a microaggregate fraction (< 250  $\mu\text{m}$ ) by dry sieving. The threshold of 250  $\mu\text{m}$  between macroaggregates and microaggregates was chosen based on Tisdall and Oades (1982). Soil aggregate fractions were then used to re-compose model soils. In order to preserve soil structure, the remaining aggregate size fractions were complemented with an inert matrix replacing the removed aggregate size fraction of the original soil. Model Soil 1 (LA) was composed of soil macroaggregates mixed in a 1:1 (w/w) ratio with glass beads of 150–250  $\mu\text{m}$  size serving as inert matrix material replacing the microaggregates of the original soil. Similarly, Model Soil 2 (SA) was composed of soil microaggregates mixed at the same ratio with fine quartz gravel of 2000–3200  $\mu\text{m}$  size. To generate an even mixture of original soil aggregates and the respective inert matrix a Turbula mixer (Willy A. Bachofen AG, Muttenz, Switzerland) was used. The proportions of the aggregate size fractions in the model soils were different from the original soil, and 50% microaggregates may be more than what is found in most natural or agricultural soils (often less than 10 %). Nevertheless, we chose to use equal amounts of micro- and macroaggregates, in order to be able to separate the effects of aggregate size from effects of aggregate amount (soil mass). These proportions were still

well in the range of common top soils (e.g., Cantón et al., 2009; Gajić et al., 2010; Six et al., 2000). The physicochemical properties of the two soils were determined by analysing three random samples of each model soil. Texture of the complete model soils was determined using the pipette method (Gee and Bauder, 1986) and pH was measured potentiometrically in a stirred slurry of 10 g soil in 20 ml of 0.01 M CaCl<sub>2</sub>, as recommended in Hendershot et al. (2007). Additionally organic carbon (C<sub>org</sub>) and total nitrogen (TN) were analysed in both aggregate size fractions without the inert material, using the method described by Walthert et al. (2010). The two model soils displayed very similar physicochemical properties (Table 2.1), except for the C:N ratio that was lower in macroaggregates than in microaggregates. The latter was due to the slightly lower organic carbon content in concert with slightly higher TN values in the macroaggregates. The high calcium carbonate (CaCO<sub>3</sub>) content of the source material of our model soils ( $390 \pm 3$  g CaCO<sub>3</sub> kg<sup>-1</sup>; Samaritani et al., 2011) buffered the systems at an alkaline pH of  $8.00 \pm 0.02$  for LA and  $7.56 \pm 0.01$  for SA respectively (Table 2.1), ensuring that the activity of key N-transforming enzymes was not hampered by too low pH, and that the potential for simultaneous production and consumption of N<sub>2</sub>O in our experiment was fully intact (Blum et al., 2018; Frame et al., 2017).

**Table 2.1:** Physicochemical properties of the two aggregate size fractions (macroaggregates and microaggregates) and added leaf litter. C<sub>org</sub> and TN of the aggregates were measured in triplicates. The leaf litter was analyzed in quadruplicates. Final pH and texture of model soil 1 and 2 were measured in duplicates (means  $\pm$  SD). Significant differences in the t-tests ( $P < 0.05$ ) are highlighted in bold.

		Macroaggregates	Microaggregates	Macroaggregates vs. Microaggregates	Litter ( <i>Salix v. L.</i> )
C <sub>org</sub>	g kg <sup>-1</sup>	19.22 $\pm$ 0.55	21.56 $\pm$ 2.39	P = 0.229	459.9 $\pm$ 2.55
Total N	g kg <sup>-1</sup>	1.58 $\pm$ 0.02	1.35 $\pm$ 0.14	P = 0.106	27.39 $\pm$ 0.15
C:N ratio		12.16 $\pm$ 0.22	15.99 $\pm$ 0.71	<b>P = 0.007</b>	16.79 $\pm$ 0.06
		Model soil 1	Model soil 2	Model soil 1 vs. Model soil 2	
pH (CaCl <sub>2</sub> )		8 $\pm$ 0.02	7.56 $\pm$ 0.01	<b>P = 0.009</b>	
sand	%	71.25 $\pm$ 0.05	70.7 $\pm$ 0.50	P = 0.469	
silt	%	20 $\pm$ 0.30	21.1 $\pm$ 0.60	P = 0.285	
clay	%	8.75 $\pm$ 0.25	8.2 $\pm$ 0.10	P = 0.240	

### 2.2.2 Mesocosms

For the mesocosm experiments, transparent polyvinyl chloride (PVC) cylinders with polymethyl methacrylate (PMMA) couplings were used. A mesocosm comprised a bottom column section, containing the soil material and a drainage layer as described below, and the upper headspace section with a detachable headspace chamber (Fig. 2.1). Each column section was equipped with two suction cups (Rhizon MOM Soil Moisture Samplers, Rhizosphere Research Products, Netherlands; pore size  $0.15\ \mu\text{m}$ ) for soil solution sampling. The suction cups were horizontally inserted at 5 cm and 20 cm below soil surface. For redox potential measurements, two custom-made Pt electrodes (tip with diameter of 1 mm and contact length of 5 mm) were placed horizontally at a  $90^\circ$  angle to the suction cups at the same depths, with the sensor tip being located 5 cm from the column wall. A Ag/AgCl reference electrode (B 2820, SI Analytics, Germany) was installed as shown in Fig. 2.1. A volumetric water content (VWC) sensor (EC-5, Decagon, USA) was installed 15 cm below the soil surface. To avoid undesired waterlogging, each column section contained a 5 cm thick drainage layer composed of quartz sand with the grain size decreasing with depth from 1 mm to 5.6 mm (Fig. 2.1). The upper cylinder section was equipped with three way valves for gas sampling, and an additional vent for pressure compensation.

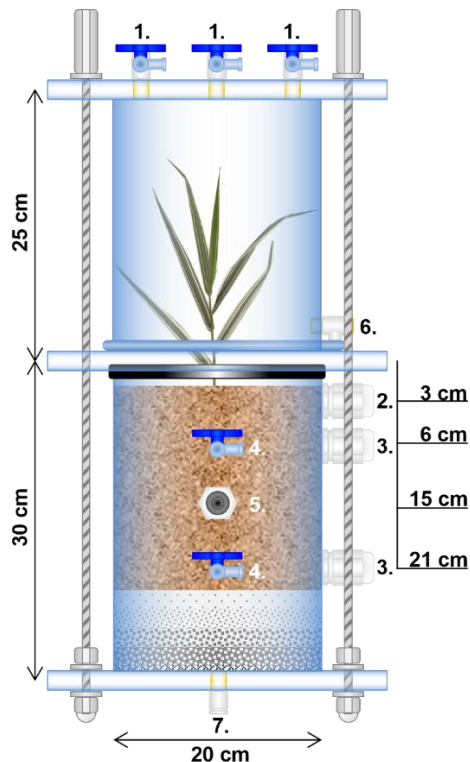


**Figure 2.1.** Schematic of a mesocosm with gas sampling valves (1), Ag/AgCl reference electrode (2), Pt redox electrodes (3), suction cups (4), volumetric water content sensors (5), vent (6), and water inlet/outlet (7). The top part is only attached during gas sampling.



### 2.2.3 Experimental setup

The mesocosm experiment had a factorial experimental design consisting of two factors (MODEL SOIL and TREATMENT), with the first factor containing two levels (macroaggregates, microaggregates) and the second factor containing three levels (unamended, litter added, plant presence). This experimental design resulted in six treatments, each replicated six times (Table 2.2). As basic material, each mesocosm contained 8.5 kg of either of the two model soils. Unamended model soils were used to investigate exclusively the effect of aggregate size, abbreviated as LAU (large aggregates, unamended) and SAU (small aggregates, unamended), respectively. In order to specifically assess the effect of enhanced availability of labile C in the detritosphere for the N<sub>2</sub>O producing or consuming soil microbial community, two sets of mesocosms were amended with freshly collected leaves of Basket Willow (*Salix viminalis* L.). Those leaves were cut into small pieces, autoclaved, and then added to the model soil components (8 g kg<sup>-1</sup> model soil) during the mixing procedure to create treatments LAL (large aggregates, litter) and SAL (small aggregates, litter), respectively. The sterilization step was included to create equal starting conditions in all litter treatments by reducing any potential effect of, and interaction with, the phyllosphere microbial community even though a direct involvement of the phyllosphere community in N<sub>2</sub>O production was unlikely according to the literature (Bringel and Couée, 2015). A third set of mesocosms was planted with cuttings collected from the same *Salix viminalis* creating treatments LAP (large aggregates, plant) and SAP (small aggregates, plant), respectively to evaluate the effects of root–soil interactions in the respective model soils. For each mesocosm one cutting was inserted 10 cm into the soil, protruding from the surface about 3 cm.

The addition of leaf litter to the model soils led to an increase of C<sub>org</sub> and TN in LAL relative to LAU by 41 % and 35 %, respectively, and in SAL relative to SAU by 58 % and 44 % respectively. The bulk density of the unamended model soil SAU (1.27 ± 0.01 g cm<sup>-3</sup>) was slightly higher than the one of LAU (1.22 ± 0.01 g cm<sup>-3</sup>; adj. *P*: < 0.0001). Regarding the litter addition treatments, the bulk density of LAL (1.13 ± 0.01 g cm<sup>-3</sup>) was significantly smaller than the one of LAU (adj. *P*: < 0.0001), whereas the bulk density of SAL (1.27 ± 0.02 g cm<sup>-3</sup>) did not differ significantly from the one of SAU. The soils in the treatments with plants exhibited a similar bulk density (LAP: 1.23 ± 0.02 g cm<sup>-3</sup>; SAP: 1.24 ± 0.01 g cm<sup>-3</sup>) as in the respective unamended treatments.

**Table 2.2:** Overview of treatments in the flooding–drying experiment. Model Soil 1, containing soil macroaggregates is abbreviated LA, whereas Model Soil 2 contains soil microaggregates and is abbreviated SA. The last character of each abbreviation stands for unamended (U), litter addition (L) and plant presence (P). Each treatment was replicated six times.

	LAU	SAU	LAL	SAL	LAP	SAP
Model Soil 1 (LA)	+	-	+	-	+	-
Model Soil 2 (SA)	-	+	-	+	-	+
Leaf litter ( <i>Salix v.</i> )	-	-	+	+	-	-
<i>Salix v.</i>	-	-	-	-	+	+

The experiments were conducted inside a climate chamber set to constant temperature ( $20 \pm 1$  °C) and relative air humidity ( $60 \pm 10\%$ ), with a light/dark cycle of 14/10 h (PAR  $116.2 \pm 13.7$   $\mu\text{mol m}^{-2} \text{s}^{-1}$ ). The experimental period was divided into four consecutive phases: The conditioning phase (Phase 1) lasted for 15 weeks and allowed the model soils to equilibrate and the plants to develop a root system. This was followed by the first experimental phase of nine days (Phase 2), serving as a reference period under steady-state conditions. During Phases 1 and 2, the soils were continuously irrigated with artificial river water ( $\text{Na}^+$ :  $0.43 \mu\text{M}$ ;  $\text{K}^+$ :  $0.06 \mu\text{M}$ ;  $\text{Ca}^{2+}$ :  $1.72 \mu\text{M}$ ;  $\text{Mg}^{2+}$ :  $0.49 \mu\text{M}$ ;  $\text{Cl}^-$ :  $4.04 \mu\text{M}$ ;  $\text{NO}_3^-$ :  $0.16 \mu\text{M}$ ;  $\text{HCO}_3^-$ :  $0.5 \mu\text{M}$ ;  $\text{SO}_4^{2-}$ :  $0.11 \mu\text{M}$ ; pH: 7.92) via suction cups, to maintain a volumetric water content of  $35 \pm 5 \%$ . In Phase 3, the mesocosms were flooded by pumping artificial river water through the drainage vent at the bottom into the cylinder ( $10 \text{ mL min}^{-1}$ , using a peristaltic pump; IPC-N-24, Ismatec, Germany) until the water level was 1 cm above the soil surface. After 48 h of flooding, the water was allowed to drain and the soil to dry for 18 days without further irrigation (Phase 4).

#### 2.2.4 Sampling and analyses

During the entire experiment, water content and redox potential were automatically logged every 5 minutes (EM5b, Decagon, USA and CR1000, Campbell scientific, USA, respectively). At selected time points during the experiment, soil-emitted gas and soil solution were sampled. For  $\text{N}_2\text{O}$  flux measurements, 20, 40 and 60 minutes after closing the mesocosms, headspace gas samples (20 mL) were collected using a syringe and transferred to pre-evacuated exetainers. The samples were analyzed for their  $\text{N}_2\text{O}$  concentration using a gas chromatograph (Agilent 6890, Santa Clara, USA; Porapak Q column, Ar/ $\text{CH}_4$  carrier gas, micro-ECD detector). Measured headspace  $\text{N}_2\text{O}$  concentrations were converted to moles using the ideal gas law and headspace volume. The  $\text{N}_2\text{O}$  efflux rates were calculated as the slope of the linear regression of

the N<sub>2</sub>O amounts at the three sampling times, relative to the exposed soil surface area (Fig. 2.1, Shrestha et al., 2012).

For soil water sampling, 20 mL of soil solution were collected using the suction cups. Water samples were analyzed for dissolved organic carbon (DOC) and TN concentrations with an elemental analyzer (Formacs<sup>HT/TN</sup>, Skalar, The Netherlands). Nitrate and ammonium concentrations were measured by ion chromatography (IC 940, Metrohm, Switzerland), and nitrite (NO<sub>2</sub><sup>-</sup>) concentrations were determined photometrically (DR 3900, Hach Lange, Germany).

### 2.2.5 Data analyses

We were interested in effects on cumulated N<sub>2</sub>O emissions during hot moments following flooding. We therefore analyzed data aggregated over this period rather than the raw full time series data. This procedure also avoided potential issues with small shifts in the timing of emissions that might have been significant but which were irrelevant for the total fluxes we focused on. The total amount of N<sub>2</sub>O emitted during the period of enhanced N<sub>2</sub>O fluxes in Phase 4,  $Q_{tot}$ , was calculated by integrating the N<sub>2</sub>O fluxes between day 11 and 25 of the experiment as follows:

$$Q_{tot} = \frac{1}{2} \sum_{n=1}^{n_{max}} [\Delta_n \times (q_n + q_{n+1})] \quad (1)$$

where  $\Delta_n$  is the time period between the  $n^{\text{th}}$  and the  $n+1^{\text{th}}$  measurement, and  $q_n$  and  $q_{n+1}$  the mean flux on the  $n^{\text{th}}$  and  $n+1^{\text{th}}$  measurement day, respectively. “ $n=1$ ” refers to day 11, and  $n_{max}$  to day 25 of Phase 4. The integrated N<sub>2</sub>O fluxes, as well as the average DOC and N-species concentrations in the soil solution during this period were analyzed by performing two-way ANOVAs with the fixed terms TREATMENT and MODEL SOIL including their interaction. In case of significant MODEL SOIL, TREATMENT or MODEL SOIL  $\times$  TREATMENT effects, their causes were inspected with the Tukey’s honestly significant difference (HSD) post hoc test. For all data, the residuals of the ANOVA models were inspected, and the Shapiro–Wilk normality test was applied to ensure that the values follow a Gaussian distribution. In case that this requirement for ANOVA was not met, the respective data set was log-transformed. Significance and confidence levels were set at  $\alpha < 0.05$ . The results of the performed ANOVAs are summarized in Table 2.3. For the statistical analyses we used GraphPad Prism (GraphPad Software Inc., 2017) and R (R Core Team, 2018).

**Table 2.3:** Results of the two-way analysis of variance (ANOVA) of the integrated fluxes ( $Q_{\text{tot}}$ ) and the mean concentrations of chemical properties in soil solution ( $n=6$ ) during the period of enhanced  $\text{N}_2\text{O}$  emissions (from day 11 to day 25). Shown are  $P$  values with significant differences ( $P < 0.05$ ) highlighted in bold characters.

	$Q_{\text{tot}}$	DOC	$\text{NO}_3^-$	$\text{NO}_2^-$	$\text{NH}_4^+$
TREATMENT	<b>0.0003</b>	<b>0.0133</b>	0.0988	< <b>0.0001</b>	<b>0.0007</b>
MODEL SOIL	<b>0.0002</b>	< <b>0.0001</b>	0.2181	< <b>0.0001</b>	<b>0.0004</b>
TREATMENT $\times$ MODEL SOIL	<b>0.0145</b>	< <b>0.0001</b>	0.0668	0.1174	< <b>0.0001</b>

## 2.3 Results

### 2.3.1 Soil moisture and redox potential

During Phase 1 and 2, saturation levels stabilized at  $53.0 \pm 2.1\%$  WFPS in the treatments with LA soils, and were slightly higher in SA treatments ( $57.8 \pm 2.0\%$ ) (Fig. 2.2). The flooding of the mesocosms for 48 h with artificial river water raised the WFPS for all LA soils to  $87.8 \pm 0.1\%$ , significantly exceeding the increase of WFPS in SA soils ( $80.6 \pm 0.1\%$ ). The water release from the system after the simulated flood resulted in an immediate drop of the WFPS, except for the LAU treatment (Fig. 2.2). This was followed by slow drying for 1 week, and a more marked decrease in WFPS during the second week after the flood. During the latter period, the plant treatments dried faster than the other treatments. As a result, at the end of the experiment, WFPS was still above pre-flood values in unamended and litter treatments, while WFPS levels in the treatments with plants were lower than before the flooding.

The time course of the redox potential measured in 5 cm and 20 cm depth exhibited distinct patterns depending on the respective model soil (Fig. 2.3). In all treatments, flooding induced a rapid decrease of the redox potential to values below 250 mV within 36 hours. Upon water release, the redox potential returned rapidly to pre-flood values at both measurement depths only in SA soils. In the LA treatments (most pronounced in LAL), soils at 20 cm depth underwent a prolonged phase of continued reduced redox condition, returning to the initial redox levels only towards the end of the experiment.

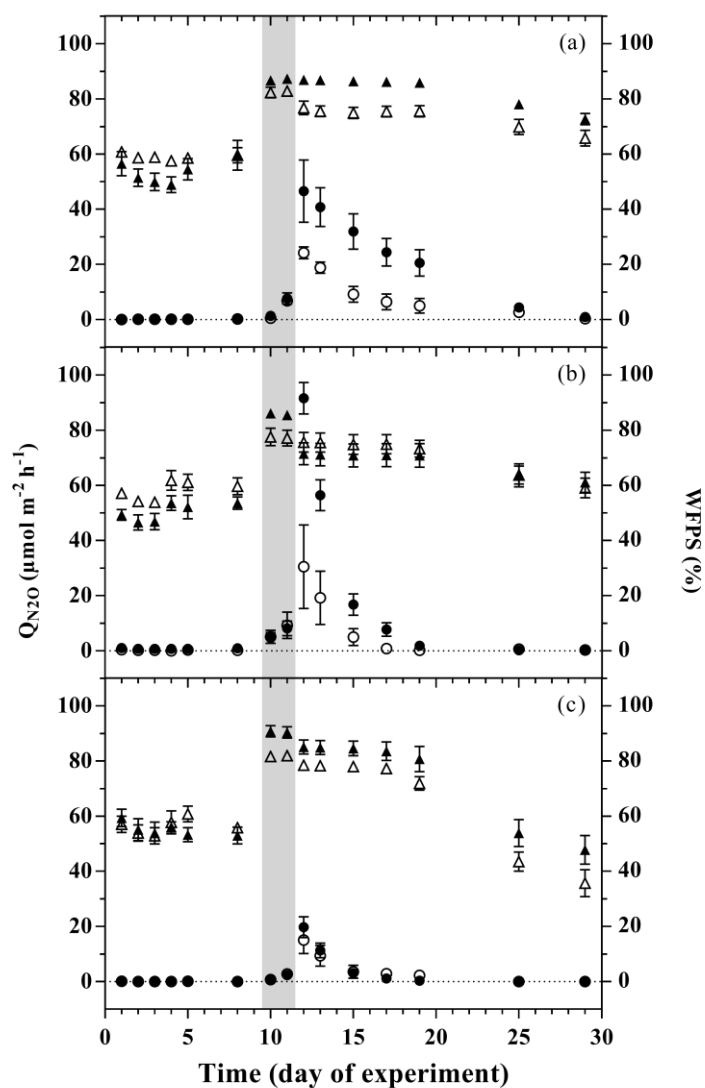


**Figure 2.2.** Mean  $N_2O$  emission during the flooding–drying experiment from large-aggregate model soil (LA; filled circles) and small-aggregate model soil (SA, open circles). The corresponding WFPS in LA (filled triangles) and SA (open triangles) are depicted on the right Y-axis. Unamended soils (A), litter addition (B) and plant treatment (C). Flooding phase indicated by the grey area. Symbols indicate means; error bars are standard error (SE);  $n=6$ .

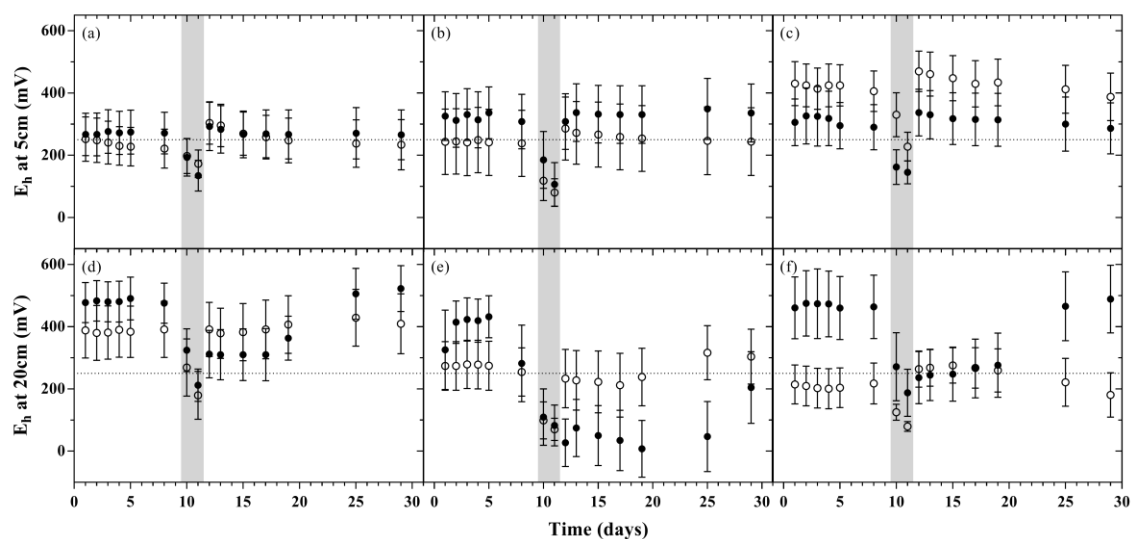


**Figure 2.3.** Redox potential relative to standard hydrogen electrode during the flooding–drying experiment in 5 cm and 20 cm depth (mean  $\pm$  SE;  $n=6$ ). Unamended soils (a and d, respectively), litter addition (b and e, respectively), plant treatment (c and f, respectively). LA (filled circles) and SA (open circles); the dotted line at 250 mV marks the threshold, below which denitrification is expected to occur.

### 2.3.2 Hydrochemistry of soil solutions

Considering individual treatments, DOC concentrations varied only little with time. Yet, the DOC concentrations were generally much higher in treatments with LA than with SA soils. This main effect of MODEL SOIL was highly significant, as was the interaction with TREATMENTS due to a smaller difference in the litter addition treatments than in the unamended and plant treatments (Table 2.3). Nitrate was the most abundant dissolved reactive N species in the soil solution, with pre-flood concentrations of 1 to 5 mM (Fig. 2.4d–f). In the unamended and plant treatments,  $\text{NO}_3^-$  concentrations were markedly higher in SA than in LA soils, whereas they were similar in both litter addition treatments. Two distinct temporal patterns in the evolution of  $\text{NO}_3^-$  concentration could be discerned. In the unamended and litter-addition treatments,  $\text{NO}_3^-$  concentrations decreased after the flooding, consistently reaching a minimum on day 19, in the case of the litter treatments below the detection limit of 0.2  $\mu\text{M}$ , before increasing again during the latter drying phase (Fig. 2.4d,e). In contrast, in the treatments with plants,  $\text{NO}_3^-$  concentrations steadily declined from concentrations of 1–2 mM to around 0.5 mM at the end of the experiment (Fig. 2.4f). Nitrite was found at significant concentrations only in LA soils, with highest concentrations in the LAU treatment right after the flooding (33.6  $\mu\text{M}$ ) and decreasing concentrations throughout the remainder of the experiment (Fig. 2.4g–i). In SA soils  $\text{NO}_2^-$  concentration was always  $< 5 \mu\text{M}$ , without much variation. Similarly, in most treatments

except SAL, ammonium ( $\text{NH}_4^+$ ) concentrations were  $< 10 \mu\text{M}$ , and particularly towards the end of the experiment very close to the detection limit (Fig. 2.4j, 2.4l). In the SAL treatment,  $\text{NH}_4^+$  concentrations peaked 5 days after the flood with concentrations of around  $70 \mu\text{M}$  (Fig. 2.4k). This deviation from the other temporal patterns prompted a significant interaction effect between MODEL SOIL and TREATMENTS.

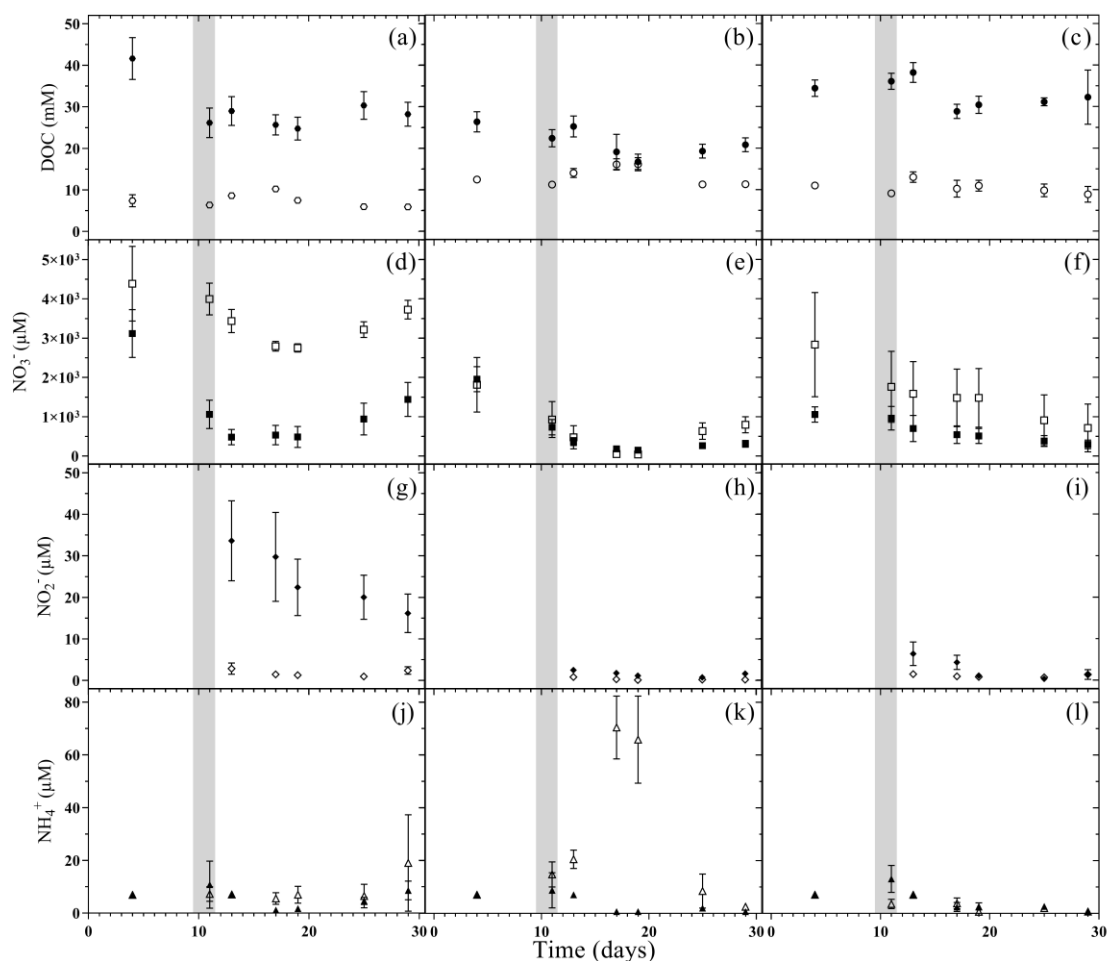


**Figure 2.4.** DOC (circles), nitrate (squares), nitrite (diamonds) and ammonium (triangles) concentrations in pore water during the flooding–drying experiment. LA (filled symbols) and SA (empty symbols). Unamended soils (a, d, g and j, respectively), litter addition (b, e, h and k, respectively) and plant treatment (c, f, j and l, respectively).; (mean  $\pm$  SE;  $n=6$ ).

### 2.3.3 Nitrous oxide emissions

During Phase 2 (i.e., before the flooding),  $\text{N}_2\text{O}$  fluxes were generally low ( $< 1 \mu\text{mol m}^{-2} \text{h}^{-1}$ ; Fig. 2.2), however, fluxes in the LAL treatment were significantly higher than in the other treatments (adj.  $P = 0.002\text{--}0.039$ ; Fig. 2.2). The flooding triggered the onset of a “hot moment”, defined here as period with strongly increased  $\text{N}_2\text{O}$  emissions, which lasted for about one week independent of the treatment (Fig. 2.2). The maximum efflux was observed immediately after

the flood. The subsequent decline in N<sub>2</sub>O emission rates followed different patterns among the various treatments. Normalizing the N<sub>2</sub>O flux to the maximum measured efflux for each replicated treatment revealed a slower decrease with time for the unamended soils than for the litter and plant treatments (Fig. S.2.1). The strongest peak emissions were observed in the LAL treatment ( $91.6 \pm 14.0 \mu\text{mol m}^{-2} \text{h}^{-1}$ ; mean  $\pm$  SD). Throughout most of the drying phase, the LAU and LAL treatments exhibited higher N<sub>2</sub>O emissions than the corresponding SAU and SAL experiments. In contrast, there was no such difference in the treatments with plant cuttings, and peak N<sub>2</sub>O emissions were overall lower than in the other treatments. The integrated N<sub>2</sub>O fluxes during the hot moment (days 11 to 25 of the experiment) were significantly higher for the LAU and LAL than for all other treatments (Fig. 2.5), and the aggregate size effect was also significant within the unamended (adj. P = 0.045) and litter-addition treatments (adj. P = 0.008). The integrated N<sub>2</sub>O emissions in the two plant treatments did not differ significantly from each other, but were significantly smaller than in the LAU (adj. P = 0.001), and the LAL (adj. P = 0.005) treatments. Overall, the effects of MODEL SOIL and TREATMENTS were significant, as was the interaction between the two factors due to the different aggregate size effect in the plant compared to the unamended and litter addition treatments (Table 2.3).

## 2.4 Discussion

In our experiment, we could confirm the occurrence of periods of enhanced N<sub>2</sub>O emissions in the drying phase shortly after flooding, as expected based on previous research (Baldwin and Mitchell, 2000; Groffman and Tiedje, 1988; Rabot et al., 2014; Shrestha et al., 2012). We observed that the six treatments had a substantial effect on the magnitude and temporal pattern of N<sub>2</sub>O emissions that could only be captured by observations at relatively high temporal resolution. The fast occurrence of strong N<sub>2</sub>O fluxes over a comparatively short period in the litter-amended treatment on the one side, and the relatively weak response to the flooding in the plant treatment on the other, suggests complex interactive mechanisms related to distinct microhabitat effects leading to characteristic periods of enhanced N<sub>2</sub>O emission. Rabot et al. (2014) explained N<sub>2</sub>O emission peaks during the desaturation phase with the release of previously produced and entrapped N<sub>2</sub>O. Such a mechanism may partly contribute to high N<sub>2</sub>O emissions in our experiment initially, but the continuing depletion of NO<sub>3</sub><sup>-</sup> and NO<sub>2</sub><sup>-</sup> during the phase of high N<sub>2</sub>O emissions indicates that the flooding and drying has strong effects on N transformations mediated by microorganisms in the soil (e.g., the balance and overall rates of nitrification, nitrifier–denitrification, and denitrification). Hence, physical controls alone clearly do not explain the observed timing and extent of hot moments with regard to N<sub>2</sub>O



emission. In the following sections we will discuss how the effect of flooding on microbial N<sub>2</sub>O production is modulated by differential microhabitat formation (and hence redox conditions) in the various treatments.

#### 2.4.1 Effect of aggregate size on N<sub>2</sub>O emissions

LA model soils exhibited both higher peak and total N<sub>2</sub>O emissions during the hot moment in the drying phase than SA model soils (Figs. 2 and 5). By contrast, in the presence of a growing willow, there was no detectable effect of aggregate size on the overall N<sub>2</sub>O emission (further discussion below). The aggregate size effects observed in the unamended and litter treatments can be explained by factors controlling (i) gas diffusion (e.g., water film distribution, tortuosity of the intra-aggregate pore space) and (ii) decomposition of encapsulated soil organic matter (SOM) regulating the extent of N<sub>2</sub>O formation (Neira et al., 2015). In order to isolate the effect of aggregate size (i.e., to minimize the effect of other factors that are likely to influence gas diffusion), we created model soils of similar soil structure and texture (see Materials and Methods). We thereby implicitly accepted that potential interactions of the two size fractions with each other, or with soil structures larger than 4 mm could not be assessed in this experiment. Although this approach thus represents only an approximation of real-world conditions it was still an improvement compared to experiments where no attempts were made to conserve soil structure. Similarly, the bulk soil chemical properties of the two aggregate size fractions, such as C<sub>org</sub> content and TN, are essentially the same. Differences in the initial C:N ratio and pH, although statistically significant, can be considered equivalent in the ecological context, e.g., in terms of organic matter degradability. Therefore, we assume in the following that the differences in N<sub>2</sub>O emissions among the treatments can mainly be attributed to size-related aggregate properties and their interactions with litter addition or rhizosphere effects.

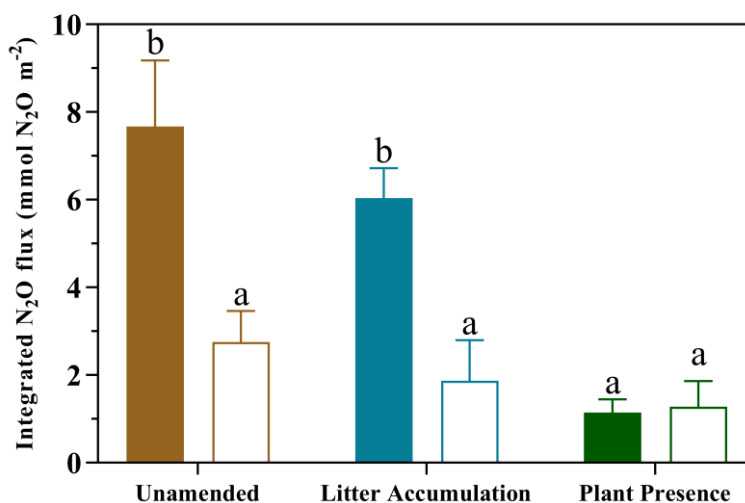


**Figure 2.5.** Integrated N<sub>2</sub>O fluxes over the 14 days period of elevated N<sub>2</sub>O emissions in the drying phase of the flooding–drying experiment (mean ± SE; n= 6). Black bars represent Model Soil 1 (macroaggregates 250–4000µm) whereas Model Soil 2 (microaggregates < 250µm) is depicted as white bars. Significant differences among the six treatments are denoted by different lower case letters at adj. P < 0.05.

During Phase 3 with near-saturated conditions, no aggregate size effect was observed. High WFPS seem to have limited the gas diffusion (O<sub>2</sub> and N<sub>2</sub>O) independent of the aggregate size, limiting soil–atmosphere gas exchange in both model soils equally (Neira et al., 2015; Thorbjørn et al., 2008). As a consequence of inhibited gas exchange/soil aeration, a sharp drop in the redox potential was observed in all treatments, indicating a rapid decline in O<sub>2</sub> availability to suboxic/anoxic conditions. Together with an incipient decrease in soil solution NO<sub>3</sub><sup>-</sup>, this indicates that N<sub>2</sub>O production is primarily driven by denitrification in this phase.

The aggregate size effects on the formation of moments of enhanced N<sub>2</sub>O emission became evident during the subsequent drying period. During the initial drying phase, when a heterogeneous distribution of water films around soil particles/aggregates develops (Young and Ritz, 2000), the macroaggregates in the LA model soils appear to foster micro-environmental conditions that are more beneficial to N<sub>2</sub>O production. This could be related to the longer diffusive distances for re-entering O<sub>2</sub> caused by the higher tortuosity of the intra-aggregate pore space of macroaggregates, as reported by Ebrahimi and Or (2016). This may have helped to maintain, or even extend, reducing conditions due to microbial activity inside the core of macroaggregates during drying. Thus, on the one hand, large aggregates favor the emergence of anoxic microhabitats expanding the zones where denitrification occurs. On the other hand, the overall higher porosity of the LA soils supports a better aeration in drained parts of the soil

---

(Sey et al., 2008), and aerobic processes (e.g., nitrification) are supported. As a result, ideal conditions for spatially coupled nitrification–denitrification are created (Baldwin and Mitchell, 2000; Koschorreck and Darwich, 1998). Indeed, the emergence of heterogeneously distributed, spatially confined oxygen minimum zones during soil drying may be reflected by the high variability of the redox conditions observed in replicate mesocosms and, on average, the tendency towards lower redox potentials for a prolonged period of time in the subsoils of the LA model soils (Fig. 2.3d–f). In this context, the relevance of water films for the emergence of periods of enhanced N<sub>2</sub>O emissions is further highlighted by the fact that elevated flux rates were only observed as long as the WFPS was above 65%. This is consistent with work by Rabot et al. (2014) and Balaine et al. (2013), who found similar soil water saturation thresholds for elevated N<sub>2</sub>O emissions from soils, attributing this phenomenon to suboptimal environmental conditions for both nitrification and denitrification at lower saturation levels.

Given the arguments above, we assume that N<sub>2</sub>O emissions during the drying phase originate to a large degree from heterotrophic denitrification, and that they are governed mainly by the aggregate-size dependent redox conditions within the semi-saturated soils. This conclusion stands in good agreement with findings from Drury et al. (2004), who found higher production of N<sub>2</sub>O due to enhanced denitrification with increasing size of intact arable soil aggregates in a laboratory incubation study. In contrast, the much lower emissions from the SA treatments can best be explained by a rapid return to pre-flood, i.e. oxic redox conditions in most of the pore space, under which N<sub>2</sub>O production driven by denitrification is inhibited. Enhanced reduction of N<sub>2</sub>O to N<sub>2</sub> in the SA versus LA treatments seems less likely as an explanation for lowered net N<sub>2</sub>O emission rates, since the relatively high redox potential represents an impediment to complete denitrification to N<sub>2</sub>. Furthermore, according to Manucharova et al. (2001) and Renault and Stengel (1994), aggregates smaller than 200 μm are simply not large (and reactive) enough (i.e., molecular diffusive distances for oxygen are too short) to develop suboxic or anoxic conditions in the center, let alone denitrifying zones. Hence, only a relatively small fraction of the total number of microaggregates in the SA soils would have been large enough (between 200 and 250 μm) to host denitrification and act as site of anaerobic N<sub>2</sub>O production. Under natural conditions, frequent hydrological disturbance in floodplains creates a highly dynamic and small-scaled mosaic of different aggregate size distributions. In this regard, our results, demonstrating the effect aggregate size has on N<sub>2</sub>O emissions, may help to understand the seemingly erratic spatial and temporal distribution of enhanced N<sub>2</sub>O emissions from floodplain areas. Moreover they imply that zones with a relatively high percentage of macroaggregates would be particularly prone to high emissions of N<sub>2</sub>O after a flood event.

### 2.4.2 Litter effect on N<sub>2</sub>O emissions

We expected that litter addition would increase N<sub>2</sub>O emissions from model soils with both small and large aggregates, as was found earlier (e.g., Loecke and Robertson, 2009; Parkin, 1987). The addition of litter to the model soils changed the temporal dynamics of the N<sub>2</sub>O emission substantially, but its effect on the net integrated N<sub>2</sub>O emission was rather minor (Fig. 2.5). More precisely, highest peak emission rates of all treatments were observed in the LAL treatment, but peak emission rates were followed by a faster return to low pre-flood emission rates in the LAL and the SAL treatments relative to the unamended treatments (Fig 2). This confirms that surplus organic carbon can, on short-term, boost N<sub>2</sub>O emissions, particularly in the large-aggregate treatment. The fast mid-term return to low N<sub>2</sub>O emission suggests that N<sub>2</sub>O production by heterotrophic denitrification either becomes limited by substrates other than carbon, and/or that the carbon added to the soils affects the redox-biogeochemistry in a way that shifts the balance between N<sub>2</sub>O production and consumption in favor of consumption. Loecke and Robertson (2009) reported similar temporal N<sub>2</sub>O emission patterns in field experiments with litter-amended soil, and attributed the observed dynamic of a rapid decline after peak emission to an increased demand for terminal electron acceptors during denitrification shortly after the carbon addition. Nitrate/nitrite limitation leads, under stable anoxic conditions, ultimately to the complete reduction of produced N<sub>2</sub>O to N<sub>2</sub> decreasing net N<sub>2</sub>O emission. Indeed, the rapid decrease in N<sub>2</sub>O emissions after the emission rate peak in the litter addition treatments was accompanied by the complete depletion of NO<sub>3</sub><sup>-</sup> in the soil solution at low redox potential, suggesting nitrate limitation. The increased demand for electron acceptors can be attributed to the increased availability of labile C compounds and nutrients provided by the mineralization of litter, and the concomitant stimulation of aggregate-associated microbial communities during the flooding (Li et al., 2016). At the same time, the litter-stimulated soil respiration increases the soil's oxygen demand, maintaining stable low redox conditions for a longer period of time during the drying phase. Since high activity of N<sub>2</sub>O reductase requires very low O<sub>2</sub> concentrations (Morley et al., 2008), such conditions may be particularly favorable for complete denitrification to N<sub>2</sub>, an additional, or alternative, explanation for the low N<sub>2</sub>O emission rates shortly after the N<sub>2</sub>O emission peak.

### 2.4.3 Effects of *Salix viminalis*

Planted willow cuttings resulted in relatively low maximum N<sub>2</sub>O emission rates (LAP: 19.75 ± 9.31 μmol m<sup>-2</sup> h<sup>-1</sup>; SAP: 15.07 ± 12.07 μmol m<sup>-2</sup> h<sup>-1</sup>; mean ± SD), independent of aggregate size. The high values for WFPS throughout the hot moment, and a low redox potential in the subsoil, imply optimal conditions for denitrification or nitrifier denitrification, but compared to

---

unamended and litter-addition treatments, only little N<sub>2</sub>O was emitted (both during peak N<sub>2</sub>O emission rates and with regards to the integrated N<sub>2</sub>O flux). *S. viminalis* suppressed peak N<sub>2</sub>O emissions, overriding the positive effect of large aggregates on N<sub>2</sub>O emissions observed otherwise. The specific mechanisms involved are uncertain. Fender et al. (2013) found in laboratory experiments with soil from a temperate broad-leaved forest planted with ash saplings (*Fraxinus excelsior* L.) N<sub>2</sub>O fluxes and plant effects very similar to the ones observed in our study. They attributed reduced N<sub>2</sub>O emissions in presence of ash partly to plant uptake of nutrients that reduced NO<sub>3</sub><sup>-</sup> availability to denitrifiers. Fast-growing plant species like *Salix* are particularly effective in removing soil inorganic N (Kowalik and Randerson, 1994). Such a causal link between reduced N<sub>2</sub>O emissions and plant growth is, however, not supported by our data. More precisely, the NO<sub>3</sub><sup>-</sup> concentrations during the hot moment of N<sub>2</sub>O emissions were always relatively high (> 0.5 mM) and above the levels observed in the litter treatments.

An alternative explanation for the reduced N<sub>2</sub>O emissions in the plant treatments could be rhizosphere aeration by aerenchyma, a physiological trait of *Salix viminalis* roots, which prevents the formation of anoxia in their close vicinity (Blom et al., 1990; Randerson et al., 2011), and thus inhibits anaerobic N<sub>2</sub>O production. Indeed, redox potentials in the topsoil were higher in SAP and LAP compared to the other treatments. By contrast, the redox potential in the saturated subsoil below was even lower than observed for the unamended soils. This indicates that the aeration effect by aerenchyma is constrained to the upper soil, or is, in the deeper soil portions, compensated by respiratory rhizosphere processes. On the other hand, aerenchyma can also aid in the gas exchange between the soil and the atmosphere, leading to an accelerated transport of N<sub>2</sub>O by bypassing the soil matrix. This phenomenon is well documented for various grasses such as *Oryza* (Baruah et al., 2010), *Triticum* (Smart and Bloom, 2001) or *Phalaris arundinacea* (Jørgensen et al., 2012). However, we are not aware of any reports on enhanced N<sub>2</sub>O emissions via aerenchyma by willows (*Salix* sp.), and indeed, our results do not indicate any increased N<sub>2</sub>O emission via plants. In fact, we observed the lowest ecosystem flux rates and lowest total integrated N<sub>2</sub>O emissions in the mesocosms with *S. viminalis*.

According to Fender et al. (2013), in vegetated soils, microbial respiration is stimulated by deposition of root exudates, which in concert with root respiration in a highly saturated pore space, leads to severe and ongoing oxygen depletion. Under such stable anoxic conditions complete denitrification would take place generating N<sub>2</sub> and not N<sub>2</sub>O as the dominant final product and therefore N<sub>2</sub>O emissions would be low.

While oxygen depletion by root-exudation-stimulated microbial respiration likely occurs in the

rhizosphere of any plant, rhizosphere aeration is restricted to plants possessing aerenchyma. However, the latter is a characteristic of many plants adapted to temporary flooding, and has been described also for *Poaceae*, or for ash. Furthermore, it is reasonable to expect this trait to be found in other *Salicaceae* like *Populus sp.* and other species of softwood floodplain forests. In areas with monospecific stands of, for example *Salix sp.*, which are often found on restored river banks, this N<sub>2</sub>O-emission reducing trait can be a welcome side effect.

## 2.5 Conclusion

In this study, we investigated the distinct effects of aggregate size, surplus organic carbon from litter and vegetation on N<sub>2</sub>O emission from model soils after flooding. Flooding and drying were always associated with hot moments of N<sub>2</sub>O production, most likely due to heterotrophic denitrification as result of suboxic O<sub>2</sub> levels at high WFPS. Our results demonstrate that aggregate size is a very important factor in modulating N<sub>2</sub>O emission from soils under changing pore space water saturation. Aggregates of a diameter > 250 µm appear to foster suboxic microhabitats that favor denitrification and associated N<sub>2</sub>O emission. This soil aggregate size effect may be amplified in the presence of excess carbon substrate, as long as heterotrophic denitrification, as the main N<sub>2</sub>O producing process, is not electron-acceptor limited, and extremely reducing conditions in organic rich soils do not promote complete denitrification leading to further reduction of N<sub>2</sub>O to N<sub>2</sub>. On the other hand, the higher porosity of the soils with macroaggregates may aid in the formation of microsites at the surface of aggregates where nitrification is re-initialized during drying, supporting favorable conditions for spatially coupled nitrification–denitrification. The mechanisms by which processes in the rhizosphere of *Salix viminalis* effectively suppress N<sub>2</sub>O emissions, and thus mask any aggregate size effect, remain ambiguous. Distinct physiological features of *Salix viminalis*, its root metabolism, in combination with microbial respiration can lead to the simultaneous aeration of some parts of the rhizosphere, and the formation of strongly reducing zones in others. In both cases, redox conditions seem to be impedimental for extensive net N<sub>2</sub>O production.

Our results demonstrate the importance and complexity of the interplay between soil aggregate size, labile organic C availability, respiratory processes in the rhizosphere, and plant-induced aeration of soils under changing soil water content. Those interactions emerged as modulators of N<sub>2</sub>O emissions by controlling the O<sub>2</sub> distribution in the soil matrix. Indeed, O<sub>2</sub> appears as the unifying master variable that ultimately sets the boundary conditions for N<sub>2</sub>O production and/or consumption.

The main scope of this work was to expand our knowledge on the controls on net N<sub>2</sub>O emissions from floodplain soils. The systematic relationships observed in this study are likely to help anticipating where and when hotspots and hot moments of N<sub>2</sub>O emissions are most likely to occur in hydrologically dynamic soil systems like floodplain soils. Further understanding of the complex interaction between plants and soil microorganisms, the detritosphere, and soil aggregation, as well as their influence on N turnover and N<sub>2</sub>O accumulation in soils, should focus on how the parameters tested affect the actual activity of the nitrifying and denitrifying communities, with an in-depth investigation into the biogeochemical pathways involved.

*Data availability.* Data will be openly available at <https://datadryad.org/>

*Competing interests.* The authors declare that they have no conflict of interest.

*Authors contributions.* The initial concept of the experiment was developed by JL, MFL and PAN. ML planned the experiment in detail, set it up and performed it. PAN supervised the measurement of N<sub>2</sub>O gas concentrations, whereas ML conducted all other measurements and data analyses. ML wrote the manuscript with major contributions by JL, MFL and PAN.

## **Acknowledgements**

The authors thank the Department of Evolutionary Biology and Environmental Studies of the University of Zurich and René Husi for performing the GC measurements. We are also very grateful to the Environmental Geoscience research group in the Department of Environmental Sciences of the University of Basel and Judith Kobler–Waldis for helping us with the IC measurements. We thank the Central Laboratory and Daniel Christen, Roger Köchli and Nouredine Hajjar of the Swiss Federal Institute for Forest, Snow and Landscape Research (WSL) for assistance with chemical analyses. This study was funded by the Swiss National Science Foundation (SNSF) under the grant number 200021\_147002 as well as by financial resources of WSL and the University of Basel.

---

## References

- Baggs, E. M.: A review of stable isotope techniques for N<sub>2</sub>O source partitioning in soils: recent progress, remaining challenges and future considerations, *Rapid Commun. Mass Spectrom.*, 22(11), 1664–1672, doi:10.1002/rcm.3456, 2008.
- Baggs, E. M.: Soil microbial sources of nitrous oxide: Recent advances in knowledge, emerging challenges and future direction, *Curr. Opin. Environ. Sustain.*, 3(5), 321–327, doi:10.1016/j.cosust.2011.08.011, 2011.
- Balaine, N., Clough, T. J., Beare, M. H., Thomas, S. M., Meenken, E. D. and Ross, J. G.: Changes in Relative Gas Diffusivity Explain Soil Nitrous Oxide Flux Dynamics, *Soil Sci. Soc. Am. J.*, 77(5), 1496–1505, doi:10.2136/sssaj2013.04.0141, 2013.
- Baldwin, D. S. and Mitchell, A. M.: The effects of drying and re-flooding on the sediment and soil nutrient dynamics of lowland river–floodplain systems: a synthesis, *Regul. Rivers Res. Manag.*, 16(5), 457–467, doi:10.1002/1099-1646(200009/10)16:5<457::AID-RRR597>3.3.CO;2-2, 2000.
- Ball, B. C.: Soil structure and greenhouse gas emissions: A synthesis of 20 years of experimentation, *Eur. J. Soil Sci.*, 64(3), 357–373, doi:10.1111/ejss.12013, 2013.
- Baruah, K. K., Gogoi, B., Gogoi, P. and Gupta, P. K.: N<sub>2</sub>O emission in relation to plant and soil properties and yield of rice varieties, *Agron. Sustain. Dev.*, 30(4), 733–742, doi:10.1051/agro/2010021, 2010.
- Bateman, E. J. and Baggs, E. M.: Contributions of nitrification and denitrification to N<sub>2</sub>O emissions from soils at different water-filled pore space, *Biol. Fertil. Soils*, 41(6), 379–388, doi:10.1007/s00374-005-0858-3, 2005.
- Beare, M. H., Gregorich, E. G. and St-Georges, P.: Compaction effects on CO<sub>2</sub> and N<sub>2</sub>O production during drying and rewetting of soil, *Soil Biol. Biochem.*, 41(3), 611–621, doi:10.1016/j.soilbio.2008.12.024, 2009.
- Bender, S. F., Plantenga, F., Neftel, A., Jocher, M., Oberholzer, H.-R., Köhl, L., Giles, M., Daniell, T. J. and van der Heijden, M. G.: Symbiotic relationships between soil fungi and plants reduce N<sub>2</sub>O emissions from soil, *ISME J.*, 8(6), 1336–1345, doi:10.1038/ismej.2013.224, 2014.
- Blom, C. W. P. M., Bögemann, G. M., Laan, P., van der Sman, A. J. M., van de Steeg, H. M. and Voeselek, L. A. C. J.: Adaptations to flooding in plants from river areas, *Aquat. Bot.*, 38(1), 29–47, doi:10.1016/0304-3770(90)90097-5, 1990.
- Blum, J. M., Su, Q., Ma, Y., Valverde-Pérez, B., Domingo-Félez, C., Jensen, M. M. and Smets, B. F.: The pH dependency of N-converting enzymatic processes, pathways and microbes: Effect on net N<sub>2</sub>O production, *Environ. Microbiol.*, doi:10.1111/1462-2920.14063, 2018.
- Böttcher, J., Weymann, D., Well, R., Von Der Heide, C., Schwen, A., Flessa, H. and Duijnsveld, W. H. M.: Emission of groundwater-derived nitrous oxide into the atmosphere: model simulations based on a <sup>15</sup>N field experiment, *Eur. J. Soil Sci.*, 62(2), 216–225, doi:10.1111/j.1365-2389.2010.01311.x, 2011.
- Bringel, F. and Couée, I.: Pivotal roles of phyllosphere microorganisms at the interface between plant functioning and atmospheric trace gas dynamics., *Front. Microbiol.*, 6(MAY), 486, doi:10.3389/fmicb.2015.00486, 2015.
- Butterbach-Bahl, K., Baggs, E. M., Dannenmann, M., Kiese, R. and Zechmeister-Boltenstern, S.: Nitrous oxide emissions from soils: how well do we understand the processes and their controls?, *Philos. Trans. R. Soc. Lond. B. Biol. Sci.*, 368(1621), 20130122, doi:10.1098/rstb.2013.0122, 2013.
- Cantón, Y., Solé-Benet, A., Asensio, C., Chamizo, S. and Puigdefábregas, J.: Aggregate stability in range sandy
-



- loam soils Relationships with runoff and erosion, *CATENA*, 77(3), 192–199, doi:10.1016/j.catena.2008.12.011, 2009.
- Ciais, P., Sabine, C., Bala, G., Bopp, L., Brovkin, V., Canadell, J., Chhabra, A., DeFries, R., Galloway, J., Heimann, M., Jones, C., Quéré, C. Le, Myneni, R. B., Piao, S. and Thornton, P.: Carbon and Other Biogeochemical Cycles, in *Climate Change 2013 - The Physical Science Basis*, edited by Intergovernmental Panel on Climate Change, pp. 465–570, Cambridge University Press, Cambridge, 2013.
- Diba, F., Shimizu, M. and Hatano, R.: Effects of soil aggregate size, moisture content and fertilizer management on nitrous oxide production in a volcanic ash soil, *Soil Sci. Plant Nutr.*, 57(5), 733–747, doi:10.1080/00380768.2011.604767, 2011.
- Drury, C. ., Yang, X. ., Reynolds, W. . and Tan, C. .: Influence of crop rotation and aggregate size on carbon dioxide production and denitrification, *Soil Tillage Res.*, 79(1), 87–100, doi:10.1016/j.still.2004.03.020, 2004.
- Ebrahimi, A. and Or, D.: Microbial community dynamics in soil aggregates shape biogeochemical gas fluxes from soil profiles – upscaling an aggregate biophysical model, *Glob. Chang. Biol.*, 22(9), 3141–3156, doi:10.1111/gcb.13345, 2016.
- Elliott, A. E. T. and Coleman, D. C.: Let the soil work for us, *Ecol. Bull.*, (39), 22–32, 1988.
- Fender, A.-C., Leuschner, C., Schützenmeister, K., Gansert, D. and Jungkunst, H. F.: Rhizosphere effects of tree species – Large reduction of N<sub>2</sub>O emission by saplings of ash, but not of beech, in temperate forest soil, *Eur. J. Soil Biol.*, 54, 7–15, doi:10.1016/j.ejsobi.2012.10.010, 2013.
- Forster, P., Ramaswamy, V., Artaxo, P., Berntsen, T., Betts, R., Fahey, D. W., Haywood, J., Lean, J., Lowe, D. C., Myhre, G., Nganga, J., Prinn, R., Raga, G., Schulz, M. and Van Dorland, R.: Changes in Atmospheric Constituents and in Radiative Forcing, in *Climate Change 2007: The Physical Science Basis*, edited by S. Solomon, D. Qin, M. Manning, Z. Chen, M. Marquis, K. B. Averyt, M. Tignor, and H. L. Miller, pp. 129–234, Cambridge University Press, Cambridge, United Kingdom and New York, NY, USA, 2007.
- Frame, C. H., Lau, E., Joseph Nolan, E., Goepfert, T. J. and Lehmann, M. F.: Acidification enhances hybrid N<sub>2</sub>O production associated with aquatic ammonia-oxidizing microorganisms, *Front. Microbiol.*, 7(JAN), 1–23, doi:10.3389/fmicb.2016.02104, 2017.
- Gajić, B., Đurović, N. and Dugalić, G.: Composition and stability of soil aggregates in Fluvisols under forest, meadows, and 100 years of conventional tillage, *J. Plant Nutr. Soil Sci.*, 173(4), 502–509, doi:10.1002/jpln.200700368, 2010.
- Gee, G. W. and Bauder, J. W.: Particle-size Analysis, in *Physical and Mineralogical Methods-Agronomy Monograph no. 9*, edited by A. Klute, pp. 383–411, American Society of Agronomy-Soil Science Society of America, Madison, WI., 1986.
- Goldberg, S. D., Knorr, K. H., Blodau, C., Lischeid, G. and Gebauer, G.: Impact of altering the water table height of an acidic fen on N<sub>2</sub>O and NO fluxes and soil concentrations, *Glob. Chang. Biol.*, 16(1), 220–233, doi:10.1111/j.1365-2486.2009.02015.x, 2010.
- GraphPad Software Inc.: GraphPad Prism 7.04, La Jolla, CA, www.graphpad.com, 2017.
- Groffman, P. M. and Tiedje, J. M.: Denitrification Hysteresis During Wetting and Drying Cycles in Soil, *Soil Sci. Soc. Am. J.*, 52(6), 1626, doi:10.2136/sssaj1988.03615995005200060022x, 1988.

- Hartmann, D. J., Klein Tank, A. M. G., Rusticucci, M., Alexander, L. V, Brönnimann, S., Charabi, Y. A.-R., Dentener, F. J., Dlugokencky, E. J., Easterling, D. R., Kaplan, A., Soden, B. J., Thorne, P. W., Wild, M. and Zhai, P.: Observations: Atmosphere and Surface, in *Climate Change 2013 - The Physical Science Basis*, edited by Intergovernmental Panel on Climate Change, pp. 159–254, Cambridge University Press, Cambridge., 2013.
- Hefting, M., Clément, J.-C., Dowrick, D., Cosandey, A. C., Bernal, S., Cimpian, C., Tatur, A., Burt, T. P. and Pinay, G.: Water table elevation controls on soil nitrogen cycling in riparian wetlands along a European climatic gradient, *Biogeochemistry*, 67(1), 113–134, doi:10.1023/B:BIOG.0000015320.69868.33, 2004.
- Heincke, M. and Kaupenjohann, M.: Effects of soil solution on the dynamics of N<sub>2</sub>O emissions: a review, *Nutr. Cycl. Agroecosystems*, 55(2), 133–157, doi:10.1023/A:1009842011599, 1999.
- Hendershot, W. H., Lalonde, H. and Duquette, M.: Soil Reaction and Exchangeable Acidity, in *Soil Sampling and Methods of Analysis*, edited by M. R. Carter and E. G. Gregorich, pp. 173–178, Crc Press Inc, Boca Raton, FL., 2007.
- Hill, A. R.: Buried organic-rich horizons: their role as nitrogen sources in stream riparian zones, *Biogeochemistry*, 104(1–3), 347–363, doi:10.1007/s10533-010-9507-5, 2011.
- Hu, H.-W., Macdonald, C. A., Trivedi, P., Holmes, B., Bodrossy, L., He, J.-Z. and Singh, B. K.: Water addition regulates the metabolic activity of ammonia oxidizers responding to environmental perturbations in dry subhumid ecosystems, *Environ. Microbiol.*, 17(2), 444–461, doi:10.1111/1462-2920.12481, 2015.
- Jahangir, M. M. R., Roobroeck, D., Van Cleemput, O. and Boeckx, P.: Spatial variability and biophysicochemical controls on N<sub>2</sub>O emissions from differently tilled arable soils, *Biol. Fertil. Soils*, 47(7), 753–766, doi:10.1007/s00374-011-0580-2, 2011.
- Jørgensen, C. J., Struwe, S. and Elberling, B.: Temporal trends in N<sub>2</sub>O flux dynamics in a Danish wetland - effects of plant-mediated gas transport of N<sub>2</sub>O and O<sub>2</sub> following changes in water level and soil mineral-N availability, *Glob. Chang. Biol.*, 18(1), 210–222, doi:10.1111/j.1365-2486.2011.02485.x, 2012.
- Khalil, K., Renault, P. and Mary, B.: Effects of transient anaerobic conditions in the presence of acetylene on subsequent aerobic respiration and N<sub>2</sub>O emission by soil aggregates, *Soil Biol. Biochem.*, 37(7), 1333–1342, doi:10.1016/j.soilbio.2004.11.029, 2005.
- Koschorreck, M. and Darwich, A.: Nitrogen dynamics in seasonally flooded soils in the Amazon floodplain, *Wetl. Ecol. Manag.*, 11, 317–330, 1998.
- Kowalik, P. J. and Randerson, P. F.: Nitrogen and phosphorus removal by willow stands irrigated with municipal waste water – A review of the Polish experience, *Biomass and Bioenergy*, 6(1–2), 133–139, doi:10.1016/0961-9534(94)90092-2, 1994.
- Kuzyakov, Y. and Blagodatskaya, E.: Microbial hotspots and hot moments in soil: Concept & review, *Soil Biol. Biochem.*, 83, 184–199, doi:10.1016/j.soilbio.2015.01.025, 2015.
- Li, X., Sørensen, P., Olesen, J. E. and Petersen, S. O.: Evidence for denitrification as main source of N<sub>2</sub>O emission from residue-amended soil, *Soil Biol. Biochem.*, 92, 153–160, doi:10.1016/j.soilbio.2015.10.008, 2016.
- Loecke, T. D. and Robertson, G. P.: Soil resource heterogeneity in terms of litter aggregation promotes nitrous oxide fluxes and slows decomposition, *Soil Biol. Biochem.*, 41(2), 228–235, doi:10.1016/j.soilbio.2008.10.017, 2009.
- Luster, J., Göttlein, A., Nowack, B. and Sarret, G.: Sampling, defining, characterising and modeling the

- rhizosphere – the soil science tool box, *Plant Soil*, 321(1–2), 457–482, doi:10.1007/s11104-008-9781-3, 2009.
- Manucharova, N. A., Stepanov, A. L. and Umarov, M. M.: Microbial transformation of nitrogen in water-stable aggregates of various soil types, *EURASIAN SOIL Sci.*, 34(10), 1125–1131, 2001.
- Morley, N., Baggs, E. M., Dörsch, P. and Bakken, L.: Production of NO, N<sub>2</sub>O and N<sub>2</sub> by extracted soil bacteria, regulation by NO<sub>2</sub><sup>-</sup> and O<sub>2</sub> concentrations, *FEMS Microbiol. Ecol.*, 65(1), 102–112, doi:10.1111/j.1574-6941.2008.00495.x, 2008.
- Myrold, D. D., Pett-Ridge, J. and Bottomley, P. J.: Nitrogen Mineralization and Assimilation at Millimeter Scales, in *Methods in Enzymology*, vol. 496, pp. 91–114, Elsevier Inc., 2011.
- Neira, J., Ortiz, M., Morales, L. and Acevedo, E.: Oxygen diffusion in soils: Understanding the factors and processes needed for modeling, *Chil. J. Agric. Res.*, 75(August), 35–44, doi:10.4067/S0718-58392015000300005, 2015.
- Oades, J. M.: Soil organic matter and structural stability: mechanisms and implications for management, *Plant Soil*, 76(1–3), 319–337, doi:10.1007/BF02205590, 1984.
- Parkin, T. B.: Soil Microsites as a Source of Denitrification Variability, *Soil Sci. Soc. Am. J.*, 51, 1194–1199, 1987.
- Philippot, L., Hallin, S., Börjesson, G. and Baggs, E. M.: Biochemical cycling in the rhizosphere having an impact on global change, *Plant Soil*, 321(1–2), 61–81, doi:10.1007/s11104-008-9796-9, 2009.
- R Core Team: R: A Language and Environment for Statistical Computing, R Found. Stat. Comput., Vienna, <https://www.R-project.org/>, 2018.
- Rabot, E., Hénault, C. and Cousin, I.: Temporal Variability of Nitrous Oxide Emissions by Soils as Affected by Hydric History, *Soil Sci. Soc. Am. J.*, 78(2), 434, doi:10.2136/sssaj2013.07.0311, 2014.
- Randerson, P. F., Moran, C. and Bialowiec, A.: Oxygen transfer capacity of willow (*Salix viminalis* L.), *Biomass and Bioenergy*, 35(5), 2306–2309, doi:10.1016/j.biombioe.2011.02.018, 2011.
- Ravishankara, A. R., Daniel, J. S. and Portmann, R. W.: Nitrous Oxide (N<sub>2</sub>O): The Dominant Ozone-Depleting Substance Emitted in the 21<sup>st</sup> Century, *Science (80-. )*, 326(5949), 123–125, doi:10.1126/science.1176985, 2009.
- Renault, P. and Stengel, P.: Modeling Oxygen Diffusion in Aggregated Soils: I. Anaerobiosis inside the Aggregates, *Soil Sci. Soc. Am. J.*, 58(4), 1017, doi:10.2136/sssaj1994.03615995005800040004x, 1994.
- Robertson, G. P. and Groffman, P. M.: Nitrogen Transformations, in *Soil Microbiology, Ecology and Biochemistry*, pp. 421–446, Elsevier., 2015.
- Ruser, R., Flessa, H., Russow, R., Schmidt, G., Buegger, F. and Munch, J. C.: Emission of N<sub>2</sub>O, N<sub>2</sub> and CO<sub>2</sub> from soil fertilized with nitrate: Effect of compaction, soil moisture and rewetting, *Soil Biol. Biochem.*, 38(2), 263–274, doi:10.1016/j.soilbio.2005.05.005, 2006.
- Samaritani, E., Shrestha, J., Fournier, B., Frossard, E., Gillet, F., Guenat, C., Niklaus, P. A., Pasquale, N., Tockner, K., Mitchell, E. A. D. and Luster, J.: Heterogeneity of soil carbon pools and fluxes in a channelized and a restored floodplain section (Thur River, Switzerland), *Hydrol. Earth Syst. Sci.*, 15(6), 1757–1769, doi:10.5194/hess-15-1757-2011, 2011.
- Sey, B. K., Manceur, A. M., Whalen, J. K., Gregorich, E. G. and Rochette, P.: Small-scale heterogeneity in carbon dioxide, nitrous oxide and methane production from aggregates of a cultivated sandy-loam soil, *Soil Biol. Biochem.*, 40(9), 2468–2473, doi:10.1016/j.soilbio.2008.05.012, 2008.

- Shrestha, J., Niklaus, P. a, Frossard, E., Samaritani, E., Huber, B., Barnard, R. L., Schleppe, P., Tockner, K. and Luster, J.: Soil nitrogen dynamics in a river floodplain mosaic., *J. Environ. Qual.*, 41(6), 2033–45, doi:10.2134/jeq2012.0059, 2012.
- Six, J., Paustian, K., Elliott, E. T. and Combrink, C.: Soil Structure and Organic Matter, *Soil Sci. Soc. Am. J.*, 64(2), 681, doi:10.2136/sssaj2000.642681x, 2000.
- Six, J., Bossuyt, H., Degryze, S. and Denef, K.: A history of research on the link between (micro)aggregates, soil biota, and soil organic matter dynamics, *Soil Tillage Res.*, 79(1), 7–31, doi:10.1016/j.still.2004.03.008, 2004.
- Smart, D. R. and Bloom, A. J.: Wheat leaves emit nitrous oxide during nitrate assimilation, *Proc. Natl. Acad. Sci.*, 98(14), 7875–7878, doi:10.1073/pnas.131572798, 2001.
- Spott, O., Russow, R. and Stange, C. F.: Formation of hybrid N<sub>2</sub>O and hybrid N<sub>2</sub> due to codenitrification: First review of a barely considered process of microbially mediated N-nitrosation, *Soil Biol. Biochem.*, 43(10), 1995–2011, doi:10.1016/j.soilbio.2011.06.014, 2011.
- Stolk, P. C., Hendriks, R. F. A., Jacobs, C. M. J., Moors, E. J. and Kabat, P.: Modelling the effect of aggregates on N<sub>2</sub>O emission from denitrification in an agricultural peat soil, *Biogeosciences*, 8(9), 2649–2663, doi:10.5194/bg-8-2649-2011, 2011.
- Thorbjørn, A., Moldrup, P., Blendstrup, H., Komatsu, T. and Rolston, D. E.: A Gas Diffusivity Model Based on Air-, Solid-, and Water-Phase Resistance in Variably Saturated Soil, *Vadose Zo. J.*, 7(4), 1276, doi:10.2136/vzj2008.0023, 2008.
- Tisdall, J. M. and Oades, J. M.: Organic matter and water-stable aggregates in soils, *J. Soil Sci.*, 33(2), 141–163, doi:10.1111/j.1365-2389.1982.tb01755.x, 1982.
- Totsche, K. U., Amelung, W., Gerzabek, M. H., Guggenberger, G., Klumpp, E., Knief, C., Lehndorff, E., Mikutta, R., Peth, S., Prechtel, A., Ray, N. and Kögel-Knabner, I.: Microaggregates in soils, *J. Plant Nutr. Soil Sci.*, 1–33, doi:10.1002/jpln.201600451, 2017.
- Vieten, B., Conen, F., Neftel, A. and Alewell, C.: Respiration of nitrous oxide in suboxic soil, *Eur. J. Soil Sci.*, 60(3), 332–337, doi:10.1111/j.1365-2389.2009.01125.x, 2009.
- Walthert, L., Graf, U., Kammer, A., Luster, J., Pezzotta, D., Zimmermann, S. and Hagedorn, F.: Determination of organic and inorganic carbon,  $\delta^{13}\text{C}$ , and nitrogen in soils containing carbonates after acid fumigation with HCl, *J. Plant Nutr. Soil Sci.*, 173(2), 207–216, doi:10.1002/jpln.200900158, 2010.
- Young, I. . and Ritz, K.: Tillage, habitat space and function of soil microbes, *Soil Tillage Res.*, 53(3–4), 201–213, doi:10.1016/S0167-1987(99)00106-3, 2000.
- Zhu, X., Burger, M., Doane, T. a and Horwath, W. R.: Ammonia oxidation pathways and nitrifier denitrification are significant sources of N<sub>2</sub>O and NO under low oxygen availability, *Pnas*, 110(16), 6328–6333, doi:10.1073/pnas.1219993110/-/DCSupplemental.www.pnas.org/cgi/doi/10.1073/pnas.1219993110, 2013.

## Chapter 3

# Microhabitat effects on source partitioning and reduction of nitrous oxide during flood-induced emissions from floodplain soils

Martin Ley<sup>a,b</sup>, Jörg Luster<sup>a</sup>, Pascal A. Niklaus<sup>c</sup>, Martin Hartmann<sup>d</sup>, Thomas Kuhn<sup>b</sup>, Beat Frey<sup>a</sup>, Moritz F. Lehmann<sup>b</sup>

<sup>a</sup>Swiss Federal Institute for Forest, Snow and Landscape Research WSL, Research Unit Forest Soils and Biogeochemistry, Zürcherstrasse 111, 8903 Birmensdorf, Switzerland

<sup>b</sup>University of Basel, Department of Environmental Sciences, Research Group Biogeochemistry, Bernoullistrasse 30, 4056 Basel, Switzerland

<sup>c</sup>University of Zürich, Department of Evolutionary Biology and Environmental Studies, Winterthurerstrasse 190, 8057 Zurich, Switzerland

<sup>d</sup>Swiss Federal Institute of Technology Zurich, Department of Environmental Systems Science, Sustainable Agroecosystems, Universitätsstrasse 2, 8092 Zürich, Switzerland

*Corresponding author:* Martin Ley (martin.ley@unibas.ch)

Keywords: stable isotopes, <sup>15</sup>N site preference, functional genes, next generation sequencing, nitrous oxide emissions

In revision with Soil Biology and Biogeochemistry

## Abstract

Floodplains are temporary hotspots of nitrous oxide (N<sub>2</sub>O) emissions due to soil heterogeneity and dynamic hydrology. However, how soil aggregation and plant-soil interactions control N<sub>2</sub>O emission dynamics during short floods, and how this is linked to the population dynamics and activity of N-cycling microbial communities, is not well understood. Here, we simulated flood events in microcosms with two soils differing in aggregate structure. Microcosms were either planted with basket willow (*Salix viminalis* L.), mixed with leaf litter, or left unamended. We combined N<sub>2</sub>O dual-isotope mapping with high-throughput sequencing of ribosomal markers

and quantitative polymerase chain reaction (qPCR) of functional genes involved in N-cycling to disentangle major processes that produce and consume N<sub>2</sub>O.

The two soils harbored distinct microbial communities, which were resistant to flooding, indicating that aggregate size is a key determinant of the soil microbiome composition. Litter addition also affected soil microbial community composition strongly, whereas the presence of willow had little effect. Nitrogen-cycling gene abundances revealed a higher potential for bacterial denitrification and for N<sub>2</sub>O reduction than for ammonia oxidation. Aggregate size had a significant impact on the abundance of most of these genes, whereas litter addition, and the presence of willow only affected the abundance of ammonia-oxidizing bacteria and archaea. Consistent with the structure of the microbiome, the isotope data revealed that N<sub>2</sub>O production during the flood phase was almost exclusively due to bacterial denitrification in all experimental treatments, yet most of the produced N<sub>2</sub>O was further reduced to N<sub>2</sub>. In the post-flooding phase, most of the net N<sub>2</sub>O production continued to derive from bacterial denitrification in anoxic micro-sites. However, the aeration of the inter-aggregate pore space led to additional contributions by oxidative N<sub>2</sub>O production, the magnitude of which depended on treatment and time point within the drying phase. Furthermore, immediately after flood water recession, N<sub>2</sub>O reduction was temporarily disrupted to a large degree, supporting the maximum net N<sub>2</sub>O efflux found at this time. The presence of willow largely attenuated effects of aggregate-size and flooding on N<sub>2</sub>O production pathways and the degree of N<sub>2</sub>O reduction.

Our findings highlight the importance of microhabitat formation in regulating source partitioning and reduction of N<sub>2</sub>O, mostly by controlling oxygen availability and distribution, but also by modifying soil microbiome composition. This study will thus advance our understanding of where and when hotspots and moments of N<sub>2</sub>O emissions in floodplain soils are most likely to occur.

### **3.1 Introduction**

Every year, an estimated 5 – 14 Tg of nitrous oxide (N<sub>2</sub>O), a potent greenhouse gas and an ozone-depleting agent in the Earth's stratosphere, is released from natural terrestrial sources (Ciais et al., 2013; Ravishankara et al., 2009). Floodplains are hotspots of N transformations (Shrestha et al., 2012), mostly because of high spatial heterogeneity in vegetation and soil properties and the dynamic hydrology (Fournier et al., 2013). However, the contribution of floodplains to the global N<sub>2</sub>O budget is uncertain, in part because duration and magnitude of N<sub>2</sub>O emissions are difficult to predict and to attribute to specific factors.

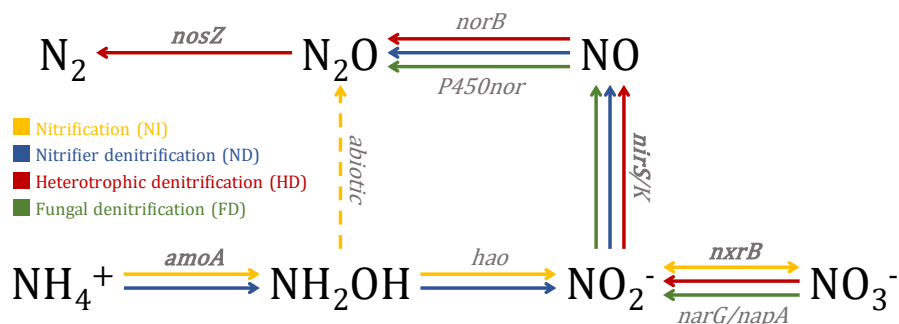


**Figure 3.1.** Schematic depicting the four most important  $N_2O$  producing processes; shown are the individual reaction steps, how they are interlinked, and major functional genes involved (abbreviations in italic). Functional genes measured in this study are indicated in bold.

$N_2O$  in soils is formed by various biotic and abiotic processes (Spott et al., 2011), with the most important ones shown in Fig. 3.1. Under oxic conditions,  $N_2O$  can be formed during the first step of nitrification (NI), when microbially-produced hydroxylamine ( $NH_2OH$ ) decomposes abiotically. Nitrification is mediated by ammonia oxidizing bacteria (AOB) and nitrite oxidizing bacteria (NOB) (Laughlin et al., 2008; Pester et al., 2014; Zhang et al., 2015). In addition, ammonia oxidizing archaea (AOA) can contribute to  $N_2O$  formation, but the exact pathway is not fully understood (Lehtovirta-Morley, 2018). Under suboxic to anoxic conditions, some AOBs and NOBs reduce nitrite ( $NO_2^-$ ) to nitric oxide (NO) and  $N_2O$  in a process known as nitrifier-denitrification (Arp and Stein, 2003; Cantera and Stein, 2007; Daims et al., 2016; Freitag et al., 1987; Starkenburg et al., 2008; Wrage et al., 2001). Under the same conditions, denitrifying bacteria reduce  $NO_3^-$  to  $NO_2^-$  and then further to NO,  $N_2O$ , and  $N_2$  (Braker et al., 2000; Knowles, 1982), and some fungi perform “incomplete” denitrification with  $N_2O$  as the final product (Laughlin and Stevens, 2002; Maeda et al., 2015). Other processes, known to produce  $N_2O$ , but not further considered in this study, are fungal co-denitrification (Shoun et al., 2012; Spott et al., 2011), dissimilatory reduction of nitrate ( $NO_3^-$ ) to ammonium (Rütting et al., 2011), and abiotic chemodenitrification (Jones et al., 2015; Stanton et al., 2018). Since many of these processes can occur simultaneously in the same soil volume, it is challenging to attribute soil  $N_2O$  emissions to a specific production process.

Natural abundance stable isotope ratio measurements of  $N_2O$  have emerged as a versatile, non-invasive alternative to  $^{15}N$  tracer techniques to deduce  $N_2O$  source processes (Baggs, 2008; Ostrom and Ostrom, 2012; Toyoda et al., 2011; Wolf et al., 2015). The simultaneous measurement of  $\delta^{15}N_{bulk}$ ,  $\delta^{18}O$  and the intramolecular distribution of the heavy ( $^{15}N$ ) and light N ( $^{14}N$ ) atoms between the central ( $\alpha$ ) and outer ( $\beta$ ) positions in the linear, asymmetric  $N_2O$  molecule, also known as  $^{15}N$  site preference ( $^{15}N$  SP), enables distinguishing between major

process groups and estimating the magnitude of N<sub>2</sub>O reduction (e.g., Lewicka-Szczebak et al., 2017). Although recent studies revealed considerable overlap in process-specific isotopic signatures and isotope enrichment effects, for given systems, this approach can provide useful information about temporal changes in the relative contribution of different oxidative and reductive N transforming processes, as well as the magnitude of N<sub>2</sub>O reduction (Decock and Six, 2013; Zou et al., 2014). While for the interpretation of  $\delta^{15}\text{N}_{\text{bulk}}$  and  $\delta^{18}\text{O}$ , the potential origins of the N and O atoms in the N<sub>2</sub>O molecule need to be considered (Kool et al., 2010, 2007; Lewicka-Szczebak et al., 2016; Snider et al., 2012, 2013), <sup>15</sup>N SP is considered to be independent of the isotopic composition of the substrate and is therefore considered process-specific (Toyoda and Yoshida, 1999). Two distinct process groups can be identified based on specific ranges of <sup>15</sup>N SP. The first group comprises NI and fungal denitrification (FD) with <sup>15</sup>N SP values of  $\sim 32 \pm 4 \text{ ‰}$ , and the second group ND and heterotrophic denitrification (HD) with comparatively low <sup>15</sup>N SP of  $\sim -2 \pm 4 \text{ ‰}$  (Decock and Six, 2013; Denk et al., 2017). Furthermore, N<sub>2</sub>O reduction to N<sub>2</sub> is associated with a distinct enrichment in <sup>15</sup>N<sup>bulk</sup>, <sup>18</sup>O<sub>N<sub>2</sub>O</sub> and a concomitant increase of <sup>15</sup>N SP of the residual pool of N<sub>2</sub>O (Decock and Six, 2013; Zou et al., 2014). For ecosystems where N<sub>2</sub>O production and consumption occur simultaneously or alternatingly, the combination of isotopomer maps with mixing models (Fig. S3.1, details of the calculation see Materials and Methods) allows estimating both the contributions of the two process groups to N<sub>2</sub>O and the magnitude of N<sub>2</sub>O reduction (Lewicka-Szczebak et al., 2017). Soil aggregation is a key factor affecting N<sub>2</sub>O production in soils, since it constrains the structure of the pore space network (Rabbi et al., 2016; Ruamps et al., 2011), and in turn oxygen diffusion and pore water flow (Wang et al., 2019; Wilpiseski et al., 2019). Unsurprisingly, aggregate structure therefore is a key determinant of microbial community structure and N transformations (Bach et al., 2018; Kravchenko et al., 2014; Mummey et al., 2006; Rillig et al., 2017).

Soil organic C inputs through litter accumulation and root exudation are other important determinants of soil N cycling and N<sub>2</sub>O emissions because they promote heterotrophic processes and, together with root respiration, promote anoxic soil volumes (Henry et al., 2008), in which denitrification is enhanced (Philippot et al., 2009). The patchy accumulation of plant litter is a common phenomenon in floodplains, which can lead to marked shifts in the bacterial and fungal community structure (Prescott and Grayston, 2013), and to the development of hot spots of N transformation processes (Hill, 2011). Similarly, the release of root exudates of living vegetation and dead, exfoliated root cells affect the rhizosphere microbiota by providing a broad spectrum of degradable organic substrates (Cline and Zak, 2015; Craine et al., 2015; Philippot



et al., 2013; Reese et al., 2018). These effects on the soil microbiome vary with plant community (Hrynkiewicz et al., 2012; Zhang et al., 2016). Certain plants also actively aerate their rhizosphere where they stimulate nitrification (Philippot et al., 2009).

In addition to the spatial effects of soil aggregation and organic C inputs, periodic flooding/drying cycles cause temporal dynamics regarding carbon, nutrient and oxygen availability, which are characteristic for floodplain soils. These cycles alter temporarily gaseous and liquid diffusion rates, which can lead to the formation of steep redox gradients. Furthermore, they induce the dispersal of N and C compounds, and promote microbial motility (Blagodatsky and Smith, 2012; Wilpiseski et al., 2019). Overall, such a heterogeneous distribution in space and time of oxygen, substrates, and soil microorganisms can lead to the simultaneous occurrence of different N transforming processes, with intermittent shifts in the contribution of N<sub>2</sub>O producing and consuming processes to total N<sub>2</sub>O emissions (Hu et al., 2015; Schlüter et al., 2018; Yamamoto et al., 2017). Indeed, inundation appears to be a key driver modulating denitrifying and ammonia oxidizing soil communities (Gleeson et al., 2010; Tomasek et al., 2017; Wang et al., 2017).

To gain insight into the spatio-temporal variation of N<sub>2</sub>O formation and reduction in floodplain soils, we studied the effects of simulated short floods in mesocosms filled with two different soil aggregate mixtures receiving different soil C inputs. In a previous report (see chapter 2), we showed that the different combinations of experimental factors influenced both the temporal pattern and the total amount of N<sub>2</sub>O emitted during a two-week period of elevated emissions in the drying phase after flooding. To deepen our process understanding of microbial N<sub>2</sub>O production and consumption, we combined different molecular and isotopic methods. First, we characterized the soil prokaryotic and fungal communities by amplicon sequencing of phylogenetic markers. Second, we quantified the abundances of functional genes that are indicative of specific reactions involved in N<sub>2</sub>O producing processes (Fig. 3.1). Third, we analyzed the isotopomeric composition of soil-emitted N<sub>2</sub>O in order to deduce the proportion of N<sub>2</sub>O source processes and the extent of partial N<sub>2</sub>O reduction.

## 3.2 Material and methods

### 3.2.1 Experimental setup

A two-factorial experiment was established comprising a two-level factor MODEL SOIL (macroaggregates and microaggregates) and a three-level factor TREATMENT (unamended, litter-added, or plant presence). The resulting six treatment combinations were replicated six times each (see also chapter 2). To establish the MODEL SOIL factor, macroaggregates (250 –

4000  $\mu\text{m}$ ) and microaggregates ( $< 250 \mu\text{m}$ ) were isolated from a N-rich carbonaceous gleyic Fluvisol. Subsequently, two model soils were constructed, using either the macro- or the microaggregates and complemented these with inert material of a size approximately comparable to the respective other fraction (2000 – 3200  $\mu\text{m}$  quartz sand, or 150 – 250  $\mu\text{m}$  glass beads). Cylindrical mesocosms were then filled with 8.5 kg of the different model soil (1:1 w/w ratio of soil aggregates:inert material), respectively. To establish the treatment combinations, the model soils were either planted with basket willow (*Salix viminalis* L.; one cutting per replicate), mixed with willow leaf litter (8 g dry matter per replicate), or left unamended.

The mesocosms were kept in a climate chamber ( $20 \pm 1 \text{ }^\circ\text{C}$ ,  $60 \pm 10 \%$  relative air humidity, 14h:10h light:dark cycle). For 15 weeks, the soils were continuously irrigated with artificial river water using suction cups to achieve a volumetric water content of  $35 \pm 5 \%$ . This conditioning phase allowed the soils to equilibrate and the plants to develop a root system. This was followed by a first experimental phase of 9 days under the same constant soil moisture conditions. Then, the mesocosms were flooded from the bottom until the water level was 1 cm above the soil surface. After 48 hours of inundation, the water was drained, and the soil allowed to dry for 18 days without further irrigation.

### 3.2.2 Air, soil water and soil sampling

Soil-emitted  $\text{N}_2\text{O}$  was analyzed once before flooding, twice during soil inundation, and seven times during the drying phase after flooding. For this, a hood was mounted on top of a mesocosm (see chapter 2), and 150 ml of headspace air were collected after 60 minutes using a gas-tight syringe. The gas sample was then transferred into a muffled and pre-evacuated serum glass vial closed with a butyl rubber stopper and an aluminum crimp. Samples were stored at room temperature in the dark until analysis. Soil water was collected by means of suction cups on most of the gas sampling events, 0.2  $\mu\text{m}$  filtered and stored at  $4 \text{ }^\circ\text{C}$  until analysis (see chapter 2).

For DNA extraction, soil was sampled with an 8 mm i.d. corer at 3 – 7 cm and 18 – 22 cm depth before flooding (day 2), shortly after recession of the flood water (day 12), and at the end of the experiment (day 33). After sampling, the holes were filled with sterile glass beads (150  $\mu\text{m}$  – 250  $\mu\text{m}$ ) to avoid undesired chimney effects. Moist soil samples were transferred into 2 ml Eppendorf Safe-Lock tubes and stored at  $-80 \text{ }^\circ\text{C}$ .

### 3.2.3 Microbiological analyses

#### 3.2.3.1 Soil DNA extraction, PCR and amplicon sequencing

DNA from soils were extracted using the DNeasy PowerSoil Kit (Qiagen, Hilden, Germany) following the manufacturer's instructions. Extracted DNA was quantified using a NanoDrop ND-1000 spectrophotometer (NanoDrop Technologies), then split into aliquots and diluted to a concentration of 2.67 ng  $\mu\text{l}^{-1}$ .

Each sample with 20 ng soil DNA was amplified in triplicates by PCR using the HotStar Taq amplification kit (Qiagen, Hilden, Germany), as previously described (Frey et al., 2020), on a Veriti 96 well thermal cycler (Applied Biosystems, Foster City, CA, USA). The small-subunit (16S) rRNA gene sequences of the V3 – V4 region for prokaryotes and the internal transcribed spacer region 2 (ITS2) for fungi was targeted (Frey et al., 2016). Successful amplification was verified by electrophoresis of aliquots of every PCR product on a 2 % agarose gel. Triplicate PCR products of each sample were subsequently pooled to ensure sufficient coverage of the whole spectrum of present taxa (for primer details see supplementary material Table S3.1). The pooled bacterial and fungal amplicons were sent to the Génome Québec Innovation Center (McGill University, Montreal, Canada) for barcoding, using the Fluidigm Access Array technology and paired-end sequencing on the Illumina MiSeq v3 platform (Illumina Inc., San Diego, CA, USA).

For quality control of the 16S rRNA and ITS2 gene sequences, sequence clustering, and the taxonomic classification and assignment, the processing pipeline described in detail by Herzog et al. (2019) was used, with the following modifications: instead of creating exact sequence variants (ESVs), the sequences were clustered into operational taxonomic units (OTUs) of at least 97% sequence identity using the cluster-size function in VSEARCH (Rognes et al., 2016). Further, the taxonomic classification was performed using the Ribosomal Database Project (RDP) classifier (Wang et al., 2007) implemented in MOTHUR (Schloss et al., 2009) with a minimum bootstrap support of 80 %. For taxonomic assignment of the OTUs, matching centroid sequences of the V3–V4 region in prokaryotic 16S ribosomal sequences and of fungal ITS2 were queried against the RDP, version 14 (Cole et al., 2009). Prior to further analysis, sequences identified as chloroplasts or mitochondria (prokaryotic dataset) and plants (eukaryotic dataset) as well as unknown sequences were removed. Raw sequences have been deposited in the NCBI Sequence Read Archive under the BioProject accession number PRJNA673594.

### 3.2.3.2 Quantitative PCR of nitrogen cycling genes

Functional marker genes encoding for enzymes catalyzing nitrification (bacterial *amoA*, archaeal *amoA*, *nxrB*), and denitrification (*nirS*, *nosZ*) were targeted according to Frey et al. (2020). For each functional gene, 6.6  $\mu\text{l}$  of template DNA (2.67  $\text{ng } \mu\text{l}^{-1}$ ) were added to 8.4  $\mu\text{l}$  of gene specific master mix. The master mix for each sample comprised 7.5  $\mu\text{l}$  QuantiTect SYBR Green PCR master mix (Qiagen, Hirlen, Germany), 0.15  $\mu\text{l}$  each of forward and reverse primer (100  $\mu\text{M}$ ; Table S3.1), 0.5  $\mu\text{l}$  water (HPLC grade), and 0.1  $\mu\text{l}$  of Bovine Serum Albumin (30  $\text{mg } \text{ml}^{-1}$ ). Each functional gene was amplified using a specific thermal profile (supplementary material Table S3.1) using an ABI7500 Fast Real-Time PCR system (Applied Biosystems, Lincoln, CA, USA). Primer specificity was verified by melting curve analyses at the end of each qPCR run. Amplification efficiency was calculated using the equation in Philippot et al. (2011) and resulted in an estimated range between 82 % and 92 %. Gene copy numbers were quantified for each run by a series of diluted cloned plasmids containing inserts of the respective gene (Frey et al., 2020).

### 3.2.4 Natural abundance stable isotope analyses

#### 3.2.4.1 Soil-emitted $\text{N}_2\text{O}$

The isotopic composition of  $\text{N}_2\text{O}$  in the gas samples was analyzed using an isotope ratio mass spectrometer (IRMS; Thermo Finnigan Delta V Plus, Thermo Fisher Scientific, Bremen, Germany) operating in continuous flow mode coupled to a customized purge and trap system (modified after McIlvin and Casciotti, 2010). Each measurement sequence comprised three  $\text{N}_2\text{O}$  gas standards (Standard 1, 2 and 3; supplementary material Table S3.2) in synthetic air with an isotopic composition determined by J. Mohn at the Swiss Federal Laboratories for Materials Science and Technology (EMPA), one ambient air sample and 10 – 15 headspace samples. Standard 3 with atmospheric isotopic composition was thereby used as an internal quality control. The manually-loaded samples were purged from the serum bottles (160 ml total volume) for 25 minutes by the helium carrier gas (purity >99.995 %, Air Liquide, France; 60  $\text{ml } \text{min}^{-1}$ ). Water was removed in three stages by a cryogenic EtOH trap at  $-60\text{ }^\circ\text{C}$ , a Nafion membrane loop and a 30 cm  $\text{Mg}(\text{ClO}_4)_2$  column trap. A Carbosorb trap was used to remove  $\text{CO}_2$ . Nitrous oxide was cryogenically trapped and concentrated using liquid  $\text{N}_2$ , and further purified in a GC-column (Rt-Q-BOND, Restek, 30 m  $\times$  0.32 mm) to separate the  $\text{N}_2\text{O}$  from any remaining  $\text{CO}_2$ . The IRMS collector was configured to simultaneously detect mass to ion-charge ( $m/z$ ) ratios of 30, 31, 44, 45, and 46. The peak areas were adjusted for linearity effects and normalized to 20 volt-seconds prior calibration against the reference gas (100 % nitrous

oxide;  $\delta^{15}\text{N}_{\text{N}_2\text{O}}$ :  $-0.25 \text{ ‰}$ ,  $\delta^{18}\text{O}_{\text{N}_2\text{O}}$ :  $39.96 \pm 0.02 \text{ ‰}$ ,  $\delta^{15}\text{N}^\alpha$ :  $-0.9 \pm 0.01 \text{ ‰}$ ,  $\delta^{15}\text{N}^\beta$ :  $0.4 \pm 0.03 \text{ ‰}$ ; Air Liquide, France). The calibration of the  $\text{N}_2\text{O}$  reference gas relative to international standards was also conducted by J. Mohn (EMPA) using a quantum cascade laser absorption spectrometer (mini-QCLAS; Aerodyne Research Inc, USA). A non-linear solver in MatLab (version R2016b, MathWorks, USA) using the equations of Frame and Casciotti (2010) and Frame et al. (2017) was applied to obtain values for  $\delta^{15}\text{N}^\alpha$ ,  $\delta^{15}\text{N}^{\text{bulk}}$  and  $\delta^{18}\text{O}_{\text{N}_2\text{O}}$  from  $m/z = 31/30$ ,  $45/44$ , and  $46/44$ , respectively, followed by a two-point correction using measurements of standards 1 and 2. All measured ratios of heavy to light isotopes ( $^{\text{H/L}}\text{R}$ ) are reported in the common delta ( $\delta$ ) notation relative to the respective international standard (Vienna Standard Mean Ocean Water, VSMOW, for  $\delta^{18}\text{O}$  and AIR- $\text{N}_2$  for  $\delta^{15}\text{N}$ ; eq. 1):

$$\delta X_{\text{sample}} = \frac{{}^{\text{H/L}}\text{R}_{\text{sample}} - {}^{\text{H/L}}\text{R}_{\text{standard}}}{{}^{\text{H/L}}\text{R}_{\text{standard}}} \times 1000 \text{ (in permil, ‰)} \quad (1)$$

Where  $\delta X_{\text{sample}}$  stands for the  $\delta^{15}\text{N}^{\text{bulk}}$ ,  $\delta^{15}\text{N}^\alpha$ ,  $\delta^{15}\text{N}^\beta$ ,  $\delta^{18}\text{O}_{\text{N}_2\text{O}}$  or  $\delta^{18}\text{O}_{\text{H}_2\text{O}}$  whereas  ${}^{\text{H/L}}\text{R}_{\text{sample}}$  and  ${}^{\text{H/L}}\text{R}_{\text{standard}}$  denote the isotopic ratio of the respective atom in the sample and of the standard. The analytical precision is given as the standard deviation of measurements of the internal Standard 3 being  $0.2 \text{ ‰}$  for both  $\delta^{15}\text{N}^{\text{bulk}}$  and  $\delta^{18}\text{O}_{\text{N}_2\text{O}}$  and  $0.4 \text{ ‰}$  for  $^{15}\text{N}$  SP.

We used the relationship:

$$\delta^{15}\text{N}^{\text{bulk}} = (\delta^{15}\text{N}^\alpha + \delta^{15}\text{N}^\beta)/2 \quad (2)$$

to calculate values for  $\delta^{15}\text{N}^\beta$  and, in turn,  $^{15}\text{N}$  SP:

$$^{15}\text{N} \text{ SP} = \delta^{15}\text{N}^\alpha - \delta^{15}\text{N}^\beta \quad (3)$$

The isotopic signatures of soil-derived  $\text{N}_2\text{O}$  were separated from background  $\text{N}_2\text{O}$  by using the following mass balance equation:

$$\delta_{\text{chamber}} = \frac{(\delta_{\text{atm}} \times C_{\text{atm}} + \delta_{\text{soil}} \times C_{\text{soil}})}{(C_{\text{atm}} + C_{\text{soil}})} \quad (4)$$

Where  $\delta_{\text{chamber}}$ ,  $\delta_{\text{atm}}$  and  $\delta_{\text{soil}}$  stand for either  $\delta^{15}\text{N}^{\text{bulk}}$ ,  $\delta^{18}\text{O}_{\text{N}_2\text{O}}$  or  $^{15}\text{N}$  SP of the gas mixture (chamber) and the two  $\text{N}_2\text{O}$  sources (atmosphere and soil), whereas  $C_{\text{chamber}}$  and  $C_{\text{atm}}$  denote the

---

measured concentrations of N<sub>2</sub>O inside the mesocosm chamber and in the background air, respectively. In rare cases where soil-derived N<sub>2</sub>O was less than 30 % of the background N<sub>2</sub>O concentration, isotopic values were excluded from further analysis since the error in the mass balance equation increases with decreasing proportion of soil derived N<sub>2</sub>O (Opdyke et al., 2009; Ostrom et al., 2007).

#### 3.2.4.2 Soil-solution NO<sub>x</sub> and soil water

The N isotopic composition of NO<sub>x</sub> in soil solution (NO<sub>x</sub> = NO<sub>3</sub><sup>-</sup> + NO<sub>2</sub><sup>-</sup>) were measured using the denitrifier method according to Sigman et al. (2001) and Casciotti et al. (2002). Briefly, soil solution samples with a 20 nmol target content of NO<sub>x</sub> were injected into 3 ml of nitrate-free nutrient solution inoculated with knock-out mutants of *P. chlororaphis* (ATCC # 13985) in helium-purged 20 ml vials. The overnight conversion of NO<sub>x</sub> to N<sub>2</sub>O was stopped by adding 100 µl of 10 M NaOH. The produced N<sub>2</sub>O was subsequently analyzed on the same IRMS as used for the soil-emitted N<sub>2</sub>O samples in sequences of up to 60 samples with three international standards (USGS32, USGS34 and IAEA-NO-3; supplementary material Table S3.2) re-measured every 10 samples. For quality control, two additional lab standards (supplementary material Table S3.2) were measured at least once every sequence. The NO<sub>x</sub>-N isotope composition is reported in the delta notation relative to AIR-N<sub>2</sub>.

The isotopic measurements of δ<sup>18</sup>O<sub>H<sub>2</sub>O</sub> of two randomly picked soil water samples from each experimental treatment per sampling day were carried out at the University of Basel Stable Isotope Ecology Laboratory (BaSIEL) at the Botanical Institute, Basel, Switzerland. Water samples were analyzed by thermal conversion in an elemental analyzer (TC/EA) coupled to a Delta V Plus IRMS through a ConFlo IV interface (Thermo Fisher Scientific, Bremen, Germany). O-isotope ratios were normalized to the V-SMOW scale using calibrated in-house standards with δ<sup>18</sup>O<sub>H<sub>2</sub>O</sub> values of -10.88 ‰ and +4.42 ‰, respectively. The long-term analytical precision for δ<sup>18</sup>O<sub>H<sub>2</sub>O</sub> in the laboratory is 0.24 ‰, based on repeated analyses of an in-house quality control standard (Newberry et al. (2017)). The δ<sup>18</sup>O<sub>H<sub>2</sub>O</sub> values showed little variation (-10.23 ± 0.15 ‰, mean ± SD) and was subsequently used to calculate expected endmember O-isotopic signatures of N<sub>2</sub>O produced by HD, ND, or FD, where H<sub>2</sub>O serves as O-atom substrate (see below).

#### 3.2.5 N<sub>2</sub>O source partitioning and N<sub>2</sub>O reduction

Source partitioning of the most common N<sub>2</sub>O producing processes and the magnitude of N<sub>2</sub>O reduction were simultaneously estimated using the dual-isotope mapping approach introduced

by Lewicka-Szczebak et al. (2017), and modified according to most recent insights from Yu et al. (2020).

To derive experiment-specific  $\delta^{18}\text{O}_{\text{N}_2\text{O}}$  endmember ranges ( $\delta^{18}\text{O}_{\text{N}_2\text{O\_ambient}}$ ) for HD, nitrifier denitrification (ND) and FD, literature values ( $\delta^{18}\text{O}_{\text{N}_2\text{O\_literature}}$ ) compiled by Yu et al. (2020; relative to a  $\delta^{18}\text{O}_{\text{H}_2\text{O}}$  of 0 ‰) were adjusted to the  $\delta^{18}\text{O}$  of ambient soil water in this study ( $\delta^{18}\text{O}_{\text{H}_2\text{O\_ambient}}$ ) following Lewicka-Szczebak et al. (2020), using eq. (5):

$$\text{endmember } \delta^{18}\text{O}_{\text{N}_2\text{O\_ambient}} = \delta^{18}\text{O}_{\text{N}_2\text{O\_literature}} + \delta^{18}\text{O}_{\text{H}_2\text{O\_ambient}} \text{ (‰)} \quad (5)$$

For NI, a range of  $\delta^{18}\text{O}_{\text{N}_2\text{O}}$  values of  $23.5 \pm 3$  ‰ was adopted from Yu et al. (2020), since previous studies showed, that  $\delta^{18}\text{O}_{\text{N}_2\text{O}}$  values from  $\text{NH}_3^+$  oxidation were similar to atmospheric oxygen (Frame and Casciotti, 2010; Sutka et al., 2006). Together with the process specific ranges in  $^{15}\text{N}$  SP also taken from Yu et al. (2020), these new endmember ranges represent the expected process-specific isotopic signatures of  $\text{N}_2\text{O}$  produced in our experiment used in the assessment of  $\text{N}_2\text{O}$  source partitioning (see also supplementary material Table S3.3). Due to the considerable overlap of the  $^{15}\text{N}$  SP and  $\delta^{18}\text{O}_{\text{N}_2\text{O}}$  values for ND and HD, these two processes were combined into one group represented by a common endmember ( $\delta_{\text{ND\&HD}}$ ). Despite the distinct ranges for NI and FD in  $\delta^{18}\text{O}_{\text{N}_2\text{O}}$  observed in pure culture studies, these two processes were also grouped and represented by one common endmember ( $\delta_{\text{NI\&FD}}$ ). Since in soils a simultaneous contribution by NI and FD cannot *a priori* be excluded and the isotopic values are in addition influenced by the degree of  $\text{N}_2\text{O}$  reduction, the relative contribution of each process cannot be distinguished with this method. The mean values of the fractionation factors  $\epsilon^{15}\text{N}$  SP (-3.7 ‰) and  $\epsilon^{18}\text{O}$  (-15.8 ‰), used to estimate isotopic shifts during  $\text{N}_2\text{O}$  reduction and to calculate the slope of the reduction line ( $\epsilon^{15}\text{N}$  SP/  $\epsilon^{18}\text{O}$  = 0.23), were taken from the laboratory soil experiment conducted by Jinuntuya-Nortman et al. (2008) spanning the same range of water filled pore space as in this study, and are well within the range of other soil studies (e.g., Lewicka-Szczebak et al., 2014; Well and Flessa, 2009).

The dual-isotope mapping approach is based on the positioning of measured and background-corrected, sample values relative to a mixing line between two process group endmembers, and a reduction line in a  $^{15}\text{N}$  SP vs.  $\delta^{18}\text{O}_{\text{N}_2\text{O}}$  diagram (Fig. S3.1). This enables the assessment of the relative importance of each of the two process groups, and the extent of  $\text{N}_2\text{O}$  reduction, depending on two scenarios differing with regards to the sequential order of  $\text{N}_2\text{O}$  mixing versus reduction.

**Scenario reduction-mixing (R-M):** In this scenario, the reduction line (with a slope derived from the fractionation factors mentioned above) originating from the  $\delta_{ND\&HD}$  endmember coordinates intersects with the mixing line passing through the  $\delta_{NI\&FD}$  endmember and the sample coordinates (Fig. S3.1a). Here, it is assumed that only  $N_2O$  produced by ND and/or HD gets partially reduced to  $N_2$  before it mixes with unreduced  $N_2O$  from other sources.

**Scenario mixing-reduction (M-R):** Here, the mixing line stretching between the two endmember points of  $\delta_{NI\&FD}$  and  $\delta_{ND\&HD}$  is intersected by the reduction line that runs through the sample coordinates. This way, it is assumed that  $N_2O$  produced by both process groups mixes first followed by partial reduction of the mixture.

The coordinates (i.e., the  $^{15}N$  SP vs.  $\delta^{18}O_{N_2O}$ , respectively) of these intersections can now be used in a two-endmember mixing model combined with the Rayleigh distillation model to account for the isotope effect of partial  $N_2O$  reduction (eq. 6), to calculate the residual fraction of unreduced  $N_2O$ .

$$\delta_{soil} = (\delta_{ND\&HD} \times (1 - f_{NI\&FD}) + \delta_{NI\&FD} \times f_{NI\&FD}) + \epsilon_{red} \times \ln(rN_2O) \quad (6)$$

In Equation 6,  $\delta_{soil}$  denotes either the  $^{15}N$  SP or  $\delta^{18}O_{N_2O}$  value of the soil emitted  $N_2O$ . The isotopic signatures of the two combined endmembers are denoted by  $\delta_{ND\&HD}$  and  $\delta_{NI\&FD}$ , respectively. The  $N_2O$  source partitioning into the two process groups is represented by  $f_{NI\&FD}$ , the fraction of  $N_2O$  produced by NI and FD, and  $f_{ND\&HD}$ , the complementary fraction produced by HD and ND (i.e.,  $f_{ND\&HD} = 1 - f_{NI\&FD}$ ).  $\epsilon_{red}$  is the net isotope effects associated with  $N_2O$  reduction, and the emitted, unreduced fraction of produced  $N_2O$  is denoted as residual  $N_2O$  ( $rN_2O$ ) (between 1 and 0). The Rayleigh model assumes closed system conditions, under which  $N_2O$  is first accumulated and subsequently partially reduced. Lewicka-Szczebak et al. (2017) could demonstrate in soil incubation experiments similar to ours that  $N_2O$  reduction follows a closed-system pattern attesting to the validity of the use of the Rayleigh distillation model.

Since in scenario R-M the fraction of  $rN_2O$  only refers to the total  $N_2O$  production by the ND&HD process group, it is necessary to consider also the  $N_2O$  produced by the NI&FD process group (Verhoeven et al., 2019). Therefore, the residual  $N_2O$  for the entire  $N_2O$  production by all processes ( $rN_2O_{total}$ ) is calculated (eq. 7):

$$rN_2O_{total} = \frac{1}{f_{ND\&HD}/rN_2O - f_{ND\&HD} + 1} \quad (7)$$



Similarly, to obtain the gross contribution of the ND&HD process group to total N<sub>2</sub>O production ( $f_{ND\&HD,gross}$ ) in scenario R-M, we must take into account the reduced N<sub>2</sub>O, using Equation 8:

$$f_{ND\&HD,gross} = \frac{f_{ND\&HD}/rN_2O}{f_{ND\&HD}/rN_2O - f_{ND\&HD} + 1} \quad (8)$$

In scenario M-R, a proportional reduction of N<sub>2</sub>O after mixing is assumed, therefore the following relations apply:

$$rN_2O = rN_2O_{total} \quad (9)$$

and

$$f_{ND\&HD} = f_{ND\&HD,gross} \quad (10)$$

Note that each scenario defines that all N<sub>2</sub>O production and consumption in the soils follow only the respective sequential order. However, in nature, mixing and reduction can occur simultaneously to a varying extent. The resulting estimates of  $f_{ND\&HD,gross}$  and  $rN_2O_{total}$ , provided by the two scenarios, should therefore be interpreted as a parameter range.

### 3.2.6 Statistical analysis

All data analyses were conducted using the statistical software R version 3.5.2 (R Core Team, 2018). After inspection of the rarefaction curves, subsets of all samples from the prokaryotic 16S and the fungal ITS2 datasets were taken by random selection of sequences using the *rarefy\_even\_depth* function implemented in the package ‘phyloseq’ (McMurdie and Holmes, 2013). This resulted in an equal sequencing depth of 10714 reads per sample for 16S rRNA gene and 8102 reads for ITS2, respectively.

Dynamics in the relative abundance of the prokaryotic and fungal communities were analyzed at the taxonomic class level of each dataset with functions of the package ‘phyloseq’. Alpha diversity indices (OTU richness and Shannon index) were calculated for the prokaryotic and fungal datasets using the *estimate\_richness* function in the package ‘phyloseq’, whereas Smith and Wilson’s evenness index ( $E_{var}$ ; Smith and Wilson, 1996) was calculated using the *evenness* function in the ‘microbiome’ package (Lathi and Shetty, 2012-2019). For analysis of beta diversity, both datasets were scaled by square root-transforming the relative abundance of the

sample counts. This standardized dataset was used to create a resemblance matrix, using the sample-wise Bray-Curtis dissimilarity. The effects of the experimental factors on bacterial and fungal community structure were tested using permutational multivariate analysis of variance (PERMANOVA), applying the *adonis* function in the package ‘vegan’ (Oksanen et al., 2019). In each PERMANOVA,  $10^4$  randomized permutations were applied. To test for effects of the factors TREATMENT (3 levels) and MODEL SOIL (2 levels) these factors defined the blocking structure for permutation on the MESOCOSM (36 levels) stratum, while the latter provided the blocking structure when testing the effects of the factors DAY OF EXPERIMENT (3 levels) and DEPTH (2 levels). To take potential heteroscedasticity into account, group dispersions were tested according each PERMANOVA design using the *permutest.betadisper* function in the ‘vegan’ package. For visualization of differences in community structure between treatments and non-metrical multidimensional scaling (NMDS) with three dimensions was used by applying the *ordinate* function of the ‘phyloseq’ package. Time-series of functional gene abundance and prokaryotic and fungal alpha- and beta-diversity were analyzed by linear-mixed models summarized by ANOVA (ASReml, VSNI; Butler et al., 2017), with the fixed effects TREATMENT, MODEL SOIL, DEPTH, and DAY OF EXPERIMENT, and temporal residual correlations. MESOCOSM, and its respective two- and three-way interactions with DAY OF EXPERIMENT and DEPTH were random terms. We further modelled the temporal correlation of residuals at these different levels. However, the serial correlations were very weak and we therefore carried out all analyses using *aov* with the respective random terms included in the Error() option. These analyses gave near-identical results.

To identify significant temporal changes in functional gene abundances and prokaryotic and fungal alpha-diversity, day-wise comparisons were calculated by creating an equivalent model with the package ‘lmerTest’ (Kuznetsova et al., 2017), followed by the comparison of user-defined contrasts with the *glht* function in the ‘multcomp’ package (Hothorn et al., 2008). Obtained *P*-values were adjusted using Holm’s correction method (Holm, 1979).

### 3.3 Results

#### 3.3.1 Prokaryotic and fungal communities

The alpha diversity of both the prokaryotic and fungal communities in terms of OTU richness, Shannon’s diversity, differed neither among treatments, nor between soil layers (Table S3.4, Table S3.5). Also, differences between pre-flood and post-flood diversity and changes during the drying phase were not statistically significant or small. Fungal species were generally less evenly distributed than bacterial species (e.g., lower  $E_{\text{var}}$  index values). Changes in evenness of

the bacterial communities were mainly observed in soils with macroaggregates directly after the flood phase where the species evenness generally decreased in the topsoils and increased in the subsoils (Table S3.4). In the fungal communities, species evenness significantly increased only in the subsoil of the litter added soils with microaggregates, whereas in the other treatments no significant changes were found (Table S3.5). Prokaryotic communities were clearly separated by aggregate size (Table 3.1; Fig. 3.2a).

**Table 3.1:** Main effects of experimental factors on microbial community composition computed by PERMANOVA based on Bray-Curtis dissimilarity of square-root transformed relative abundances of prokaryotic (Prok.) and fungal OTUs. Significant effects ( $P_{\text{perm}} < 0.05$ ) are reported, non-significant effects are indicated as ns. Marked results ( $\dagger$ ) had significantly different group dispersions ( $P < 0.05$ ). Significance values are based on  $10^4$  permutations. Sum of squares and mean sum of squares are denoted as SS and MS, respectively.

	Df	SS		MS		$F_{\text{model}}$		$R^2$		$P_{\text{perm}}$	
		Prok.	Fungi	Prok.	Fungi	Prok.	Fungi	Prok.	Fungi	Prok.	Fungi
TREATMENT	2	ns	1	ns	0.53	ns	3.4	ns		ns	0.001 $\dagger$
MODEL SOIL	1	0.3	ns	0.3	ns	2.87	ns	0.014	ns	0.007 $\dagger$	ns
DEPTH	1	0.13	ns	0.13	ns	1.26	ns	0.006	ns	0.014	ns
DAY OF EXPERIMENT	2	0.32	ns	0.16	ns	1.53	ns	0.015	ns	0.001	ns

At the class level, this was reflected mainly by a larger contribution of *Planctomycetacia* and a smaller contribution of *Betaproteobacteria* in the treatments with macroaggregates compared to those with microaggregates (Fig. 3.3a). Soil depth and sampling day had additional significant, but on the class level small effects (Table 3.1, Fig. 3.3a). The addition of litter led to a pronounced separation in both the prokaryotic and the fungal communities (Fig. 3.2a, b), but this led to a significant effect of soil amendment only for the fungi (Table 3.1). Most prominently, the litter added soils with macroaggregates exhibited a much higher contribution of *Eurotiomycetes* than all other treatments (Fig. 3.3b).

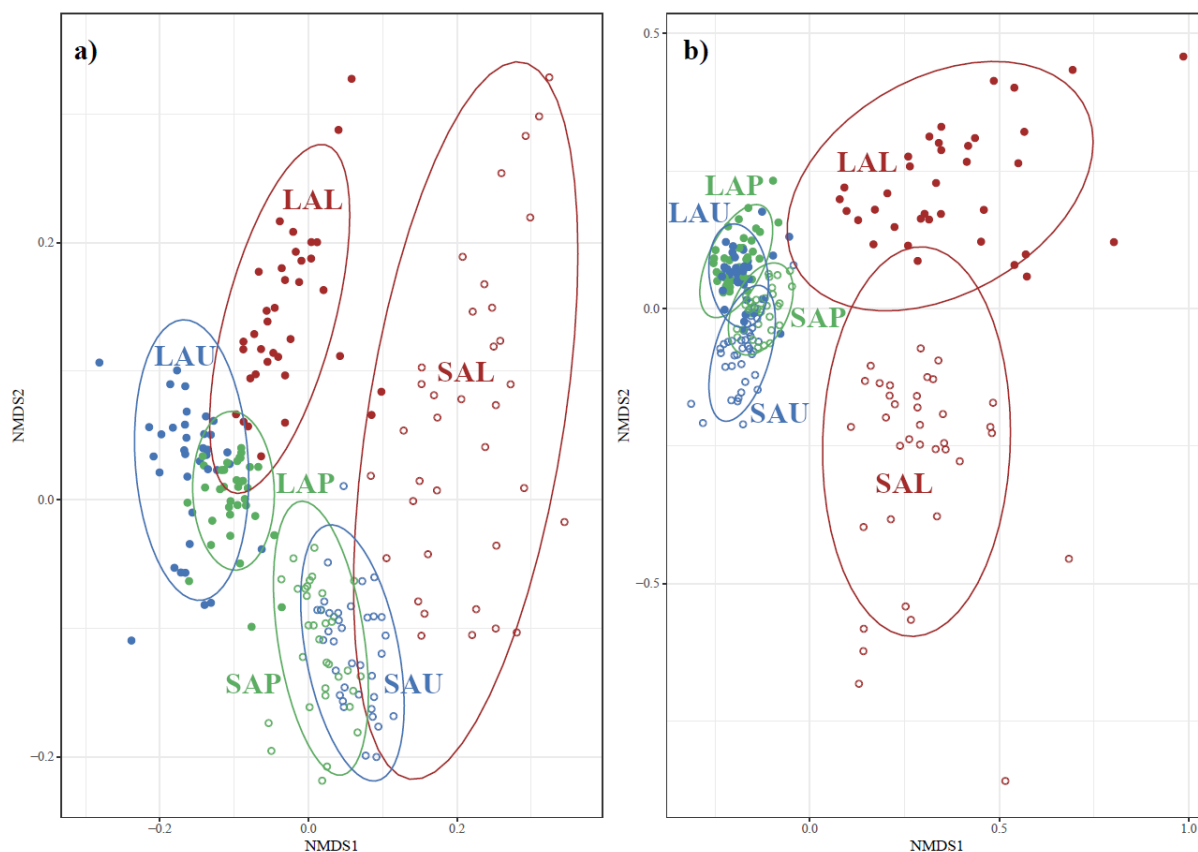


**Figure 3.2.** Non-metrical multidimensional scaling (NMDS) ordination of a) prokaryotic (stress: 0.095; dim.: 3) and b) fungal (stress: 0.084; dim.: 3) community structure in soils from different treatments of a flooding experiment with model floodplain soils. Filled and open symbols represent large aggregates (LA) and small aggregates (SA), respectively. Blue symbols indicate unamended soils (LAU and SAU treatments), red symbols soils with litter addition (LAL and SAL treatments), and green symbols soils with plants (LAP and SAP treatments), respectively. The ellipses represent the 95 % confidence intervals from the centroid of the respective cluster.

A pronounced increase of *Pezizomycetes* with time was observed in both model soils with plants (Fig. 3.3b), but the temporal effect on the whole fungal community was not significant (Table 3.1). The class *Soil Crenarchaeotic Group*, comprising many ammonia oxidizing species, made up most of the archaea (Fig. S3.2). Particularly large numbers of methanogenic Archaea of the classes *Methanobacteria* and *Methanomicrobia*, contributing together 54 % of the total archaeal community, were found in the subsoil of the litter added soils with microaggregates.

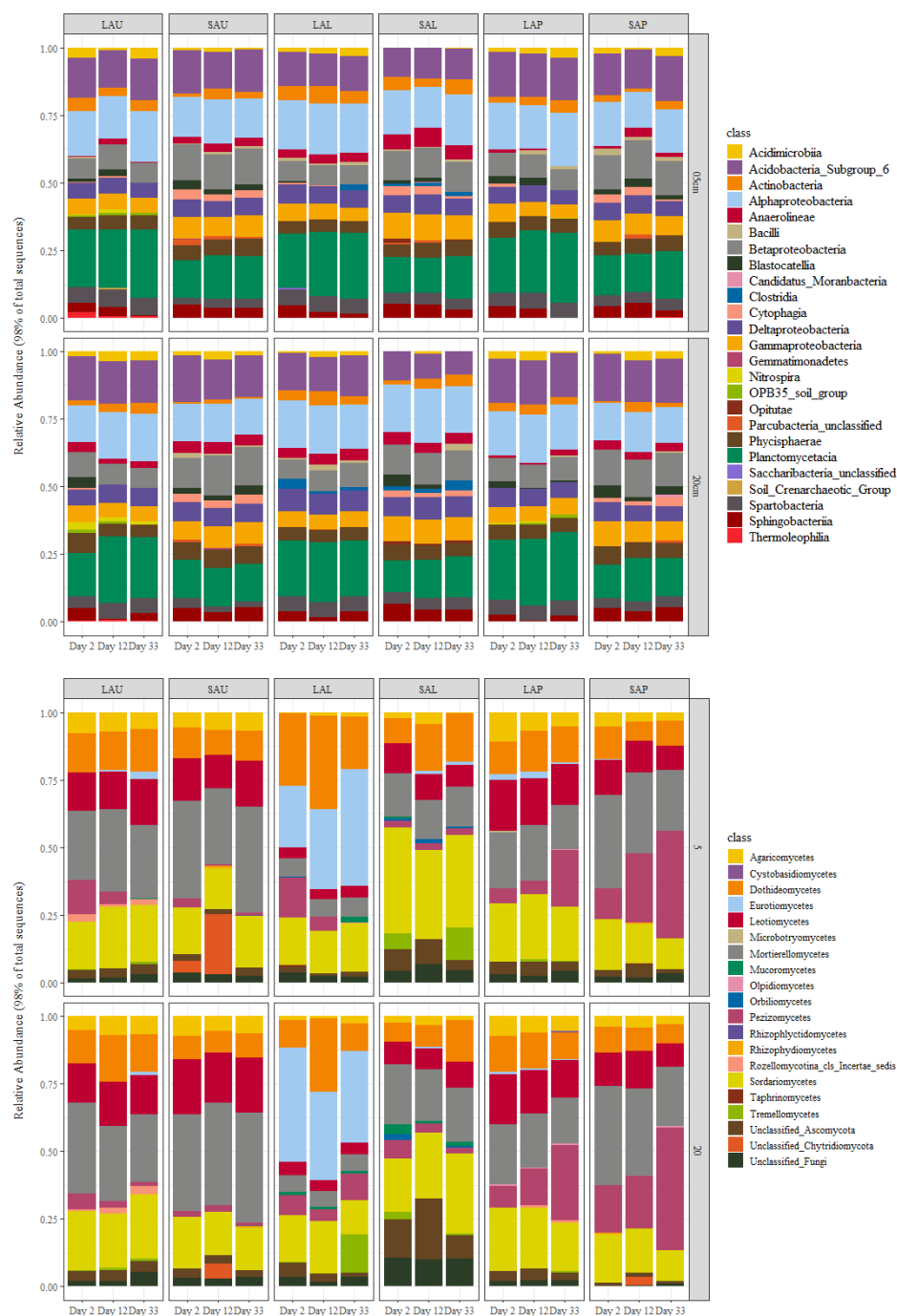


**Figure 3.3.** Relative abundance of taxonomic groups of prokaryotes (a) and fungi (b) at the class level in the topsoils (5cm) and the subsoils (20cm) from a flooding experiment with model floodplain soils. In the three-letter treatment denotation, LA and SA stand for large and small aggregates, respectively, and the last letter U for unamended, L for litter addition, and P for plant presence. Values are means of replicated treatments ( $n = 6$ ).

### 3.3.2 Abundance of key N-cycling genes

Independent of the treatment, soil depth, and time, *nosZ* genes were most abundant in term of copy numbers per g soil one order of magnitude more abundant than those of bacterial *amoA*,

*nxrB*, and *nirS* genes. Archeal *amoA* were least abundant, with copy numbers one order of magnitude lower than for bacterial *amoA* (Fig. 3.4).

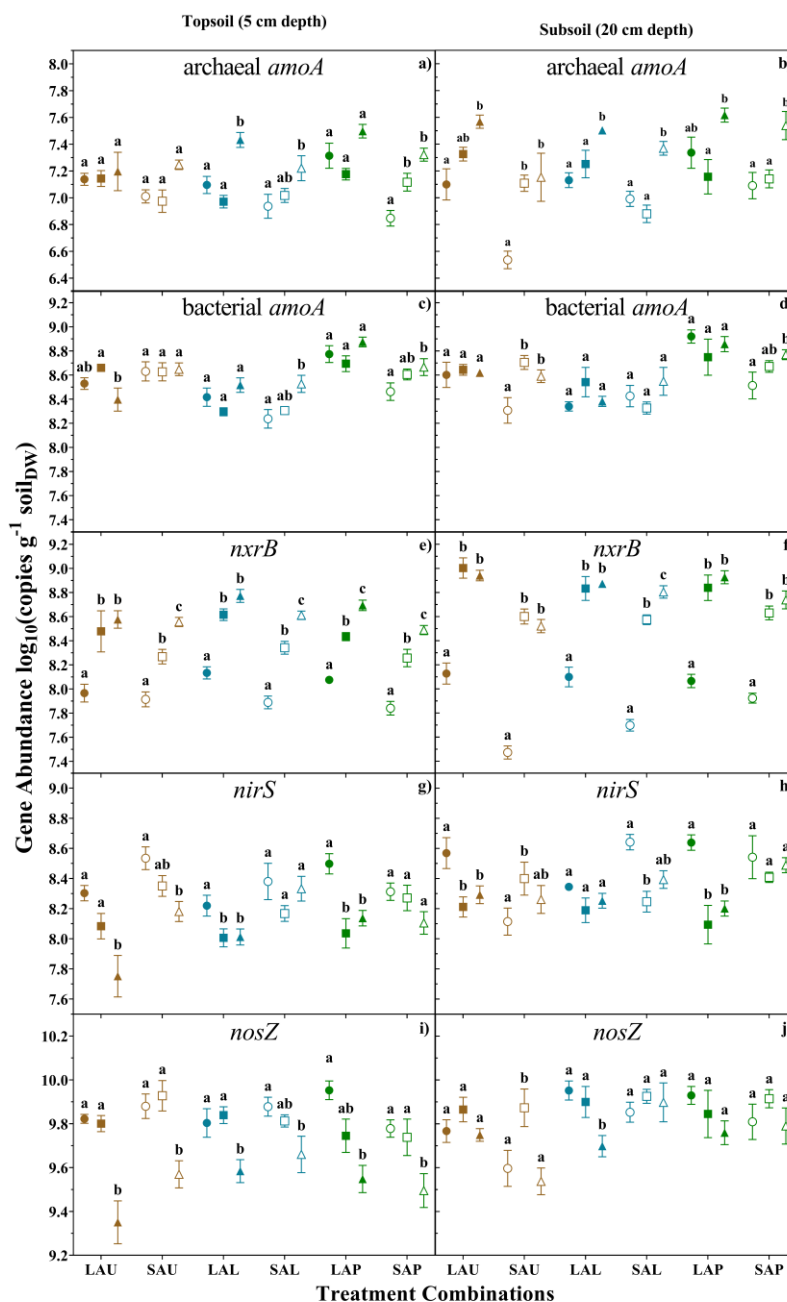


**Figure 3.4.** Log-transformed abundances of N-cycling functional genes for the six treatments of a flooding experiment with model floodplain soils in 5 cm (a, c, e, g and i) and 20 cm depth (b, d, f, h and j), respectively. In the three-letter treatment denotation, LA and SA stand for large and small aggregates, respectively, and the last letter U for unamended, L for litter addition, and P for plant presence. Shown are data for Day 2 (before flooding), Day 12 (peak emissions after flooding), Day 33 (end of the drying phase), as mean  $\pm$  standard error (SE) ( $n = 6$ ); significant changes based on adjusted  $P$  values ( $P < 0.05$ ) for multiple comparisons after Holm (1979) are reported as lower-case letters.

The treatments affected significantly only the abundance of nitrifier genes, whereas the denitrifier genes remained mainly unaffected. Aggregate size significantly affected archaeal *amoA* and *nxB* genes with higher abundances in soils with macroaggregates (Fig. 3.4a, b, e, f; Table 3.2). For *nxB* genes, this effect was much stronger in the subsoil, leading to a significant interaction between MODEL SOIL and DEPTH. The addition of litter or plant presence (TREATMENT) significantly affected the abundance of both bacterial and archaeal functional genes involved in ammonia oxidation (Table 3.2). The effects were much more pronounced, however, for the bacterial *amoA* genes where gene abundance was generally highest in treatments with plants and lowest in treatments with litter addition (Fig. 3.4c, d).

In contrast to the different treatments, flooding, and subsequent drying (expressed in the factor DAY OF EXPERIMENT) significantly affected all functional genes (Table 3.2). However, these effects were clearly weaker for bacterial *amoAs* than for the other genes. The most pronounced effect was observed for *nxB* genes, with a marked increase after flooding into the drying phase (Fig. 3.4e, f). The overall increase in *nxB* genes was more pronounced in the subsoil, which led to a highly significant interaction between DAY OF EXPERIMENT and DEPTH (Table 3.2). By contrast, the abundances of the denitrifier gene *nirS* decreased after flooding (Fig. 3.4g, h), in many cases more prominently in soils with macroaggregates (significant interaction between MODEL SOIL and DAY OF EXPERIMENT, Table 3.2). Towards the end of the drying phase, archaeal *amoAs* increased in abundance irrespective of soil depth (Fig. 3.4a, b). By contrast, *nosZ* genes decreased (Fig. 3.4i, j), but mainly in the topsoil (significant interaction between DAY OF EXPERIMENT and DEPTH).

**Table 3.2:** Main effects and interactions of experimental factors on functional gene abundance. F and P values of significant effects and interaction are reported as follows: ‘\*’  $P < 0.05$ , ‘\*\*’  $P < 0.01$  and ‘\*\*\*’  $P < 0.001$ . Non-significant effects and interactions are indicated as ns.

	Archaeal <i>amoA</i>	Bacterial <i>amoA</i>	<i>nxB</i>	<i>nirS</i>	<i>nosZ</i>
TREATMENT	$F_{(2, 30)} = 10.6^{***}$	$F_{(2, 30)} = 39^{***}$	ns	ns	ns
MODEL SOIL	$F_{(1, 30)} = 52^{***}$	$F_{(1, 30)} = 5.3^*$	$F_{(1, 30)} = 53^{***}$	$F_{(1, 30)} = 12.4^{**}$	ns
DEPTH	$F_{(1, 30)} = 7.5^{**}$	ns	$F_{(1, 30)} = 71^{***}$	$F_{(1, 30)} = 42^{***}$	$F_{(1, 30)} = 25^{***}$
DAY OF EXPERIMENT	$F_{(2, 30)} = 63^{***}$	$F_{(2, 30)} = 5.3^{**}$	$F_{(2, 30)} = 565^{***}$	$F_{(2, 30)} = 36^{***}$	$F_{(2, 30)} = 52^{***}$
TREATMENT × MODEL SOIL	ns	$F_{(2, 30)} = 4.5^*$	ns	ns	ns
TREATMENT × DEPTH	ns	ns	$F_{(2, 30)} = 4.4^*$	ns	$F_{(2, 30)} = 5.4^{**}$
TREATMENT × DAY OF EXP.	$F_{(4, 60)} = 2.7^*$	$F_{(4, 60)} = 2.9^*$	ns	$F_{(4, 60)} = 3.2^*$	$F_{(4, 60)} = 3.1^*$
MODEL SOIL × DEPTH	$F_{(1, 30)} = 4.4^*$	ns	$F_{(1, 30)} = 13.8^{***}$	$F_{(1, 30)} = 5.5^*$	ns
MODEL SOIL × DAY OF EXP.	ns	$F_{(2, 60)} = 4.3^*$	ns	$F_{(2, 60)} = 8.3^{***}$	$F_{(2, 60)} = 4.0^*$
DAY OF EXP. × DEPTH	ns	ns	$F_{(2, 60)} = 49.0^{***}$	$F_{(2, 60)} = 3.6^*$	$F_{(2, 60)} = 19.0^{***}$

### 3.3.3 $^{15}\text{N}$ enrichment of $\text{NO}_x$ in the soil solution

$\text{NO}_x$  compounds measured in the soil solution of all treatments before flooding were characterized by mean  $\delta^{15}\text{N}_{\text{NO}_x}$  values between 5‰ and 10‰ (Fig. 3.5). Since  $\text{NO}_2^-$  concentrations were always at least one order of magnitude lower than those of  $\text{NO}_3^-$  (see chapter 2), the measured  $\delta^{15}\text{N}_{\text{NO}_x}$  can be considered representative of the nitrate N isotope composition. The flooding of the mesocosms induced a phase of nitrate reduction, indicated by a decline in nitrate concentration accompanied by an increase in  $\delta^{15}\text{N}_{\text{NO}_x}$ . This effect was most prominent in the unamended and litter added soils with macroaggregates. In the drying phase, nitrate concentrations continued to decline, and  $\delta^{15}\text{N}_{\text{NO}_x}$  further increased, at least initially. Maximum  $\delta^{15}\text{N}_{\text{NO}_x}$  values were observed in litter added and planted soils with macroaggregates ( $46.2 \pm 4.1$  ‰ and  $41.4 \pm 11.9$  ‰, respectively; mean  $\pm$  SD), whereas the unamended and planted soils with microaggregates were characterized by relatively low  $^{15}\text{NO}_x$  enrichments. The decline of  $\delta^{15}\text{N}_{\text{NO}_x}$  observed for the litter added soils with both, macro- and microaggregates towards the end of the drying phase may indicate a contribution of “light” nitrate produced by ammonium oxidation, which, particularly at the low  $\text{NO}_x$  concentrations observed, can mask the  $^{15}\text{NO}_x$  enrichment due to fractional  $\text{NO}_x$  reduction.

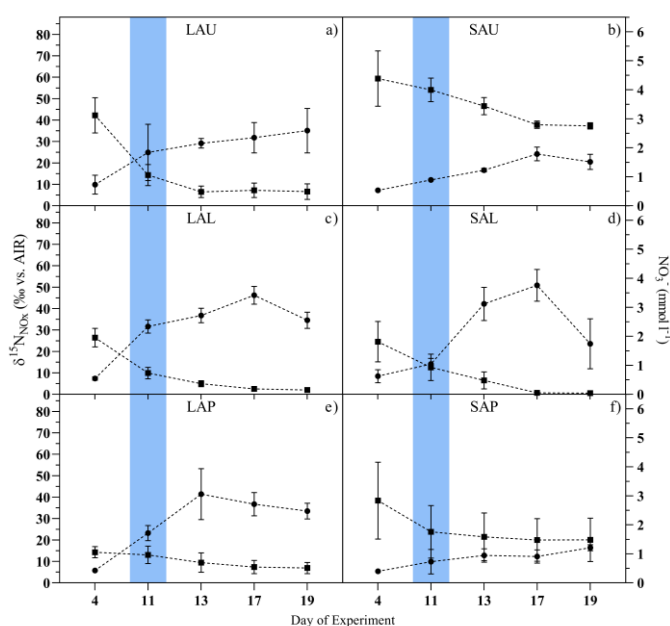


**Figure 3.5.**  $\delta^{15}\text{N}$  of  $\text{NO}_x$  in soil solution (connected black dots; mean  $\pm$  SE;  $n = 2 - 6$ ) at different time points of a flooding experiment using model floodplain soils. In the three-letter treatment denotation, LA and SA stand for large and small aggregates, respectively, and the last letter U for unamended, L for litter addition, and P for plant presence. In addition,  $\text{NO}_3^-$  concentrations are depicted as connected black squares (mean  $\pm$  SE;  $n = 6$ ), as taken from Ley et al. (2018); the blue shading indicates the period of flooding.



### 3.3.4 Source partitioning and reduction of soil emitted N<sub>2</sub>O

The isotopic signatures of soil-emitted N<sub>2</sub>O during the flood-induced period of enhanced emissions revealed temporal dynamics that varied depending on the treatments (Fig. 3.6). Respective treatment effects on the N<sub>2</sub>O production/consumption dynamics in terms of source partitioning between the two process groups ND&HD and NI&FD are indicated in the <sup>15</sup>N SP vs.  $\delta^{18}\text{O}_{\text{N}_2\text{O}/\text{H}_2\text{O}}$  maps (Fig. 3.7). The contribution of ND&HD (i.e.,  $f_{\text{ND\&HD}_{\text{gross}}}$ ), varied markedly depending on the model scenario, whereas the contribution of the residual N<sub>2</sub>O (i.e.,  $r\text{N}_2\text{O}_{\text{total}}$ ) did not differ much between the two scenarios (Fig. 3.8). Overall, scenario M-R yielded lower estimated  $f_{\text{ND\&HD}_{\text{gross}}}$  and higher  $r\text{N}_2\text{O}_{\text{total}}$  values than scenario R-M.

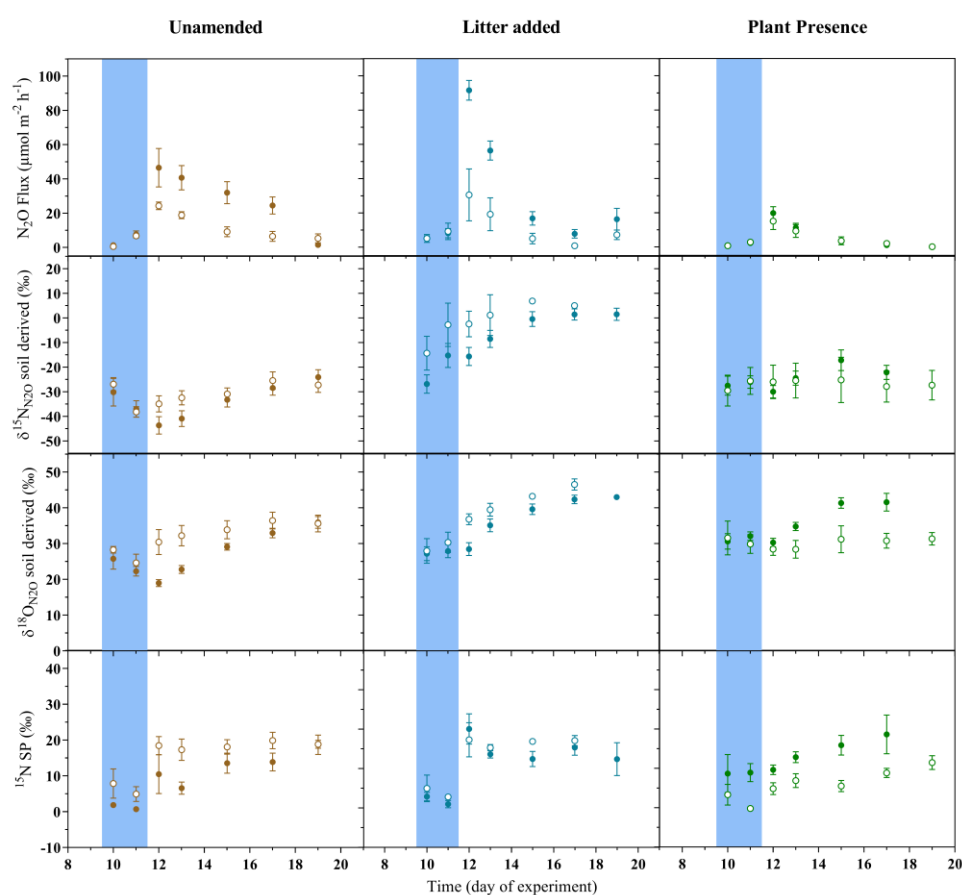


**Figure 3.6.** Efflux and isotopic signature ( $\delta^{15}\text{N}_{\text{N}_2\text{O}}$ ,  $\delta^{18}\text{O}_{\text{N}_2\text{O}}$ , and <sup>15</sup>N SP) of N<sub>2</sub>O emitted at different time points during a flooding experiment with model floodplain soils (filled symbols: large aggregates LA; open symbols: small aggregates SA) that were unamended (left panels, LAU and SAU treatments), mixed with leaf litter from willow (middle panels, LAL and SAL treatments), or planted with willow cuttings (right panels, LAP and SAP treatments); shown are mean  $\pm$  SE for 2 to 6 replicates; efflux data are taken from Ley et al. (2018); the blue shading indicates the period of flooding.

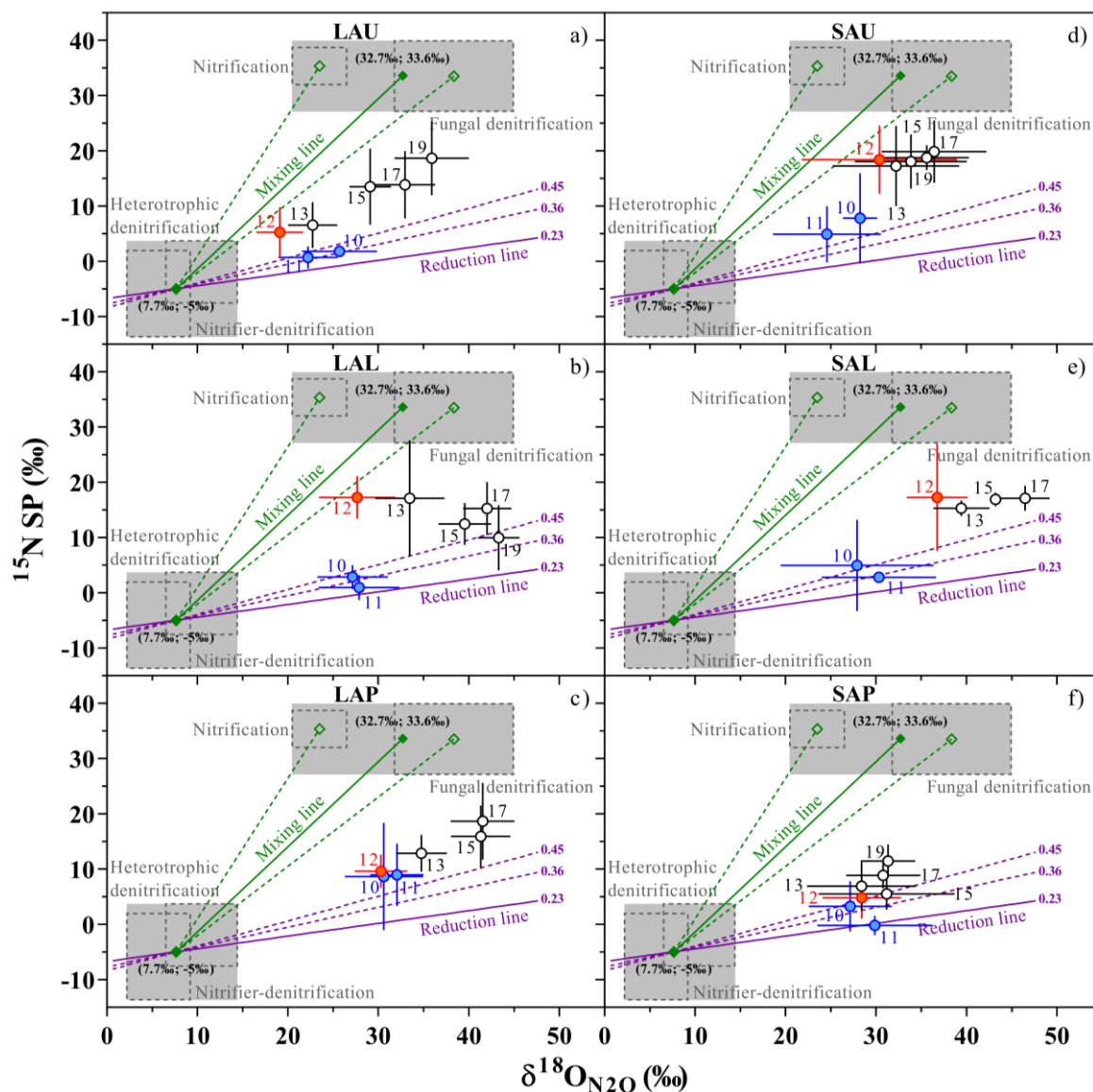


**Figure 3.7.** Dual isotope maps ( $^{15}\text{N SP}$  vs.  $\delta^{18}\text{O}_{\text{N}_2\text{O}}$ ) of  $\text{N}_2\text{O}$  emitted at different time points. LA and SA stand for large and small aggregates, respectively, and the last letter U for unamended, L for litter addition, and P for plant presence, respectively. Numbers indicate the day of the experiment (blue: during the artificial flood; red: beginning of drying phase, peak emissions; black: further drying). Shown are mean values  $\pm$  SD for 2 to 6 replicates. Gray dashed-lined boxes delineate ranges of potential source processes taken from Yu et al. (2020; see supplementary material, Table S3.3). The  $\delta^{18}\text{O}_{\text{N}_2\text{O}}$  values of source process ranges are calculated under the consideration of the respective ambient substrate  $\delta^{18}\text{O}$ : nitrifier-denitrification (ND), heterotrophic denitrification (HD) and FD:  $\delta^{18}\text{O}_{\text{H}_2\text{O}} = -10.2$  ‰ (this study); and nitrification (NI):  $\delta^{18}\text{O}_{\text{O}_2} = 23.5$  ‰. Common endmember isotope values for the process groups ND&HD and NI&FD are shown in parentheses and connected by the mixing line (solid green) used in the M-R model scenario (see also Fig. S3.1). The green dashed lines indicate the hypothetical mixing lines between the ND&HD process group and nitrification or fungal

---

denitrification alone. The N<sub>2</sub>O reduction line used in the reduction-mixing (R-M) scenario (see also Fig. S3.1) is indicated by the purple solid line, calculated from the mean fractionation factors reported in Jinuntuya-Nortman et al. (2008). The purple dashed lines indicate reduction lines as used by Buchen et al. (2018; slope 0.36) or with the mean slope as reported by Yu et al. (2020; slope 0.45).

With the incipient increase in soil-derived N<sub>2</sub>O emission rates during the two-day flood phase, the isotopic composition of the emitted N<sub>2</sub>O did not differ much among the treatments, with  $\delta^{15}\text{N}_{\text{N}_2\text{O}}$ ,  $\delta^{18}\text{O}_{\text{N}_2\text{O}}$  and  $^{15}\text{N}$  SP values mostly in the range of -40 to -20 ‰, 20 to 30 ‰, and -5 and 10 ‰, respectively (Fig. 3.6). The only exception was somewhat higher  $\delta^{15}\text{N}_{\text{N}_2\text{O}}$  values in the litter added soils with microaggregates. In this phase, most data points in the  $^{15}\text{N}$  SP vs.  $\delta^{18}\text{O}_{\text{N}_2\text{O}/\text{H}_2\text{O}}$  map were positioned on, or close to, the reduction line starting from the ND&HD endmember N<sub>2</sub>O isotope signature (Fig. 3.7, blue symbols), indicating an initial contribution almost completely by bacterial denitrification (ND&HD; Fig. 3.7, Fig. 3.8). In both model scenarios, an average of between 20 and 50 % of unreduced N<sub>2</sub>O was emitted in this phase (Fig. 3.8).

On day 12, the first day of the drying phase, when N<sub>2</sub>O emission rates were highest,  $^{15}\text{N}$  SP increased strongly in both variants of the untreated and litter added model soils with macro- or microaggregates, respectively (Fig. 3.6). The corresponding shifts in the  $^{15}\text{N}$  SP vs.  $\delta^{18}\text{O}_{\text{N}_2\text{O}}$  diagrams (Fig. 3.7) indicate a temporarily increased relative contribution of the NI&FD process group (Fig. 3.8). This contribution was particularly high (around 40 %) in the litter added soils with macroaggregates (both model scenario), and the unamended and litter added soils with microaggregates (M-R scenario only). Irrespective of the model scenario, a particularly low degree of N<sub>2</sub>O reduction to N<sub>2</sub> was indicated for the unamended and litter added model soils with macroaggregates.

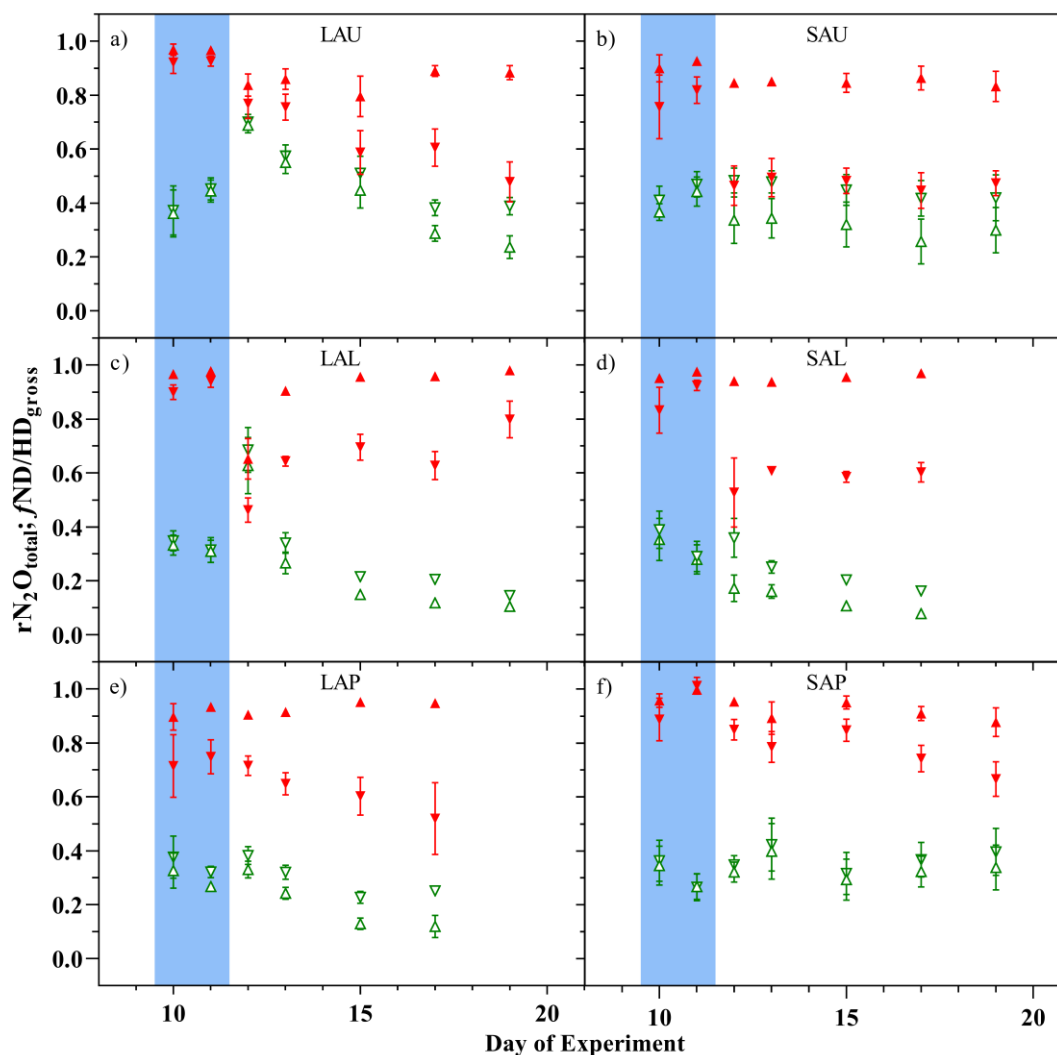


**Figure 3.8.** Contribution of the ND&HD process group to gross  $\text{N}_2\text{O}$  production ( $f\text{ND}\&\text{HD}_{\text{gross}}$ ; red, filled symbols) and residual  $\text{N}_2\text{O}$  produced by both ND&HD and FD&NI process groups ( $r\text{N}_2\text{O}_{\text{total}}$ ; green, open symbols) at different time points during a flooding experiment using model floodplain soils. LA and SA stand for large and small aggregates, respectively, and the last letter U for unamended, L for litter addition, and P for plant presence. These data represent model estimates considering either a M-R scenario (downward-pointing triangles,  $\nabla$  and  $\blacktriangledown$ ) or a R-M scenario (upward-pointing triangles,  $\triangle$  and  $\blacktriangle$ ) (see Fig. S3.1). Shown are mean values  $\pm$  SE for 2 to 6 replicates (see text). The blue shading indicates the period of flooding.

In the later post-flood phase, when  $\text{N}_2\text{O}$  efflux rates decreased again, the  $\text{N}_2\text{O}$  emitted from the unamended soils with micro- and macroaggregates, and litter added soils with micro- and macroaggregates became systematically enriched in both  $^{15}\text{N}$  and  $^{18}\text{O}$  (Fig. 3.6).  $^{15}\text{N}$  SP changes were rather subtle during the entire post-flood phase, except for a steady  $^{15}\text{N}$  SP increase in the unamended and planted soils with macroaggregates. The  $\delta^{18}\text{O}_{\text{N}_2\text{O}}$  increased during the post-flood phase in all treatments but more strongly for treatments with macroaggregates than with

microaggregates (Fig. 3.7). The estimated source partitioning between the two process groups remained relatively constant in treatments with microaggregates (Fig. 3.8). By contrast, in the unamended and the planted soils with macroaggregates, the contribution of the ND&HD process group decreased further (M-R scenario only), whereas in the litter added soils with macroaggregates both model scenarios indicated an anew increase of reductive N<sub>2</sub>O production. Similarly, the calculated fraction of residual N<sub>2</sub>O remained approximately constant in the treatments with microaggregates, but decreased in treatments with macroaggregates, most prominently in the unamended and the litter added soils with macroaggregates.

### 3.4 Discussion

The results from this laboratory experiment with model floodplain soils revealed diverse effects of microhabitats related to soil aggregates, the detritosphere and the rhizosphere on the production pathways of N<sub>2</sub>O and their temporal dynamics during flood-induced phases of elevated emissions, as well as on the related soil microbiome. In the following, we first discuss the differential effects of the experimental treatments and the related microhabitats on the prokaryotic and fungal community structure, followed by a discussion of the potential for specific N transforming processes related to N<sub>2</sub>O production and reduction to occur at different time points. This evaluation of the functional potential provides the basis, upon which we then discuss in detail the processes of N<sub>2</sub>O production and reduction, and their dynamics as constrained by the isotopic signature of the soil-emitted N<sub>2</sub>O.

#### 3.4.1 Treatment-specific, flood-resilient soil microbiomes with a similar potential to produce N<sub>2</sub>O

Our experimental treatments resulted in distinct, but similarly diverse microbial communities. Aggregate size was identified as a major driver differentiating prokaryotic and, to a minor extent, also fungal communities. This observation is in line with recent reports on microbial assemblages in agricultural soils, showing that macro- and microaggregates can hold communities that are distinct from each other (Bach et al., 2018; Davinic et al., 2012; Trivedi et al., 2017). The aggregate-size-specific colonization could be linked to differences in environmental conditions in microhabitats of the intra-aggregate pore space of differently sized aggregates (Kravchenko et al. (2014). This can have direct consequences for the functional diversity of N-cycling microbes (Wilpieszski et al., 2019) and therefore for the production and consumption of N<sub>2</sub>O.

Among the soil amendments, litter addition exerted the most pronounced effect on the soil microbiome. It strongly altered the bacterial and fungal community structures at the class level,

especially in combination with macroaggregates. The introduction of a detritusphere, and along with it a broad range of substrates, was previously found to promote the succession of bacterial and fungal specialists for the decomposition of distinct parts of decaying plant material (Bastian et al., 2009; McMahon et al., 2005). Especially the high relative abundance of *Eurotiomycetes*, *Sordariomycetes* and *Dothiomycetes* in the fungal communities confirmed such a shift towards a saprotrophic community.

In contrast to litter addition, and irrespective of aggregate size, plant presence and related root-soil interactions altered the microbial community only to a minor degree. This is in accordance with earlier studies, e.g., by Urbanová et al. (2015), who found no significant effect of different forest trees on the bacterial communities in bulk soil. Effects of root-soil interactions on the soil microbiome appear to be restricted to a relatively narrow rhizosphere zone, as found, e.g., by Turner et al. (2013) for agricultural plants.

Small, but significant temporal changes of soil prokaryotic communities, as found in our experiment, have been observed before, e.g., by Wilson et al. (2011), and can likely be attributed to sudden flood-induced changes in substrate availability. Also, new microbial niches may have become available during the wetting/drying cycle. In contrast, the relative resilience of the fungal communities to short-term flooding, as also observed by Graupner et al. (2017), could be linked to the development of hyphal networks throughout the soil, allowing fungi to escape temporarily unfavorable environmental conditions. This may also explain why prokaryotic communities were more affected by soil depth than fungal communities.

Based on the compilations of Zumft (1997) and Philippot et al. (2007), and irrespective of treatment, we identified genera potentially comprising denitrifying taxa within the most abundant prokaryotic classes *Planctomycetacia*, *Alphaproteobacteria*, *Betaproteobacteria*, but also the less abundant classes *Actinobacteria*, *Gammaproteobacteria* and *Physisphaerae*. *Betaproteobacteria* also comprised one genus potentially harboring nitrifying taxa, and the important nitrite-oxidizing bacterial taxa *Nitrospira* were found at high relative abundance in the subsoil of treatments with microaggregates. Within those fungal classes, that were particularly abundant in the litter addition treatments, we identified genera known to comprise taxa capable of fungal denitrification, such as *Aspergillus* and *Penicillium* (both *Eurotiomycetes*) in the litter added model soils with macroaggregates, and *Fusarium* and *Cylindrocarpon* (both *Sordariomycetes*) in both litter added model soils with micro- and macroaggregates, respectively (Maeda et al., 2015; Mothapo et al., 2015).

The overall rather subtle flood-related changes in microbial diversity and community structure may be taken as indication for the resilience of the microbial community to fluctuations in redox

conditions during drying-rewetting cycles, which is consistent with observations made by Fierer et al. (2003). Likewise, the microbial community data indicate a treatment- and time-independent potential for N<sub>2</sub>O production by both denitrifiers and nitrifiers, which seems to remain intact throughout flooding and drying phases.

### 3.4.2 Flood-induced changes in the abundance of functional genes related to N<sub>2</sub>O production pathways

Compared to the small effects on the microbial diversity and community structure, flooding led to distinct alterations of DNA-based functional gene abundance. The latter has been identified as a good proxy for specific process potentials, since it has been shown to correspond well with the enzyme activity encoded by the respective genes (Deslippe et al., 2014). Yet, in some studies the abundance of functional genes related to denitrification and nitrification were not correlated with N<sub>2</sub>O fluxes (Niklaus et al., 2016; Qin et al., 2019). This, however, may be because the net N<sub>2</sub>O efflux from soil may not correspond directly with N<sub>2</sub>O production, as is also indicated by the isotopic data in our experiment.

Populations of AOA and AOB seemed to be adapted to a life in floodplain soils, since the rapid changes of redox conditions during the flooding/drying cycle had no effects on the abundance of the related genes. The ~10 times higher copy numbers of bacterial compared to archaeal *amoA* genes in all treatments are characteristic for N-rich carbonate-containing soils, since high total N contents and alkaline pH appear to favor AOB over AOA (Lehtovirta-Morley, 2018; Levy-Booth et al., 2014). The higher abundance of archaeal *amoA* genes in the treatments with macroaggregates than microaggregates agrees well with the findings by Nahidan et al. (2017). The growth of AOA, but not of AOB, in all treatments during the post-flood phase, which was larger in the subsoil, can be explained by the relatively low oxygen (O<sub>2</sub>) requirement of the AOA-specific pathway of NH<sub>3</sub> oxidation that allows AOA to occur also in low-oxygen zones (Schleper and Nicol, 2010). This would enable AOA to grow better than the more oxygen-dependent AOB under prolonged low redox potentials, as observed in our experiment in most of the subsoils during drying (see chapter 2). Such a physiological trait of AOA could be beneficial also in situations, where additional O<sub>2</sub> consumption by heterotrophic processes interferes with nitrification, which may explain the particularly strong increase of archaeal *amoA* in the treatments with litter addition and plant growth, as well as the generally lower abundance of bacterial *amoA* in the litter addition treatments.

The remarkable increase of the *nxrB* gene abundance during the flood phase in all treatments highlights the ability of the versatile NOB to shift between multiple metabolisms under limited O<sub>2</sub> availability (Daims et al., 2016; Freitag et al., 1987). For example, since NOBs can carry

the *nirK* gene, they are able to compete with heterotrophic denitrifiers and denitrifying fungi. Yet, the conversion of  $\text{NO}_3^-$  back to  $\text{NO}_2^-$  by NOB would provide additional substrate for nitrifier denitrification by AOB rather than for denitrifiers, since AOB and NOB often occur in close spatial relationship (Daims et al., 2016). Our *nxrB* gene data suggest that NOBs are particularly competitive in LA, which is indirectly supported by the flood related decline of *nirS* abundance in macroaggregates, possibly because of this competition (see also below). The continuing growth of *nxrB*-bearing microorganisms during the drying phase mainly in model soils with microaggregates may be related to the faster return to oxic conditions in microaggregates (see chapter 2), allowing them to sooner resume aerobic  $\text{NO}_2^-$  oxidation activity than in macroaggregates.

In most natural environments, the abundance of *nirS* genes is found to be higher than of *nirK* genes (Bothe et al., 2000; Maeda et al., 2017; Morales et al., 2010; Zhao et al., 2020). Therefore, we used the abundance of *nirS* as a proxy for the heterotrophic denitrification potential, despite the smaller phylogenetic diversity of *nirS*- than *nirK*-bearing microorganisms (Decleyre et al., 2016; Philippot et al., 2009; Starkenburg et al., 2008). While Blaud et al. (2018) found copy numbers of *nirS* genes similar to our study in a young floodplain forest soil, their *nirS* abundance was similar in different aggregate size fractions, in contrast to our findings, i.e., that microaggregates generally harbored more *nirS* genes than macroaggregates. This discrepancy could be explained by the relatively high N content of our soils compared to those investigated by Blaud et al. (2018), given a study by Li et al. (2020) who showed that the *nirS* abundance in microaggregates increased more strongly than in macroaggregates when nutrients were added. Somewhat surprising was the observed decrease of *nirS* gene abundance during flooding, mainly in macroaggregates. This might be explained by the above-mentioned emerging competition for  $\text{NO}_2^-$  and  $\text{NO}_3^-$  by other microbial groups, such as *nirK* bearing microorganisms like AOBs, NOBs or denitrifying fungi, thus limiting the ability of *nirS* bearing microbes to grow. Such a competition is indicated by the generally opposing trends between *nirS* and *nxrB* copy numbers during flooding.

The *nosZ*-gene-bearing community was affected by none of the experimental factors, and the abundance of the *nosZ* gene was always higher than of the other investigated N-cycling genes in all treatments. Both might be attributed to the broad spectrum of microhabitat preferences by the phylogenetically diverse groups of microorganisms comprising the *nosZ* gene, even including non-denitrifiers (Graf et al., 2014). Therefore, and despite the decrease in the abundance of *nosZ* during drying (mainly in the topsoil), we consider the genetic potential for  $\text{N}_2\text{O}$  reduction to be similar for the whole suite of experimental conditions.



### 3.4.3 N<sub>2</sub>O production by bacterial denitrification during flooding

Based on the isotopic signatures of soil emitted N<sub>2</sub>O during flooding, gross N<sub>2</sub>O production was dominated almost exclusively by the ND&HD process group, irrespective of treatment or N<sub>2</sub>O mixing scenario. This makes the high level of pore water saturation appear as the overarching controlling factor of N<sub>2</sub>O production during this phase. A more frequent reductive N<sub>2</sub>O production is the consequence of stable anoxic conditions throughout the soil column, as indicated by low redox potentials (see chapter 2), and the associated depletion of alternative terminal electron acceptors. Nitrate reduction as most likely N<sub>2</sub>O producing pathway is also indicated by the incipient enrichment of  $\delta^{15}\text{N}_{\text{NOx}}$  (Fig. 3.5). A greater fractional substrate consumption in all treatments with macroaggregates than with microaggregates suggest that soil aggregation supports a greater activity and/or higher abundance of N<sub>2</sub>O-producing denitrifiers. Such oxygen-limited conditions are also conducive to the enhanced transcription of the highly abundant *nosZ* genes, and thus N<sub>2</sub>O reduction (Bergaust et al., 2010; Brenzinger et al., 2015; Buchen et al., 2018). Indeed, relatively high levels of partial N<sub>2</sub>O reduction during the flooding phase, indicated by low levels of residual N<sub>2</sub>O (Fig. 3.8), were estimated by both scenarios of the isotope mapping approach in all treatments. It is therefore likely that extensive N<sub>2</sub>O reduction was at least partly responsible for the relatively low net N<sub>2</sub>O emissions during flooding.

### 3.4.4 N<sub>2</sub>O production pathways in the post-flood phase

After flood recession, markedly increased net N<sub>2</sub>O fluxes were observed in all treatments. At the same time, although heterotrophic denitrification and/or nitrifier-denitrification were still the dominant N<sub>2</sub>O production pathways in most cases, the source partitioning rapidly shifted towards higher contributions from the NI&FD process group. The degree and the dynamics of these contributions depended on the treatment and modelling scenario (Fig. 3.8).

Soil aggregation appeared to promote N<sub>2</sub>O production by the NI&FD process group, considering on the one hand that the most pronounced, and scenario-independent, yet temporary, effect was found in the litter added soils with macroaggregates, and on the other that there was a steady increase of the respective contribution during the entire drying phase in the unamended and planted soils with macroaggregates in the M-R scenario. A factor that could have promoted the concomitant N<sub>2</sub>O production by bacterial denitrification and nitrification is the structural control on gas diffusion in macroaggregates. The complex pore space geometry in macroaggregates creates a heterogeneous small-scale distribution of micro-niches with potentially different redox conditions, as demonstrated by Schlüter et al. (2018). In combination with the still high pore water saturation, as previously reported in chapter 2, this structural

---

characteristic intrinsic to macroaggregates could have led to the co-existence of oxic microhabitats in a well aerated inter-aggregate pore space and anoxic microhabitats within the macroaggregates. This in turn would support the simultaneous activity of both aerobic and anaerobic N<sub>2</sub>O production as previously described by (Hu et al., 2015; Yamamoto et al., 2017). A steady increase of the NI&FD process group contribution, as calculated under M-R scenario assumptions for the unamended and planted soils with macroaggregates, could then be attributed to a systematic increase in the number of more oxygenated zones, where AOBs gradually resume aerobic ammonia oxidation activity. At the same time, N<sub>2</sub>O production by the ND&HD process group became more and more limited to anoxic micro-niches located deeper within the macroaggregates.

Litter addition appeared to have multifaceted effects, depending on the stage within the drying phase. On one hand, highest contributions of the NI&FD process group during peak N<sub>2</sub>O emissions in the litter added model soil with macroaggregates (and in the M-R modelling scenario also in the litter added soil with microaggregates) may be attributed to the fast re-aeration of macropores in the early post-flood phase, promoted by the improvement of the soil structure by buried litter as described by Jarecke et al. (2016). Such an effect would have likely stimulated the source contribution of nitrification rather than of fungal denitrification. Yet, considering the increased abundance of fungal genera comprising potentially denitrifying fungi like *Fusarium spp.* and *Cylindrocarpon spp.* found in the litter added model soils with macro- and microaggregates, respectively, a certain contribution to N<sub>2</sub>O production by fungal denitrification cannot be fully excluded. On the other hand, the return to dominantly N<sub>2</sub>O production by the ND&HD group after peak emissions and throughout the remaining drying phase in both litter addition treatments, may be explained by the functionality of litter as a carbon resource. The presence of readily degradable carbon compounds from the decomposing litter likely stimulated the activity of denitrifiers competing with other heterotrophs and increased the oxygen demand, leading to stable anoxic conditions in the soil columns (Müller and Clough, 2014). Such a reduced O<sub>2</sub> availability was also indicated by the continuously low redox potentials throughout the period of enhanced emissions (see chapter 2), and, in the subsoil of the litter added soil with microaggregates, by the high abundance of methanogenic archaea. Additional evidence for a high denitrifying activity was provided by the almost complete consumption of NO<sub>3</sub><sup>-</sup> in both litter addition treatments accompanied by a strong enrichment in <sup>15</sup>N of the remaining N oxides (Fig. 3.5).

For the unamended and the litter added model soils with microaggregates, the two modelling scenarios led to particularly large differences in the estimated contribution of the NI&FD

process group to N<sub>2</sub>O production during the entire post-flood phase (Fig. 3.8b, d). Again, the two scenarios reflect extreme cases of the combined effects of N<sub>2</sub>O reduction and mixing of the different N<sub>2</sub>O sources, and a co-occurrence of both scenarios is plausible, yet there are indications as to which scenario is more realistic. Considering the less reducing conditions reflected by the high redox potentials in the subsoils of the unamended soils with microaggregates, and the lack of an additional C source stimulating extensive heterotrophic respiration, a sufficient aeration of certain parts of the pore space can be assumed despite the still high WFPS (see chapter 2). As a result, soil gases would also be able to mix more easily. Therefore, the estimates derived from the M-R scenario appear more plausible. In this case, the stable, almost equal contributions to N<sub>2</sub>O production by both process groups reflect the return of nitrifying conditions in aerated parts of the soils, whereas still enough zones in the soil would sustain anoxic conditions for bacterial denitrification. By contrast, under the extensive anoxic conditions promoted by litter decomposition in the litter added soil with microaggregates, as discussed above, it seems more plausible that source partitioning follows the R-M scenario.

In contrast to the other treatments, the changes in source partitioning relative to the flood phase were rather subtle in both variants of planted model soils, i.e., reductive N<sub>2</sub>O production by ND&HD remained remarkably high throughout the drying phase. This is consistent with the previously reported low redox potentials observed for these treatments, especially in the subsoils, where ambient redox conditions were optimal for the formation of denitrification hotspots (see chapter 2). Such reductive conditions in planted soils likely occur due to stimulated microbial respiration by the release of root exudates, which, in concert with root respiration in a highly saturated pore space can lead to severe and ongoing oxygen depletion (Fender et al., 2013). The observed stability in source partitioning further implies that, once anoxic micro-niches have developed in the planted soils, they can be sustained over several days of drying. To some extent this is surprising, since willow root systems, particularly in macroaggregated soils, are known to aerate the rhizosphere via aerenchyma (Randerson et al., 2011). That this process may happen to some degree is suggested by the increasing contribution of the NI&FD process group to N<sub>2</sub>O production with continued soil drying in the M-R scenario. Further insight into N<sub>2</sub>O produced by the ND&HD process group can be obtained from the relative <sup>15</sup>N enrichment of the emitted N<sub>2</sub>O (Fig. 3.6) and the relative abundance of bacterial *amoA* and *nirS* genes (Fig. 3.4). Since nitrifier denitrification is known to be associated with a large N isotope effect ( $\eta_{\text{NH}_4^+ \rightarrow \text{N}_2\text{O}}$ :  $-61.3 \pm 3.1$  ‰; Yoshida, 1988), the particularly low  $\delta^{15}\text{N}_{\text{N}_2\text{O}}$  values measured during peak emissions in the unamended soil with macroaggregates, and to a lesser extent in the unamended soils with microaggregates, point to a large contribution

of this process. At the same time, bacterial *amoA* was about three times more abundant than *nirS* in the unamended model soils with macroaggregates, providing further evidence that the potential for nitrifier denitrification was higher than for heterotrophic denitrification. The higher  $\delta^{15}\text{N}_{\text{N}_2\text{O}}$  values in all other treatments throughout the drying phase may in turn be attributed to the presence of easily degradable carbon compounds from buried litter or root exudation that promotes heterotrophic denitrification.

#### 3.4.5 N<sub>2</sub>O reduction during the drying phase

Consistent with the isotopic constraints on the balance between reductive and oxidative N<sub>2</sub>O production during the initial drying phase, an abrupt decrease in partial N<sub>2</sub>O reduction (i.e., increase in  $r\text{N}_2\text{O}_{\text{total}}$ ) after flood water recession was observed in the unamended and litter added model soil with macroaggregates, respectively (Fig. 3.8). Considering the still large contributions by the ND&HD process group to N<sub>2</sub>O production this suggests a strong aggregate size effect on N<sub>2</sub>O consumption in denitrifying microhabitats. Although the high abundance of *nosZ* genes always indicates a strong N<sub>2</sub>O reduction potential in all treatments, such an apparent accumulation of N<sub>2</sub>O suggests a disruption of the complete denitrification chain at the final step (i.e., N<sub>2</sub>O reduction to N<sub>2</sub>) by the re-aeration of the pore space. It is known that in low-O<sub>2</sub> settings, and in the case of rapid transitions from anoxic to oxic conditions (as was likely the case after the flooding), the activity of N<sub>2</sub>O reductase may be suppressed (Freymond et al., 2013; Morley et al., 2008). Such disruption of N<sub>2</sub>O reduction in parallel with a strong decrease in the  $f\text{ND}\&\text{HD}_{\text{gross}}$  values corresponded with the highest N<sub>2</sub>O flux rates observed in this study, highlighting the susceptibility of this factor combination to support hot spots and moments of N<sub>2</sub>O emissions. Litter addition appeared to accelerate the return to higher levels of partial N<sub>2</sub>O reduction during further drying. Again, this can be explained by the presence of more easily degradable organic matter that stimulates heterotrophic microbial activity (Li et al., 2016), leading to a higher systemic O<sub>2</sub> demand than in the unamended soils.

The low fractions of  $r\text{N}_2\text{O}_{\text{total}}$  in all treatments with microaggregates throughout the post-flood phase imply that N<sub>2</sub>O reduction zones within these soils are more resilient to pore space aeration. Since microaggregates smaller than 200  $\mu\text{m}$  have molecular diffusive distances simply too short to sustain suboxic or anoxic conditions in their centers (Manucharova et al., 2001; Renault and Stengel, 1994), this phenomenon might be attributed rather to the internal pore structure of larger microaggregates (200 to 250  $\mu\text{m}$ ). Once water-saturated, pore water evaporation is hindered by their low porosity and small pore diameters (Chun et al., 2008; Dexter, 1988). This in turn provides efficient diffusion barriers necessary for the formation of stable anoxic micro-niches, in which denitrification can proceed to completion throughout the

experiment. Furthermore, microaggregates tend to arrange themselves more densely, which could lead to the temporary formation of strongly diffusion-limited clusters under high water content. The particularly high degree of N<sub>2</sub>O reduction in the litter added soil with microaggregates may be attributed to the above-mentioned O<sub>2</sub> depletion associated with decaying plant litter, which likely helped to maintain anoxic conditions within the microaggregates. Moreover, in this treatment, nitrate was almost completely consumed at the end of the experiment. When soil nitrate concentrations are close to the detection limit, N<sub>2</sub>O may be the only terminal electron acceptor left for denitrification (Butterbach-Bahl et al., 1998; Chapuis-Lardy et al., 2007).

The presence of a growing *Salix v.* root system appeared to override any aggregate-size effect and led to stable N<sub>2</sub>O reduction at high levels throughout the experiment in the planted model soil with both, macro- and microaggregates, respectively. At the same time, the N<sub>2</sub>O flux rates during the post-flood phase were significantly lower compared to all other treatments. The direct effects of the vegetation in this context remain ambivalent. On the one hand, root respiration in combination with root exudation of labile C compounds and decomposition of dead root cells could have caused a similar O<sub>2</sub>-depleting effect as decaying litter, and, thus, have helped to sustain anoxic microhabitats (Fender et al., 2013). On the other hand, the improved soil structure by root growth and pore aeration by aerenchyma could have led to a lower total number of such anoxic denitrifying microhabitats, keeping overall N<sub>2</sub>O fluxes induced by incomplete denitrification relatively low.

### **3.5 Conclusion**

Taken together, the molecular and isotopic data from our factorial experiment provided new insights into the dynamics of N<sub>2</sub>O production and reduction in floodplain soils during flooding-drying cycles, and how they are affected by soil and plant-related drivers.

Under highly reducing conditions during the flood phase, emitted N<sub>2</sub>O was almost entirely produced by bacterial denitrification, and was partially reduced. Neither soil aggregate size nor soil amendments had any significant effect. By contrast, N<sub>2</sub>O emissions during the post-flood phase appeared to be the result of the interplay of oxidative and reductive N<sub>2</sub>O production in combination with N<sub>2</sub>O reduction, and the balance between the different N<sub>2</sub>O production/reduction processes depended strongly on the experimental factors. Immediately after flood water recession, soil aggregation and structural support by buried leaf litter facilitated the re-aeration of the interaggregate pore space, leading, on the one hand, to a particularly high contribution of nitrifier-produced N<sub>2</sub>O, and, on the other, to the disruption of

N<sub>2</sub>O reduction. Together with the still high N<sub>2</sub>O production by bacterial denitrification in the anoxic interior of aggregates, this resulted in particularly high N<sub>2</sub>O emissions. Upon further drying, the buried leaf litter seemed to play an important role. The elevated O<sub>2</sub> demand by heterotrophic decomposition of the leaf material seemed to re-establish extensive anoxic conditions and thus supported a high degree of reductive N<sub>2</sub>O production and of N<sub>2</sub>O reduction throughout the drying phase, whereas in absence of buried leaf litter, the contribution of N<sub>2</sub>O produced by nitrifiers increased steadily with further drying. In the absence of macroaggregates, the maintenance of anoxic microsites seemed even more dependent on the presence of litter as a C source. The presence of a growing willow largely mitigated the effects of both flooding and soil aggregation on the pathways of N<sub>2</sub>O production and the degree of N<sub>2</sub>O reduction. This may be due to opposing effects of root exudation of easily degradable C compounds on one hand, and rhizosphere aeration via aerenchyma on the other.

In summary, the results of our experiment imply that soil aggregation and buried litter promote conditions of N<sub>2</sub>O production, which can lead to particularly high temporary N<sub>2</sub>O emissions after flooding, whereas the presence of *Salix viminalis* appears to have a buffering effect in this regard. The mitigating effect of willow-planted soils towards lower N<sub>2</sub>O emissions appears as a highly desirable trait in the context of restoration of river floodplains. Furthermore, while we could clearly demonstrate the diagnostic value of the isotopic composition of emitted N<sub>2</sub>O in combination with data on the soil microbiome to deduce N<sub>2</sub>O production pathways and the degree of N<sub>2</sub>O reduction, the isotope mapping approach has limitations that are related to the ambiguity of isotopic enrichment and site preference values associated to specific processes. Since we found molecular evidence that buried leaf litter may promote fungal denitrifiers, improved, or alternative, methods are needed to disentangle N<sub>2</sub>O production by nitrification versus fungal denitrification in floodplain soils.

*Data availability.* All data are openly available at [www.envidat.ch](http://www.envidat.ch)

*Conflicts of interest.* The authors declare that they have no known competing financial interests or personal relationships that could have appeared to influence the work reported in this paper.

*Authors contributions.* The initial concept of the experiment was developed by JL, MFL and PAN. ML planned and designed the experiments in detail, set them up and conducted them. PAN supervised the measurement of N<sub>2</sub>O gas concentrations and helped with data analysis, ML conducted all other measurements and data analyses. MH designed and provided training for

the bioinformatics pipeline. TK and MFL supervised IRMS measurements and isotope data interpretation. ML wrote the manuscript together with MFL and JL, with input from all other co-authors.

### **Acknowledgements**

The authors thank Dr. Daniel B. Nelson of the Physiological Plant Ecology group at the Botanical Institute of the University of Basel for conducting the isotopic measurements of the pore water. We thank Beat Stierli of the research unit Forest Soils and Biogeochemistry, research group Rhizosphere Processes of the Swiss Federal Institute for Forest, Snow and Landscape Research (WSL) for his assistance with molecular biological analyses. This study was funded by the Swiss National Science Foundation (SNSF) under the grant number 200021\_147002, as well as by financial resources of WSL and the University of Basel.

---

## References

- Arp, D.J., Stein, L.Y., 2003. Metabolism of Inorganic N Compounds by Ammonia-Oxidizing Bacteria. *Critical Reviews in Biochemistry and Molecular Biology* 38, 471–495. doi:10.1080/10409230390267446
- Bach, E.M., Williams, R.J., Hargreaves, S.K., Yang, F., Hofmockel, K.S., 2018. Greatest soil microbial diversity found in micro-habitats. *Soil Biology and Biochemistry* 118, 217–226. doi:10.1016/j.soilbio.2017.12.018
- Baggs, E.M., 2008. A review of stable isotope techniques for N<sub>2</sub>O source partitioning in soils: recent progress, remaining challenges and future considerations. *Rapid Communications in Mass Spectrometry* 22, 1664–1672. doi:10.1002/rcm.3456
- Bastian, F., Bouziri, L., Nicolardot, B., Ranjard, L., 2009. Impact of wheat straw decomposition on successional patterns of soil microbial community structure. *Soil Biology and Biochemistry* 41, 262–275. doi:10.1016/j.soilbio.2008.10.024
- Bergaust, L., Mao, Y., Bakken, L.R., Frostegard, A., 2010. Denitrification Response Patterns during the Transition to Anoxic Respiration and Posttranscriptional Effects of Suboptimal pH on Nitrogen Oxide Reductase in *Paracoccus denitrificans*. *Applied and Environmental Microbiology* 76, 6387–6396. doi:10.1128/AEM.00608-10
- Blagodatsky, S., Smith, P., 2012. Soil physics meets soil biology: Towards better mechanistic prediction of greenhouse gas emissions from soil. *Soil Biology and Biochemistry* 47, 78–92. doi:10.1016/j.soilbio.2011.12.015
- Blaud, A., van der Zaan, B., Menon, M., Lair, G.J., Zhang, D., Huber, P., Schiefer, J., Blum, W.E.H., Kitzler, B., Wei, E.H., van Gaans, P., Banwart, S., 2018. The abundance of nitrogen cycle genes and potential greenhouse gas fluxes depends on land use type and little on soil aggregate size. *Applied Soil Ecology* 125, 1–11. doi:10.1016/j.apsoil.2017.11.026
- Bothe, H., Jost, G., Schloter, M., Ward, B.B., Witzel, K.-P., 2000. Molecular analysis of ammonia oxidation and denitrification in natural environments. *FEMS Microbiology Reviews* 24, 673–690. doi:10.1111/j.1574-6976.2000.tb00566.x
- Braker, G., Zhou, J., Wu, L., Devol, A.H., Tiedje, J.M., 2000. Nitrite reductase genes (*nirK* and *nirS*) as functional markers to investigate diversity of denitrifying bacteria in pacific northwest marine sediment communities. *Applied and Environmental Microbiology* 66, 2096–2104. doi:10.1128/AEM.66.5.2096-2104.2000
- Brenzinger, K., Dörsch, P., Braker, G., 2015. pH-driven shifts in overall and transcriptionally active denitrifiers control gaseous product stoichiometry in growth experiments with extracted bacteria from soil. *Frontiers in Microbiology* 6, 1–11. doi:10.3389/fmicb.2015.00961
- Buchen, C., Lewicka-Szczebak, D., Flessa, H., Well, R., 2018. Estimating N<sub>2</sub>O processes during grassland renewal and grassland conversion to maize cropping using N<sub>2</sub>O isotopocules. *Rapid Communications in Mass Spectrometry* 32, 1053–1067. doi:10.1002/rcm.8132
- Butler, D.G., Cullis, B.R., Gilmour, A.R., Gogel, B.J., Thompson, R., 2017. ASReml-R Reference Manual Version 4. ASReml-R Reference Manual 176.
- Butterbach-Bahl, K., Gasche, R., Huber, C., Kreutzer, K., Papen, H., 1998. Impact of N-input by wet deposition on N-trace gas fluxes and CH<sub>4</sub>-oxidation in spruce forest ecosystems of the temperate zone in Europe. *Atmospheric Environment* 32, 559–564. doi:10.1016/S1352-2310(97)00234-3



- Cantera, J.J.L., Stein, L.Y., 2007. Molecular diversity of nitrite reductase genes (*nirK*) in nitrifying bacteria. *Environmental Microbiology* 9, 765–776. doi:10.1111/j.1462-2920.2006.01198.x
- Casciotti, K.L., Sigman, D.M., Hastings, M.G., Böhlke, J.K., Hilkert, A., 2002. Measurement of the oxygen isotopic composition of nitrate in seawater and freshwater using the denitrifier method. *Analytical Chemistry* 74, 4905–4912. doi:10.1021/ac020113w
- Chapuis-Lardy, L., Wrage, N., Metay, A., Chotte, J.L., Bernoux, M., 2007. Soils, a sink for N<sub>2</sub>O? A review. *Global Change Biology* 13, 1–17. doi:10.1111/j.1365-2486.2006.01280.x
- Chun, H.C., Giménez, D., Yoon, S.W., 2008. Morphology, lacunarity and entropy of intra-aggregate pores: Aggregate size and soil management effects. *Geoderma* 146, 83–93. doi:10.1016/j.geoderma.2008.05.018
- Ciais, P., Sabine, C., Bala, G., Al., E., Bopp, L., Brovkin, V., Canadell, J., Chhabra, A., DeFries, R., Galloway, J., Heimann, M., Jones, C., Quéré, C. le, Myneni, R., Piao, S., Thornton, P., Al., E., 2013. Carbon and Other Biogeochemical Cycles, in: Intergovernmental Panel on Climate Change (Ed.), *Climate Change 2013 - The Physical Science Basis*. Cambridge University Press, Cambridge, pp. 465–570. doi:10.1017/CBO9781107415324.015
- Cline, L.C., Zak, D.R., 2015. Soil microbial communities are shaped by plant-driven changes in resource availability during secondary succession. *Ecology* 96, 3374–3385. doi:10.1890/15-0184.1
- Cole, J.R., Wang, Q., Cardenas, E., Fish, J., Chai, B., Farris, R.J., Kulam-Syed-Mohideen, A.S., McGarrell, D.M., Marsh, T., Garrity, G.M., Tiedje, J.M., 2009. The Ribosomal Database Project: Improved alignments and new tools for rRNA analysis. *Nucleic Acids Research* 37, 141–145. doi:10.1093/nar/gkn879
- Craine, J.M., Brookshire, E.N.J., Cramer, M.D., Hasselquist, N.J., Koba, K., Marin-Spiotta, E., Wang, L., 2015. Ecological interpretations of nitrogen isotope ratios of terrestrial plants and soils. *Plant and Soil* 396, 1–26. doi:10.1007/s11104-015-2542-1
- Daims, H., Lückner, S., Wagner, M., 2016. A New Perspective on Microbes Formerly Known as Nitrite-Oxidizing Bacteria. *Trends in Microbiology* 24, 699–712. doi:10.1016/j.tim.2016.05.004
- Davinic, M., Fultz, L.M., Acosta-Martinez, V., Calderón, F.J., Cox, S.B., Dowd, S.E., Allen, V.G., Zak, J.C., Moore-Kucera, J., 2012. Pyrosequencing and mid-infrared spectroscopy reveal distinct aggregate stratification of soil bacterial communities and organic matter composition. *Soil Biology and Biochemistry* 46, 63–72. doi:10.1016/j.soilbio.2011.11.012
- Decleyre, H., Heylen, K., Bjorn, T., Willems, A., 2016. Highly diverse *nirK* genes comprise two major clades that harbour ammonium-producing denitrifiers. *BMC Genomics* 17, 155. doi:10.1186/s12864-016-2465-0
- Decock, C., Six, J., 2013. How reliable is the intramolecular distribution of <sup>15</sup>N in N<sub>2</sub>O to source partition N<sub>2</sub>O emitted from soil? *Soil Biology and Biochemistry* 65, 114–127. doi:10.1016/j.soilbio.2013.05.012
- Denk, T.R.A., Mohn, J., Decock, C., Lewicka-Szczepak, D., Harris, E., Butterbach-Bahl, K., Kiese, R., Wolf, B., 2017. The nitrogen cycle: A review of isotope effects and isotope modeling approaches. *Soil Biology and Biochemistry* 105, 121–137. doi:10.1016/j.soilbio.2016.11.015
- Deslippe, J.R., Jamali, H., Jha, N., Saggari, S., 2014. Denitrifier community size, structure and activity along a gradient of pasture to riparian soils. *Soil Biology and Biochemistry* 71, 48–60. doi:10.1016/j.soilbio.2014.01.007
- Dexter, A.R., 1988. Advances in characterization of soil structure. *Soil and Tillage Research* 11, 199–238. doi:https://doi.org/10.1016/0167-1987(88)90002-5

- Fender, A.-C., Leuschner, C., Schützenmeister, K., Gansert, D., Jungkunst, H.F., 2013. Rhizosphere effects of tree species – Large reduction of N<sub>2</sub>O emission by saplings of ash, but not of beech, in temperate forest soil. *European Journal of Soil Biology* 54, 7–15. doi:10.1016/j.ejsobi.2012.10.010
- Fierer, N., Schimel, J.P., Holden, P.A., 2003. Influence of Drying-Rewetting Frequency on Soil Bacterial Community Structure. *Microbial Ecology* 45, 63–71. doi:10.1007/s00248-002-1007-2
- Fournier, B., Guenat, C., Bullinger-Weber, G., Mitchell, E.A.D., 2013. Spatio-temporal heterogeneity of riparian soil morphology in a restored floodplain. *Hydrology and Earth System Sciences* 17, 4031–4042. doi:10.5194/hess-17-4031-2013
- Frame, C.H., Casciotti, K.L., 2010. Biogeochemical controls and isotopic signatures of nitrous oxide production by a marine ammonia-oxidizing bacterium. *Biogeosciences* 7, 2695–2709. doi:10.5194/bg-7-2695-2010
- Frame, C.H., Lau, E., Joseph Nolan, E., Goepfert, T.J., Lehmann, M.F., 2017. Acidification enhances hybrid N<sub>2</sub>O production associated with aquatic ammonia-oxidizing microorganisms. *Frontiers in Microbiology* 7, 1–23. doi:10.3389/fmicb.2016.02104
- Freitag, A., Rudert, M., Bock, E., 1987. Growth of *Nitrobacter* by dissimilatory nitrate reduction. *FEMS Microbiology Letters* 48, 105–109. doi:10.1111/j.1574-6968.1987.tb02524.x
- Frey, B., Carnol, M., Dharmarajah, A., Brunner, I., Schleppei, P., 2020. Only Minor Changes in the Soil Microbiome of a Sub-alpine Forest After 20 Years of Moderately Increased Nitrogen Loads. *Frontiers in Forests and Global Change* 3, 1–18. doi:10.3389/ffgc.2020.00077
- Frey, B., Rime, T., Phillips, M., Stierli, B., Hajdas, I., Widmer, F., Hartmann, M., 2016. Microbial diversity in European alpine permafrost and active layers. *FEMS Microbiology Ecology* 92, fiw018. doi:10.1093/femsec/fiw018
- Freymond, C. v., Wenk, C.B., Frame, C.H., Lehmann, M.F., 2013. Year-round N<sub>2</sub>O production by benthic NO<sub>x</sub> reduction in a monomictic south-alpine lake. *Biogeosciences* 10, 8373–8383. doi:10.5194/bg-10-8373-2013
- Gleeson, D.B., Müller, C., Banerjee, S., Ma, W., Siciliano, S.D., Murphy, D. V., 2010. Response of ammonia oxidizing archaea and bacteria to changing water filled pore space. *Soil Biology and Biochemistry* 42, 1888–1891. doi:10.1016/j.soilbio.2010.06.020
- Graf, D.R.H., Jones, C.M., Hallin, S., 2014. Intergenomic Comparisons Highlight Modularity of the Denitrification Pathway and Underpin the Importance of Community Structure for N<sub>2</sub>O Emissions. *PLoS ONE* 9, e114118. doi:10.1371/journal.pone.0114118
- Graupner, N., Röhl, O., Jensen, M., Beisser, D., Begerow, D., Boenigk, J., 2017. Effects of short-term flooding on aquatic and terrestrial microeukaryotic communities: a mesocosm approach. *Aquatic Microbial Ecology* 80, 257–272. doi:10.3354/ame01853
- Henry, S., Texier, S., Hallet, S., Bru, D., Dambreville, C., Chèneby, D., Bizouard, F., Germon, J.C., Philippot, L., 2008. Disentangling the rhizosphere effect on nitrate reducers and denitrifiers: insight into the role of root exudates. *Environmental Microbiology* 10, 3082–3092. doi:10.1111/j.1462-2920.2008.01599.x
- Herzog, C., Hartmann, M., Frey, B., Stierli, B., Rumpel, C., Buchmann, N., Brunner, I., 2019. Microbial succession on decomposing root litter in a drought-prone Scots pine forest. *The ISME Journal* 13, 2346–2362. doi:10.1038/s41396-019-0436-6
- Hill, A.R., 2011. Buried organic-rich horizons: their role as nitrogen sources in stream riparian zones. *Biogeochemistry* 104, 347–363. doi:10.1007/s10533-010-9507-5

- Holm, S., 1979. A Simple Sequentially Rejective Multiple Test Procedure. *Scandinavian Journal of Statistics* 6, 65–70.
- Hothorn, T., Bretz, F., Westfall, P., 2008. Simultaneous Inference in General Parametric Models. *Biometrical Journal* 50, 346–363. doi:10.1002/bimj.200810425
- Hryniewicz, K., Toljander, Y.K., Baum, C., Fransson, P.M.A., Taylor, A.F.S., Weih, M., 2012. Correspondence of ectomycorrhizal diversity and colonisation of willows (*Salix* spp.) grown in short rotation coppice on arable sites and adjacent natural stands. *Mycorrhiza* 22, 603–613. doi:10.1007/s00572-012-0437-z
- Hu, H.-W., Chen, D., He, J.-Z., 2015. Microbial regulation of terrestrial nitrous oxide formation: understanding the biological pathways for prediction of emission rates. *FEMS Microbiology Reviews* 39, 729–749. doi:10.1093/femsre/fuv021
- Jarecke, K.M., Loecke, T.D., Burgin, A.J., 2016. Coupled soil oxygen and greenhouse gas dynamics under variable hydrology. *Soil Biology and Biochemistry* 95, 164–172. doi:10.1016/j.soilbio.2015.12.018
- Jinuntuya-Nortman, M., Sutka, R.L., Ostrom, P.H., Gandhi, H., Ostrom, N.E., 2008. Isotopologue fractionation during microbial reduction of  $N_2O$  within soil mesocosms as a function of water-filled pore space. *Soil Biology and Biochemistry* 40, 2273–2280. doi:10.1016/j.soilbio.2008.05.016
- Jones, L.C., Peters, B., Lezama Pacheco, J.S., Casciotti, K.L., Fendorf, S., 2015. Stable isotopes and iron oxide mineral products as markers of chemodenitrification. *Environmental Science and Technology* 49, 3444–3452. doi:10.1021/es504862x
- Knowles, R., 1982. Denitrification. *Microbiological Reviews* 46, 43–70. doi:10.1016/0968-0004(76)90171-7
- Kool, D.M., Wrage, N., Oenema, O., Dolfing, J., van Groenigen, J.W., 2007. Oxygen exchange between (de)nitrification intermediates and  $H_2O$  and its implications for source determination of  $NO_3^-$  and  $N_2O$ : a review. *Rapid Communications in Mass Spectrometry* 21, 3569–3578. doi:10.1002/rcm.3249
- Kool, D.M., Wrage, N., Zechmeister-Boltenstern, S., Pfeiffer, M., Brus, D., Oenema, O., van Groenigen, J.W., 2010. Nitrifier denitrification can be a source of  $N_2O$  from soil: A revised approach to the dual-isotope labelling method. *European Journal of Soil Science* 61, 759–772. doi:10.1111/j.1365-2389.2010.01270.x
- Kravchenko, A.N., Negassa, W.C., Guber, A.K., Hildebrandt, B., Marsh, T.L., Rivers, M.L., 2014. Intra-aggregate Pore Structure Influences Phylogenetic Composition of Bacterial Community in Macroaggregates. *Soil Science Society of America Journal* 78, 1924–1939. doi:10.2136/sssaj2014.07.0308
- Kuznetsova, A., Brockhoff, P.B., Christensen, R.H.B., 2017. lmerTest Package: Tests in Linear Mixed Effects Models. *Journal of Statistical Software* 82. doi:10.18637/jss.v082.i13
- Lathi, L., Shetty, S., 2012-2019, microbiome R package <http://microbiome.github.io>.
- Laughlin, R.J., Stevens, R.J., 2002. Evidence for Fungal Dominance of Denitrification and Codenitrification in a Grassland Soil. *Soil Science Society of America Journal* 66, 1540. doi:10.2136/sssaj2002.1540
- Laughlin, R.J., Stevens, R.J., Müller, C., Watson, C.J., 2008. Evidence that fungi can oxidize  $NH_4^+$  to  $NO_3^-$  in a grassland soil. *European Journal of Soil Science* 59, 285–291. doi:10.1111/j.1365-2389.2007.00995.x
- Lehtovirta-Morley, L.E., 2018. Ammonia oxidation: Ecology, physiology, biochemistry and why they must all come together. *FEMS Microbiology Letters* 365, 1–9. doi:10.1093/femsle/fny058
- Levy-Booth, D.J., Prescott, C.E., Grayston, S.J., 2014. Microbial functional genes involved in nitrogen fixation, nitrification and denitrification in forest ecosystems. *Soil Biology and Biochemistry* 75, 11–25. doi:10.1016/j.soilbio.2014.03.021

- 
- Lewicka-Szczebak, D., Augustin, J., Giesemann, A., Well, R., 2017. Quantifying N<sub>2</sub>O reduction to N<sub>2</sub> based on N<sub>2</sub>O isotopocules – validation with independent methods (helium incubation and <sup>15</sup>N gas flux method). *Biogeosciences* 14, 711–732. doi:10.5194/bg-14-711-2017
- Lewicka-Szczebak, D., Dyckmans, J., Kaiser, J., Marca, A., Augustin, J., Well, R., 2016. Oxygen isotope fractionation during N<sub>2</sub>O production by soil denitrification. *Biogeosciences* 13, 1129–1144. doi:10.5194/bg-13-1129-2016
- Lewicka-Szczebak, D., Piotr Lewicki, M., Well, R., 2020. N<sub>2</sub>O isotope approaches for source partitioning of N<sub>2</sub>O production and estimation of N<sub>2</sub>O reduction-validation with the <sup>15</sup>N gas-flux method in laboratory and field studies. *Biogeosciences* 17, 5513–5537. doi:10.5194/bg-17-5513-2020
- Lewicka-Szczebak, D., Well, R., Köster, J.R., Fuß, R., Senbayram, M., Dittert, K., Flessa, H., 2014. Experimental determinations of isotopic fractionation factors associated with N<sub>2</sub>O production and reduction during denitrification in soils. *Geochimica et Cosmochimica Acta* 134, 55–73. doi:10.1016/j.gca.2014.03.010
- Ley, M., Lehmann, M.F., Niklaus, P.A., Luster, J., 2018. Alteration of nitrous oxide emissions from floodplain soils by aggregate size, litter accumulation and plant–soil interactions. *Biogeosciences* 15, 7043–7057. doi:10.5194/bg-15-7043-2018
- Li, P.-P., Zhang, S.-Q., Li, F., Zhang, Y., Han, Y., 2020. Long term combined fertilization and soil aggregate size on the denitrification and community of denitrifiers. *Applied Soil Ecology* 156, 103718. doi:10.1016/j.apsoil.2020.103718
- Li, X., Sørensen, P., Olesen, J.E., Petersen, S.O., 2016. Evidence for denitrification as main source of N<sub>2</sub>O emission from residue-amended soil. *Soil Biology and Biochemistry* 92, 153–160. doi:10.1016/j.soilbio.2015.10.008
- Maeda, K., Spor, A., Edel-Hermann, V., Heraud, C., Breuil, M.C., Bizouard, F., Toyoda, S., Yoshida, N., Steinberg, C., Philippot, L., 2015. N<sub>2</sub>O production, a widespread trait in fungi. *Scientific Reports* 5, 9697. doi:10.1038/srep09697
- Maeda, K., Toyoda, S., Philippot, L., Hattori, S., Nakajima, K., Ito, Y., Yoshida, N., 2017. Relative Contribution of *nirK*- and *nirS*- Bacterial Denitrifiers as Well as Fungal Denitrifiers to Nitrous Oxide Production from Dairy Manure Compost. *Environmental Science & Technology* 51, 14083–14091. doi:10.1021/acs.est.7b04017
- Manucharova, N.A., Stepanov, A.L., Umarov, M.M., 2001. Microbial transformation of nitrogen in water-stable aggregates of various soil types. *EURASIAN SOIL SCIENCE* 34, 1125–1131.
- McIlvin, M.R., Casciotti, K.L., 2010. Fully automated system for stable isotopic analyses of dissolved nitrous oxide at natural abundance levels. *Limnology and Oceanography: Methods* 8, 54–66. doi:10.4319/lom.2010.8.54
- McMahon, S.K., Williams, M.A., Bottomley, P.J., Myrold, D.D., 2005. Dynamics of Microbial Communities during Decomposition of Carbon-13 Labeled Ryegrass Fractions in Soil. *Soil Science Society of America Journal* 69, 1238–1247. doi:10.2136/sssaj2004.0289
- McMurdie, P.J., Holmes, S., 2013. Phyloseq: An R Package for Reproducible Interactive Analysis and Graphics of Microbiome Census Data. *PLoS ONE* 8. doi:10.1371/journal.pone.0061217
- Morales, S.E., Cosart, T., Holben, W.E., 2010. Bacterial gene abundances as indicators of greenhouse gas emission in soils. *ISME Journal* 4, 799–808. doi:10.1038/ismej.2010.8
-

- Morley, N., Baggs, E.M., Dörsch, P., Bakken, L., 2008. Production of NO, N<sub>2</sub>O and N<sub>2</sub> by extracted soil bacteria, regulation by NO<sub>2</sub><sup>-</sup> and O<sub>2</sub> concentrations. *FEMS Microbiology Ecology* 65, 102–112. doi:10.1111/j.1574-6941.2008.00495.x
- Mothapo, N., Chen, H., Cubeta, M.A., Grossman, J.M., Fuller, F., Shi, W., 2015. Phylogenetic, taxonomic and functional diversity of fungal denitrifiers and associated N<sub>2</sub>O production efficacy. *Soil Biology and Biochemistry* 83, 160–175. doi:10.1016/j.soilbio.2015.02.001
- Müller, C., Clough, T.J., 2014. Advances in understanding nitrogen flows and transformations: Gaps and research pathways. *Journal of Agricultural Science* 152, S34–S44. doi:10.1017/S0021859613000610
- Mummey, D., Holben, W., Six, J., Stahl, P., 2006. Spatial Stratification of Soil Bacterial Populations in Aggregates of Diverse Soils. *Microbial Ecology* 51, 404–411. doi:10.1007/s00248-006-9020-5
- Nahidan, S., Nourbakhsh, F., Henneberger, R., Lazzaro, A., Zeyer, J., 2017. Aggregate Size Distribution of Ammonia-Oxidizing Bacteria and Archaea at Different Landscape Positions. *Geomicrobiology Journal* 34, 895–902. doi:10.1080/01490451.2017.1297511
- Newberry, S.L., Nelson, D.B., Kahmen, A., 2017. Cryogenic vacuum artifacts do not affect plant water-uptake studies using stable isotope analysis. *Ecohydrology* 10, 1–10. doi:10.1002/eco.1892
- Niklaus, P.A., le Roux, X., Poly, F., Buchmann, N., Scherer-Lorenzen, M., Weigelt, A., Barnard, R.L., 2016. Plant species diversity affects soil–atmosphere fluxes of methane and nitrous oxide. *Oecologia* 181, 919–930. doi:10.1007/s00442-016-3611-8
- Oksanen, J., Blanchet, F.G., Friendly, M., Kindt, R., Legendre, P., Mcglinn, D., Minchin, P.R., O’hara, R.B., Simpson, G.L., Solymos, P., Stevens, H.H., Szoecs, E., Wagner, H., 2019. *vegan: Community Ecology Package*. R Package Version 2.5-5. doi:https://cran.r-project.org/package=vegan
- Opdyke, M.R., Ostrom, N.E., Ostrom, P.H., 2009. Evidence for the predominance of denitrification as a source of N<sub>2</sub>O in temperate agricultural soils based on isotopologue measurements. *Global Biogeochemical Cycles* 23, 1–10. doi:10.1029/2009GB003523
- Ostrom, N.E., Ostrom, P.H., 2012. The Isotopomers of Nitrous Oxide: Analytical Considerations and Application to Resolution of Microbial Production Pathways, in: *Handbook of Environmental Isotope Geochemistry*. Springer Berlin Heidelberg, Berlin, Heidelberg, pp. 453–476. doi:10.1007/978-3-642-10637-8\_23
- Ostrom, N.E., Pitt, A., Sutka, R., Ostrom, P.H., Grandy, A.S., Huizinga, K.M., Robertson, G.P., 2007. Isotopologue effects during N<sub>2</sub>O reduction in soils and in pure cultures of denitrifiers. *Journal of Geophysical Research* 112, G02005. doi:10.1029/2006JG000287
- Pester, M., Maixner, F., Berry, D., Rattei, T., Koch, H., Lückner, S., Nowka, B., Richter, A., Spieck, E., Lebedeva, E., Loy, A., Wagner, M., Daims, H., 2014. *NxrB* encoding the beta subunit of nitrite oxidoreductase as functional and phylogenetic marker for nitrite-oxidizing *Nitrospira*. *Environmental Microbiology* 16, 3055–3071. doi:10.1111/1462-2920.12300
- Philippot, L., Andert, J., Jones, C.M., Bru, D., Hallin, S., 2011. Importance of denitrifiers lacking the genes encoding the nitrous oxide reductase for N<sub>2</sub>O emissions from soil. *Global Change Biology* 17, 1497–1504. doi:10.1111/j.1365-2486.2010.02334.x
- Philippot, Laurent, Čuhel, J., Saby, N.P.A., Chêneby, D., Chroňáková, A., Bru, D., Arrouays, D., Martin-Laurent, F., Šimek, M., 2009. Mapping field-scale spatial patterns of size and activity of the denitrifier community. *Environmental Microbiology* 11, 1518–1526. doi:10.1111/j.1462-2920.2009.01879.x

- Philippot, L., Hallin, S., Börjesson, G., Baggs, E.M., 2009. Biochemical cycling in the rhizosphere having an impact on global change. *Plant and Soil* 321, 61–81. doi:10.1007/s11104-008-9796-9
- Philippot, L., Hallin, S., Schloter, M., 2007. Ecology of Denitrifying Prokaryotes in Agricultural Soil, in: *Advances in Agronomy*. pp. 249–305. doi:10.1016/S0065-2113(07)96003-4
- Philippot, L., Raaijmakers, J.M., Lemanceau, P., van der Putten, W.H., 2013. Going back to the roots: the microbial ecology of the rhizosphere. *Nature Reviews Microbiology* 11, 789–799. doi:10.1038/nrmicro3109
- Prescott, C.E., Grayston, S.J., 2013. Tree species influence on microbial communities in litter and soil: Current knowledge and research needs. *Forest Ecology and Management* 309, 19–27. doi:10.1016/j.foreco.2013.02.034
- Qin, H., Xing, X., Tang, Y., Hou, H., Yang, J., Shen, R., Zhang, W., Liu, Y., Wei, W., 2019. Linking soil N<sub>2</sub>O emissions with soil microbial community abundance and structure related to nitrogen cycle in two acid forest soils. *Plant and Soil* 435, 95–109. doi:10.1007/s11104-018-3863-7
- R Core Team, 2018. R: A Language and Environment for Statistical Computing. R Foundation for Statistical Computing Vienna, <https://www.R-project.org/>.
- Rabbi, S.M.F., Daniel, H., Lockwood, P. V., Macdonald, C., Pereg, L., Tighe, M., Wilson, B.R., Young, I.M., 2016. Physical soil architectural traits are functionally linked to carbon decomposition and bacterial diversity. *Scientific Reports* 6, 33012. doi:10.1038/srep33012
- Randerson, P.F., Moran, C., Bialowiec, A., 2011. Oxygen transfer capacity of willow (*Salix viminalis* L.). *Biomass and Bioenergy* 35, 2306–2309. doi:10.1016/j.biombioe.2011.02.018
- Ravishankara, A.R., Daniel, J.S., Portmann, R.W., 2009. Nitrous Oxide (N<sub>2</sub>O): The Dominant Ozone-Depleting Substance Emitted in the 21st Century. *Science* 326, 123–125. doi:10.1126/science.1176985
- Reese, A.T., Lulow, K., David, L.A., Wright, J.P., 2018. Plant community and soil conditions individually affect soil microbial community assembly in experimental mesocosms. *Ecology and Evolution* 8, 1196–1205. doi:10.1002/ece3.3734
- Renault, P., Stengel, P., 1994. Modeling Oxygen Diffusion in Aggregated Soils: I. Anaerobiosis inside the Aggregates. *Soil Science Society of America Journal* 58, 1017. doi:10.2136/sssaj1994.03615995005800040004x
- Rillig, M.C., Muller, L.A.H., Lehmann, A., 2017. Soil aggregates as massively concurrent evolutionary incubators. *The ISME Journal* 11, 1943–1948. doi:10.1038/ismej.2017.56
- Rognes, T., Flouri, T., Nichols, B., Quince, C., Mahé, F., 2016. VSEARCH: a versatile open source tool for metagenomics. *PeerJ* 4, e2584. doi:10.7717/peerj.2584
- Ruamps, L.S., Nunan, N., Chenu, C., 2011. Microbial biogeography at the soil pore scale. *Soil Biology and Biochemistry* 43, 280–286. doi:10.1016/j.soilbio.2010.10.010
- Rütting, T., Huygens, D., Staelens, J., Müller, C., Boeckx, P., 2011. Advances in <sup>15</sup>N-tracing experiments: new labelling and data analysis approaches. *Biochemical Society Transactions* 39, 279–283. doi:10.1042/BST0390279
- Schleper, C., Nicol, G.W., 2010. Ammonia-Oxidising Archaea – Physiology, Ecology and Evolution, in: *Advances in Microbial Physiology*. Elsevier Ltd, pp. 1–41. doi:10.1016/B978-0-12-381045-8.00001-1
- Schloss, P.D., Westcott, S.L., Ryabin, T., Hall, J.R., Hartmann, M., Hollister, E.B., Lesniewski, R.A., Oakley, B.B., Parks, D.H., Robinson, C.J., Sahl, J.W., Stres, B., Thallinger, G.G., Van Horn, D.J., Weber, C.F., 2009. Introducing mothur: Open-Source, Platform-Independent, Community-Supported Software for

- Describing and Comparing Microbial Communities. *Applied and Environmental Microbiology* 75, 7537–7541. doi:10.1128/AEM.01541-09
- Schlüter, S., Henjes, S., Zawallich, J., Bergaust, L., Horn, M., Ippisch, O., Vogel, H.-J., Dörsch, P., 2018. Denitrification in Soil Aggregate Analogues—Effect of Aggregate Size and Oxygen Diffusion. *Frontiers in Environmental Science* 6, 1–10. doi:10.3389/fenvs.2018.00017
- Shoun, H., Fushinobu, S., Jiang, L., Kim, S.-W., Wakagi, T., 2012. Fungal denitrification and nitric oxide reductase cytochrome P450nor. *Philosophical Transactions of the Royal Society of London. Series B, Biological Sciences* 367, 1186–94. doi:10.1098/rstb.2011.0335
- Shrestha, J., Niklaus, P. a, Frossard, E., Samaritani, E., Huber, B., Barnard, R.L., Schleppei, P., Tockner, K., Luster, J., 2012. Soil nitrogen dynamics in a river floodplain mosaic. *Journal of Environmental Quality* 41, 2033–45. doi:10.2134/jeq2012.0059
- Sigman, D.M., Casciotti, K.L., Andreani, M., Barford, C., Galanter, M., Böhlke, J.K., 2001. A Bacterial Method for the Nitrogen Isotopic Analysis of Nitrate in Seawater and Freshwater. *Analytical Chemistry* 73, 4145–4153. doi:10.1021/ac010088e
- Smith, B., Wilson, B.J., 1996. A consumer's guide to evenness indices. *Oikos* 70–82.
- Snider, D.M., Venkiteswaran, J.J., Schiff, S.L., Spoelstra, J., 2013. A new mechanistic model of  $\delta^{18}\text{O}\text{-N}_2\text{O}$  formation by denitrification. *Geochimica et Cosmochimica Acta* 112, 102–115. doi:10.1016/j.gca.2013.03.003
- Snider, D.M., Venkiteswaran, J.J., Schiff, S.L., Spoelstra, J., 2012. Deciphering the oxygen isotope composition of nitrous oxide produced by nitrification. *Global Change Biology* 18, 356–370. doi:10.1111/j.1365-2486.2011.02547.x
- Spott, O., Russow, R., Stange, C.F., 2011. Formation of hybrid  $\text{N}_2\text{O}$  and hybrid  $\text{N}_2$  due to codenitrification: First review of a barely considered process of microbially mediated N-nitrosation. *Soil Biology and Biochemistry* 43, 1995–2011. doi:10.1016/j.soilbio.2011.06.014
- Stanton, C.L., Reinhard, C.T., Kasting, J.F., Ostrom, N.E., Haslun, J.A., Lyons, T.W., Glass, J.B., 2018. Nitrous oxide from chemodenitrification: A possible missing link in the Proterozoic greenhouse and the evolution of aerobic respiration. *Geobiology* 16, 597–609. doi:10.1111/gbi.12311
- Starkenbug, S.R., Arp, D.J., Bottomley, P.J., 2008. Expression of a putative nitrite reductase and the reversible inhibition of nitrite-dependent respiration by nitric oxide in *Nitrobacter winogradskyi* Nb-255. *Environmental Microbiology* 10, 3036–3042. doi:10.1111/j.1462-2920.2008.01763.x
- Sutka, R.L., Ostrom, N.E., Ostrom, P.H., Breznak, J.A., Gandhi, H., Pitt, A.J., Li, F., 2006. Distinguishing nitrous oxide production from nitrification and denitrification on the basis of isotopomer abundances. *Applied and Environmental Microbiology* 72, 638–644. doi:10.1128/AEM.72.1.638-644.2006
- Tomasek, A., Staley, C., Wang, P., Kaiser, T., Lurndahl, N., Kozarek, J.L., Hondzo, M., Sadowsky, M.J., 2017. Increased denitrification rates associated with shifts in prokaryotic community composition caused by varying hydrologic connectivity. *Frontiers in Microbiology* 8, 1–12. doi:10.3389/fmicb.2017.02304
- Toyoda, S., Yano, M., Nishimura, S., Akiyama, H., Hayakawa, A., Koba, K., Sudo, S., Yagi, K., Makabe, A., Tobari, Y., Ogawa, N.O., Ohkouchi, N., Yamada, K., Yoshida, N., 2011. Characterization and production and consumption processes of  $\text{N}_2\text{O}$  emitted from temperate agricultural soils determined via isotopomer ratio analysis. *Global Biogeochemical Cycles* 25, 1–17. doi:10.1029/2009GB003769

- Toyoda, S., Yoshida, N., 1999. Determination of nitrogen isotopomers of nitrous oxide on a modified isotope ratio mass spectrometer. *Analytical Chemistry* 71, 4711–4718. doi:10.1021/ac9904563
- Trivedi, P., Delgado-Baquerizo, M., Jeffries, T.C., Trivedi, C., Anderson, I.C., Lai, K., McNee, M., Flower, K., Pal Singh, B., Minkey, D., Singh, B.K., 2017. Soil aggregation and associated microbial communities modify the impact of agricultural management on carbon content. *Environmental Microbiology* 19, 3070–3086. doi:10.1111/1462-2920.13779
- Turner, T.R., Ramakrishnan, K., Walshaw, J., Heavens, D., Alston, M., Swarbreck, D., Osbourn, A., Grant, A., Poole, P.S., 2013. Comparative metatranscriptomics reveals kingdom level changes in the rhizosphere microbiome of plants. *The ISME Journal* 7, 2248–2258. doi:10.1038/ismej.2013.119
- Urbanová, M., Šnajdr, J., Baldrian, P., 2015. Composition of fungal and bacterial communities in forest litter and soil is largely determined by dominant trees. *Soil Biology and Biochemistry* 84, 53–64. doi:10.1016/j.soilbio.2015.02.011
- Verhoeven, E., Barthel, M., Yu, L., Celi, L., Said-Pullicino, D., Sleutel, S., Lewicka-Szczepak, D., Six, J., Decock, C., 2019. Early season N<sub>2</sub>O emissions under variable water management in rice systems: Source-partitioning emissions using isotope ratios along a depth profile. *Biogeosciences* 16, 383–408. doi:10.5194/bg-16-383-2019
- Wang, B., Brewer, P.E., Shugart, H.H., Lerdau, M.T., Allison, S.D., 2019. Soil aggregates as biogeochemical reactors and implications for soil–atmosphere exchange of greenhouse gases—A concept. *Global Change Biology* 25, 373–385. doi:10.1111/gcb.14515
- Wang, Q., Garrity, G.M., Tiedje, J.M., Cole, J.R., 2007. Naïve Bayesian Classifier for Rapid Assignment of rRNA Sequences into the New Bacterial Taxonomy. *Applied and Environmental Microbiology* 73, 5261–5267. doi:10.1128/AEM.00062-07
- Wang, Y., Uchida, Y., Shimomura, Y., Akiyama, H., Hayatsu, M., 2017. Responses of denitrifying bacterial communities to short-term waterlogging of soils. *Scientific Reports* 7, 803. doi:10.1038/s41598-017-00953-8
- Well, R., Flessa, H., 2009. Isotopologue enrichment factors of N<sub>2</sub>O reduction in soils. *Rapid Communications in Mass Spectrometry* 23, 2996–3002. doi:10.1002/rcm.4216
- Wilpiseski, R.L., Aufrecht, J.A., Retterer, S.T., Sullivan, M.B., Graham, D.E., Pierce, E.M., Zablocki, O.D., Palumbo, A. v., Elias, D.A., 2019. Soil aggregate microbial communities: Towards understanding microbiome interactions at biologically relevant scales. *Applied and Environmental Microbiology* 1–18. doi:10.1128/aem.00324-19
- Wilson, J.S., Baldwin, D.S., Rees, G.N., Wilson, B.P., 2011. The effects of short-term inundation on carbon dynamics, microbial community structure and microbial activity in floodplain soil. *River Research and Applications* 27, 213–225. doi:10.1002/rra.1352
- Wolf, B., Merbold, L., Decock, C., Tuzson, B., Harris, E., Six, J., Emmenegger, L., Mohn, J., 2015. First on-line isotopic characterization of N<sub>2</sub>O above intensively managed grassland. *Biogeosciences* 12, 2517–2531. doi:10.5194/bg-12-2517-2015
- Wrage, N., Velthof, G.L., van Beusichem, M.L., Oenema, O., 2001. Role of nitrifier denitrification in the production of nitrous oxide. *Soil Biology and Biochemistry* 33, 1723–1732. doi:10.1016/S0038-0717(01)00096-7



- 
- Yamamoto, A., Akiyama, H., Nakajima, Y., Hoshino, Y.T., 2017. Estimate of bacterial and fungal N<sub>2</sub>O production processes after crop residue input and fertilizer application to an agricultural field by <sup>15</sup>N isotopomer analysis. *Soil Biology and Biochemistry* 108, 9–16. doi:10.1016/j.soilbio.2017.01.015
- Yoshida, N., 1988. <sup>15</sup>N-depleted N<sub>2</sub>O as a product of nitrification. *Nature*. doi:10.1038/335528a0
- Yu, L., Harris, E., Lewicka-Szczebak, D., Barthel, M., Blomberg, M.R.A., Harris, S.J., Johnson, M.S., Lehmann, M.F., Liisberg, J., Müller, C., Ostrom, N.E., Six, J., Toyoda, S., Yoshida, N., Mohn, J., 2020. What can we learn from N<sub>2</sub>O isotope data? – Analytics, processes and modelling. *Rapid Communications in Mass Spectrometry* 34, 1–14. doi:10.1002/rcm.8858
- Zhang, C., Liu, G., Xue, S., Wang, G., 2016. Soil bacterial community dynamics reflect changes in plant community and soil properties during the secondary succession of abandoned farmland in the Loess Plateau. *Soil Biology and Biochemistry* 97, 40–49. doi:10.1016/j.soilbio.2016.02.013
- Zhang, J., Müller, C., Cai, Z., 2015. Heterotrophic nitrification of organic N and its contribution to nitrous oxide emissions in soils. *Soil Biology and Biochemistry* 84, 199–209. doi:10.1016/j.soilbio.2015.02.028
- Zhao, S., Zhou, J., Yuan, D., Wang, W., Zhou, L., Pi, Y., Zhu, G., 2020. *NirS*-type N<sub>2</sub>O-producers and *nosZ* II-type N<sub>2</sub>O-reducers determine the N<sub>2</sub>O emission potential in farmland rhizosphere soils. *Journal of Soils and Sediments* 20, 461–471. doi:10.1007/s11368-019-02395-3
- Zou, Y., Hirono, Y., Yanai, Y., Hattori, S., Toyoda, S., Yoshida, N., 2014. Isotopomer analysis of nitrous oxide accumulated in soil cultivated with tea (*Camellia sinensis*) in Shizuoka, central Japan. *Soil Biology and Biochemistry* 77, 276–291. doi:10.1016/j.soilbio.2014.06.016
- Zumft, W.G., 1997. Cell biology and molecular basis of denitrification. *Microbiology and Molecular Biology Reviews* : MMBR 61, 533–616.



## Chapter 4

# Pioneer plant *Phalaris arundinacea* modifies temporal patterns of enhanced N<sub>2</sub>O emissions, source partitioning and N<sub>2</sub>O reduction from floodplain soils after a short-term flood event

Martin Ley<sup>a,b</sup>, Moritz F. Lehmann<sup>b</sup>, Pascal A. Niklaus<sup>c</sup>, Beat Frey<sup>a</sup>, Jörg Luster<sup>a</sup>

<sup>a</sup>Swiss Federal Institute for Forest, Snow and Landscape Research WSL, Research Unit Forest Soils and Biogeochemistry, Zürcherstrasse 111, 8903 Birmensdorf, Switzerland

<sup>b</sup>University of Basel, Department of Environmental Sciences, Research Group Biogeochemistry, Bernoullistrasse 30, 4056 Basel, Switzerland

<sup>c</sup>University of Zürich, Department of Evolutionary Biology and Environmental Studies, Winterthurerstrasse 190, 8057 Zurich, Switzerland

*Corresponding author:* Martin Ley (martin.ley@unibas.ch)

Keywords: stable isotopes, <sup>15</sup>N site preference, functional gene transcripts, nitrous oxide emissions

### Abstract

Short-term flood events trigger periods of enhanced emissions of the ozone-depleting greenhouse gas nitrous oxide (N<sub>2</sub>O). However, the temporal post-flood dynamics in source partitioning of major microbial N<sub>2</sub>O production pathways and N<sub>2</sub>O reduction are still poorly understood. In a field manipulation experiment, conducted in the zone of a river floodplain strongly exposed to regular flood perturbations, we studied the effect of the presence/absence of pioneer vegetation on the interplay of these source and sink functions as determinants of the magnitude of N<sub>2</sub>O emissions. A combined approach of analyses of the isotopomeric signatures of soil-emitted N<sub>2</sub>O and RNA-based molecular techniques was applied during a three-week post-flood phase. During times of high emissions directly after flooding, N<sub>2</sub>O flux rates did not differ significantly in magnitude between bare plots and plots covered by the pioneer plant *Phalaris arundinacea*. However, elevated N<sub>2</sub>O fluxes were maintained for a longer period at the *Phalaris* plots, whereas flux rates from bare plots gradually decreased. Peak emissions were always the result of a mixed source contribution by oxidative and reductive processes, although the fraction of oxidative processes was higher in the *Phalaris* plots. After the first week of the

post-flood phase, emissions from bare plots originated almost exclusively from nitrifier denitrification and/or heterotrophic denitrification, whereas the proportional source contribution from oxidative and reductive processes in the *Phalaris* plots remained stable. N<sub>2</sub>O reduction was initially less pronounced in the bare plots shortly after the flood but intensified over the course of the drying period. By contrast, *Phalaris* plots showed little variation in the extent of N<sub>2</sub>O reduction during the entire drying period. These findings were largely supported by the results from the analysis of transcript abundance of key marker genes. Together, they indicate that periods of enhanced N<sub>2</sub>O emissions were mostly the consequence of a flood-stimulated microbial community dominated by denitrification-capable microorganisms. The plant-related development of soil structure and macropore aeration seemed to provide a stable, yet more heterogeneous distribution of redox gradients, creating diverse microhabitats that support robust patterns in source partitioning of simultaneous oxidative and reductive N<sub>2</sub>O production. By contrast, the poorly structured, highly water-saturated bare sediments seemed to create more extensive anoxia in the deeper sections of the soils, promoting denitrification processes and efficient N<sub>2</sub>O reduction. These findings should help to improve our assessment of the climate regulation function and greenhouse gas budget from river floodplain ecosystems.

## 4.1 Introduction

The prediction of emissions of potent greenhouse gases (GHG), such as the ozone-depleting nitrous oxide (N<sub>2</sub>O), from natural and near-natural terrestrial ecosystems is challenging, leading to great uncertainties in the estimation of annual GHG budgets from soils under natural vegetation, ranging between 3.3 – 9.0 Tg N-N<sub>2</sub>O yr<sup>-1</sup> (Ravishankara et al., 2009; Ciais et al., 2013). River floodplains, natural and restored, are particularly difficult to assess since these transition zones between aquatic and terrestrial systems are marked by a high small-scale heterogeneity in soil properties and diverse vegetation (Fournier et al., 2013; Schirmer et al., 2014). This structural diversity creates hotspots of carbon (C) and nitrogen (N) transformations and must be therefore considered when evaluating related ecosystem services, such as the removal of reactive N species and/or C storage (McClain et al., 2003; European Environment Agency (EEA), 2020). In riparian zones with little hydrological disturbances biogeochemical N transformations generally do not lead to enhanced emissions of N<sub>2</sub>O (Audet et al., 2014; Mafa-Attoye et al., 2020). By contrast, in floodplains, frequent short-term inundation seems to directly affect N-cycling processes in such a way that periods of elevated N<sub>2</sub>O emission rates have been repeatedly observed (Jacinthe et al., 2012; Peter et al., 2012; Shrestha et al., 2012). This highlights the necessity to include flood frequency into the assessment of N<sub>2</sub>O emission

budgets, since these flood-induced short-term periods of high emissions can make up to 50 % of the cumulative annual N<sub>2</sub>O emissions from an otherwise relatively low-emitting ecosystem (Molodovskaya et al., 2012; Hansen et al., 2014). The temporal confinement of high N<sub>2</sub>O emission rates to post-flood phases highlights the need of an in-depth understanding of the site-specific controls on N<sub>2</sub>O production and consumption processes in association with flooding to adequately assess the overall N<sub>2</sub>O budget of floodplains. This becomes even more important considering the projected increase in frequency and intensity of heavy precipitation, which is likely to increase the probability of flash floods (Handmer et al., 2012).

The arguably most relevant N-transformations in context of GHG production and climate change are nitrification, nitrifier denitrification and heterotrophic denitrification (Spott et al., 2011), all producing N<sub>2</sub>O as intermediate N species or by product. Nitrification (NI), mediated by autotrophic ammonia oxidizing bacteria (AOB) and nitrite oxidizing bacteria (NOB), produces N<sub>2</sub>O under oxic conditions during ammonia oxidation when hydroxylamine (NH<sub>2</sub>OH) decomposes abiotically (Laughlin et al., 2008; Pester et al., 2014; Zhang et al., 2015). Ammonia oxidizing archaea (AOA) produce lower amounts of N<sub>2</sub>O, but the exact pathway is not yet fully understood (Stieglmeier et al., 2014; Lehtovirta-Morley, 2018). Under suboxic to anoxic conditions, some AOBs and NOBs form N<sub>2</sub>O via nitrifier denitrification (ND) either by reducing nitrite (NO<sub>2</sub><sup>-</sup>) to nitric oxide (NO) or by direct reduction of NH<sub>2</sub>OH to N<sub>2</sub>O (Arp and Stein, 2003; Starkenburg et al., 2008; Caranto et al., 2016; Kozłowski et al., 2016). Under the same conditions, denitrifying heterotrophic bacteria (HD) reduce NO<sub>3</sub><sup>-</sup> and NO<sub>2</sub><sup>-</sup> to gaseous NO, N<sub>2</sub>O, and N<sub>2</sub> (Knowles, 1982; Braker et al., 2000). Heterotrophic denitrification can also be performed by fungi (FD), but with N<sub>2</sub>O as the final product (Laughlin and Stevens, 2002; Maeda et al., 2015). To expand our still limited knowledge about the relationship between the relative contributions of specific N<sub>2</sub>O source processes and site-specific environmental conditions during periods of increased N<sub>2</sub>O emissions from floodplain soils, it is important to assess the temporal dynamics regarding the source contributions of major microbial N cycling processes in response to flood events. The only biological sink of N<sub>2</sub>O discovered so far is the bacterial N<sub>2</sub>O reduction to N<sub>2</sub>, the last step of complete denitrification (Baggs, 2008; Vieten et al., 2009). N<sub>2</sub>O reduction in soils is an important modulator (i.e., mitigator) of soil N<sub>2</sub>O emissions. However, there is little information regarding the sensitivity of this process towards hydrological perturbations in floodplain systems.

The activity and efficiency of the above-mentioned microbial N<sub>2</sub>O producing and consuming processes is tightly linked to the physical and chemical properties of soils, constraining, for example, diffusive gas transport as well as the availability of suitable terminal electron

acceptors ( $O_2$ , or reactive N species) and biodegradable C sources. The latter, in turn, are controlled by factors such as soil development and vegetation type. Floodplain soils directly adjacent to the river shoreline consist mainly of young sediment deposits with a limited soil development (Fournier et al., 2013; Schomburg et al., 2018), in which buried organic detritus can form hotspots of N transformation (Hill, 2011). In this dynamic alluvial zone, physically resilient pioneer plants can form patchy vegetation patterns (Samaritani et al., 2011), promoting soil structuring and stabilization of the sediments (Angers and Caron, 1998; Gurnell, 2014). In addition, fine roots and root exudates can bind mineral particles with organic detritus which act as nuclei for early soil aggregation, thereby altering soil aeration, substrate distribution and pore water dynamics (Oades, 1984; Six et al., 2004). The increased availability of biodegradable substrates can further stimulate the activity of N-transforming microorganisms (Philippot et al., 2009; Robertson and Groffman, 2015). Another common trait of plants adapted to water-saturated soil conditions is the ability to ventilate the rhizosphere (Colmer, 2003). This leads to a diversification of soil microhabitats, with various levels of oxygen availability affecting  $N_2O$  producing and reducing processes on a small scale. Some species also seem to convey  $N_2O$  to the atmosphere via plant-internal physiological structures allowing  $N_2O$  to bypass the soil matrix (Smart and Bloom, 2001; Rückauf et al., 2004; Baruah et al., 2010; Jørgensen et al., 2012). However, the ongoing discourse about the role of specific types of pioneer vegetation in the formation and reduction of  $N_2O$ , or on the activity of major N transforming consortia of microorganisms under post-flood changing environmental conditions highlights the need to better understand the complex interactions between plant, microbes, and soil.

The use of natural abundance stable isotope ratio measurements of  $N_2O$  has emerged as a versatile, non-invasive method to identify  $N_2O$  source processes (Baggs, 2008; Toyoda et al., 2011; Ostrom and Ostrom, 2012; Wolf et al., 2015). The isotopic analysis of the linear, asymmetric  $N_2O$  molecule involves three isotopic parameters:  $\delta^{15}N_{\text{bulk}}$ ,  $\delta^{18}O$  and the intramolecular distribution of the heavy ( $^{15}N$ ) and light N ( $^{14}N$ ) atoms between the central ( $\alpha$ ) and outer ( $\beta$ ) positions, also known as  $^{15}N$  site preference ( $^{15}N$  SP). The combined application of these isotopic parameters in dual-isotope maps, e.g.,  $\delta^{15}N_{\text{bulk}}$  vs.  $^{15}N$  SP or  $\delta^{18}O$  vs.  $^{15}N$  SP, can be used to distinguish between major process groups and to indirectly estimate the magnitude of  $N_2O$  reduction (Lewicka-Szczebak et al., 2017). The dual-isotope mapping approach introduced by Lewicka-Szczebak et al. (2017) has been successfully applied in field (Buchen et al., 2018; Verhoeven et al., 2019), and experimental studies (see chapter 3). These studies confirmed the suitability of the dual-isotope mapping approach for the combined estimation of source partitioning (i.e., proportional contribution of different oxidative and

reductive N<sub>2</sub>O producing processes), and the magnitude of N<sub>2</sub>O reduction in ecosystems where N<sub>2</sub>O production and consumption occur simultaneously or alternately.

Here we evaluate results from a plant removal experiment in a river floodplain to assess the effects of pioneer vegetation on parameters related to N<sub>2</sub>O emission from floodplain soils during hot moments after flooding. Specifically, our objective is to investigate and understand the temporal patterns of, and controls on, 1) N<sub>2</sub>O emissions from, and N<sub>2</sub>O concentrations in, vegetated versus bare soils, 2) the N<sub>2</sub>O source contribution by major microbial process groups, and of the transcriptional activity of related key marker genes, and 3) the reduction of produced N<sub>2</sub>O to N<sub>2</sub>. The approach selected to address these objectives is a combination of gas flux measurements, RNA-based molecular techniques, and the analyses of the natural-abundance isotopic composition of the emitted N<sub>2</sub>O, which is described in detail in Chapter 3, and is based on the N<sub>2</sub>O isotope mapping approach by Lewicka-Szczebak et al. (2017).

## 4.2 Methods

### 4.2.1 Site description and experimental design

This study was performed within the framework of a field manipulation experiment conducted at sites in a 2 km-long restored section of the Thur River floodplain at Niederneunforn (NE Switzerland; 47°35'28" N, 8°46'26" E). Due to the nivo-pluvial hydrologic regime of the Thur River and the lack of any reservoir within its catchment, this floodplain is regularly subject to flash floods occurring mainly during snow melt in late spring and after heavy summer rainfall (Fournier et al., 2013). The soils of the studied site, located in a highly disturbed zone close to the river channel, were composed of  $79 \pm 6$  % sand,  $14.7 \pm 5$  % silt, and  $6.4 \pm 1.4$  % clay (Schomburg et al., 2019) and were classified as loamy sands (IUSS Working Group WRB, 2015). The dominant vegetation in this zone consisted of *Phalaris arundinacea*, *Urtica dioica* and the invasive neophyte *Impatiens glandulifera*. The  $1.5 \times 1.5$  m plots were set up 3 – 8 m from the mean water line, corresponding to a mean annual river discharge of  $46.8 \text{ m}^3 \text{ s}^{-1}$ , and were arranged in a randomized complete-plot design. A detailed description of the full experimental setup can be found in Schomburg et al. (2019). Two different treatments were investigated: unmanipulated plots with vegetation (*P. arundinacea*), and plots, where vegetation was regularly removed, referred to as “*Phalaris* plots” and “bare plots”, respectively. Each treatment was replicated six times, with two replicates assigned to each of three blocks ( $2 \times 2 \times 3 = 12$  plots in total).

Each plot was equipped with four custom-made Pt electrodes (tip with diameter of 1 mm and contact length of 5 mm) inserted vertically in every plot to a depth of 15 cm and 30 cm, and a

custom-made Ag/AgCl reference electrode filled with 3 M KCl. All these electrodes were connected to a CR1000 data logger (Campbell Scientific, Shepshed, UK) via multiplexers (AM 16/32A, Campbell Scientific, Shepshed, UK) for hourly redox potential ( $E_h$ ) measurements. Three volumetric water content (VWC) sensors of various types (EC-5, EC-TM, 10-HS and 5-TE, Decagon, USA) were placed at 15 cm, 30 cm, and 45 cm below the soil surface of each plot, respectively, and were connected to EM50 data loggers (Decagon, USA). VWC and soil temperature was measured every 30 minutes. Water filled pore space (WFPS) was calculated by dividing a given measured VWC by the VWC during inundation – assuming pore water saturation at this time point. Two suction cups (high-flow porous ceramic cups, Soil Moisture Equipment Corp., Santa Barbara, CA, USA) per plot were installed at 15 cm and 30 cm depth, respectively, for collecting soil solution by applying a vacuum of 50 to 60 kPa. To collect  $N_2O$  from soil pore space, three gas tubes per plot with a 1-m gas permeable part (Accurel<sup>®</sup> PP V8/2 HF, Membrana GmbH, Wuppertal, Germany) were horizontally installed 15 cm, 30 cm, and 45 cm below the soil surface (for details see Fig. S4.2). Two cylindrical, PVC static gas chamber rings with a 30 cm diameter and 30 cm height (20 cm above surface, 10 cm below surface), and closable with a vented lid were installed in each plot for measuring  $N_2O$  emissions at the soil-atmosphere interface.

On May 13<sup>th</sup>, 2016, a strong flood event (max. discharge  $550 \text{ m}^3 \text{ s}^{-1}$ ) occurred after heavy rainfall, which led to the inundation of the research site for 48 hours (Schomburg et al., 2019). This event initiated the sampling campaign conducted 2, 5, 10 and 22 days after flood water recession, and ending shortly before the next flood (Fig. 4.1). On each sampling day, the gas chambers on the different plots were closed, and 30 mL of headspace gas were collected, respectively, 2, 20, 40 and 60 minutes after closure. With the final sampling, an additional 150 mL of headspace gas was collected for  $N_2O$  isotopic analysis. An additional 30 mL and 160 mL of ambient air was collected 2 m above ground to determine the background  $N_2O$  concentration and its isotopic composition, respectively. Further, 30 mL of soil air was sampled in each plot from all three depths, to measure the  $N_2O$  concentration in the pore air. All gaseous samples were taken with gas-tight syringes and injected into muffled, pre-evacuated exetainers (30 mL) or glass serum vials (160 mL).  $N_2O$  concentrations were determined at the University of Zurich by gas chromatography (Agilent 6890, Santa Clara, USA; Porapak Q column, Ar/ $CH_4$  carrier gas, micro-ECD detector), and  $N_2O$  surface flux rates were calculated from the  $N_2O$  concentration change with time in the chamber, as described in chapter 2.

Soil samples were taken from each plot directly after gas flux measurements with a custom-made auger (2.5 cm in diameter) at 7.5 – 22.5 cm, 22.5 – 37.5 cm, and 37.5 – 52.5 cm below



soil surface (144 samples in total). For RNA and DNA extraction, each core segment was rapidly homogenized, and field-moist subsamples were transferred into 2 ml and 5 ml sterile, RNase free Eppendorf tubes. These aliquots were subsequently shock-frozen using liquid nitrogen, before stored at -80 °C.

Pore water samples were filtered (0.45 µm) and subsequently analyzed for dissolved organic carbon (DOC) and TN concentrations with an elemental analyzer (TOC-V Shimadzu, Switzerland; Formacs<sup>HT/TN</sup>, Skalar, The Netherlands). Nitrate and ammonium concentrations in the soil solution were measured by ion chromatography (DX-120, Dionex, California, USA) and flow injection analysis (FIAS 300, UV/VIS Spectrometer Lambda 2S, PerkinElmer, Germany), respectively.

#### 4.2.2 Stable isotope analyses and isotopic mass balances

The isotopic composition of gaseous N<sub>2</sub>O samples was analyzed using a customized purge and trap system (McIlvin & Casiotti, 2010) coupled to a continuous-flow isotope ratio mass spectrometer (IRMS; Thermo Finnigan Delta V<sup>plus</sup>, Thermo Fisher Scientific, Bremen, Germany), configured to simultaneously detect mass to ion-charge (m/z) ratios of 30, 31, 44, 45, and 46. Samples were purged with helium, and the target gas N<sub>2</sub>O was then purified (using water and CO<sub>2</sub> traps), separated from any remaining CO<sub>2</sub> using a GC-column (Rt-Q-BOND, Restek, 15 m × 0.32 mm), and cryogenically pre-concentrated using a liquid N<sub>2</sub> trap. Measured isotopic ratios were pre-calibrated against a reference gas (100 % N<sub>2</sub>O; Air Liquide, France). The calibration of the N<sub>2</sub>O reference gas for bulk and site-specific isotopic composition relative to international standards was conducted by J. Mohn (Swiss Federal Laboratories for Materials Science and Technology (EMPA), Switzerland) using a quantum cascade laser absorption spectrometer (mini-QCLAS; Aerodyne Research Inc, USA). The mass-to-charge ratios of N<sub>2</sub>O (m/z 45/44, and 46/44) and of the fragment ion NO<sup>+</sup> (31/30) were converted to the delta (δ) notation δ<sup>15</sup>N<sub>N<sub>2</sub>O</sub><sup>bulk</sup> (vs. AIR-N<sub>2</sub>), δ<sup>18</sup>O<sub>N<sub>2</sub>O</sub> (vs. Vienna Standard Mean Ocean Water, VSMOW) and site-specific δ<sup>15</sup>N<sub>N<sub>2</sub>O</sub><sup>α</sup> using the equations published in Frame et al. (2017) and Frame and Casciotti (2010). Subsequently, a two-point correction using measurements of two isotopically different standards of N<sub>2</sub>O in synthetic air (Table S4.1) was applied for each measurement sequence (Mohn et al., 2014). Values for δ<sup>15</sup>N<sub>N<sub>2</sub>O</sub><sup>β</sup> were calculated using the relationship δ<sup>15</sup>N<sub>N<sub>2</sub>O</sub><sup>bulk</sup> = (δ<sup>15</sup>N<sub>N<sub>2</sub>O</sub><sup>α</sup> + δ<sup>15</sup>N<sub>N<sub>2</sub>O</sub><sup>β</sup>)/2 to obtain <sup>15</sup>N SP (<sup>15</sup>N SP = δ<sup>15</sup>N<sub>N<sub>2</sub>O</sub><sup>α</sup> - δ<sup>15</sup>N<sub>N<sub>2</sub>O</sub><sup>β</sup>). The analytical precision is given as the standard deviation of measurements of the internal Standard 3 provided by EMPA (Table S4.1), measured in every measurement sequence (0.2 ‰ for both δ<sup>15</sup>N<sup>bulk</sup> and <sup>15</sup>N SP, and 0.1 ‰ for δ<sup>18</sup>O<sub>N<sub>2</sub>O</sub>). Isotopic signatures of soil-derived N<sub>2</sub>O were calculated using the following mass balance equation:

$$\delta_{chamber} \times (C_{atm} + C_{soil}) = (\delta_{atm} \times C_{atm} + \delta_{soil} \times C_{soil}) \quad (1)$$

$\delta_{chamber}$ ,  $\delta_{atm}$  and  $\delta_{soil}$  represent either  $\delta^{15}\text{N}^{\text{bulk}}$ ,  $\delta^{18}\text{O}_{\text{N}_2\text{O}}$  or  $^{15}\text{N}$  SP of the gas mixture (chamber) and the two  $\text{N}_2\text{O}$  sources (atmosphere and soil), respectively.  $C_{soil}$  and  $C_{atm}$  denotes the calculated soil  $\text{N}_2\text{O}$  concentrations and measured  $\text{N}_2\text{O}$  concentrations in the background air, respectively. Samples where soil-derived  $\text{N}_2\text{O}$  was less than 30 % of the background  $\text{N}_2\text{O}$  concentration, were excluded from further analysis.

For later adjustment of literature  $\delta^{18}\text{O}_{\text{N}_2\text{O}}$  values to represent expectable ranges of distinct process groups that apply to the study site, the isotopic composition of soil pore water was determined for each sampling day and for each plot, using an elemental analyzer (TC/EA) coupled to a Delta V Plus isotope ratio mass spectrometer (IRMS) through a ConFlo IV interface (Thermo Fisher Scientific, Bremen, Germany) at the University of Basel Stable Isotope Ecology Laboratory (BaSIEL), Switzerland.  $\text{O}_{\text{H}_2\text{O}}$  isotope ratios were converted to the  $\delta$  notation and normalized to the VSMOW scale using calibrated in-house standards. Literature source  $\delta^{18}\text{O}_{\text{N}_2\text{O}}$  values for ND, HD and FD compiled in Yu et al. (2020) were subsequently adapted relative to the mean  $\delta^{18}\text{O}_{\text{H}_2\text{O}}$  of the pore water ( $-11.84 \pm 0.88$  ‰ (mean  $\pm$  SD) in this study, following recommendations in Lewicka-Szczebak et al. (2020). Since  $\delta^{18}\text{O}_{\text{N}_2\text{O}}$  values of NI are not affected by the isotopic signature of ambient water, and similar to the  $\delta^{18}\text{O}$  of atmospheric oxygen (Frame and Casciotti, 2010; Sutka et al., 2006), the respective value range (20.5 ‰ to 26.5 ‰) was adopted unchanged from Yu et al. (2020).

#### 4.2.3 $\text{N}_2\text{O}$ source partitioning and fractional $\text{N}_2\text{O}$ reduction

The quantitative estimation of source partitioning of the most common  $\text{N}_2\text{O}$  producing processes and partial  $\text{N}_2\text{O}$  reduction were calculated using the dual-isotope mapping approach introduced by Lewicka-Szczebak et al. (2017, 2020). This method is based on the determination of intercepts between a mixing line and a reduction line with a fixed slope constructed relative to the isotope values of each sample in a  $^{15}\text{N}$  SP vs.  $\delta^{18}\text{O}_{\text{N}_2\text{O}}$  diagram. The slope of the reduction line of 0.23 was calculated based on reported fractionation factors  $\epsilon^{15}\text{N}$  SP (-3.7 ‰) and  $\epsilon^{18}\text{O}$  (-15.8 ‰) from Jinuntuya-Nortman et al. (2008). This slope is well within the range of other soil studies (e.g., Lewicka-Szczebak et al., 2014; Well and Flessa, 2009). Due to the considerable overlap of the combined  $^{15}\text{N}$  SP and  $\delta^{18}\text{O}_{\text{N}_2\text{O}}$  signatures for ND and HD, one common endmember ( $\delta_{\text{ND\&HD}}$ ) was created to represent these two processes. NI and FD were also grouped and represented by one common endmember  $\text{N}_2\text{O}$  isotope signature ( $\delta_{\text{NI\&FD}}$ ), even though pure culture studies reported distinct ranges for in  $\delta^{18}\text{O}_{\text{N}_2\text{O}}$  for these two processes. A

list of all isotopic parameters can be found in the supplementary material (Table S4.2). These endmember  $^{15}\text{N}$  SP and  $\delta^{18}\text{O}_{\text{N}_2\text{O}}$  values and the slope of the reduction line were used in the equations and calculation procedure presented in the supplement of Wu et al. (2019) to estimate the gross contribution of the ND&HD process group to total  $\text{N}_2\text{O}$  production ( $f_{\text{ND\&HD,gross}}$ ) and the residual fraction of all originally produced  $\text{N}_2\text{O}$  after partial reduction ( $r\text{N}_2\text{O}_{\text{total}}$ ). However, the dual isotope mapping approach takes two model scenarios into account. These scenarios differ in their assumptions regarding the sequential order of  $\text{N}_2\text{O}$  mixing versus reduction. In the first scenario (scenario R-M), it is assumed that only  $\text{N}_2\text{O}$  from nitrifier denitrification and/or heterotrophic bacterial denitrification gets partially reduced to  $\text{N}_2$  prior mixing with unreduced  $\text{N}_2\text{O}$  from the other processes (Fig. S4.1a). In the second scenario (scenario M-R), all  $\text{N}_2\text{O}$  produced by different processes/process groups is mixed first, followed by partial reduction of the mixed  $\text{N}_2\text{O}$  (Fig. S4.1b). These two scenarios yield two distinct estimates for  $f_{\text{ND\&HD,gross}}$  and  $r\text{N}_2\text{O}_{\text{total}}$  for each data point in the  $^{15}\text{N}$  SP vs.  $\delta^{18}\text{O}_{\text{N}_2\text{O}}$  space of the isotope map.

#### 4.2.4 Nucleic acid extraction, quality control and reverse transcription

Total RNA and DNA were extracted using the RNeasy<sup>®</sup> PowerSoil<sup>®</sup> Total RNA Kit in conjunction with the RNeasy<sup>®</sup> PowerSoil<sup>®</sup> DNA Elution Kit (Qiagen, Hilden, Germany) according to the manufacturers protocol from  $3.8 \pm 0.1$  g of fresh soil per sample. During the phenolic isolation procedure of the nucleic acids, we used a ready-to-use Phenol:Chloroform:Isoamyl alcohol (25:24:1, pH: 7.5 – 8.0, in TE-Buffer; Carl Roth<sup>®</sup> GmbH + Co. KG, Karlsruhe, Germany) as proposed by the manufacturer of the extraction kits. Extracted RNA was quantified using a NanoDrop ND-1000 spectrophotometer (NanoDrop Technologies). Integrity of extracted total RNA was further assessed using a Bioanalyzer (2100 Expert, Agilent Technologies, Inc., Santa Clara, USA) on 24 randomly picked RNA extracts. The visual inspection of the electropherograms and calculated RNA Integrity number (RIN; range: 5.8 – 8.1) confirmed sufficient quality of obtained RNA for further downstream processing.

Reverse transcription of mRNA into complementary DNA (cDNA) was conducted using the QuantiTect<sup>®</sup> Reverse Transcription Kit (Qiagen, Hilden, Germany) following the manufacturers protocol. This two-step process included an initial elimination of eventually present remaining genomic DNA from the extraction procedure prior reverse-transcription of mRNA. Both steps were conducted on a thermal cycler (Veriti, Applied Biosystems, Foster City, USA). Reverse-transcription products were stored at  $-20$  °C until further used.

#### 4.2.5 Quantitative PCR of nitrogen cycling gene transcripts

Transcripts of functional marker genes encoding for enzymes catalyzing the aerobic oxidation of ammonia to  $\text{NH}_2\text{OH}$  (bacterial *amoA*, archaeal *amoA*) and  $\text{NO}_2^-$  to  $\text{NO}_3^-$  (*nirS*) during nitrification, and the anaerobic reduction of  $\text{NO}_2^-$  to  $\text{NO}$  (*nirS*) and  $\text{N}_2\text{O}$  to  $\text{N}_2$  (*nosZ*) during denitrification were targeted according to Frey et al. (2020). For each functional gene, 6.6  $\mu\text{l}$  of template cDNA (2.67  $\text{ng } \mu\text{l}^{-1}$ ) were added to 8.4  $\mu\text{l}$  of gene-specific master mix. The master mix for each sample comprised 7.5  $\mu\text{l}$  QuantiTect SYBR Green PCR master mix (Qiagen, Hilden, Germany), 0.15  $\mu\text{l}$  each of forward and reverse primer (100  $\mu\text{M}$ ; Table S4.3), 0.5  $\mu\text{l}$  water (HPLC grade), and 0.1  $\mu\text{l}$  of BSA (30mg/ml). Each functional gene transcript was amplified using a specific thermal profile (Table S4.3) using an ABI7500 Fast Real-Time PCR system (Applied Biosystems, Lincoln, CA, USA). Melting curve analyses were conducted at the end of each qPCR run to verify primer specificity. Amplification efficiency was calculated using the equation in (Philippot et al., 2011), resulting in estimated efficiencies always higher than the set threshold of 80 % for run acceptance. Gene transcript abundances were quantified for each run by a series of diluted cloned plasmids, containing inserts of the respective gene (Frey et al., 2020), and finally normalized to copy numbers per gram dry soil.

#### 4.2.6 Statistical analyses

Significant effects and interactions on hydrochemical parameters and N cycling gene transcripts were identified by using linear mixed models applying advanced residual maximum likelihood techniques implemented in the R package ‘ASReml’ (VSNI, Hemel Hempstead, UK; Butler et al., 2017), according to the randomized complete block design of the experiment and summarized by analyses of variance (ANOVA; Type I, Kenward-Roger’s method for adjustment of the denominator degrees of freedom). The predictors plot type (two levels: “*Phalaris*” and “bare”), soil depth (three levels: 7.5 – 22.5 cm, 22.5 – 37.5 cm and 37.5 – 52.5 cm), sampling day (four levels: day02, day05, day10 and day22), and temporal residual correlations were set as fixed effects. Random effects were the individual plots and their two- and three-way interactions with soil depth and sampling day. The response variables “ $\text{N}_2\text{O}$  flux”, “isotope values of soil-emitted  $\text{N}_2\text{O}$ ”, “ $\text{rN}_2\text{O}_{\text{total}}$ ” and “ $f\text{ND\&HD}_{\text{gross}}$ ” were assessed with a similar model structure but without the depth component. Day-wise comparisons were calculated by creating equivalent models with the package ‘lmerTest’ (Kuznetsova et al., 2017). User-defined contrasts were subsequently compared with the ‘multcomp’ package (Hothorn et al., 2008), and resulting *P*-values were adjusted for multiple comparison using the Benjamini-Hochberg method (Benjamini and Hochberg, 1995), if the same contrasts were tested multiple times. Response variables were log-transformed, if the *a posteriori* inspection of model

residuals at the lowest stratum revealed that the requirements for normality and homoscedasticity were not met. The significance and confidence levels for all tested hypotheses were at  $\alpha < 0.05$ . All statistical analyses were conducted in the R environment (R Core Team, 2021).

## 4.3 Results

### 4.3.1 Physicochemical parameters of pore water

The flood event led to a rapid and almost complete saturation (80-100 %) of the pore space, and the overall temporal course and depth distribution of the average WFPS was similar in both plot types (Fig. 4.1). After flooding, in 15 cm soil depth, the WFPS in the *Phalaris* plots was equivalent to the WFPS in the bare plots and return to pre-flood conditions was fast. Further below, the decrease in WFPS was more gradual, and, overall, significantly lower in the vegetated than in the bare plots. The average redox potential in both plot types and all depths were subject to considerable fluctuations, with *Phalaris* plots having the tendency towards stronger amplitudes compared to bare plots (Fig. 4.1). During the saturation period, the redox potential particularly in the vegetated plots temporarily decreased. After the first week into the drying phase, these plots tended to display higher redox potentials in 30 cm depth than in 15 cm depth. A subtle trend toward an increasing redox potential toward the end of the experiment could only be discerned in the bare plots.

**Table 4.1:** ANOVA table of effects and interactions of experimental factors on soil N<sub>2</sub>O concentrations, solute concentrations in soil solution, redox potentials, and water-filled pore space (WFPS). Significance levels are indicated as follows: ‘\*’ P < 0.05, ‘\*\*’ P < 0.01 and ‘\*\*\*’ P < 0.001. Non-significant effects and interactions are indicated as ns.

	N <sub>2</sub> O (μmol m <sup>-3</sup> )	NH <sub>4</sub> <sup>+</sup> (μmol l <sup>-1</sup> )	NO <sub>3</sub> <sup>-</sup> (μmol l <sup>-1</sup> )	DOC (μmol l <sup>-1</sup> )
type	ns	ns	ns	ns
depth	ns	ns	ns	ns
day	$F_{\text{inc}}(3, 90) = 6.77^{***}$	$F_{\text{inc}}(3, 41.3) = 6.13^{**}$	$F_{\text{inc}}(3, 16.6) = 20.38^{***}$	$F_{\text{inc}}(3, 21) = 84.68^{***}$
type×depth	ns	$F_{\text{inc}}(1, 15.7) = 4.83^*$	ns	$F_{\text{inc}}(1, 6.7) = 7.13^*$
type×day	$F_{\text{inc}}(3, 90) = 6.39^{***}$	ns	$F_{\text{inc}}(3, 18.6) = 3.35^*$	$F_{\text{inc}}(3, 22) = 9.12^{***}$
depth×day	ns	ns	$F_{\text{inc}}(3, 15.7) = 6^{**}$	$F_{\text{inc}}(3, 17.6) = 11.9^{***}$
type×depth×day	ns	ns	ns	ns

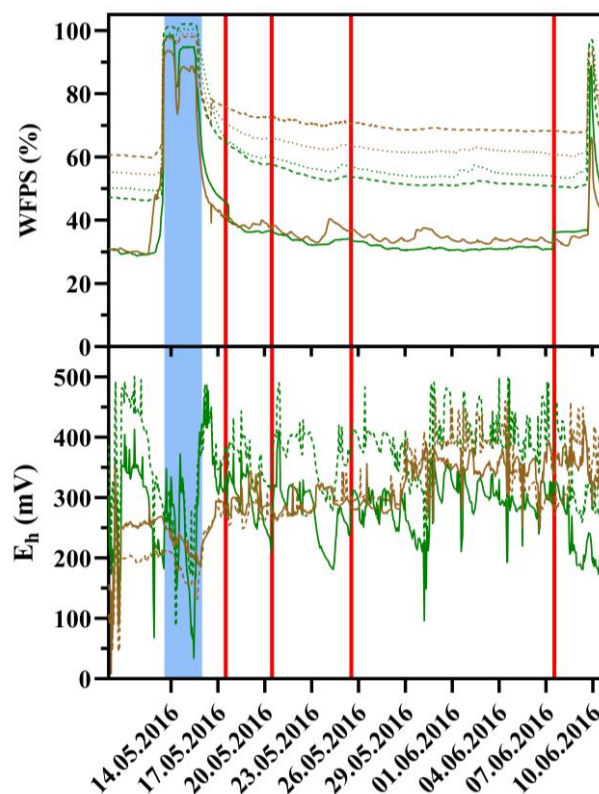


**Fig. 4.1.** Average water-filled pore space (WFPS; upper panel) and redox potential ( $E_h$ ; lower panel) in 15 cm (solid line), 30 cm (dashed line) and 45 cm (dotted line) depth. The blue-shaded area denotes the flood period and red lines indicate the sampling days

Ammonium ( $\text{NH}_4^+$ ) concentrations in pore water were low, often close to, or below, the detection limit of the used method. Maximum concentrations ranged between 2.5  $\mu\text{M}$  and 3  $\mu\text{M}$  and 2.6  $\mu\text{M}$  and were similar in both plot types.  $\text{NH}_4^+$  concentrations showed a tendency to decrease with time, at least in 30 cm depth (Fig. 4.2; Table 4.1). By contrast, nitrate ( $\text{NO}_3^-$ ) concentrations were up to three orders of magnitude higher and generally followed an increasing trend, especially in 15 cm depth, where the trends in mean  $\text{NO}_3^-$  concentration were quite similar between both plot types (Fig. 4.2). In 30 cm depth, mean  $\text{NO}_3^-$  concentrations in bare plots increased stronger than in the *Phalaris* plots (Table 4.1). DOC concentrations displayed a similar temporal pattern as  $\text{NO}_3^-$  (Fig. 4.2). The increasingly higher DOC concentrations in the *Phalaris* plots in 15 cm below soil surface caused a series of significant interaction effects of type, day, and depth (Table 4.1). Overall, however, the differences in hydrochemistry between the two plot types were rather small, and the presence/absence of *P. arundinacea* had no significant effect on the assessed parameters (Table 4.1).

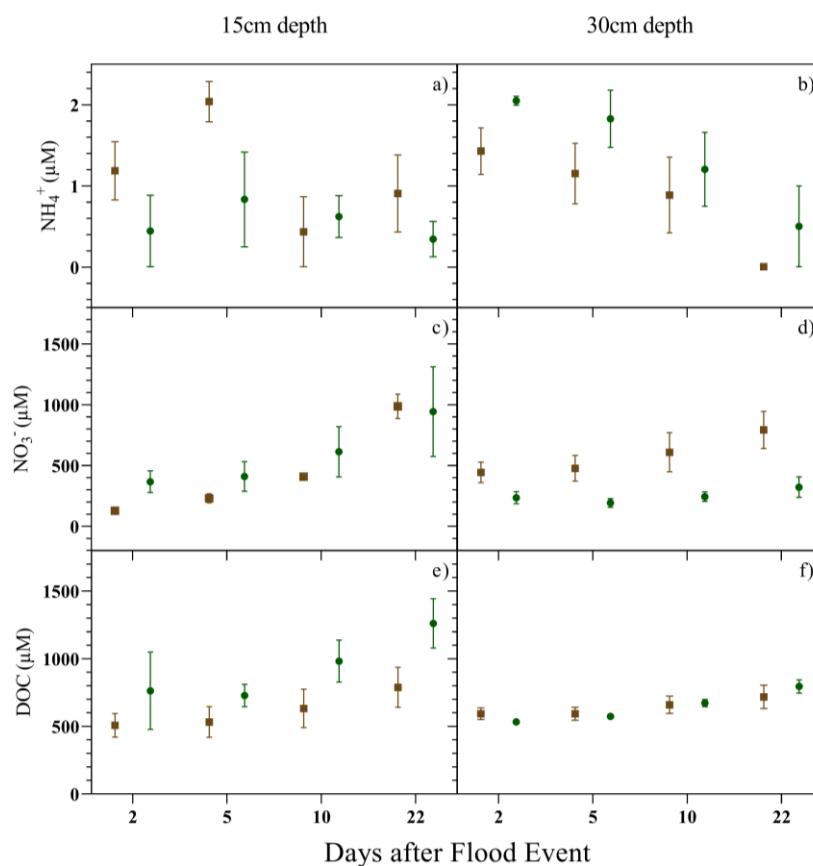


**Fig. 4.2.** Temporal patterns of ammonium ( $\text{NH}_4^+$ ; a and b), nitrate ( $\text{NO}_3^-$ ; c and d) and dissolved organic carbon (DOC; e and f) in soil solution collected at 15 cm (left column) and 30 cm (right column) soil depth during the observation period. Average values from bare plots are indicated as filled brown squares and from *Phalaris* plots as filled green circles. Values are reported as mean  $\pm$  SE for 2 to 6 replicates.

#### 4.3.2 $\text{N}_2\text{O}$ fluxes and soil concentrations

The flood event led to a substantial increase in net  $\text{N}_2\text{O}$  fluxes relative to the pre-flood emission rates (Fig. 4.3). However, after the flood event, the scatter of  $\text{N}_2\text{O}$  flux rates between the replicates of each plot type was quite high, with fluxes ranging from 0.7 to 9.9  $\mu\text{mol m}^{-2} \text{h}^{-1}$  in the bare plots, and from 0.7 to 12.3  $\mu\text{mol m}^{-2} \text{h}^{-1}$  in *Phalaris* plots, respectively. In the bare plots, maximum mean  $\text{N}_2\text{O}$  emission rates were measured on the second day after the flood and continuously decreased afterwards, whereas mean flux rates from plots with *P. arundinacea* reached their maximum a couple of days later and remained relatively stable thereafter (Fig. 4.3). The average  $\text{N}_2\text{O}$  flux rates between the two plot types were not significantly different for the first two observation dates after flooding. However, for days 10 and 22 after the flood event, plots with *P. arundinacea* emitted significantly more  $\text{N}_2\text{O}$  than the bare plots (Fig. 4.3, Table 4.2).

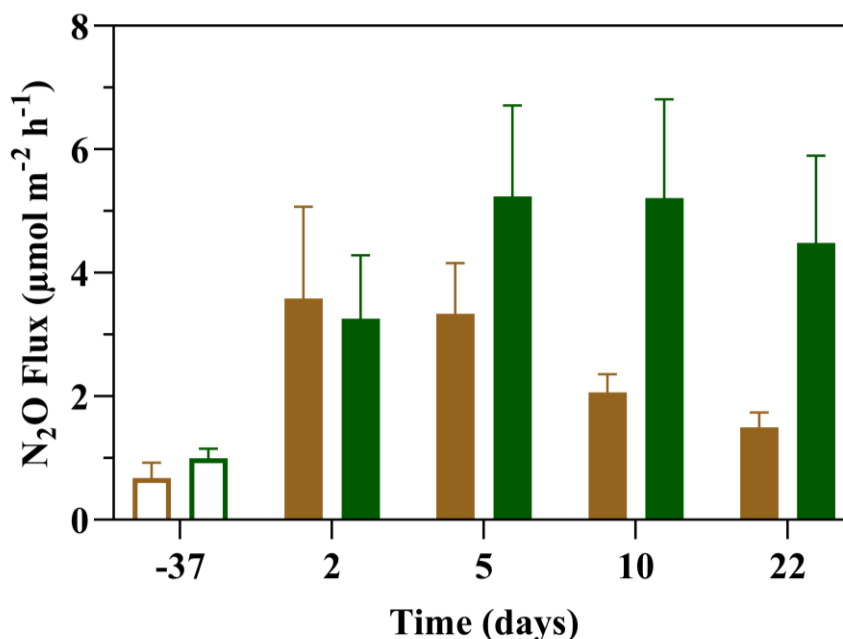


**Fig. 4.3.** N<sub>2</sub>O efflux rates (mean ± SE; n = 6) from bare (filled brown squares) and *Phalaris* plots (filled green circles). Reference efflux rates taken prior the flood event are shown as an open brown bar and an open green bar for the bare and for the *Phalaris* plots, respectively.

**Table 4.2:** Comparison between bare plots and *Phalaris* plots with regards to soil-emitted N<sub>2</sub>O flux rates, the source partitioning of the ND&HD process group to gross N<sub>2</sub>O production ( $f_{\text{ND\&HD}_{\text{gross}}}$ ) and the residual fraction of unreduced N<sub>2</sub>O relative to total N<sub>2</sub>O production ( $r_{\text{N}_2\text{O}_{\text{total}}}$ ) assessed under the model assumptions of Scenario R-M and Scenario M-R, respectively. Data are shown for 2, 5, 10 and 22 days after the flood event. Significant changes between sampling days are reported based on adjusted P values for multiple comparisons (Benjamini and Hochberg, 1995). Significance levels are indicated as follows: ‘\*’ P ≤ 0.05, ‘\*\*’ P ≤ 0.01, ‘\*\*\*’ P ≤ 0.001. Non-significant effects and interactions are indicated as ns.

	$f_{\text{ND\&HD}_{\text{gross}}}$			$r_{\text{N}_2\text{O}_{\text{total}}}$	
	N <sub>2</sub> O Flux	Scenario R-M	Scenario M-R	Scenario R-M	Scenario M-R
day 02	ns	P = 0.002**	P = 0.013*	P = 0.033*	P = 0.012*
day 05	ns	ns	ns	ns	ns
day 10	P = 0.035*	ns	ns	ns	ns
day 22	P = 0.010*	ns	ns	ns	ns

The measured individual N<sub>2</sub>O concentrations in the pore space of each plot were quite variable, especially in the *Phalaris* plots during the first two sampling days (Fig. 4.4). The highest mean N<sub>2</sub>O concentrations in the soil profiles were observed in both plot types at 45 cm depth reaching



$554 \pm 84 \mu\text{mol m}^{-3}$  in the bare plots and  $417 \pm 148 \mu\text{mol m}^{-3}$  in the *Phalaris* plots on day 2 and day 5, respectively (mean  $\pm$  SE; n = 6). The mean N<sub>2</sub>O concentrations decreased steadily at all depths, resulting in no major changes in the depth distribution of N<sub>2</sub>O concentrations. However, from day 10 onwards, differences in N<sub>2</sub>O concentrations in the soils began to emerge between the two plot types, with higher concentrations in the *Phalaris* plots than in the bare plots (Table 4.1). This emerging differentiation in soil N<sub>2</sub>O concentrations is consistent with the observed temporal N<sub>2</sub>O emission patterns of relatively higher emissions from *Phalaris* plots relative to the bare plots from that time point on.

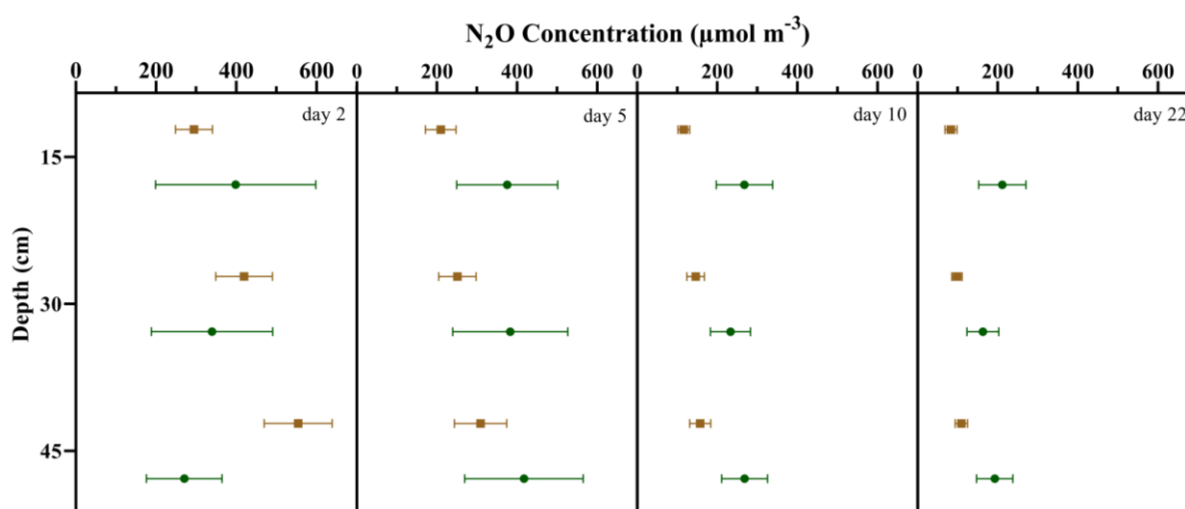


**Fig. 4.4.** Temporal changes of N<sub>2</sub>O concentration in three soil depths (mean  $\pm$  SE; n = 6) in bare (filled brown squares) and *Phalaris* plots (filled green circles).

#### 4.3.3 Stable isotope ratios of soil-emitted N<sub>2</sub>O

The analysis of the isotopic composition of soil-emitted N<sub>2</sub>O revealed that the presence/absence of *P. arundinacea* and time had both significant effects on all isotopic parameters ( $\delta^{15}\text{N}_{\text{N}_2\text{O}}$ ,  $\delta^{18}\text{O}_{\text{N}_2\text{O}}$  and  $^{15}\text{N}$  SP; Table 4.3).  $^{15}\text{N}$  SP values for emitted N<sub>2</sub>O was consistently lower in plots with *P. arundinacea* compared to that emitted from bare plots, with an overall average of  $8.4 \pm 1.3 \text{ ‰}$  and  $15 \pm 0.7 \text{ ‰}$ , respectively (mean  $\pm$  SE; n = 24; Fig. 4.5, Table 4.4). Further, we observed a continuous increase in  $\delta^{15}\text{N}_{\text{N}_2\text{O}}$  values in both plot types, yet, with significantly more negative values observed in the bare plots than in *Phalaris* plots, particularly during the first two sampling dates (Fig. 4.5, Table 4.4). By contrast, significant differences in the  $\delta^{18}\text{O}_{\text{N}_2\text{O}}$  between the two plot types became apparent only from the fifth day after the flood event onward, with the  $\delta^{18}\text{O}_{\text{N}_2\text{O}}$  values from *Phalaris* plots being lower than in N<sub>2</sub>O from bare plots (Table 4.4).

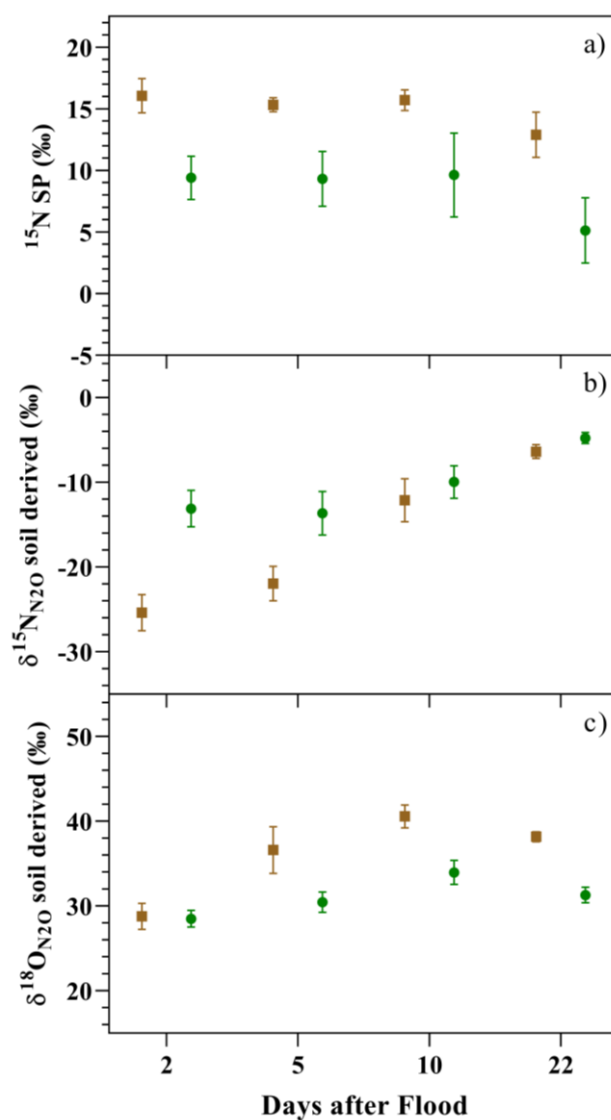


**Fig. 4.5.** Temporal changes of a)  $^{15}\text{N}$  SP, b)  $\delta^{15}\text{N}_{\text{bulk}}$  and c)  $\delta^{18}\text{O}_{\text{N}_2\text{O}}$  of background-corrected  $\text{N}_2\text{O}$  values (mean  $\pm$  SE;  $n = 6$ ) emitted from bare (filled brown squares) and *Phalaris* plots (filled green circles).

**Table 4.3:** ANOVA table of effects and interactions of experimental factors on isotopic signatures of soil-emitted  $\text{N}_2\text{O}$ . Significance levels are indicated as follows: ‘\*’  $P \leq 0.05$ , ‘\*\*’  $P \leq 0.01$ , ‘\*\*\*’  $P \leq 0.001$ . Non-significant effects and interactions are indicated as ns.

	$^{15}\text{N}$ SP	$\delta^{15}\text{N}_{\text{bulk}}$	$\delta^{18}\text{O}_{\text{N}_2\text{O}}$
Type	$F_{(1, 10)} = 7.49^*$	$F_{(1, 10)} = 8.31^*$	$F_{(1, 10)} = 10.6^{**}$
Day	$F_{(3, 30)} = 4.07^*$	$F_{(3, 30)} = 36.06^{***}$	$F_{(3, 30)} = 19.9^{***}$
Type $\times$ Day	ns	$F_{(3, 30)} = 5.9^{**}$	$F_{(3, 30)} = 3.7^*$

**Table 4.4:** Day-wise comparison between bare plots and *Phalaris* plots with regards to the isotopic signatures of soil-emitted N<sub>2</sub>O. Data are shown for 2, 5, 10 and 22 days after the flood event. Significant changes between sampling days are reported based on adjusted P values for multiple comparisons (Benjamini and Hochberg, 1995). Significance levels are indicated as follows: ‘\*’ P ≤ 0.05, ‘\*\*’ P ≤ 0.01, ‘\*\*\*’ P ≤ 0.001. Non-significant effects and interactions are indicated as ns.

	<sup>15</sup> N SP	δ <sup>15</sup> N <sup>bulk</sup>	δ <sup>18</sup> O <sub>N<sub>2</sub>OH<sub>2</sub>O</sub>
day 02	P = 0.036*	P < 0.001***	ns
day 05	P = 0.036*	P = 0.006**	P = 0.004**
day 10	P = 0.036*	ns	P = 0.003**
day 22	P = 0.027*	ns	P = 0.003**

#### 4.3.4 N<sub>2</sub>O source partitioning and estimates of partial N<sub>2</sub>O reduction

The isotopic signatures of samples of soil-emitted N<sub>2</sub>O from both plot types were mostly clustering between the mixing and the designated N<sub>2</sub>O reduction line in the dual-isotope maps (Fig. 4.6), clearly indicating the combined effects of mixing of N<sub>2</sub>O from different process groups, and partial reduction of N<sub>2</sub>O. A few samples from *Phalaris* plots with <sup>15</sup>N SP values ranging between -1.1 – -3.7 ‰ were close to, or slightly below the reduction line (Fig. 4.6). The dual-isotope maps revealed a higher variability in δ<sup>18</sup>O<sub>N<sub>2</sub>O</sub> and confirmed the higher <sup>15</sup>N SP values in the bare plots compared to *Phalaris* plots (Fig. 4.6).

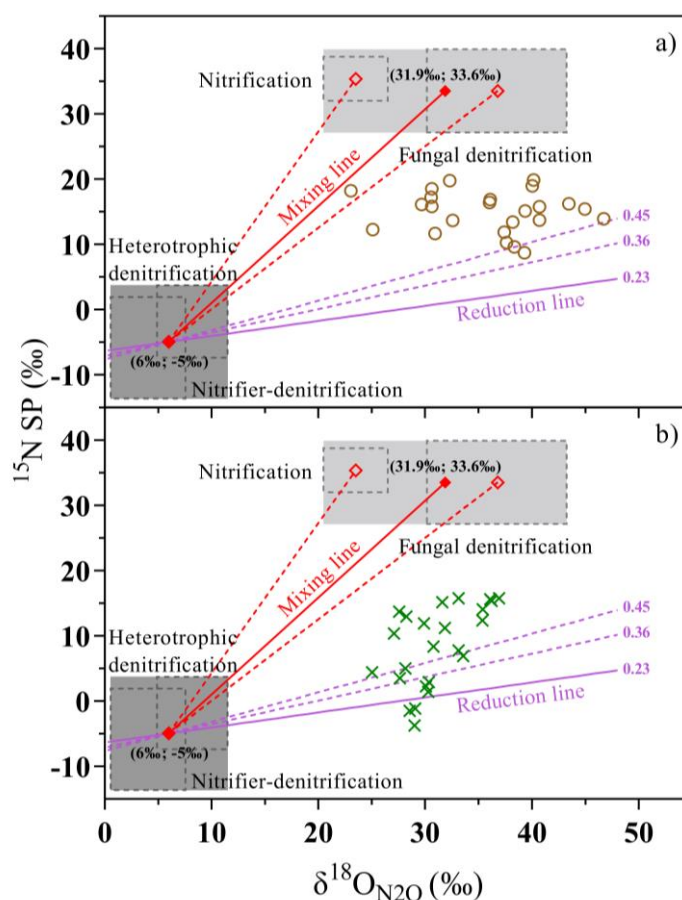


**Fig. 4.6.** Dual isotope maps ( $^{15}\text{N}$  SP vs.  $\delta^{18}\text{O}_{\text{N}_2\text{O}}$ ) of  $\text{N}_2\text{O}$  emitted at different time points. Isotopic signatures of individual samples of  $\text{N}_2\text{O}$  from bare plots a) are indicated as open brown circles. The isotopic values for  $\text{N}_2\text{O}$  from *Phalaris* plots b) are demarked as green crosses. Gray dashed-lined boxes delineate ranges of potential source processes adopted from Yu et al. (2020; see supplementary material, Table S4.1). The  $\delta^{18}\text{O}_{\text{N}_2\text{O}}$  values of the endmember source ranges are calculated with consideration of the respective ambient substrate  $\delta^{18}\text{O}$ : for nitrifier-denitrification (ND), heterotrophic denitrification (HD) and fungal denitrification (FD):  $\delta^{18}\text{O}_{\text{H}_2\text{O}} = -11.8$  ‰ (this study); and nitrification (NI):  $\delta^{18}\text{O}_{\text{O}_2} = 23.5$  ‰. Common endmember isotope values for the process groups ND&HD and NI&FD are shown in parentheses and connected by the mixing line (solid red) used in the mixing-reduction (M-R) model scenario. The red dashed lines indicate the hypothetical mixing lines between the ND&HD process group and nitrification or fungal denitrification alone. The  $\text{N}_2\text{O}$  reduction line used in the reduction-mixing (R-M) scenario is indicated by the solid purple line, calculated from the mean fractionation factors reported in Jinuntuya-Nortman et al. (2008). The dashed purple lines indicate reduction lines as used by Buchen et al. (2018; slope 0.36) or with the mean slope as reported by Yu et al. (2020; slope 0.45)

$\text{N}_2\text{O}$  emissions could largely be attributed to the ND&HD process group, with an overall contribution ( $f_{\text{ND\&HD}_{\text{gross}}}$ ) in both plot types of more than 90 % in the R-M scenario and of about  $68 \pm 16$  % (mean  $\pm$  SD) in the M-R scenario (Fig. 4.7a). However, two days after the flood event, when  $\text{N}_2\text{O}$  emissions were highest in the bare plots, the NI&FD process group was estimated to contribute on average about 25 % in the R-M scenario and about 50 % in the M-R scenario to gross  $\text{N}_2\text{O}$  production. By contrast, in *Phalaris* plots, even during peak emissions,  $\text{N}_2\text{O}$  source partitioning was consistently dominated by the ND&HD process group where average contributions by the NI&FD process group did not exceed 10 % and 30 % in the R-M and M-R scenarios, respectively. This difference in the source composition of  $\text{N}_2\text{O}$  at the beginning of the observation period, regardless of applied scenario, revealed a significant difference between the two plot types (Table 4.2). However, this difference between the two plot types was only temporarily observable under the assumptions of scenario R-M but still relevant enough to cause a significant interaction between plot type and sampling day (Fig. 4.7a, Table 4.5). Nevertheless, in the M-R scenario a significant effect of pioneer vegetation on the course of  $\text{N}_2\text{O}$  source partitioning could be observed ( Fig. 4.7a, Table 4.5).

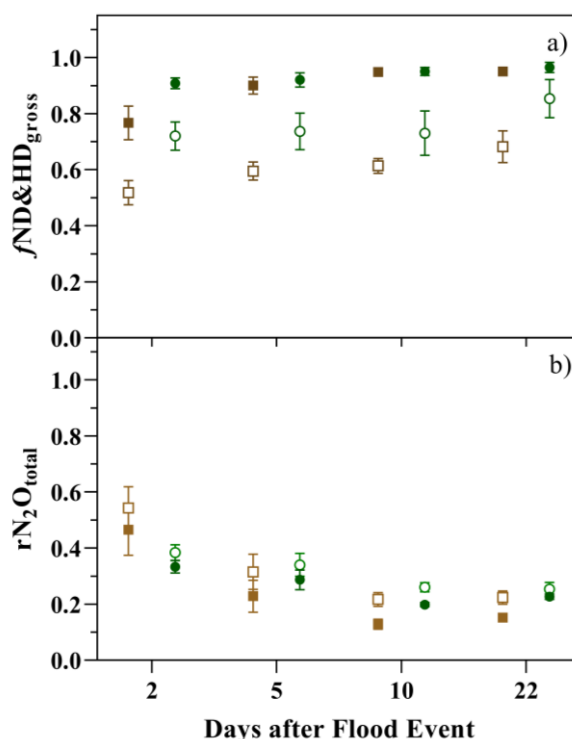


**Fig. 4.7.** Temporal patterns of a) source contribution of the ND&HD process group to gross  $\text{N}_2\text{O}$  production ( $f_{\text{ND\&HD}_{\text{gross}}}$ ) and b) residual  $\text{N}_2\text{O}$  produced by both ND&HD and FD&NI process groups ( $r_{\text{N}_2\text{O}_{\text{total}}}$ ). Data from bare plots and *Phalaris* plots are indicated as squares and circles, respectively. Model estimates considering either a “mixing-reduction” scenario (M-R) or a “reduction-mixing” scenario (R-M) are depicted as open and filled symbols, respectively. Shown are mean values  $\pm$  SE ( $n = 6$ ).

In general, the R-M and M-R scenarios yielded similar estimates of the residual N<sub>2</sub>O fractions after partial N<sub>2</sub>O reduction (Fig. 4.7b). Overall, the remaining N<sub>2</sub>O fraction of originally produced N<sub>2</sub>O that ultimately got emitted was estimated to be only about  $25 \pm 14\%$  in the R-M scenario and  $32 \pm 14\%$  in the M-R scenario (mean  $\pm$  SD). However, both scenarios estimated an average rN<sub>2</sub>O<sub>total</sub> of about  $50 \pm 20\%$  and  $30 \pm 10\%$  (mean  $\pm$  SD) when highest mean N<sub>2</sub>O flux rates were observed from bare plots (day 2) and *Phalaris* plots (day 5), respectively. Significant differences in the extent of N<sub>2</sub>O reduction between the *Phalaris* and the bare plots were only observed two days after the flood event, where the estimated rN<sub>2</sub>O<sub>total</sub> was higher in the bare soils than in *Phalaris* plots (Fig. 4.7b, Table 4.2). However, this effect also diminished over the observation period under the assumptions of both scenarios still causing a significant interaction between plot type and sampling day (Table 4.5).

**Table 4.5:** ANOVA table of effects and interactions of experimental factors on soil-emitted N<sub>2</sub>O flux rates, the source partitioning of the ND&HD process group to gross N<sub>2</sub>O production (fND&HD<sub>gross</sub>) and the residual fraction of unreduced N<sub>2</sub>O relative to total N<sub>2</sub>O production (rN<sub>2</sub>O<sub>total</sub>), assessed for scenarios R-M and M-R, respectively. Significance levels are indicated as follows: ‘\*’ P  $\leq$  0.05, ‘\*\*’ P  $\leq$  0.01, ‘\*\*\*’ P  $\leq$  0.001. Non-significant effects and interactions are indicated as ns.

	fND&HD <sub>gross</sub>			rN <sub>2</sub> O <sub>total</sub>	
	N <sub>2</sub> O Flux	Scenario R-M	Scenario M-R	Scenario R-M	Scenario M-R
Type	ns	ns	$F_{(1,9.4)} = 5.9^*$	ns	ns
Day	ns	$F_{(3,27.6)} = 7.5^{***}$	$F_{(3,26.8)} = 4.1^*$	$F_{(3,27.7)} = 21.3^{***}$	$F_{(3,27.4)} = 18.4^{***}$
Type $\times$ Day	$F_{(3,30)} = 3.03^*$	$F_{(3,27.7)} = 3.1^*$	ns	$F_{(3,27.8)} = 4.0^*$	$F_{(3,27.5)} = 3.1^*$

#### 4.3.5 Abundance of key functional gene transcripts

The quantification of gene transcripts using qPCR confirmed the presence of highly active microbial populations involved in major oxidative and reductive N transformation processes (Fig. 4.8). It further enabled us to assess the temporal and spatial patterns in gene expression of all targeted genes, despite the high variability in gene transcripts between replicate plots. By far the most abundant N-transformation gene transcripts were those of *nxB*, with an overall average of  $1.3 \times 10^8$  and  $1.2 \times 10^8$  copies g<sup>-1</sup> dry soil, detected in the *Phalaris* plots and in the bare plots, respectively (Fig. 4.8e, f). The second most abundant gene transcripts, at similar level, were *nosZ* and *nirS* (Fig. 4.8g, h, i, j). The *nirS* gene transcripts were about 8.5 times more abundant than the bacterial *amoA* gene transcripts in both plot types. Bacterial *amoA* was

generally on the order of four and ten times more abundant than archaeal *amoA* in the bare plots and *Phalaris* plots, respectively (Fig. 4.8a, b, c, d). The ANOVA models revealed that the abundance of all investigated functional gene transcripts was subject to significant temporal changes (Table 4.6). In the bacterial *amoA* and N<sub>2</sub>O reductase (*nosZ*) gene transcripts no statistically significant change in abundance was found over the observation period in all depths of plots covered with *P. arundinacea*. By contrast, significant changes in the temporal pattern of gene transcription of archaeal *amoA*, *nxrB* and *nirS* occurred in both plot types and all soil depths. In general, gene expression of the assessed genes was similar on day 2 and 5 after the flood event in both plot types and for most depths, except for *nxrB* transcripts, which decreased significantly already on day 5. Such a decrease was observed for all other genes ten days after the flood event where we detected significantly less copy numbers on the third sampling day.

**Table 4.6:** ANOVA table of effects and interactions of experimental factors on functional gene transcript abundance. Significance levels are indicated as follows: ‘\*’ P <0.05, ‘\*\*\*’ P <0.01 and ‘\*\*\*\*’ P <0.001. Non-significant effects and interactions are indicated as ns.

	<i>nirS</i>	<i>nosZ</i>	<i>nxrB</i>	archaeal <i>amoA</i>	bacterial <i>amoA</i>
Type	ns	ns	ns	ns	ns
Depth	ns	ns	ns	ns	ns
Day	$F_{(3, 30)} = 24.9^{****}$	$F_{(3, 32.8)} = 14.9^{****}$	$F_{(3, 38.4)} = 14.8^{****}$	$F_{(3, 30)} = 34.2^{****}$	$F_{(3, 30)} = 8.6^{****}$
Type × Depth	ns	ns	ns	ns	ns
Type × Day	ns	ns	ns	ns	ns
Depth × Day	ns	ns	ns	ns	ns
Type × Depth × Day	ns	ns	ns	ns	ns

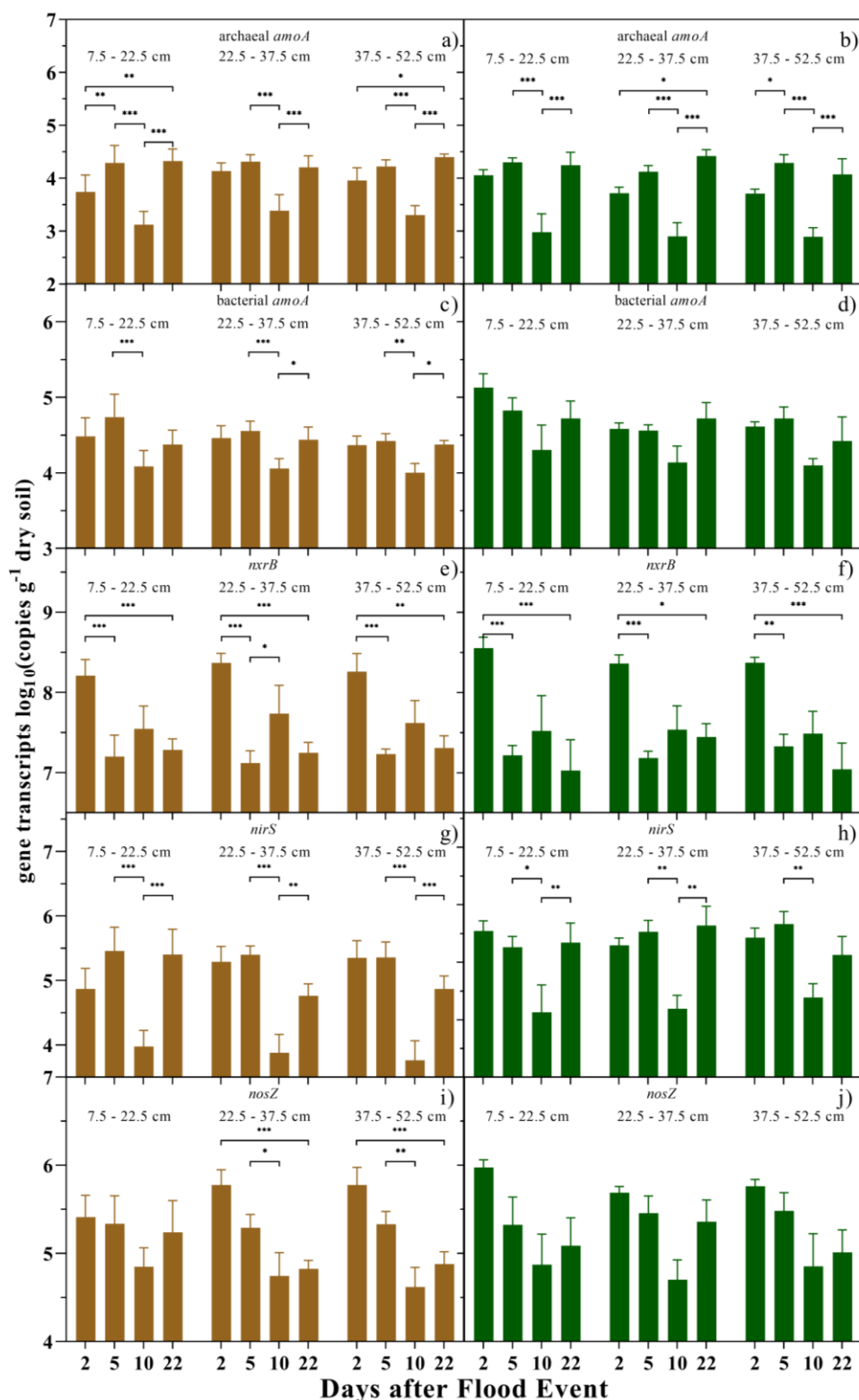


**Fig. 4.8.** Log-transformed transcript abundances of N-cycling functional genes from three depth sections of the bare plots (brown bars; a, c, e, g and i) and *Phalaris* plots (green bars; b, d, f, h and j), respectively. Data are shown for 2, 5, 10 and 22 days after the flood event as mean  $\pm$  SE ( $n = 6$ ). Significant differences between sampling days are reported based on adjusted P values for multiple comparisons (Benjamini-Hochberg, 1995). Significance levels are indicated as follows: ‘\*’  $P \leq 0.05$ , ‘\*\*’  $P \leq 0.01$ , ‘\*\*\*’  $P \leq 0.001$ .



---

## 4.4 Discussion

In the first section of the following discussion, the focus will be on how the presence/absence of *P. arundinacea* affected the specific temporal patterns of the enhanced post-flood N<sub>2</sub>O emissions and the role of N<sub>2</sub>O reduction in controlling these emissions in both plot types. Since the R-M and M-R scenarios applied in the isotope mapping approach yielded very similar estimates for rN<sub>2</sub>O<sub>total</sub>, these results will not be discussed separately. The second section will elaborate on how *P. arundinaceae* functions as an ecosystem engineer shaping the balance between major microbial N cycling processes. However, due to the different estimates in gross N<sub>2</sub>O source partitioning (e.g.,  $f_{ND\&HD_{gross}}$ ) in the two scenarios, the plausibility of each scenario will be addressed first for both soil types.

Although there is an ongoing discourse about a potential transport of N<sub>2</sub>O via plant-specific physiological traits of *P. arundinacea* like aerenchyma (Rückauf et al., 2004; Jørgensen et al., 2012) such plant-related gas fluxes were not explicitly investigated in this study. Therefore, the N<sub>2</sub>O emissions assessed from the *Phalaris* plots in this study represent soil fluxes without including the plant shoot. It is thus possible that a certain fraction of N<sub>2</sub>O was not accounted for in the *Phalaris* plots of the field experiment. However, this would not have changed the conclusion reached that *P. arundinacea* promotes emissions of N<sub>2</sub>O.

In addition, it became evident that the interpretation of microbial gene transcripts extracted from different soil depths in relation to isotopic signatures of soil-emitted N<sub>2</sub>O should be conducted cautiously. Although it can provide valuable additional information about the current biogeochemical processes taking place, complex interactions between environmental conditions and unassessed steps following gene transcription, like enzyme production and finally enzyme activity, can lead to a temporal offset between observed gene transcript abundance and isotopic signatures of N<sub>2</sub>O. Further, microbe-specific differences in reaction time in their gene transcription in response to environmental changes can also lead to such temporal offsets. For this reason, the gene transcription data were used prudently in the following discussion.

### 4.4.1 Pioneer vegetation shapes N<sub>2</sub>O emission patterns in the riparian zone

A period of enhanced N<sub>2</sub>O emissions after the flood event was expected from previous studies in this area (Shrestha et al., 2012), enabling a detailed investigation of N<sub>2</sub>O emission patterns and their connection to the presence/absence of pioneer vegetation. The N<sub>2</sub>O emission rates thereby significantly exceeded the average emission rates found during the undisturbed reference period in this floodplain, reaching magnitudes comparable to those repeatedly observed from various temperate wetlands and even fertilized croplands (Jacinthe et al., 2012;

---

Oertel et al., 2016). These strong flux rates stand in contrast to the observations made in riparian ecosystems with little or no disturbance (Audet et al., 2014; Davis et al., 2019). However, flood-related, sporadically occurring events of high N<sub>2</sub>O emissions can make up a large fraction of annual cumulative emissions (Clar and Anex, 2020; Molodovskaya et al., 2012). Our findings, even though the study presented here comprised only one post-flood phase, therefore indicate the importance to integrate these periods into assessments of GHG budgets of floodplains to avoid underestimation.

N<sub>2</sub>O emissions reached their maximum flux rates of similar magnitude in both plot types within the first week after the flood event. However, the different residual fractions of originally produced N<sub>2</sub>O between the two plot types that got emitted at this point indicated that the presence of pioneer vegetation must have a regulating effect on the extent of N<sub>2</sub>O reduction that controlled the strength of peak N<sub>2</sub>O emission rates to a certain degree. In turn, the significantly larger rN<sub>2</sub>O<sub>total</sub> fractions observed in the bare plots than in the *Phalaris* plots under peak emissions two days after the flood event not only could partially explain these high emissions but also highlight the susceptibility of N<sub>2</sub>O reduction to flood-related perturbances in sediments without plant cover. However, the transcript numbers of the *nosZ* gene, encoding the N<sub>2</sub>O reductase enzyme, were comparable between bare and *Phalaris* plots during peak emissions, indicating that denitrifying bacteria tried to actively use the entire denitrification pathway in both plot types to an equal extent. This apparently contradicts the observed differences in rN<sub>2</sub>O<sub>total</sub> but can be explained, for example, by the circumstance that the flood-related changes in environmental conditions within the different plot types likely did not affect gene expression at the transcription level but probably on a subsequent step, such as enzyme activity. In case of the bare plots, it seems that an efficient initial re-aeration of the pore space in the uppermost segment of the bare soils temporarily inhibited the oxygen-sensitive N<sub>2</sub>O reductase enzymes (Morley et al., 2008), allowing more N<sub>2</sub>O to reach the soil surface during the first days after the flood event. By contrast, the consistently low rN<sub>2</sub>O<sub>total</sub> estimates in the *Phalaris* plots indicated that N<sub>2</sub>O reductase was continuously active without disruption, even though the soils desaturated rapidly and allowed fast aeration of the macropore space. This interpretation is corroborated by the constant transcription of the *nosZ* gene, which, in turn, suggests that in the presence of *P. arundinacea*, stable anoxic microhabitats were present within a matrix of less reducing conditions in the soil throughout the observation period. It is likely that root respiration and the more abundant macroaggregates (250 – 2000 μm) in the *Phalaris* plots found by Schomburg et al. (2019) would not only locally limit oxygen availability (Fender et al., 2013) but also impede gas diffusion into anoxic denitrification hotspots inside the aggregates therefore

---

physically protecting the functionality of the N<sub>2</sub>O reductase. These soil aggregates, once water-saturated, can form persistent internal diffusion barriers protecting anoxic microhabitats even under progressing soil drying and re-aeration of the inter-aggregate pore space. This ability to efficiently exclude oxygen from denitrification hotspots could be linked to their longer, more complex intra-aggregate pore structure, and the higher capability of smaller pores to resist water loss (Ebrahimi and Or, 2016; Li et al., 2020).

The effect of pioneer vegetation on N<sub>2</sub>O emission rates emerged primarily in the later part of the observation period. After the first week of the post-flood phase, N<sub>2</sub>O emissions from *Phalaris* plots remained stable at relatively high levels and those from bare plots gradually returned to pre-flood flux rates. At this time, it became evident that these increasingly different emission rates must be the result of a higher production activity of N<sub>2</sub>O source processes in the *Phalaris* plots than in bare plots, since at the same time, the rN<sub>2</sub>O<sub>total</sub> estimates were similar in both plot types. Indeed, the  $\delta^{15}\text{N}^{\text{bulk}}$  values of emitted N<sub>2</sub>O from both plot types further increased, corroborating that N<sub>2</sub>O reduction was still ongoing (Mohn et al., 2013). This implies that both plot types contained persistent anoxic microsites, supporting N<sub>2</sub>O reduction over an extended period. Such confined anoxic areas have previously been found in proximity of buried organic matter, where the increased availability of labile C compounds and nutrients stimulates the activity of heterotrophic decomposers, and therefore increasing the oxygen demand in the soil (Parkin, 1987; Loecke and Robertson, 2009; Li et al., 2016). Considering the slowly increasing redox potentials, such an accumulation of sedimented organic matter would be essential, particularly in the bare soils to sustain local anoxic hotspots for reductive N<sub>2</sub>O production and reduction since these soils lack other complex structures to prevent complete re-oxygenation. However, in areas where organic matter accumulated, the continuously high pore water saturation in the lower depths of the bare plots would have further increased the O<sub>2</sub> limitation by creating extensive diffusion barriers. This suggests that anaerobic N<sub>2</sub>O production and reduction mainly occurred in the deeper parts of the soil profile, where organic matter decomposition and high WFPS would function as the main controls on O<sub>2</sub> availability rather than soil aggregates. Such reducing conditions would also make a constant *de novo* production of N<sub>2</sub>O reductase enzymes unnecessary, allowing denitrifying bacteria to reduce *nosZ* transcription, as seen in the steady decrease in *nosZ* transcript abundance in the deeper sections of bare plots. In the presence of *P. arundinacea*, in addition to detritus accumulation, root respiration and microbial mineralization of root exudates may support the formation of persistent anoxic conditions in certain areas of the soil system, like soil aggregates (Fender et al., 2013). However, since most of the root system of *P. arundinacea* can be found

in the upper 20 cm of soils (Klimešová and Šrůtek, 1995), it is reasonable to assume, that these plant-related oxygen consumption processes would be more relevant in the topsoil of the *Phalaris* plots. This is supported by the observation of lower redox potentials in 15 cm than in 30 cm depth, where increasing recalcitrance of older buried organic matter, and less root deposits, would in turn reduce soil respiration with increasing soil depth. Overall, it appears that plant-soil interactions, leading to incipient soil aggregation and expansion of the pore network, in combination with locally high oxygen demand by the plant roots and microorganism created a resilient soil environment that compensated for the effects of rapid flood-related changes in pore water saturation and redox conditions. These conditions promoted a constant production of N<sub>2</sub>O by both aerobic and anaerobic processes, leading to continuously high emissions from the *Phalaris* plots. By contrast, oxygen diffusion was more severely hindered in the bare plots by the unstructured, highly water saturated sediments, intensified by enhanced local oxygen consumption by decomposition processes in proximity of sedimented organic matter. Bare soils therefore seemed to have provided more persistent microhabitats favorable for anaerobic N<sub>2</sub>O production and more efficient reduction of N<sub>2</sub>O to N<sub>2</sub> at least in the deeper parts of the plots. The assumption of such persistent anoxic conditions even in the later post-flood phase is supported by the intensified reduction of N<sub>2</sub>O to N<sub>2</sub> reflected by decreasing rN<sub>2</sub>O<sub>total</sub> values, since the N<sub>2</sub>O reductase enzyme requires the exclusion of oxygen to function properly. Such a decrease in N<sub>2</sub>O:N<sub>2</sub> production ratio would be also in line with the continuous decrease of N<sub>2</sub>O emission rates observed in the bare soils after the first week into the post-flood phase.

#### 4.4.2 Simultaneous activity of oxidative and reductive processes causes prolonged N<sub>2</sub>O emissions from soils under *P. arundinacea* stands

The presence of pioneer vegetation in the plots covered by *P. arundinacea* substantially impacted the N<sub>2</sub>O source partitioning, which can be related to the improved soil porosity, enhanced pore connectivity and soil aggregation (Schomburg et al., 2019), and consequently the soil redox conditions. Indeed, the soil structure in the *Phalaris* plots was more conducive to soil aeration (i.e., less reducing conditions in the macropore network after the flood event), as indicated by rapid desaturation of large parts of the pore space at all depths, and the rapid return of the redox potentials back to pre-flood conditions (Fig. 4.1). This may have allowed nitrifying microorganisms colonizing the macropore space to return to aerobic metabolisms relatively fast after the flood water recession, which is supported by the generally higher abundance of bacterial *amoA* transcripts in the *Phalaris* plots (Fig. 4.8d). Therefore, a continuous contribution of the NI&FD process group to the formation of N<sub>2</sub>O from early on is plausible. Further, a more

developed soil structure in the *Phalaris* plots would not only have facilitated the diffusion of oxygen but also of N<sub>2</sub>O produced by different source processes under varying redox conditions in different parts of the soils. In such a system, complete denitrification, and therefore partial N<sub>2</sub>O reduction to N<sub>2</sub>, would be constrained to anoxic microsites, either physically protected within some of the newly formed soil aggregates, large enough to efficiently limit gas diffusion, or in proximity of decomposing organic matter, where respiratory processes limit the availability of oxygen. It is therefore likely that a large fraction of N<sub>2</sub>O from different sources first mixes before getting partially reduced after diffusing into such denitrification hotspots. Thus, the M-R scenario seems to represent the predominant dynamics with regards to source contribution by the two process groups more realistically in the *Phalaris* plots. In this scenario, estimated source partitioning was remarkably stable throughout the whole drying period. Although nitrifier denitrification and heterotrophic bacterial denitrification has generally contributed about 75 % of N<sub>2</sub>O production, a steady and relatively high contribution by the NI&FD process group was also observed, even under peak emissions. This combined constant activity of oxidative and reductive processes ultimately resulted in the observed prolonged enhanced N<sub>2</sub>O emissions from the *Phalaris* plots. This suggests that *P. arundinacea*, as an ecosystem engineer, was able to modify the soil system to simultaneously maintain oxic and anoxic zones in close proximity to each other over an extended period of time (Philippot et al., 2009). The high redox potentials observed directly after the flood event prior the initial sampling day indicate a rapid re-aeration of the inter-aggregate pore space, creating suitable conditions for nitrification in the larger pores of the soil volume. Further, *P. arundinacea* possesses aerenchyma (highly porous plant tissues) as an adaptation to its flood-prone habitat, which enables this plant to aerate its rhizosphere (Colmer, 2003; Jørgensen et al., 2012). This additional oxygen supply would ensure a certain stability in redox conditions to the proximity of plant roots beneficial for aerobic processes like nitrification, thereby buffering flood-related disturbance effects on source partitioning. In turn, denitrifying processes would be sustained in areas of the soil where root respiration of *P. arundinacea* and heterotrophic decomposition of root exudates and dead root material would limit the availability of O<sub>2</sub>.

In case of the bare soils, gas diffusion is likely physically impeded due to the combination of its sandy texture, its poorly developed soil structure, and the persistently high pore water saturation in 30 cm and 45 cm soil depths. In addition, oxygen availability is further limited in proximity of sedimented, decomposing organic material. Taken together, such conditions would promote the formation of stable anoxic hotspots of bacterial denitrification in deeper layers of the soils in which N<sub>2</sub>O gets reduced prior mixing with N<sub>2</sub>O from other sources.

Therefore, it is likely that the R-M scenario reflects the dynamics in source partitioning in the bare soils more accurately than the M-R scenario. In the R-M scenario, it became evident that peak emissions in the bare plots were the result of simultaneous N<sub>2</sub>O production by both process groups, where the NI&FD process group contributed about 20 % to gross N<sub>2</sub>O production. The fast and extensive desaturation of the topmost investigated section of the bare soils together with a notably higher *amoA* gene transcription in 7.5 - 22.5 cm depth (Fig. 4.1, Fig. 4.8c) indicated that nitrifying microorganisms already began to switch from anaerobic back to aerobic pathways directly after flood water recession. In this transition phase, a temporary metabolic disbalance between the individual steps of nitrification could have led to the formation of N<sub>2</sub>O by decomposition of intermediates (Zhu et al., 2013; Prosser et al., 2020). However, this disbalance seems to be overcome after the first week indicated by almost complete absence of contribution of nitrifying processes to N<sub>2</sub>O emissions (e.g., an *f*ND&HD of almost 100 %). Due to this rapid decline in estimated contributions of the NI&FD process group to gross N<sub>2</sub>O production, even a potential contribution from fungal denitrification, which cannot be fully excluded, would be of minor importance, even though it has been shown that fungal communities are resilient to short-term flooding (Graupner et al., 2017). Furthermore, the simultaneous decrease in mean NH<sub>4</sub><sup>+</sup> concentrations with increasing NO<sub>3</sub><sup>-</sup> concentrations at 15 cm depth after the first post-flood week (Fig. 4.2a, c). would rather support the assumption of an initial contribution of nitrification rather than fungal denitrification. In turn, denitrifying processes in deeper, still highly saturated sections of the soil columns became the almost only source of N<sub>2</sub>O in the later drying phase, which is in line with previous studies demonstrating that short-term flooding could lead to enhanced denitrification rates even weeks after the flood event (Tomasek et al., 2019).

## 4.5 Conclusion

In this field manipulation experiment, the effects of the presence/absence of pioneer vegetation on N<sub>2</sub>O emission patterns and their underlying production and consumption processes after a short-term flood event have been studied. Gas flux measurements were combined with natural abundance stable isotope analysis and RNA-based molecular techniques. Although no major effect of *P. arundinacea* on the magnitude of N<sub>2</sub>O emission rates was found, it became evident that the soil structuring effect of pioneer vegetation and plant-soil interactions created environmental conditions that promote longer periods of constantly high N<sub>2</sub>O emissions. These emissions originated from multiple oxidative and reductive processes, where nitrification made up a substantial fraction. By contrast, the initially high but gradually decreasing N<sub>2</sub>O emissions

from bare plots derived almost exclusively from denitrifying processes. This dominance of denitrification seemed to be the result of extensive long-lasting anoxia in deeper sections of the soil column promoted by poor pore water drainage and elevated O<sub>2</sub> demand by heterotrophic decomposition of sedimented organic matter. It is therefore likely that areas covered by *P. arundinacea* would turn into transient but longer-lasting hotspots, ultimately emitting more N<sub>2</sub>O after flood disturbances than unvegetated sandbars.

The investigation of the role of N<sub>2</sub>O reduction in the formation of elevated N<sub>2</sub>O emissions, functioning as the biological sink of N<sub>2</sub>O, revealed that during most of the time only 15 to 30 % of originally produced N<sub>2</sub>O reached the soil surface. This high N<sub>2</sub>O removal efficiency emphasizes the importance of N<sub>2</sub>O reduction in the temporal development of N<sub>2</sub>O emission rates, especially in case of the bare soils. However, the observed sensitivity of N<sub>2</sub>O reduction to the presence of oxygen could pose a risk for stronger emissions of N<sub>2</sub>O if soil conditions become less favorable for N<sub>2</sub>O reduction. Mitigation strategies should thus focus on the promotion of complete denitrification by, e.g., planting fast-growing vegetation known to buffer the negative effects of flood perturbation on N<sub>2</sub>O reduction like *Salix viminalis* and/or plants known to sequester high amounts of carbon thereby creating a high O<sub>2</sub> demand by heterotrophs and thus ideal conditions for N<sub>2</sub>O reduction.

Overall, these findings improve our understanding of the post-flood microbial N<sub>2</sub>O production and consumption process dynamics involved in the emergence of periods of enhanced N<sub>2</sub>O emissions in presence/absence of an ecosystem engineer like *P. arundinacea*. This information will help to improve the assessment of the climate regulation function and GHG budget of hydrologically active river floodplain ecosystems.

*Data availability.* All data are openly available at [www.envidat.ch](http://www.envidat.ch)

*Conflicts of interest.* The authors declare that they have no conflicts of interests.

*Authors contributions.* The concept of the field manipulation experiment was developed and installed by JL. ML planned and designed the sampling campaign in detail and conducted it. PAN supervised the measurement of N<sub>2</sub>O gas concentrations and helped with data analysis, ML conducted all other measurements and data analyses. MFL supervised IRMS measurements and isotope data interpretation. ML wrote the manuscript together with MFL and JL, with input from all other co-authors.

**Acknowledgements**

The authors thank Dr. Daniel B. Nelson of the Physiological Plant Ecology group at the Botanical Institute of the University of Basel for conducting the isotopic measurements of the pore water. We thank Dr. Thomas Kuhn of the Aquatic and Isotope Biogeochemistry research group at the University of Basel for his assistance with IRMS measurements and analyses. We are also very grateful to Roger Köchli of the research unit Forest Soils and Biogeochemistry, research group Soil Functions and Soil Protection of the Swiss Federal Institute for Forest, Snow and Landscape Research (WSL) for his assistance in the field. This study was funded by the Swiss National Science Foundation (SNSF) under the grant number 200021\_147002, as well as by financial resources of WSL and the University of Basel.



---

## References

- Angers, D.A., Caron, J., 1998. Plant-induced changes in soil structure: Processes and feedbacks, in: Plant-Induced Soil Changes: Processes and Feedbacks. Springer Netherlands, Dordrecht, pp. 55–72. doi:10.1007/978-94-017-2691-7\_3
- Arp, D.J., Stein, L.Y., 2003. Metabolism of Inorganic N Compounds by Ammonia-Oxidizing Bacteria. *Critical Reviews in Biochemistry and Molecular Biology* 38, 471–495. doi:10.1080/10409230390267446
- Audet, J., Hoffmann, C.C., Andersen, P.M., Baattrup-Pedersen, A., Johansen, J.R., Larsen, S.E., Kjaergaard, C., Elsgaard, L., 2014. Nitrous oxide fluxes in undisturbed riparian wetlands located in agricultural catchments: Emission, uptake and controlling factors. *Soil Biology and Biochemistry* 68, 291–299. doi:10.1016/j.soilbio.2013.10.011
- Baggs, E.M., 2008. A review of stable isotope techniques for N<sub>2</sub>O source partitioning in soils: recent progress, remaining challenges and future considerations. *Rapid Communications in Mass Spectrometry* 22, 1664–1672. doi:10.1002/rcm.3456
- Baruah, K.K., Gogoi, B., Gogoi, P., Gupta, P.K., 2010. N<sub>2</sub>O emission in relation to plant and soil properties and yield of rice varieties. *Agronomy for Sustainable Development* 30, 733–742. doi:10.1051/agro/2010021
- Benjamini, Y., Hochberg, Y., 1995. Controlling the False Discovery Rate: A Practical and Powerful Approach to Multiple Testing. *Journal of the Royal Statistical Society: Series B (Methodological)* 57, 289–300. doi:10.1111/j.2517-6161.1995.tb02031.x
- Braker, G., Zhou, J., Wu, L., Devol, A.H., Tiedje, J.M., 2000. Nitrite reductase genes (*nirK* and *nirS*) as functional markers to investigate diversity of denitrifying bacteria in pacific northwest marine sediment communities. *Applied and Environmental Microbiology* 66, 2096–2104. doi:10.1128/AEM.66.5.2096-2104.2000
- Buchen, C., Lewicka-Szczebak, D., Flessa, H., Well, R., 2018. Estimating N<sub>2</sub>O processes during grassland renewal and grassland conversion to maize cropping using N<sub>2</sub>O isotopocules. *Rapid Communications in Mass Spectrometry* 32, 1053–1067. doi:10.1002/rcm.8132
- Butler, D.G., Cullis, B.R., Gilmour, A.R., Gogel, B.J., Thompson, R., 2017. ASReml-R Reference Manual Version 4. ASReml-R Reference Manual 176.
- Caranto, J.D., Vilbert, A.C., Lancaster, K.M., 2016. Nitrosomonas europaea cytochrome P460 is a direct link between nitrification and nitrous oxide emission. *Proceedings of the National Academy of Sciences* 113, 14704–14709. doi:10.1073/pnas.1611051113
- Ciais, P., Sabine, C., Bala, G., Al., E., Bopp, L., Brovkin, V., Canadell, J., Chhabra, A., DeFries, R., Galloway, J., Heimann, M., Jones, C., Quéré, C. le, Myneni, R., Piao, S., Thornton, P., Al., E., 2013. Carbon and Other Biogeochemical Cycles, in: Intergovernmental Panel on Climate Change (Ed.), *Climate Change 2013 - The Physical Science Basis*. Cambridge University Press, Cambridge, pp. 465–570. doi:10.1017/CBO9781107415324.015
- Colmer, T.D., 2003. Long-distance transport of gases in plants: a perspective on internal aeration and radial oxygen loss from roots. *Plant, Cell & Environment* 26, 17–36. doi:10.1046/j.1365-3040.2003.00846.x
- Davis, M.P., Groh, T.A., Jaynes, D.B., Parkin, T.B., Isenhardt, T.M., 2019. Nitrous Oxide Emissions from Saturated Riparian Buffers: Are We Trading a Water Quality Problem for an Air Quality Problem? *Journal of Environment Quality* 48, 261. doi:10.2134/jeq2018.03.0127

- 
- Ebrahimi, A., Or, D., 2016. Microbial community dynamics in soil aggregates shape biogeochemical gas fluxes from soil profiles – upscaling an aggregate biophysical model. *Global Change Biology* 22, 3141–3156. doi:10.1111/gcb.13345
- European Environment Agency (EEA), 2020. Floodplains: a natural system to preserve and restore, Report: EEA N024. doi:10.2800/431107
- Fender, A.-C., Leuschner, C., Schützenmeister, K., Gansert, D., Jungkunst, H.F., 2013. Rhizosphere effects of tree species – Large reduction of N<sub>2</sub>O emission by saplings of ash, but not of beech, in temperate forest soil. *European Journal of Soil Biology* 54, 7–15. doi:10.1016/j.ejsobi.2012.10.010
- Fournier, B., Guenat, C., Bullinger-Weber, G., Mitchell, E.A.D., 2013. Spatio-temporal heterogeneity of riparian soil morphology in a restored floodplain. *Hydrology and Earth System Sciences* 17, 4031–4042. doi:10.5194/hess-17-4031-2013
- Frame, C. H., Casciotti, K.L., 2010. Biogeochemical controls and isotopic signatures of nitrous oxide production by a marine ammonia-oxidizing bacterium. *Biogeosciences* 7, 2695–2709. doi:10.5194/bg-7-2695-2010
- Frame, C H, Casciotti, K.L., 2010. Biogeochemical controls and isotopic signatures of nitrous oxide production by a marine ammonia-oxidizing bacterium. *Biogeosciences* 7, 2695–2709. doi:10.5194/bg-7-2695-2010
- Frame, C.H., Lau, E., Joseph Nolan, E., Goepfert, T.J., Lehmann, M.F., 2017. Acidification enhances hybrid N<sub>2</sub>O production associated with aquatic ammonia-oxidizing microorganisms. *Frontiers in Microbiology* 7, 1–23. doi:10.3389/fmicb.2016.02104
- Francis Clar, J.T., Anex, R.P., 2020. Flux intensity and diurnal variability of soil N<sub>2</sub>O emissions in a highly fertilized cropping system. *Soil Science Society of America Journal* 84, 1983–1994. doi:10.1002/saj2.20132
- Frey, B., Carnol, M., Dharmarajah, A., Brunner, I., Schleppei, P., 2020. Only Minor Changes in the Soil Microbiome of a Sub-alpine Forest After 20 Years of Moderately Increased Nitrogen Loads. *Frontiers in Forests and Global Change* 3, 1–18. doi:10.3389/ffgc.2020.00077
- Graupner, N., Röhl, O., Jensen, M., Beisser, D., Begerow, D., Boenigk, J., 2017. Effects of short-term flooding on aquatic and terrestrial microeukaryotic communities: a mesocosm approach. *Aquatic Microbial Ecology* 80, 257–272. doi:10.3354/ame01853
- Gurnell, A., 2014. Plants as river system engineers. *Earth Surface Processes and Landforms* 39, 4–25. doi:10.1002/esp.3397
- Handmer, J., Honda, Y., Kundzewicz, Z.W., Arnell, N., Benito, G., Hatfield, J., Mohamed, I.F., Peduzzi, P., Wu, S., Sherstyukov, B., Takahashi, K., Yan, Z., 2012. Changes in impacts of climate extremes: human systems and ecosystems. In: *Managing the Risks of Extreme Events and Disasters to Advance Climate Change Adaptation. A Special Report of Working Groups I and II of the Intergovernmental Panel on Climate Change (IPCC)* 231–290.
- Hansen, M., Clough, T.J., Elberling, B., 2014. Flooding-induced N<sub>2</sub>O emission bursts controlled by pH and nitrate in agricultural soils. *Soil Biology and Biochemistry* 69, 17–24. doi:10.1016/j.soilbio.2013.10.031
- Hill, A.R., 2011. Buried organic-rich horizons: their role as nitrogen sources in stream riparian zones. *Biogeochemistry* 104, 347–363. doi:10.1007/s10533-010-9507-5
- Hothorn, T., Bretz, F., Westfall, P., 2008. Simultaneous Inference in General Parametric Models. *Biometrical Journal* 50, 346–363. doi:10.1002/bimj.200810425
-

- 
- IUSS Working Group WRB, 2015. World Reference Base for Soil Resources 2014, update 2015., World Soil Resources Reports No. 106. FAO, Rome.
- Jacinthe, P.A., Bills, J.S., Tedesco, L.P., Barr, R.C., 2012. Nitrous Oxide Emission from Riparian Buffers in Relation to Vegetation and Flood Frequency. *Journal of Environmental Quality* 41, 95–105. doi:10.2134/jeq2011.0308
- Jinuntuya-Nortman, M., Sutka, R.L., Ostrom, P.H., Gandhi, H., Ostrom, N.E., 2008. Isotopologue fractionation during microbial reduction of N<sub>2</sub>O within soil mesocosms as a function of water-filled pore space. *Soil Biology and Biochemistry* 40, 2273–2280. doi:10.1016/j.soilbio.2008.05.016
- Jørgensen, C.J., Struwe, S., Elberling, B., 2012. Temporal trends in N<sub>2</sub>O flux dynamics in a Danish wetland - effects of plant-mediated gas transport of N<sub>2</sub>O and O<sub>2</sub> following changes in water level and soil mineral-N availability. *Global Change Biology* 18, 210–222. doi:10.1111/j.1365-2486.2011.02485.x
- Klimešová, J., Šrůtek, M., 1995. Vertical distribution of underground organs of *Phalaris arundinacea* and *Urtica dioica* in a floodplain: a comparison of two methods. *Preslia* 67, 47–53.
- Knowles, R., 1982. Denitrification. *Microbiological Reviews* 46, 43–70. doi:10.1016/0968-0004(76)90171-7
- Kozłowski, J.A., Kits, K.D., Stein, L.Y., 2016. Comparison of Nitrogen Oxide Metabolism among Diverse Ammonia-Oxidizing Bacteria. *Frontiers in Microbiology* 7, 1–9. doi:10.3389/fmicb.2016.01090
- Kuznetsova, A., Brockhoff, P.B., Christensen, R.H.B., 2017. lmerTest Package: Tests in Linear Mixed Effects Models. *Journal of Statistical Software* 82. doi:10.18637/jss.v082.i13
- Laughlin, R.J., Stevens, R.J., 2002. Evidence for Fungal Dominance of Denitrification and Codenitrification in a Grassland Soil. *Soil Science Society of America Journal* 66, 1540. doi:10.2136/sssaj2002.1540
- Laughlin, R.J., Stevens, R.J., Müller, C., Watson, C.J., 2008. Evidence that fungi can oxidize NH<sub>4</sub><sup>+</sup> to NO<sub>3</sub><sup>-</sup> in a grassland soil. *European Journal of Soil Science* 59, 285–291. doi:10.1111/j.1365-2389.2007.00995.x
- Lehtovirta-Morley, L.E., 2018. Ammonia oxidation: Ecology, physiology, biochemistry and why they must all come together. *FEMS Microbiology Letters* 365, 1–9. doi:10.1093/femsle/fny058
- Lewicka-Szczebak, D., Augustin, J., Giesemann, A., Well, R., 2017. Quantifying N<sub>2</sub>O reduction to N<sub>2</sub> based on N<sub>2</sub>O isotopocules – validation with independent methods (helium incubation and 15N gas flux method). *Biogeosciences* 14, 711–732. doi:10.5194/bg-14-711-2017
- Lewicka-Szczebak, D., Piotr Lewicki, M., Well, R., 2020. N<sub>2</sub>O isotope approaches for source partitioning of N<sub>2</sub>O production and estimation of N<sub>2</sub>O reduction-validation with the 15N gas-flux method in laboratory and field studies. *Biogeosciences* 17, 5513–5537. doi:10.5194/bg-17-5513-2020
- Lewicka-Szczebak, D., Well, R., Köster, J.R., Fuß, R., Senbayram, M., Dittert, K., Flessa, H., 2014. Experimental determinations of isotopic fractionation factors associated with N<sub>2</sub>O production and reduction during denitrification in soils. *Geochimica et Cosmochimica Acta* 134, 55–73. doi:10.1016/j.gca.2014.03.010
- Ley, M., Lehmann, M.F., Niklaus, P.A., Luster, J., 2018. Alteration of nitrous oxide emissions from floodplain soils by aggregate size, litter accumulation and plant-soil interactions. *Biogeosciences* 15, 7043–7057. doi:10.5194/bg-15-7043-2018
- Li, P.P., Zhang, S.Q., Li, F., Zhang, Y.T., Han, Y.L., 2020. Long term combined fertilization and soil aggregate size on the denitrification and community of denitrifiers. *Applied Soil Ecology* 156. doi:10.1016/j.apsoil.2020.103718
-

- Li, X., Sørensen, P., Olesen, J.E., Petersen, S.O., 2016. Evidence for denitrification as main source of N<sub>2</sub>O emission from residue-amended soil. *Soil Biology and Biochemistry* 92, 153–160. doi:10.1016/j.soilbio.2015.10.008
- Loecke, T.D., Robertson, G.P., 2009. Soil resource heterogeneity in terms of litter aggregation promotes nitrous oxide fluxes and slows decomposition. *Soil Biology and Biochemistry* 41, 228–235. doi:10.1016/j.soilbio.2008.10.017
- Maeda, K., Spor, A., Edel-Hermann, V., Heraud, C., Breuil, M.C., Bizouard, F., Toyoda, S., Yoshida, N., Steinberg, C., Philippot, L., 2015. N<sub>2</sub>O production, a widespread trait in fungi. *Scientific Reports* 5, 9697. doi:10.1038/srep09697
- Mafa-Attoye, T.G., Baskerville, M.A., Ofosu, E., Oelbermann, M., Thevathasan, N. v., Dunfield, K.E., 2020. Riparian land-use systems impact soil microbial communities and nitrous oxide emissions in an agro-ecosystem. *Science of The Total Environment* 724, 138148. doi:10.1016/j.scitotenv.2020.138148
- McClain, M.E., Boyer, E.W., Dent, C.L., Gergel, S.E., Grimm, N.B., Groffman, P.M., Hart, S.C., Harvey, J.W., Johnston, C.A., Mayorga, E., McDowell, W.H., Pinay, G., 2003. Biogeochemical Hot Spots and Hot Moments at the Interface of Terrestrial and Aquatic Ecosystems. *Ecosystems* 6, 301–312. doi:10.1007/s10021-003-0161-9
- Mohn, J., Steinlin, C., Merbold, L., Emmenegger, L., Hagedorn, F., 2013. N<sub>2</sub>O emissions and source processes in snow-covered soils in the Swiss Alps. *Isotopes in Environmental and Health Studies* 49, 520–531. doi:10.1080/10256016.2013.826212
- Mohn, J., Wolf, B., Toyoda, S., Lin, C.T., Liang, M.C., Brüggemann, N., Wissel, H., Steiker, A.E., Dyckmans, J., Szvec, L., Ostrom, N.E., Casciotti, K.L., Forbes, M., Giesemann, A., Well, R., Doucett, R.R., Yarnes, C.T., Ridley, A.R., Kaiser, J., Yoshida, N., 2014. Interlaboratory assessment of nitrous oxide isotopomer analysis by isotope ratio mass spectrometry and laser spectroscopy: Current status and perspectives. *Rapid Communications in Mass Spectrometry* 28, 1995–2007. doi:10.1002/rcm.6982
- Molodovskaya, M., Singurindy, O., Richards, B.K., Warland, J., Johnson, M.S., Steenhuis, T.S., 2012. Temporal Variability of Nitrous Oxide from Fertilized Croplands: Hot Moment Analysis. *Soil Science Society of America Journal* 76, 1728–1740. doi:10.2136/sssaj2012.0039
- Morley, N., Baggs, E.M., Dörsch, P., Bakken, L., 2008. Production of NO, N<sub>2</sub>O and N<sub>2</sub> by extracted soil bacteria, regulation by NO<sub>2</sub>- and O<sub>2</sub> concentrations. *FEMS Microbiology Ecology* 65, 102–112. doi:10.1111/j.1574-6941.2008.00495.x
- Oades, J.M., 1984. Soil organic matter and structural stability: mechanisms and implications for management. *Plant and Soil* 76, 319–337. doi:10.1007/BF02205590
- Oertel, C., Matschullat, J., Zurba, K., Zimmermann, F., Erasmi, S., 2016. Greenhouse gas emissions from soils—A review. *Chemie Der Erde* 76, 327–352. doi:10.1016/j.chemer.2016.04.002
- Ostrom, N.E., Ostrom, P.H., 2012. The Isotopomers of Nitrous Oxide: Analytical Considerations and Application to Resolution of Microbial Production Pathways, in: *Handbook of Environmental Isotope Geochemistry*. Springer Berlin Heidelberg, Berlin, Heidelberg, pp. 453–476. doi:10.1007/978-3-642-10637-8\_23
- Parkin, T.B., 1987. Soil Microsites as a Source of Denitrification Variability. *Soil Science Society of America Journal* 51, 1194–1199.
- Pester, M., Maixner, F., Berry, D., Rattei, T., Koch, H., Lückner, S., Nowka, B., Richter, A., Spieck, E., Lebedeva, E., Loy, A., Wagner, M., Daims, H., 2014. NxrB encoding the beta subunit of nitrite oxidoreductase as

- functional and phylogenetic marker for nitrite-oxidizing *Nitrospira*. *Environmental Microbiology* 16, 3055–3071. doi:10.1111/1462-2920.12300
- Peter, S., Rechsteiner, R., Lehmann, M.F., Brankatschk, R., Vogt, T., Diem, S., Wehrli, B., Tockner, K., Durisch-Kaiser, E., 2012. Nitrate removal in a restored riparian groundwater system: functioning and importance of individual riparian zones. *Biogeosciences* 9, 4295–4307. doi:10.5194/bg-9-4295-2012
- PHILIPPOT, L., ANDERT, J., JONES, C.M., BRU, D., HALLIN, S., 2011. Importance of denitrifiers lacking the genes encoding the nitrous oxide reductase for N<sub>2</sub>O emissions from soil. *Global Change Biology* 17, 1497–1504. doi:10.1111/j.1365-2486.2010.02334.x
- Philippot, L., Hallin, S., Börjesson, G., Baggs, E.M., 2009. Biochemical cycling in the rhizosphere having an impact on global change. *Plant and Soil* 321, 61–81. doi:10.1007/s11104-008-9796-9
- Prosser, J.I., Hink, L., Gubry-Rangin, C., Nicol, G.W., 2020. Nitrous oxide production by ammonia oxidizers: Physiological diversity, niche differentiation and potential mitigation strategies. *Global Change Biology* 26, 103–118. doi:10.1111/gcb.14877
- R Core Team, 2021. R: A Language and Environment for Statistical Computing.
- Ravishankara, A.R., Daniel, J.S., Portmann, R.W., 2009. Nitrous Oxide (N<sub>2</sub>O): The Dominant Ozone-Depleting Substance Emitted in the 21st Century. *Science* 326, 123–125. doi:10.1126/science.1176985
- Robertson, G.P., Groffman, P.M., 2015. Nitrogen Transformations, in: *Soil Microbiology, Ecology and Biochemistry*. Elsevier, pp. 421–446. doi:10.1016/B978-0-12-415955-6.00014-1
- Rückauf, U., Augustin, J., Russow, R., Merbach, W., 2004. Nitrate removal from drained and reflooded fen soils affected by soil N transformation processes and plant uptake. *Soil Biology and Biochemistry* 36, 77–90. doi:10.1016/j.soilbio.2003.08.021
- Samaritani, E., Shrestha, J., Fournier, B., Frossard, E., Gillet, F., Guenat, C., Niklaus, P.A., Pasquale, N., Tockner, K., Mitchell, E.A.D., Luster, J., 2011. Heterogeneity of soil carbon pools and fluxes in a channelized and a restored floodplain section (Thur River, Switzerland). *Hydrology and Earth System Sciences* 15, 1757–1769. doi:10.5194/hess-15-1757-2011
- Schirmer, M., Luster, J., Linde, N., Perona, P., Mitchell, E.A.D., Barry, D.A., Hollender, J., Cirpka, O.A., Schneider, P., Vogt, T., Radny, D., Durisch-Kaiser, E., 2014. Morphological, hydrological, biogeochemical and ecological changes and challenges in river restoration the Thur River case study. *Hydrology and Earth System Sciences* 18, 2449–2462. doi:10.5194/hess-18-2449-2014
- Schomburg, A., Brunner, P., Turberg, P., Guenat, C., Riaz, M., le Bayon, R.C., Luster, J., 2019. Pioneer plant *Phalaris arundinacea* and earthworms promote initial soil structure formation despite strong alluvial dynamics in a semi-controlled field experiment. *CATENA* 180, 41–54. doi:10.1016/j.catena.2019.04.001
- Schomburg, A., Schilling, O.S., Guenat, C., Schirmer, M., le Bayon, R.C., Brunner, P., 2018. Topsoil structure stability in a restored floodplain: Impacts of fluctuating water levels, soil parameters and ecosystem engineers. *Science of The Total Environment* 639, 1610–1622. doi:10.1016/j.scitotenv.2018.05.120
- Shrestha, J., Niklaus, P. a, Frossard, E., Samaritani, E., Huber, B., Barnard, R.L., Schleppei, P., Tockner, K., Luster, J., 2012. Soil nitrogen dynamics in a river floodplain mosaic. *Journal of Environmental Quality* 41, 2033–45. doi:10.2134/jeq2012.0059
- Six, J., Bossuyt, H., Degryze, S., Denef, K., 2004. A history of research on the link between (micro)aggregates, soil biota, and soil organic matter dynamics. *Soil and Tillage Research* 79, 7–31. doi:10.1016/j.still.2004.03.008

- Smart, D.R., Bloom, A.J., 2001. Wheat leaves emit nitrous oxide during nitrate assimilation. *Proceedings of the National Academy of Sciences* 98, 7875–7878. doi:10.1073/pnas.131572798
- Spott, O., Russow, R., Stange, C.F., 2011. Formation of hybrid N<sub>2</sub>O and hybrid N<sub>2</sub> due to codenitrification: First review of a barely considered process of microbially mediated N-nitrosation. *Soil Biology and Biochemistry* 43, 1995–2011. doi:10.1016/j.soilbio.2011.06.014
- Starkenburger, S.R., Arp, D.J., Bottomley, P.J., 2008. Expression of a putative nitrite reductase and the reversible inhibition of nitrite-dependent respiration by nitric oxide in *Nitrobacter winogradskyi* Nb-255. *Environmental Microbiology* 10, 3036–3042. doi:10.1111/j.1462-2920.2008.01763.x
- Stieglmeier, M., Mooshammer, M., Kitzler, B., Wanek, W., Zechmeister-Boltenstern, S., Richter, A., Schleper, C., 2014. Aerobic nitrous oxide production through N-nitrosating hybrid formation in ammonia-oxidizing archaea. *ISME Journal* 8, 1135–1146. doi:10.1038/ismej.2013.220
- Sutka, R.L., Ostrom, N.E., Ostrom, P.H., Breznak, J.A., Gandhi, H., Pitt, A.J., Li, F., 2006. Distinguishing nitrous oxide production from nitrification and denitrification on the basis of isotopomer abundances. *Applied and Environmental Microbiology* 72, 638–644. doi:10.1128/AEM.72.1.638-644.2006
- Tomasek, A.A., Hondzo, M., Kozarek, J.L., Staley, C., Wang, P., Lurndahl, N., Sadowsky, M.J., 2019. Intermittent flooding of organic-rich soil promotes the formation of denitrification hot moments and hot spots. *Ecosphere* 10. doi:10.1002/ecs2.2549
- Toyoda, S., Yano, M., Nishimura, S., Akiyama, H., Hayakawa, A., Koba, K., Sudo, S., Yagi, K., Makabe, A., Tobari, Y., Ogawa, N.O., Ohkouchi, N., Yamada, K., Yoshida, N., 2011. Characterization and production and consumption processes of N<sub>2</sub>O emitted from temperate agricultural soils determined via isotopomer ratio analysis. *Global Biogeochemical Cycles* 25, 1–17. doi:10.1029/2009GB003769
- Verhoeven, E., Barthel, M., Yu, L., Celi, L., Said-Pullicino, D., Sleutel, S., Lewicka-Szczepak, D., Six, J., Decock, C., 2019. Early season N<sub>2</sub>O emissions under variable water management in rice systems: Source-partitioning emissions using isotope ratios along a depth profile. *Biogeosciences* 16, 383–408. doi:10.5194/bg-16-383-2019
- Well, R., Flessa, H., 2009. Isotopologue enrichment factors of N<sub>2</sub>O reduction in soils. *Rapid Communications in Mass Spectrometry* 23, 2996–3002. doi:10.1002/rcm.4216
- Wolf, B., Merbold, L., Decock, C., Tuzson, B., Harris, E., Six, J., Emmenegger, L., Mohn, J., 2015. First on-line isotopic characterization of N<sub>2</sub>O above intensively managed grassland. *Biogeosciences* 12, 2517–2531. doi:10.5194/bg-12-2517-2015
- Wu, D., Well, R., Cárdenas, L.M., Fuß, R., Lewicka-Szczepak, D., Köster, J.R., Brüggemann, N., Bol, R., 2019. Quantifying N<sub>2</sub>O reduction to N<sub>2</sub> during denitrification in soils via isotopic mapping approach: Model evaluation and uncertainty analysis. *Environmental Research* 179, 108806. doi:10.1016/j.envres.2019.108806
- Yu, L., Harris, E., Lewicka-Szczepak, D., Barthel, M., Blomberg, M.R.A., Harris, S.J., Johnson, M.S., Lehmann, M.F., Liisberg, J., Müller, C., Ostrom, N.E., Six, J., Toyoda, S., Yoshida, N., Mohn, J., 2020. What can we learn from N<sub>2</sub>O isotope data? – Analytics, processes and modelling. *Rapid Communications in Mass Spectrometry* 34, 1–14. doi:10.1002/rcm.8858
- Zhang, J., Müller, C., Cai, Z., 2015. Heterotrophic nitrification of organic N and its contribution to nitrous oxide emissions in soils. *Soil Biology and Biochemistry* 84, 199–209. doi:10.1016/j.soilbio.2015.02.028

Zhu, X., Burger, M., Doane, T. a, Horwath, W.R., 2013. Ammonia oxidation pathways and nitrifier denitrification are significant sources of N<sub>2</sub>O and NO under low oxygen availability. *Proceedings of the National Academy of Sciences* 110, 6328–6333. doi:10.1073/pnas.1219993110





## Chapter 5

### General Synthesis

Assessing N<sub>2</sub>O budgets of river floodplains, and thus of their climate regulation function, is a challenging task. This is due to the dynamic patchwork of various habitats with distinct properties regarding N transformations which are temporarily perturbed by sporadic flood events. A thorough understanding of the modulating effects related to specific factors which determine the occurrence of temporary hot spots of enhanced N<sub>2</sub>O emissions after flood perturbances is therefore of fundamental importance to reduce the uncertainties inherent to these N<sub>2</sub>O budgets. For this reason, the main objective of this thesis project was the systematic examination of the relative effects of factors related to microhabitat formation on the emissions, production, and consumption of N<sub>2</sub>O as well as the respective soil microbiome. The focus of the investigations was thereby on factors which often exhibit a high degree of heterogeneity within floodplains such as soil aggregation, detritus accumulation and interactions of plant roots with the soil matrix. The combined application of N<sub>2</sub>O flux measurements, natural abundance stable isotope analyses and DNA- and RNA-based molecular techniques has emerged as an efficient approach providing detailed information under controlled conditions and in the field. Although linking these different datasets with each other was sometimes challenging, these data formed a solid basis to interpret the complex dynamics of the balance between microbial N<sub>2</sub>O production and consumption after short-term flood perturbation. Furthermore, these gained insights helped to extend our mechanistic understanding of the distinct microhabitat effects regulating the magnitude and temporal patterns of enhanced N<sub>2</sub>O emissions. In the following, the main outcomes from the studies presented in this thesis project are briefly recapitulated followed by a critical examination of the gained insights. The last two sections comprise technical considerations about the used methods and recommendations for possible future projects.

### 5.1 Overview of main findings

#### 5.1.1 Mesocosm Experiment

In the first part of a comprehensive mesocosm study, presented in chapter 2, the dynamics of N<sub>2</sub>O flux rates and physicochemical parameters were investigated over a flooding-drying cycle

under controlled climatic conditions. The first objective was to characterize the modulating microhabitat effects caused by differently sized aggregate fractions, detritus accumulation or interactions with an extending root network of *Salix viminalis* on the magnitude and temporal pattern of N<sub>2</sub>O emissions. The main results were:

- The flood event initiated a phase of increased N<sub>2</sub>O emission rates relative to pre-flood emissions, where peak N<sub>2</sub>O emissions were detected immediately after flood water recession with temporal patterns and magnitudes distinct in each factor combination.
- Aggregate size had a significant impact on the magnitude of N<sub>2</sub>O flux rates with macroaggregates promoting stronger emissions than microaggregates.
- The addition of leaf litter to the soil altered the temporal emission patterns of N<sub>2</sub>O comprising higher peak emission rates and shorter periods of enhanced emission. However, litter accumulation had only a minor effect on the N<sub>2</sub>O emissions integrated over the entire phase of enhanced emissions.
- Plant-soil interactions with both aggregate size fractions suppressed strong N<sub>2</sub>O emissions leading to the lowest peak emission rates in the experiment.

The second part of the mesocosm experiment (chapter 3) focused on the elucidation of the underlying dynamics of microbial production and consumption of N<sub>2</sub>O as well as the microbial community structures involved in these processes. To this end, analyses of natural abundance stable isotope signatures of soil emitted N<sub>2</sub>O were combined with data from high throughput sequencing and qPCR of soil-extracted prokaryotic and fungal DNA. The major findings were:

- Microhabitat formation led to the development of distinct microbiomes. Specifically, prokaryotic communities were strongly affected by aggregate size whereas fungal communities changed the most under the influence of litter accumulation.
- During the flood phase, N<sub>2</sub>O was produced almost exclusively by heterotrophic denitrification and/or nitrifier denitrification regardless of factor combination.
- N<sub>2</sub>O production during the post-flood phase was characterized by the simultaneous involvement of nitrifying and denitrifying processes.
- Peak N<sub>2</sub>O emissions from macroaggregates with or without leaf litter accumulation were the result of rapid changes in source contribution and partial disruption of N<sub>2</sub>O reduction highlighting N<sub>2</sub>O reduction to N<sub>2</sub> as a major controlling factor of N<sub>2</sub>O emissions
- The degradation of buried litter and root exudates favored N<sub>2</sub>O production by denitrifying processes

### 5.1.2 Field Manipulation Experiment

In the field manipulation experiment conducted in the hydrologically most dynamic zone of a re-naturalized section of the Thur River (chapter 4), the effect of pioneer vegetation growth on the interplay of source and sink processes as determinants of the magnitude of N<sub>2</sub>O emissions was investigated. During a three-week post-flood phase, the analysis of the isotopomeric signatures of soil-emitted N<sub>2</sub>O was combined with RNA-based molecular techniques to additionally investigate the temporal changes in activity of specific groups of N transforming microorganisms. The following observations were made:

- Young, sandy sediments under a dense cover of the grass *P. arundinacea* experienced longer periods of elevated N<sub>2</sub>O emissions, whereas emissions from bare sediments gradually decreased after initial peak rates.
- Nitrification and/or fungal denitrification contributed to N<sub>2</sub>O emissions from bare plots only in the beginning of the post-flood phase, whereas this process group consistently contributed about 20-30 % to gross N<sub>2</sub>O production in plots covered by *P. arundinacea*
- N<sub>2</sub>O reduction was temporarily disturbed at the beginning of the post-flood phase in bare plots, whereas N<sub>2</sub>O reduction in the *Phalaris* plots was stable during the entire drying phase
- Denitrifying and nitrite oxidizing microorganisms were the most active N transforming microorganisms in this part of the river floodplain

## **5.2 Flood frequency – a reliable predictor of periods of enhanced N<sub>2</sub>O emissions**

The post-flood phases in the mesocosm and the field experiment were both associated with enhanced N<sub>2</sub>O emissions exceeding the reference emission rates measured before the flood events considerably. These observations are in line with previous observations made in our research area by (Shrestha et al., 2014) but also in other riparian zones (Poblador et al., 2017; Tomasek et al., 2019). This temporally constrained occurrence of enhanced N<sub>2</sub>O emissions after inundation from an ecosystem with otherwise low emissions, highlighted the relevance of short-term disturbances in the floodplain ecotone. This temporal coupling of flood events and enhanced N<sub>2</sub>O emissions further emphasizes the necessity to combine regular gas flux monitoring schedules with opportunistic sampling campaigns to gain more accurate assessments of the GHG budget of floodplain areas. This would be relevant especially in floodplain areas with a high, or projected increase in flood frequency related to climate change.

---

Further, these periods of enhanced N<sub>2</sub>O emissions emphasize that the beneficial ecosystem service of floodplains in terms of water purification by removal of nitrogen compounds can come at the expense of the formation of climate-hazardous N<sub>2</sub>O.

### **5.3 Soil aggregates – functional base units of N<sub>2</sub>O emissions**

In the mesocosm study presented in chapters 2 and 3, it became evident that the physicochemical properties related to aggregate size were a major driver of the development of the procaryotic community structure, which is consistent with previous studies (Trivedi et al., 2017). In addition, these properties decisively shaped the balance between N<sub>2</sub>O production and consumption throughout the flooding-drying cycle ultimately leading to distinct temporal patterns of N<sub>2</sub>O emissions. These temporal dynamics in N<sub>2</sub>O source partitioning and N<sub>2</sub>O reduction have not been shown so far with such high temporal resolution. We demonstrated that the N<sub>2</sub>O emissions during the post-flood period of enhanced emissions were originally produced by several simultaneously active aerobic and anaerobic N<sub>2</sub>O production pathways with the composition of source partitioning depending strongly on the aggregate size specific microhabitat conditions. The size-related increase in structural complexity inherent to macroaggregates, as demonstrated by (Schlüter et al., 2018), created a more heterogeneous distribution of oxic and anoxic microhabitats during the entire desaturation of the inter- and intra-aggregate pore network. Under such conditions, more dynamic changes in temporal patterns of source contribution and N<sub>2</sub>O reduction were discovered. This is in line with previous studies where heterogeneous distribution of redox gradients has been suggested as the cause of the simultaneous activity of aerobic and anaerobic N<sub>2</sub>O production (Hu et al., 2015; Yamamoto et al., 2017). By contrast, source partitioning in microaggregates only changed substantially as a response to the fast initial drainage at the end of the flood phase revealing that redox conditions in most microhabitats associated with microaggregates are strongly linked to the oxygenation status of the inter-aggregate pore space. The similarly strong susceptibility of microbial N<sub>2</sub>O reduction to fluctuations in redox conditions in macroaggregates after flood events revealed a crucial link between aggregate size, temporary partial interruption of N<sub>2</sub>O reduction and peak N<sub>2</sub>O emission rates. This discovery does not only highlight the pivotal role of this so far poorly constrained sink function of N<sub>2</sub>O in the occurrence of periods of enhanced emissions but will also advance our ability to identify potential hotspots of N<sub>2</sub>O emissions in floodplains.

Further, the simulation of a soil structure in the laboratory experiment allowed the observation and confirmation of the importance of this often-excluded aspect in studies of the responses of

---

biogeochemical processes to changing environmental conditions in differently sized aggregates. The inter-aggregate pore architecture of the artificial soil matrix determined the distribution of soil moisture controlling the diffusive transport processes of gases and solutes in the surrounding environment of soil aggregates. These external conditions ultimately regulated the internal physicochemical conditions of the differently sized aggregates. These observations fit neatly into the conceptual framework of soil aggregates as biogeochemical reactors with reactivities defined by aggregate size and bulk soil abiotic and biotic factors, which are described in Fig. 1.3, that shape the reaction environment (Wang et al., 2019). This relationship between aggregate associated nitrous oxide producing processes and the regulatory properties of the inter-aggregate pore space became particularly clear in the field manipulation experiment presented in chapter 4, where both plot types comprised a similar amount of macroaggregates. The significantly better pore connectivity and higher porosity in the bulk soil of *Phalaris* plots (Schomburg et al., 2019) promoted a faster decrease in pore water saturation during drying. This in turn facilitated gas exchange between microsites of N<sub>2</sub>O production and the atmosphere leading to prolonged elevated N<sub>2</sub>O emissions during the drying phase.

Based on these findings, even though potential interaction effects between the two aggregate size fractions were not investigated, it is likely that natural soils with a dominating macroaggregate fraction would become temporary hot spots of N<sub>2</sub>O emissions after short-term inundation. However, the mesocosm experiment and the field experiment showed, that these aggregate size-related effects can be altered by other factors of microhabitat formation such as litter accumulation and plant root network development as described in the following two paragraphs.

#### **5.4 Litter accumulation – Soil-structuring microhabitat, nutrient source and promoter of reductive N transformation processes**

The introduction of leaf litter into the model soils of the mesocosm experiment as well as the burial of plant detritus in the field study did not only represent specific microhabitats distinct from the surrounding soil but also functioned as an additional source of carbon and nitrogen compounds substantially altering the physicochemical properties of the entire soil. The introduction of dead plant material in the mesocosm study, and probably to some extent also the burial of plant litter in the field experiment, significantly reduced soil bulk density. This led to an improved soil structure and promoted pore space desaturation, as also described by (Jarecke et al., 2016), which facilitated the subsequent reaeration of the upper soil pore network

during the initial drying phase. The rapid return to oxic conditions in the macropore space stimulated aerobic N<sub>2</sub>O production in a previously denitrification dominated system but also partially interrupted N<sub>2</sub>O reduction. At the same time, the increased availability of carbon and nitrogen compounds did not only support the activity of nitrifying and denitrifying microorganisms but also led to a stimulation of heterotrophic degradation processes. This in turn increased the overall oxygen demand and lowered the redox potential in the soil system. This dynamic interrelation between increased gas diffusivity in the bulk soil, the presence of diffusion barriers inside the aggregates and high oxygen demand by detritus decomposition processes had a major impact on the temporal pattern of N<sub>2</sub>O emissions as well as the N<sub>2</sub>O production and consumption processes. It resulted in a compressed N<sub>2</sub>O emission pattern of short, strong increases in flux rates from oxidative and reductive source processes and partial interruption of N<sub>2</sub>O reduction followed by a rapid decrease in N<sub>2</sub>O emission rates dominated by denitrification and resuming N<sub>2</sub>O reduction. This finding is supported by the results of (Jiang et al., 2021), who found similar temporal emission patterns after straw addition to different aggregate size fractions with peak emissions explained by the simultaneous activity of nitrifying and denitrifying microorganisms. Further, this short period of highly dynamic changes in source process composition and sink efficiency in which the strongest N<sub>2</sub>O emissions occurred, revealed the potential risk of underestimating the cumulative emissions if these short but strong peak emission rates are missed during sampling campaigns. Gas flux measurements should thus begin as soon as possible after the flood event in areas of the floodplain with litter accumulation.

The easily degradable leaf litter of *Salix viminalis* used in the mesocosm study, and probably the buried plant material of unknown quality and origin in the field experiment as well, emerged as promoters of anoxic soil environments under unsaturated conditions. Both types of detritus thereby fostered reductive N<sub>2</sub>O production but also provided ideal conditions for microbial removal of nitrous oxide by complete denitrification. However, the characterization of the chemical properties and the associated degradability of the detritus were not the subject of the investigations in this project, even though denitrification is linked to the quantity and quality of buried organic deposits (Hill, 2019). Recent studies on agricultural plant residues have also demonstrated the connection between detritus quality and magnitude of N<sub>2</sub>O emissions (Rummel et al., 2020). Thus, it would be of great interest to conduct future research also on the aspect of microhabitat effects related to different qualities of autochthonous and allochthonous plant residues on N<sub>2</sub>O emissions from floodplain soils.

Another important aspect of the microhabitat effects associated with litter accumulation was their function as strong drivers of the development of microbial community structure, particularly of the fungal community as observed in the mesocosm experiment. This observation has been confirmed by other studies dealing with changes in the composition of bacterial and fungal soil microbiome (Habtewold et al., 2020). These litter-specific effects especially promoted fungal genera comprising denitrifying taxa, which increased the potential contribution of this reductive process to periods of enhanced emissions, especially given the incomplete denitrification of fungi and that N<sub>2</sub>O production by fungal denitrification of some of these taxa can be substantial (Maeda et al., 2015). Such an increase in denitrifying fungi would therefore also increase the potential for nitrous oxide formation in areas of the floodplain where litter accumulates. However, in this project the applied methods did only allow for a rough qualitative estimation of the contribution of this potentially relevant process to the observed N<sub>2</sub>O emission rates. Therefore, the role of this still poorly constrained process in the formation of periods of enhanced N<sub>2</sub>O emissions should therefore be subject of future investigation, particularly in natural systems.

### **5.5 Plant-soil interactions – Determinants of N<sub>2</sub>O production and consumption from floodplain vegetation stands**

The assessment of the interaction of two common floodplain plant species, *Phalaris arundinacea* and *Salix viminalis*, with their respective soils provided insight into distinct rhizosphere-related microhabitat effects that resulted in contrasting patterns of N<sub>2</sub>O emissions after the flood events. However, a direct comparison of the plant effects on the N<sub>2</sub>O emissions between the two experiments should be done with caution. In the mesocosm experiment the entire plant was included in the investigation of the ecosystem fluxes of N<sub>2</sub>O, whereas the emissions assessed in the field experiment represent soil N<sub>2</sub>O fluxes without including the plant shoot. Since both plants have aerenchyma as physiological adaptations to life in floodplains, and which are discussed as possible alternative transport ways for soil-produced N<sub>2</sub>O, it is possible that a certain fraction of N<sub>2</sub>O was not accounted for in the *Phalaris* plots of the field experiment. If *P. arundinacea* had indeed transported N<sub>2</sub>O via internal channels, which would be in line with observations made by (Jørgensen et al., 2012), the ecosystem fluxes of these plots would have been higher. However, this would not have changed the conclusions reached that *P. arundinacea* promotes emissions of N<sub>2</sub>O. In turn, mesocosm experiments with *S. viminalis* emitted about the same or less N<sub>2</sub>O than the unplanted model soils. These

observations show that the mere presence of such gas-transporting physiological structures in plants does not directly imply that they must lead to increased nitrous oxide emissions. However, since the assessment of mechanisms controlling the potential gas transport via plant-internal channels was not part of this project, our results are therefore inconclusive in this respect. Still, results from recent investigations on the potential of wetland plants (Wang & Reid, 2020) and even pioneer trees in riparian forests (Schindler et al., 2020) to transport N<sub>2</sub>O emphasize the need to extend our investigations of such plant-related alternative N<sub>2</sub>O transport routes to more species of floodplain vegetation. Such a detailed inventory of N<sub>2</sub>O-transporting vegetation could largely improve assessments of floodplain ecosystem services.

The presence of both *S. viminalis* and *P. arundinacea* reduced the magnitude of fluctuations in N<sub>2</sub>O reduction and N<sub>2</sub>O source partitioning during the transition from flooded to drying conditions. These plant-related controls on N<sub>2</sub>O source composition and reduction after flood events have hardly been investigated so far, which further emphasizes the importance of our studies to advance our mechanistic understanding of nitrous oxide emissions from vegetated areas in floodplains. Similar to detritus accumulation, microhabitat effects related to root respiration and the deposition of easily degradable root exudates, which stimulated heterotrophic respiration, helped to sustain anoxia in areas of bacterial denitrification activity during desaturation of the pore space. These microhabitat effects, also previously described by Fender et al. (2013), allowed N<sub>2</sub>O reduction to continuously remove large fractions of originally produced N<sub>2</sub>O. This demonstrated the important role of plant deposits in maintaining the sink function for N<sub>2</sub>O during changing redox conditions in soils.

Furthermore, the different source contributions observed in the mesocosm, and the field experiment revealed that the microhabitat effects caused by site-specific plant-soil interactions can result in substantial differences in the temporal dynamics of microbial N<sub>2</sub>O production. In addition to the plant-specific C inputs and O<sub>2</sub> consumption, soil texture and the level of aggregation functioning as additional controls of oxygen availability emerged to be the most essential drivers of N<sub>2</sub>O source partitioning. In the mesocosm experiment, the more complex pore space structure created by the relatively finer texture of the model soils, compared to the sediments in the field, and the aggregates embedded within them emerged as efficient diffusion barriers under still high WFPS. By contrast, in the field trial, the incipient soil development of the coarser textured sediments promoted by the pioneer vegetation in the *Phalaris* plots resulted in facilitated gas diffusion in the soil. The microbial N<sub>2</sub>O source partitioning resulting from the respective plant-soil combinations showed that in the mesocosm experiment peak N<sub>2</sub>O emissions were strongly dominated by only gradually decreasing bacterial denitrification, while



*P. arundinacea* stands showed stable and more diverse N<sub>2</sub>O source contribution. Therefore, site-specific soil characteristics that control gas diffusion must be included in the assessment of the microbial N<sub>2</sub>O source dynamics under vegetation.

## **5.6 Towards improved interpretation methods of natural abundance stable isotopes**

The first application of dual-isotope mapping of soil-emitted N<sub>2</sub>O in a non-agricultural context in this thesis project emerged as a versatile method to investigate source contribution and N<sub>2</sub>O reduction simultaneously. The minimal disturbance of the assessed system and the simplicity of field sampling are undoubtedly major advantages of this method and makes it suitable for application in natural and near-natural ecosystems. However, in this thesis project it became evident that this method still has the potential for further improvement. The strong dependence of the approach on ranges of previously published isotope values and fractionation factors has been discussed in a recent publication (Yu et al., 2020) and was also a constraining factor in our investigations. Consequently, this dependency limited the quantification of specific source contributions obtained by two model scenarios, as it did in previously published research (Buchen et al., 2018; Verhoeven et al., 2019). For example, in most studies including this thesis project neither the isotopic endmember signatures of the assessed processes nor the fractionation factors of N<sub>2</sub>O reduction to N<sub>2</sub> are known. For this reason and due to the strong overlap in isotopic signature ranges of some processes, e.g., nitrifier denitrification and heterotrophic denitrification, the use of averaged endmember values and isotope effects has become the standard approach to these issues (Buchen et al., 2018). However, this can lead to a less than optimal representation of the measured values by the fitted models used in this approach (e.g., measured values outside the model assumptions). It would therefore be recommendable to conduct incubation experiments under oxic and anoxic conditions, using soil material from the respective study site in combination with fungicides and nitrification inhibitors, to derive isotopic endmember signatures and fractionation factors characteristic for a given study site. In addition, the variability and dependence of endmember signatures and fractionation factors on ambient physicochemical conditions (e.g., diffusion barriers, oxygen availability, substrate limitations) and conditions related to microbial community composition (e.g., species specific N transformation pathways and rates, type of catalyzing enzymes) may also make it necessary to determine these values several times during a measurement campaign and to apply them to the respective sample values.

Another relevant aspect of the dual-isotope mapping approach is that it requires the characteristic  $\delta^{18}\text{O}$  signature of the soil pore water in each  $\text{N}_2\text{O}$  isotopomer study to adjust the respective literature endmember ranges (Lewicka-Szczebak et al., 2020). This adjustment is necessary since  $\delta^{18}\text{O}$  of the pore water can vary substantially, depending on the degree of isotopic fractionation the water underwent prior to precipitation, e.g., due to a latitude or altitude effect (Sharp, 2007). In the studies conducted in this thesis project, we followed the recommendations of (Verhoeven et al., 2019) and thus always included this parameter in the sampling strategies allowing us to adapt our endmember values accordingly. It became evident that the more depleted in  $^{18}\text{O}$  the soil pore water is, the more the ranges for nitrification and fungal denitrification converge. This convergence would justify the use of common endmember values, since with increasing overlap of the isotopic signatures of nitrification and fungal denitrification, it becomes increasingly difficult to distinguish precisely between the two process endmembers. These considerations would be especially relevant if isotopomer studies are to be conducted in, for example, mountainous regions or areas with a strong continental influence.

Another challenge related to the interpretation of the results from the dual-isotope mapping approach emerges when estimates of the two applied scenarios diverge considerably from each other. In this case both scenarios should be regarded as boundaries within which source partitioning is located rather than selecting one scenario over another. The decision to follow only one specific scenario should only be made if there is strong evidence from other data that allows to clearly exclude one of the two scenarios.

Overall, the current dual-isotope approach used in this thesis project has already proved its diagnostic value but the precision in the determination of source contribution and  $\text{N}_2\text{O}$  reduction will most likely improve if the recommendations made here are implemented during the application of the method.

## **5.7 Outlook**

This thesis project advanced our predictive understanding on how different microhabitat effects shape the N transforming microbial community dynamics, and the balance between  $\text{N}_2\text{O}$  production and consumption processes resulting in the observed magnitude and temporal patterns of elevated  $\text{N}_2\text{O}$  emissions after short-term flooding. However, during this thesis project new knowledge gaps emerged, which offer promising opportunities for future research projects:

- In the two studies conducted during this thesis project our knowledge of how various microhabitats rich in nitrogenous compounds and with a carbonate-buffered pH shaped the magnitude and temporal patterns of N<sub>2</sub>O emissions was extended. However, changes in both characteristics have a pivotal impact on the microorganisms and enzymes involved in N transformation processes and therefore also on the resulting N<sub>2</sub>O emissions. This underlines the need to further investigate the effect of different levels of N availability and soil pH on source composition of N<sub>2</sub>O and especially on the sensitivity of microbial N<sub>2</sub>O reduction during and after several flood events in various floodplains. In combination with our insights from this thesis project these new insights would result in a more generalized understanding of different microhabitat effects on post-flood microbial process dynamics resulting in periods of enhanced N<sub>2</sub>O emissions.
- The aspect of a potentially unaccounted fraction of N<sub>2</sub>O emitted via internal plant gas transport should not be neglected. The fact that in our mesocosm experiment *S. viminalis* did not increase the ecosystem fluxes of N<sub>2</sub>O but Jørgensen et al. (2012) could show that *P. arundinacea* is capable of such gas transport, indicates that the potential to function as conduits of soil-produced nitrous oxide may vary amongst species of floodplain vegetation. This highlights the need of a systematic assessment of the capability of various species of the soft and hardwood vegetation in the floodplain to plant-mediated transport of N<sub>2</sub>O, especially of taxa that also promote N<sub>2</sub>O emissions from the soils under their stands, as observed for *P. arundinacea* in our field experiment. In addition, in the river floodplain flood-related damage to the vegetation but also plant growth stage can potentially alter the ability of the plants to transport N<sub>2</sub>O, which is why these factors should also be included in the investigations. Laboratory and/or field-based investigations using flux chamber measurements in combination with stable isotope analyses of plant-emitted N<sub>2</sub>O would therefore not only improve our predictive capabilities to identify patches of specific vegetation with high potential for becoming hotspots of N<sub>2</sub>O emissions, but also would further elucidate the microbial origin of this soil-produced fraction of N<sub>2</sub>O.
- The climatic conditions prevalent during the field experiment and in the mesocosm experiment were characteristic for late spring and early summer in which the strongest most frequent periods of enhanced N<sub>2</sub>O emissions after flood events have previously been observed in our research area (Shrestha et al., 2014). Since microbial processes but also plant physiology are sensitive to changes in temperature it is crucial for our mechanistic understanding of the dynamics between microbial N<sub>2</sub>O source processes

and N<sub>2</sub>O reduction to assess the effect of various seasonal conditions in the field and/or simulated in climate chamber studies.

- Fungal denitrification is a potentially strong contributor to N<sub>2</sub>O emissions from soils, as demonstrated by several previous laboratory studies (Maeda et al., 2015; Rohe et al., 2017; Shoun et al., 2012). However, the methods applied in this thesis project so far only allow a qualitative determination of the N<sub>2</sub>O source contribution by this pathway in soil systems harboring a natural or near-natural microbiome. An expansion of the DNA- and RNA-based molecular techniques already established in this project with focus on denitrifying fungi could improve the current situation. The application of primers targeting specific marker genes of denitrifying fungi, e.g., p450nor, would not only facilitate the identification and quantification of this N<sub>2</sub>O production pathway but also provide new insights on this rarely investigated pathway outside the laboratory.

---

## References

- Buchen, C., Lewicka-Szczebak, D., Flessa, H., & Well, R. (2018). Estimating N<sub>2</sub>O processes during grassland renewal and grassland conversion to maize cropping using N<sub>2</sub>O isotopocules. *Rapid Communications in Mass Spectrometry*, *32*(13), 1053–1067. <https://doi.org/10.1002/rcm.8132>
- Fender, A.-C., Leuschner, C., Schützenmeister, K., Gansert, D., & Jungkunst, H. F. (2013). Rhizosphere effects of tree species – Large reduction of N<sub>2</sub>O emission by saplings of ash, but not of beech, in temperate forest soil. *European Journal of Soil Biology*, *54*, 7–15. <https://doi.org/10.1016/j.ejsobi.2012.10.010>
- Habtewold, J. Z., Helgason, B. L., Yanni, S. F., Janzen, H. H., Ellert, B. H., & Gregorich, E. G. (2020). Litter composition has stronger influence on the structure of soil fungal than bacterial communities. *European Journal of Soil Biology*, *98*(January), 103190. <https://doi.org/10.1016/j.ejsobi.2020.103190>
- Hill, A. R. (2019). Groundwater nitrate removal in riparian buffer zones: a review of research progress in the past 20 years. *Biogeochemistry*, *143*(3), 347–369. <https://doi.org/10.1007/s10533-019-00566-5>
- Hu, H. W., Chen, D., & He, J. Z. (2015). Microbial regulation of terrestrial nitrous oxide formation: Understanding the biological pathways for prediction of emission rates. *FEMS Microbiology Reviews*, *39*(5), 729–749. <https://doi.org/10.1093/femsre/fuv021>
- Jarecke, K. M., Loecke, T. D., & Burgin, A. J. (2016). Coupled soil oxygen and greenhouse gas dynamics under variable hydrology. *Soil Biology and Biochemistry*, *95*, 164–172. <https://doi.org/10.1016/j.soilbio.2015.12.018>
- Jiang, M., Yang, N., Zhao, J., Shaaban, M., & Hu, R. (2021). Crop straw incorporation mediates the impacts of soil aggregate size on greenhouse gas emissions. *Geoderma*, *401*(July), 115342. <https://doi.org/10.1016/j.geoderma.2021.115342>
- Jørgensen, C. J., Struwe, S., & Elberling, B. (2012). Temporal trends in N<sub>2</sub>O flux dynamics in a Danish wetland - effects of plant-mediated gas transport of N<sub>2</sub>O and O<sub>2</sub> following changes in water level and soil mineral-N availability. *Global Change Biology*, *18*(1), 210–222. <https://doi.org/10.1111/j.1365-2486.2011.02485.x>
- Lewicka-Szczebak, D., Piotr Lewicki, M., & Well, R. (2020). N<sub>2</sub>O isotope approaches for source partitioning of N<sub>2</sub>O production and estimation of N<sub>2</sub>O reduction-validation with the <sup>15</sup>N gas-flux method in laboratory and field studies. *Biogeosciences*, *17*(22), 5513–5537. <https://doi.org/10.5194/bg-17-5513-2020>
- Maeda, K., Spor, A., Edel-Hermann, V., Heraud, C., Breuil, M. C., Bizouard, F., Toyoda, S., Yoshida, N., Steinberg, C., & Philippot, L. (2015). N<sub>2</sub>O production, a widespread trait in fungi. *Scientific Reports*, *5*(1), 9697. <https://doi.org/10.1038/srep09697>
- Poblador, S., Lupon, A., Sabaté, S., & Sabater, F. (2017). Soil water content drives spatiotemporal patterns of CO<sub>2</sub> and N<sub>2</sub>O emissions from a Mediterranean riparian forest soil. *Biogeosciences*, *14*(18), 4195–4208. <https://doi.org/10.5194/bg-14-4195-2017>
- Rohe, L., Well, R., & Lewicka-Szczebak, D. (2017). Use of oxygen isotopes to differentiate between nitrous oxide produced by fungi or bacteria during denitrification. *Rapid Communications in Mass Spectrometry*, *31*(16), 1297–1312. <https://doi.org/10.1002/rcm.7909>
- Rummel, P. S., Pfeiffer, B., Pausch, J., Well, R., Schneider, D., & Dittert, K. (2020). Maize root and shoot litter quality controls short-term CO<sub>2</sub> and N<sub>2</sub>O emissions and bacterial community structure of arable soil. *Biogeosciences*, *17*(4), 1181–1198. <https://doi.org/10.5194/bg-17-1181-2020>
-

- 
- Schindler, T., Mander, Ü., Machacova, K., Espenberg, M., Krasnov, D., Escuer-Gatius, J., Veber, G., Pärn, J., & Soosaar, K. (2020). Short-term flooding increases CH<sub>4</sub> and N<sub>2</sub>O emissions from trees in a riparian forest soil-stem continuum. *Scientific Reports*, *10*(1), 3204. <https://doi.org/10.1038/s41598-020-60058-7>
- Schlüter, S., Henjes, S., Zawallich, J., Bergaust, L., Horn, M., Ippisch, O., Vogel, H. J., & Dörsch, P. (2018). Denitrification in soil aggregate analogues-effect of aggregate size and oxygen diffusion. *Frontiers in Environmental Science*, *6*(APR), 1–10. <https://doi.org/10.3389/fenvs.2018.00017>
- Schomburg, A., Brunner, P., Turberg, P., Guenat, C., Riaz, M., le Bayon, R. C., & Luster, J. (2019). Pioneer plant *Phalaris arundinacea* and earthworms promote initial soil structure formation despite strong alluvial dynamics in a semi-controlled field experiment. *CATENA*, *180*(April), 41–54. <https://doi.org/10.1016/j.catena.2019.04.001>
- Sharp, Z. (2007). Principles of stable isotope geochemistry. In *Choice Reviews Online* (Vol. 44, Issue 11). <https://doi.org/10.5860/choice.44-6251>
- Shoun, H., Fushinobu, S., Jiang, L., Kim, S. W., & Wakagi, T. (2012). Fungal denitrification and nitric oxide reductase cytochrome P450nor. *Philosophical Transactions of the Royal Society B: Biological Sciences*, *367*(1593), 1186–1194. <https://doi.org/10.1098/rstb.2011.0335>
- Shrestha, J., Niklaus, P. A., Pasquale, N., Huber, B., Barnard, R. L., Frossard, E., Schleppei, P., Tockner, K., & Luster, J. (2014). Flood pulses control soil nitrogen cycling in a dynamic river floodplain. *Geoderma*, *228–229*, 14–24. <https://doi.org/10.1016/j.geoderma.2013.09.018>
- Tomasek, A. A., Hondzo, M., Kozarek, J. L., Staley, C., Wang, P., Lurndahl, N., & Sadowsky, M. J. (2019). Intermittent flooding of organic-rich soil promotes the formation of denitrification hot moments and hot spots. *Ecosphere*, *10*(1). <https://doi.org/10.1002/ecs2.2549>
- Trivedi, P., Delgado-Baquerizo, M., Jeffries, T. C., Trivedi, C., Anderson, I. C., Lai, K., McNee, M., Flower, K., Pal Singh, B., Minkey, D., & Singh, B. K. (2017). Soil aggregation and associated microbial communities modify the impact of agricultural management on carbon content. *Environmental Microbiology*, *19*(8), 3070–3086. <https://doi.org/10.1111/1462-2920.13779>
- Verhoeven, E., Barthel, M., Yu, L., Celi, L., Said-Pullicino, D., Sleutel, S., Lewicka-Szczebak, D., Six, J., & Decock, C. (2019). Early season N<sub>2</sub>O emissions under variable water management in rice systems: Source-partitioning emissions using isotope ratios along a depth profile. *Biogeosciences*, *16*(2), 383–408. <https://doi.org/10.5194/bg-16-383-2019>
- Wang, B., Brewer, P. E., Shugart, H. H., Lerdau, M. T., & Allison, S. D. (2019). Soil aggregates as biogeochemical reactors and implications for soil–atmosphere exchange of greenhouse gases—A concept. *Global Change Biology*, *25*(2), 373–385. <https://doi.org/10.1111/gcb.14515>
- Wang, S., & Reid, M. C. (2020). Kinetics of nitrous oxide mass transfer from porewater into root aerenchyma of wetland plants. *Journal of Environmental Quality*, *49*(6), 1717–1729. <https://doi.org/10.1002/jeq2.20162>
- Yamamoto, A., Akiyama, H., Nakajima, Y., & Hoshino, Y. T. (2017). Estimate of bacterial and fungal N<sub>2</sub>O production processes after crop residue input and fertilizer application to an agricultural field by <sup>15</sup>N isotopomer analysis. *Soil Biology and Biochemistry*, *108*, 9–16. <https://doi.org/10.1016/j.soilbio.2017.01.015>
-

Yu, L., Harris, E., Lewicka-Szczebak, D., Barthel, M., Blomberg, M. R. A., Harris, S. J., Johnson, M. S., Lehmann, M. F., Liisberg, J., Müller, C., Ostrom, N. E., Six, J., Toyoda, S., Yoshida, N., & Mohn, J. (2020). What can we learn from N<sub>2</sub>O isotope data? – Analytics, processes and modelling. *Rapid Communications in Mass Spectrometry*, 34(20), 1–14. <https://doi.org/10.1002/rcm.8858>

## Supplementary Material Chapter 2

### **Alteration of nitrous oxide emissions from floodplain soils by aggregate size, litter accumulation and plant–soil interactions**

Martin Ley<sup>1,2</sup>, Moritz F. Lehmann<sup>2</sup>, Pascal A. Niklaus<sup>3</sup>, and Jörg Luster<sup>1</sup>

<sup>1</sup>Swiss Federal Institute for Forest, Snow and Landscape Research WSL, Zürcherstrasse 111, 8903 Birmensdorf, Switzerland

<sup>2</sup>Department of Environmental Sciences, University of Basel, Bernoullistrasse 30, 4056 Basel, Switzerland

<sup>3</sup>Department of Evolutionary Biology and Environmental Studies, University of Zürich, Winterthurerstrasse 190, 8057 Zurich, Switzerland

*Correspondence to:* Martin Ley ([martin.ley@wsl.ch](mailto:martin.ley@wsl.ch))



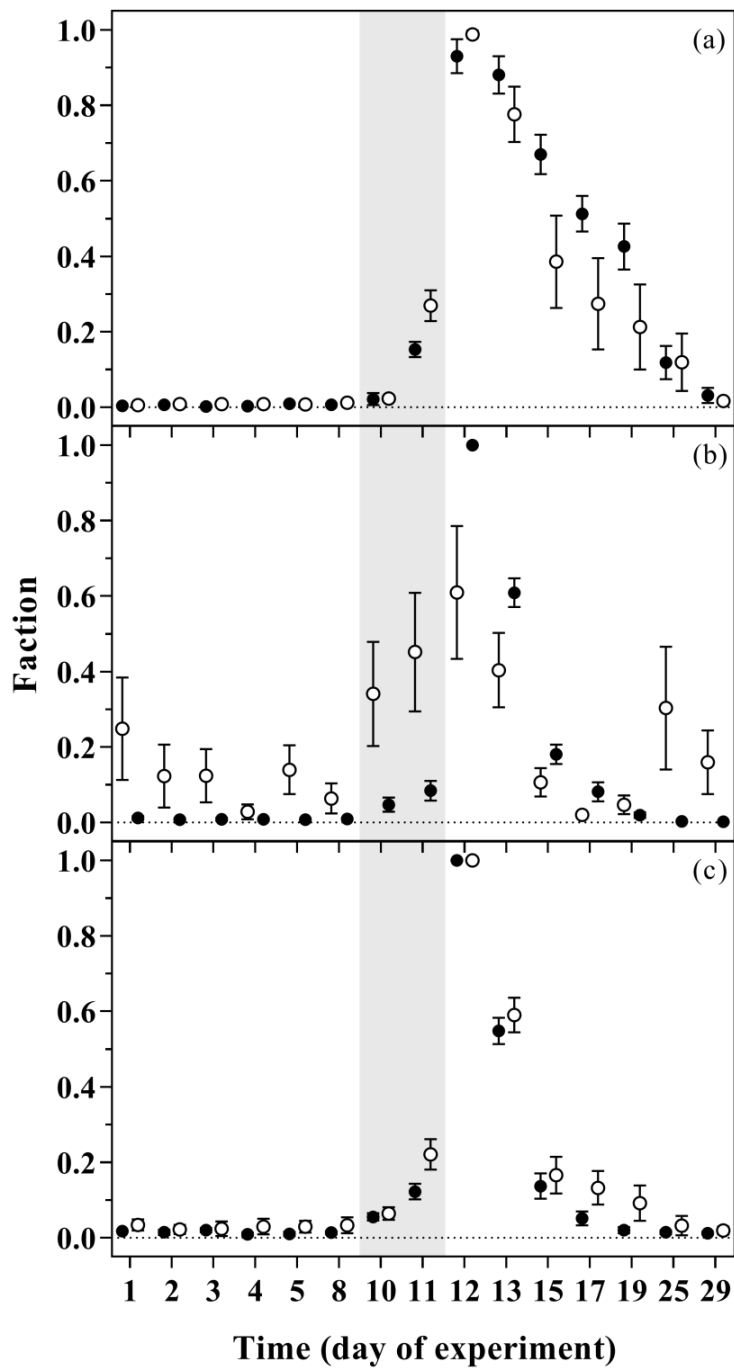


**Figure S2.2.** Mean of the normalized N<sub>2</sub>O emission fluxes during the flooding–drying experiment from large-aggregate model soil (LA; filled circles) and small-aggregate model soil (SA, open circles). Unamended soils (A), litter addition (B) and plant treatment (C). Flooding phase indicated by the grey area. Symbols indicate means; error bars are SE; n = 6.

## Supplementary Material Chapter 3

# Microhabitat effects on source partitioning and reduction of nitrous oxide during flood-induced emissions from floodplain soils

Martin Ley<sup>a,b</sup>, Jörg Luster<sup>a</sup>, Pascal A. Niklaus<sup>c</sup>, Martin Hartmann<sup>d</sup>, Thomas Kuhn<sup>b</sup>, Beat Frey<sup>a</sup>, Moritz F. Lehmann<sup>b</sup>

<sup>a</sup>Swiss Federal Institute for Forest, Snow and Landscape Research WSL, Research Unit Forest Soils and Biogeochemistry, Zürcherstrasse 111, 8903 Birmensdorf, Switzerland

<sup>b</sup>University of Basel, Department of Environmental Sciences, Research Group Biogeochemistry, Bernoullistrasse 30, 4056 Basel, Switzerland

<sup>c</sup>University of Zürich, Department of Evolutionary Biology and Environmental Studies, Winterthurerstrasse 190, 8057 Zurich, Switzerland

<sup>d</sup>Swiss Federal Institute of Technology Zurich, Department of Environmental Systems Science, Sustainable Agroecosystems, Universitätsstrasse 2, 8092 Zürich, Switzerland

*Corresponding author:* Martin Ley (martin.ley@unibas.ch)

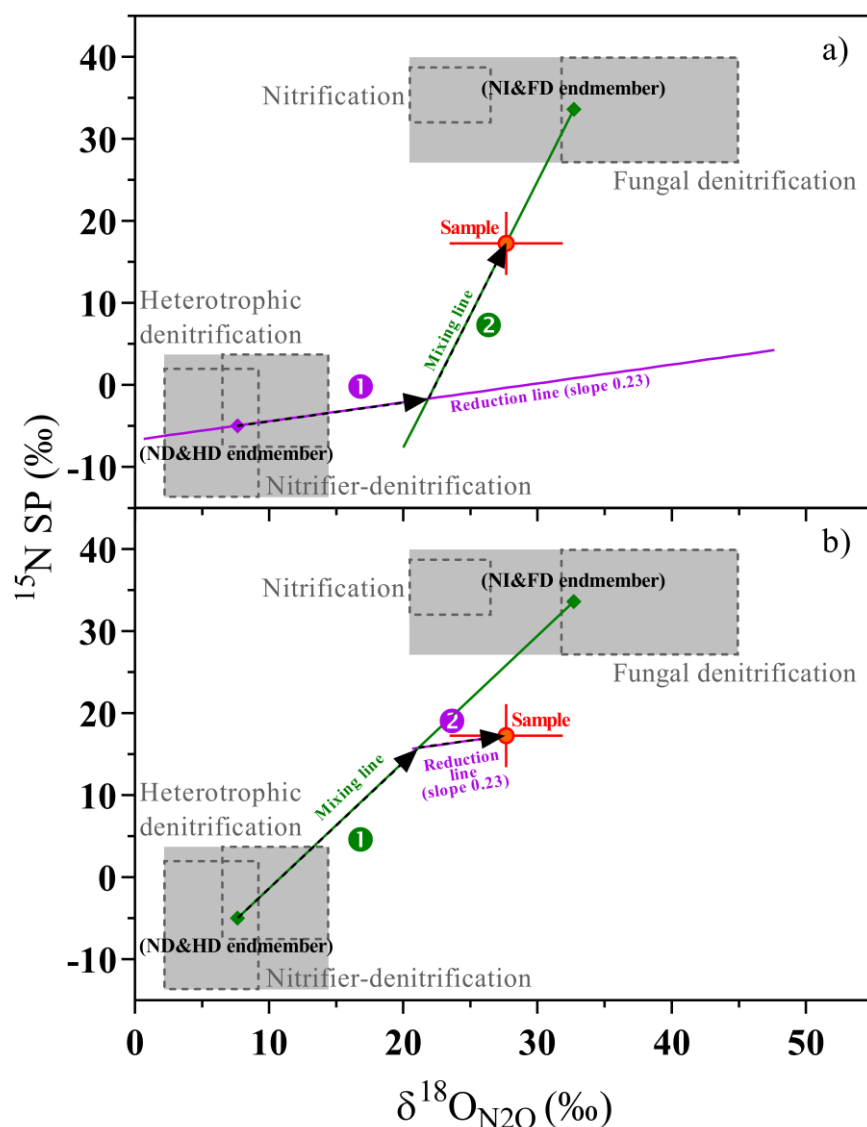


**Figure S3.1.** Schematic depicting the N<sub>2</sub>O isotopomer mapping approach, with  $\delta^{18}\text{O}_{\text{N}_2\text{O}}$  on the X axis, and  $^{15}\text{N SP}$  on the Y axis. The ranges of reference values from the literature for the four major N<sub>2</sub>O producing processes adjusted to the isotopic signature of the ambient water ( $\delta^{18}\text{O}_{\text{H}_2\text{O}}$ : -10.2 ‰) are indicated by the dashed-line boxes within the grey-shaded areas. Due to the considerable overlap for some of the processes, for N<sub>2</sub>O source partitioning estimation, we used common endmembers values for the process groups nitrifier denitrification / heterotrophic denitrification (ND&HD) and nitrification / fungal denitrification (NI&FD), respectively (central values indicated by green diamonds within grey boxes). Depending on assumptions regarding the sequential order of N<sub>2</sub>O mixing versus reduction, observational isotope data yield different estimates on the contribution of the ND&HD process group ( $f_{\text{ND\&HD}}$ ) and the residual N<sub>2</sub>O ( $f_{\text{N}_2\text{O}}$ ): a) N<sub>2</sub>O reduction first followed by mixing b) mixing first followed by N<sub>2</sub>O reduction (see text for details).

**Table S3.1:** Primer List and applied Thermal profiles for different target genes.

Target gene	Primers	Primer Sequence (5'-3')	Primers Reference	Thermal profile	Number of Cycles
16S rRNA gene (bacterial and archeal)	341F	CCTAYGGGDBGCWSCAG	Frey et al., 2016	95 °C/2 min	1
	806R	GGACTACNVGGGTHCTAAT	Frey et al., 2016	94 °C/40 sec - 58 °C/40 sec - 72 °C/1 min 72 °C/10 min	35 1
ITS2 (fungal)	ITS3	CAHCGATGAACGYRG	Tedersoo et al., 2014	95 °C/2 min	1
	ITS4	TCCTSCGCTTATTGATATGC	Tedersoo et al., 2014	94 °C/40 sec - 58 °C/40 sec - 72 °C/1 min 72 °C/10 min	38 1
bacterial amoA	amoA-1F	GGGGHTTYTACTGGTGGT	Rotthauwe et al., 1997	95 °C/15 min	1
	amoA-2R	CCCCTCKGSAAAGCCTTCTTC	Rotthauwe et al., 1997	95 °C/45 sec - 55 °C/45 sec - 72 °C/45 sec 95 °C/15 sec - 60 °C/15 sec - 95 °C/15 sec	40 1
archaeal amoA	Arch-amoA-for	CTGAYTGGGTCYTGGACATC	Wuchter et al., 2006	95 °C/15 min	1
	Arch-amoA-rev	TTCTTCTTTGTTGCCAGTA	Wuchter et al., 2006	95 °C/45 sec - 53 °C/45 sec - 72 °C/45 sec 95 °C/15 sec - 60 °C/15 sec - 95 °C/15 sec	40 1
nxrB	nxrB169f	TACATGTGGTGGAACA	Pester et al., 2014	95 °C/15 min	1
	nxrB638r	CGGTTCTGGTCRATCA	Pester et al., 2014	95 °C/45 sec - 57 °C/45 sec - 72 °C/45 sec 95 °C/15 sec - 60 °C/15 sec - 95 °C/15 sec	40 1
nirS	cd3AF	G TSAACG TSAAGGARACSGG	Throbäck et al., 2004	95 °C/15 min	1
	R3cd	GASTTCGGRTGSGTCTTGA	Throbäck et al., 2004	95 °C/45 sec - 58 °C/45 sec - 72 °C/45 sec 95 °C/15 sec - 60 °C/15 sec - 95 °C/15 sec	35 1
nosZ	nosZ-1F	WCSYTGTTTCMTCGACAGCCAG	Henry et al., 2006	95 °C/15 min	1
	nosZ-R	ATGTCGATCARCTGVKCRTTYT C	Henry et al., 2006	95 °C/15 sec - 67 °C/30 sec - 72 °C/30 sec 95 °C/15 sec - 62 °C/15 sec - 72 °C/30 sec 95 °C/15 sec - 60 °C/15 sec - 95 °C/15 sec	(Touchdown) 6 40 1

**Table S3.2:** Isotopic signatures of the N<sub>2</sub>O standards and standards used in the denitrifier method.

N <sub>2</sub> O gas standards					
	$\delta^{15}\text{N}^{\text{bulk}}$ (‰)	$\delta^{18}\text{O}_{\text{N}_2\text{O}}$ (‰)	$\delta^{15}\text{N}^{\alpha}$ (‰)	$\delta^{15}\text{N}^{\beta}$ (‰)	$^{15}\text{N}$ SP (‰)
Standard 1	-35.74	26.94	-22.21	-49.28	27.07
Standard 2	48.09	36.01	1.71	94.44	-92.73
Standard 3	6.84	35.39	17.11	-3.43	20.54
Standards used in denitrifier method					
	$\delta^{15}\text{N}$ (‰ vs. AIR-N <sub>2</sub> )	$\delta^{18}\text{O}$ (‰ vs. VSMOW)			
IAEA-NO-3	4.7	25.6			
USGS32	180	25.7			
USGS34	-1.8	-27.9			
UBN-NO3	14.15	25.6			
Deep Pacific Nitrate	~5.1	~2.1			

**Table S3.3:** Ranges of  $^{15}\text{N}$  SP and  $\delta^{18}\text{O}_{\text{N}_2\text{O}}$  (unadjusted literature values in parentheses) used in the dual-isotope maps and the isotopic fractionation factors for the reduction of  $\text{N}_2\text{O}$  to  $\text{N}_2$  used in the model calculations.

Process	$^{15}\text{N}$ SP (‰)		$\delta^{18}\text{O}_{\text{N}_2\text{O}}$ (‰)		Reference
	min	max	min	max	
Nitrification (NI)	32	38.7	20.5	26.5	Frame and Casciotti, 2010; Sutka et al., 2006
Fungal denitrification (FD)	27.2	39.9	31.8 (42)	44.9 (55.1)	Maeda et al., 2015; Rohe et al., 2017, 2014; Sutka et al., 2008
Heterotrophic bacterial denitrification (HD)	-7.5	3.7	6.5 (16.7)	13.1 (23.3)	Sutka et al., 2006; Toyoda et al., 2005
Nitrifier denitrification (ND)	-13.6	1.9	2.2 (12.4)	9.2 (19.4)	Frame and Casciotti, 2010; Sutka et al., 2006
ND&HD endmember	-5.0		7.7		This study
NI&FD endmember	33.6		32.7		This study
Fractionation factors of $\text{N}_2\text{O}$ reduction					
$\epsilon^{15}\text{N}$ SP	-3.7				Jinuntuya-Nortman et al., 2008
$\epsilon^{18}\text{O}$			-15.8		

**Table S3.4:** OTU richness, Shannon index and species evenness index ( $E_{var}$ ) for the prokaryotic communities in the topsoil (5cm depth) and subsoil (20cm depth) of the different treatments (mean  $\pm$  SE;  $n = 6$ ). LA and SA stand for large and small aggregates, respectively, and the last letter U for unamended, L for litter addition, and P for plant presence. Superscript letters indicate significant (adj.  $P < 0.05$ ) differences between sampling days in the topsoil and the subsoil, respectively.

		OTU richness			Shannon's diversity (H')			Species evenness index ( $E_{var}$ )		
		day 02	day 12	day 33	day 02	day 12	day 33	day 02	day 12	day 33
LAU	topsoil	2552 $\pm$ 13	2620 $\pm$ 51	2569 $\pm$ 65	7.0 $\pm$ 0.0	7.1 $\pm$ 0.0	7.0 $\pm$ 0.1	0.43 $\pm$ 0.00 <sup>a</sup>	0.37 $\pm$ 0.01 <sup>b</sup>	0.38 $\pm$ 0.01 <sup>b</sup>
	subsoil	2554 $\pm$ 18	2607 $\pm$ 23	2589 $\pm$ 74	7.0 $\pm$ 0.0	7.0 $\pm$ 0.0	7.0 $\pm$ 0.1	0.39 $\pm$ 0.01 <sup>a</sup>	0.45 $\pm$ 0.01 <sup>b</sup>	0.40 $\pm$ 0.01 <sup>a</sup>
LAL	topsoil	2422 $\pm$ 68 <sup>a</sup>	2489 $\pm$ 12 <sup>b</sup>	2482 $\pm$ 64 <sup>b</sup>	6.9 $\pm$ 0.1	7.0 $\pm$ 0.0	7.0 $\pm$ 0.0	0.43 $\pm$ 0.01 <sup>a</sup>	0.38 $\pm$ 0.01 <sup>b</sup>	0.38 $\pm$ 0.01 <sup>b</sup>
	subsoil	2410 $\pm$ 27	2608 $\pm$ 26	2612 $\pm$ 28	6.9 $\pm$ 0.0	7.1 $\pm$ 0.0	7.0 $\pm$ 0.0	0.40 $\pm$ 0.00 <sup>a</sup>	0.43 $\pm$ 0.01 <sup>b</sup>	0.45 $\pm$ 0.01 <sup>b</sup>
LAP	topsoil	2543 $\pm$ 23	2645 $\pm$ 33	2688 $\pm$ 40	7.0 $\pm$ 0.0	7.1 $\pm$ 0.0	7.1 $\pm$ 0.0	0.42 $\pm$ 0.01 <sup>a</sup>	0.39 $\pm$ 0.01 <sup>b</sup>	0.41 $\pm$ 0.00 <sup>a</sup>
	subsoil	2525 $\pm$ 25	2553 $\pm$ 17	2602 $\pm$ 40	7.0 $\pm$ 0.0	7.0 $\pm$ 0.0	7.1 $\pm$ 0.0	0.42 $\pm$ 0.01 <sup>a</sup>	0.43 $\pm$ 0.01 <sup>a</sup>	0.38 $\pm$ 0.00 <sup>b</sup>
SAU	topsoil	2555 $\pm$ 18	2535 $\pm$ 53	2474 $\pm$ 94	7.0 $\pm$ 0.0	7.0 $\pm$ 0.0	7.0 $\pm$ 0.0	0.41 $\pm$ 0.00	0.39 $\pm$ 0.01	0.40 $\pm$ 0.01
	subsoil	2471 $\pm$ 22	2572 $\pm$ 33	2684 $\pm$ 46	7.0 $\pm$ 0.0	7.0 $\pm$ 0.0	7.1 $\pm$ 0.0	0.42 $\pm$ 0.00 <sup>a</sup>	0.44 $\pm$ 0.01 <sup>a</sup>	0.48 $\pm$ 0.02 <sup>b</sup>
SAL	topsoil	2554 $\pm$ 24	2435 $\pm$ 47	2646 $\pm$ 13	7.0 $\pm$ 0.0	7.0 $\pm$ 0.0	7.1 $\pm$ 0.0	0.42 $\pm$ 0.01	0.40 $\pm$ 0.01	0.41 $\pm$ 0.01
	subsoil	2578 $\pm$ 45 <sup>a</sup>	2531 $\pm$ 36 <sup>b</sup>	2643 $\pm$ 28 <sup>a</sup>	7.0 $\pm$ 0.0	7.0 $\pm$ 0.0	7.1 $\pm$ 0.0	0.40 $\pm$ 0.01	0.42 $\pm$ 0.01	0.41 $\pm$ 0.01
SAP	topsoil	2540 $\pm$ 32	2522 $\pm$ 22	2608 $\pm$ 28	7.0 $\pm$ 0.0	7.0 $\pm$ 0.0	7.1 $\pm$ 0.0	0.42 $\pm$ 0.01 <sup>a</sup>	0.39 $\pm$ 0.01 <sup>b</sup>	0.39 $\pm$ 0.00 <sup>b</sup>
	subsoil	2541 $\pm$ 27	2538 $\pm$ 35	2627 $\pm$ 52	7.0 $\pm$ 0.0	6.9 $\pm$ 0.0	7.1 $\pm$ 0.0	0.43 $\pm$ 0.01	0.44 $\pm$ 0.01	0.43 $\pm$ 0.01

**Table S3.5:** OTU richness, Shannon index and species evenness index ( $E_{var}$ ) for the fungal communities in the topsoil (5cm depth) and subsoil (20cm depth) of the different treatments (mean  $\pm$  SE;  $n = 6$ ). LA and SA stand for large and small aggregates, respectively, and the last letter U for unamended, L for litter addition, and P for plant presence. Superscript letters indicate significant (adj.  $P < 0.05$ ) differences between sampling days in the topsoil and the subsoil, respectively.

		OTU Richness			Shannon's diversity ( $H'$ )			Species evenness index ( $E_{var}$ )		
		day 02	day 12	day 33	day 02	day 12	day 33	day 02	day 12	day 33
LAU	topsoil	484 $\pm$ 40	520 $\pm$ 44	439 $\pm$ 54	4.3 $\pm$ 0.1	4.1 $\pm$ 0.3	3.9 $\pm$ 0.2	0.32 $\pm$ 0.02	0.34 $\pm$ 0.01	0.31 $\pm$ 0.02
	subsoil	485 $\pm$ 31	412 $\pm$ 54	422 $\pm$ 37	3.8 $\pm$ 0.2	3.1 $\pm$ 0.4	3.7 $\pm$ 0.1	0.35 $\pm$ 0.01	0.35 $\pm$ 0.01	0.31 $\pm$ 0.02
LAL	topsoil	520 $\pm$ 24	550 $\pm$ 19	562 $\pm$ 18	4.3 $\pm$ 0.1	4.3 $\pm$ 0.1	4.2 $\pm$ 0.1	0.35 $\pm$ 0.00	0.35 $\pm$ 0.00	0.35 $\pm$ 0.00
	subsoil	534 $\pm$ 15	484 $\pm$ 17	530 $\pm$ 35	4.1 $\pm$ 0.2	3.9 $\pm$ 0.1	4.1 $\pm$ 0.2	0.35 $\pm$ 0.00	0.34 $\pm$ 0.00	0.35 $\pm$ 0.00
LAP	topsoil	319 $\pm$ 39	359 $\pm$ 31	458 $\pm$ 28	3.0 $\pm$ 0.3 <sup>a</sup>	3.2 $\pm$ 0.2 <sup>ab</sup>	3.9 $\pm$ 0.1 <sup>b</sup>	0.30 $\pm$ 0.02	0.31 $\pm$ 0.01	0.33 $\pm$ 0.02
	subsoil	542 $\pm$ 27	527 $\pm$ 55	445 $\pm$ 36	4.3 $\pm$ 0.1	4.1 $\pm$ 0.3	3.7 $\pm$ 0.2	0.35 $\pm$ 0.01	0.34 $\pm$ 0.01	0.33 $\pm$ 0.01
SAU	topsoil	441 $\pm$ 24	459 $\pm$ 26	401 $\pm$ 33	3.6 $\pm$ 0.1	3.7 $\pm$ 0.2	3.4 $\pm$ 0.1	0.34 $\pm$ 0.01	0.34 $\pm$ 0.01	0.33 $\pm$ 0.01
	subsoil	470 $\pm$ 18 <sup>a</sup>	385 $\pm$ 34 <sup>b</sup>	396 $\pm$ 17 <sup>ab</sup>	3.9 $\pm$ 0.1 <sup>a</sup>	3.4 $\pm$ 0.2 <sup>b</sup>	3.4 $\pm$ 0.1 <sup>b</sup>	0.34 $\pm$ 0.01	0.31 $\pm$ 0.01	0.33 $\pm$ 0.01
SAL	topsoil	547 $\pm$ 18 <sup>ab</sup>	467 $\pm$ 30 <sup>a</sup>	590 $\pm$ 17 <sup>b</sup>	4.2 $\pm$ 0.1	3.8 $\pm$ 0.2	4.3 $\pm$ 0.1	0.36 $\pm$ 0.01	0.35 $\pm$ 0.00	0.37 $\pm$ 0.01
	subsoil	322 $\pm$ 24 <sup>a</sup>	439 $\pm$ 51 <sup>ab</sup>	552 $\pm$ 21 <sup>b</sup>	3.3 $\pm$ 0.1 <sup>a</sup>	3.8 $\pm$ 0.2 <sup>ab</sup>	4.1 $\pm$ 0.1 <sup>b</sup>	0.28 $\pm$ 0.01 <sup>a</sup>	0.33 $\pm$ 0.01 <sup>b</sup>	0.36 $\pm$ 0.00 <sup>c</sup>
SAP	topsoil	357 $\pm$ 29	355 $\pm$ 48	459 $\pm$ 54	3.8 $\pm$ 0.1	3.4 $\pm$ 0.3	3.9 $\pm$ 0.2	0.27 $\pm$ 0.02	0.29 $\pm$ 0.01	0.32 $\pm$ 0.02
	subsoil	420 $\pm$ 45	410 $\pm$ 28	508 $\pm$ 51	4.0 $\pm$ 0.1	3.8 $\pm$ 0.1	4.1 $\pm$ 0.2	0.31 $\pm$ 0.02	0.32 $\pm$ 0.02	0.32 $\pm$ 0.02



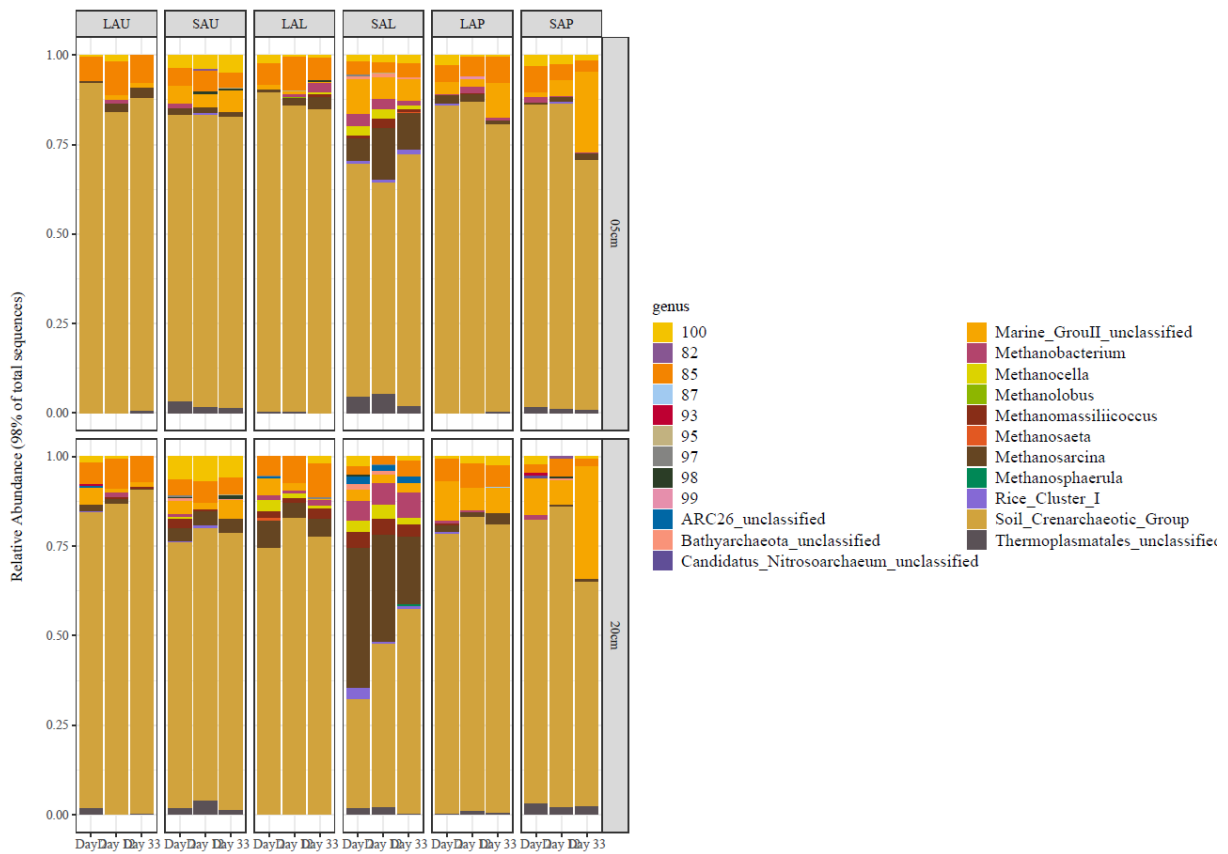


**Figure S3.2.** Relative abundance of taxonomic groups of archaea at the class level in the topsoils (5cm) and the subsoils (20cm) from a flooding experiment with model floodplain soils. LA and SA stand for large and small aggregates, respectively, and the last letter U for unamended, L for litter addition, and P for plant presence. Values are means of replicated treatments ( $n = 6$ )

---

## References

- Frame, C.H., Casciotti, K.L., 2010. Biogeochemical controls and isotopic signatures of nitrous oxide production by a marine ammonia-oxidizing bacterium. *Biogeosciences* 7, 2695–2709. doi:10.5194/bg-7-2695-2010
- Frey, B., Rime, T., Phillips, M., Stierli, B., Hajdas, I., Widmer, F., Hartmann, M., 2016. Microbial diversity in European alpine permafrost and active layers. *FEMS Microbiology Ecology* 92, fiw018. doi:10.1093/femsec/fiw018
- Henry, S., Bru, D., Stes, B., Hallet, S., Philippot, L., 2006. Quantitative detection of the *nosZ* gene, encoding nitrous oxide reductase, and comparison of the abundances of 16S rRNA, *narG*, *nirK*, and *nosZ* genes in soils. *Applied and Environmental Microbiology* 72, 5181–5189. doi:10.1128/AEM.00231-06
- Jinuntuya-Nortman, M., Sutka, R.L., Ostrom, P.H., Gandhi, H., Ostrom, N.E., 2008. Isotopologue fractionation during microbial reduction of N<sub>2</sub>O within soil mesocosms as a function of water-filled pore space. *Soil Biology and Biochemistry* 40, 2273–2280. doi:10.1016/j.soilbio.2008.05.016
- Maeda, K., Spor, A., Edel-Hermann, V., Heraud, C., Breuil, M.C., Bizouard, F., Toyoda, S., Yoshida, N., Steinberg, C., Philippot, L., 2015. N<sub>2</sub>O production, a widespread trait in fungi. *Scientific Reports* 5, 9697. doi:10.1038/srep09697
- Pester, M., Maixner, F., Berry, D., Rattei, T., Koch, H., Lückner, S., Nowka, B., Richter, A., Spieck, E., Lebedeva, E., Loy, A., Wagner, M., Daims, H., 2014. *NxrB* encoding the beta subunit of nitrite oxidoreductase as functional and phylogenetic marker for nitrite-oxidizing Nitrospira. *Environmental Microbiology* 16, 3055–3071. doi:10.1111/1462-2920.12300
- Rohe, L., Anderson, T.H., Braker, G., Flessa, H., Giesemann, A., Lewicka-Szczebak, D., Wrage-Mönnig, N., Well, R., 2014. Dual isotope and isotopomer signatures of nitrous oxide from fungal denitrification - A pure culture study. *Rapid Communications in Mass Spectrometry* 28, 1893–1903. doi:10.1002/rcm.6975
- Rohe, L., Well, R., Lewicka-Szczebak, D., 2017. Use of oxygen isotopes to differentiate between nitrous oxide produced by fungi or bacteria during denitrification. *Rapid Communications in Mass Spectrometry* 31, 1297–1312. doi:10.1002/rcm.7909
- Rotthauwe, J.H., Witzel, K.P., Liesack, W., 1997. The ammonia monooxygenase structural gene *amoA* as a functional marker: Molecular fine-scale analysis of natural ammonia-oxidizing populations. *Applied and Environmental Microbiology* 63, 4704–4712. doi:10.1128/aem.63.12.4704-4712.1997
- Sutka, R.L., Adams, G.C., Ostrom, N.E., Ostrom, P.H., 2008. Isotopologue fractionation during N<sub>2</sub>O production by fungal denitrification. *Rapid Communications in Mass Spectrometry* 22, 3989–3996. doi:10.1002/rcm.3820
- Sutka, R.L., Ostrom, N.E., Ostrom, P.H., Breznak, J.A., Gandhi, H., Pitt, A.J., Li, F., 2006. Distinguishing nitrous oxide production from nitrification and denitrification on the basis of isotopomer abundances. *Applied and Environmental Microbiology* 72, 638–644. doi:10.1128/AEM.72.1.638-644.2006
- Tedersoo, L., Bahram, M., Pölme, S., Kõljalg, U., Yorou, N.S., Wijesundera, R., Ruiz, L.V., Vasco-Palacios, A.M., Thu, P.Q., Suija, A., Smith, M.E., Sharp, C., Saluveer, E., Saitta, A., Rosas, M., Riit, T., Ratkowsky, D., Pritsch, K., Põldmaa, K., Piepenbring, M., Phosri, C., Peterson, M., Parts, K., Pärtel, K., Otsing, E., Nouhra, E., Njouonkou, A.L., Nilsson, R.H., Morgado, L.N., Mayor, J., May, T.W., Majuakim, L., Lodge, D.J., Lee, S.S., Larsson, K.-H., Kohout, P., Hosaka, K., Hiiesalu, I., Henkel, T.W., Harend, H., Guo, L., Greslebin, A., Grelet, G., Geml, J., Gates, G., Dunstan, W., Dunk, C., Drenkhan, R., Dearnaley, J., de Kesel, A., Dang, T., Chen, X., Buegger, F., Brearley, F.Q., Bonito, G., Anslan, S., Abell,

- S., Abarenkov, K., 2014. Global diversity and geography of soil fungi. *Science* 346, 1256688. doi:10.1126/science.1256688
- Throbäck, I.N., Enwall, K., Jarvis, Å., Hallin, S., 2004. Reassessing PCR primers targeting *nirS*, *nirK* and *nosZ* genes for community surveys of denitrifying bacteria with DGGE. *FEMS Microbiology Ecology* 49, 401–417. doi:10.1016/j.femsec.2004.04.011
- Toyoda, S., Mutobe, H., Yamagishi, H., Yoshida, N., Tanji, Y., 2005. Fractionation of N<sub>2</sub>O isotopomers during production by denitrifier. *Soil Biology and Biochemistry* 37, 1535–1545. doi:10.1016/j.soilbio.2005.01.009
- Wuchter, C., Abbas, B., Coolen, M.J.L., Herfort, L., van Bleijswijk, J., Timmers, P., Strous, M., Teira, E., Herndl, G.J., Middelburg, J.J., Schouten, S., Damsté, J.S.S., 2006. Archaeal nitrification in the ocean. *Proceedings of the National Academy of Sciences of the United States of America* 103, 12317–12322. doi:10.1073/pnas.0600756103

## Supplementary Material Chapter 4

# **Pioneer plant *Phalaris arundinacea* modifies temporal patterns of enhanced N<sub>2</sub>O emissions, source partitioning and N<sub>2</sub>O reduction from floodplain soils after a short-term flood event**

Martin Ley<sup>a,b</sup>, Moritz Lehmann<sup>b</sup>, Pascal A. Niklaus<sup>c</sup>, Beat Frey<sup>a</sup>, Jörg Luster<sup>a</sup>

<sup>a</sup>Swiss Federal Institute for Forest, Snow and Landscape Research WSL, Research Unit Forest Soils and Biogeochemistry, Zürcherstrasse 111, 8903 Birmensdorf, Switzerland

<sup>b</sup>University of Basel, Department of Environmental Sciences, Research Group Biogeochemistry, Bernoullistrasse 30, 4056 Basel, Switzerland

<sup>c</sup>University of Zürich, Department of Evolutionary Biology and Environmental Studies, Winterthurerstrasse 190, 8057 Zurich, Switzerland

*Corresponding author:* Martin Ley (martin.ley@unibas.ch)

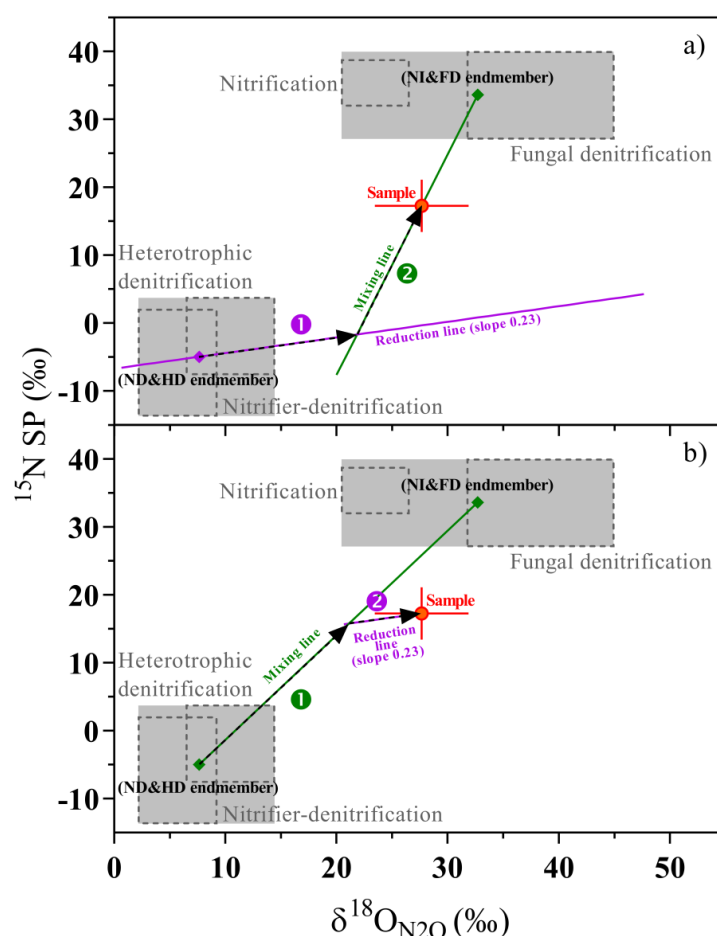


**Figure S4.1.** Schematic depicting the N<sub>2</sub>O isotopomer mapping approach, with  $\delta^{18}\text{O}_{\text{N}_2\text{O}}$  on the X axis, and  $^{15}\text{N SP}$  on the Y axis. The respective ranges of reference values, from the literature for nitrifier denitrification, heterotrophic denitrification and fungal denitrification, were adjusted to the isotopic signature of the ambient water ( $\delta^{18}\text{O}_{\text{H}_2\text{O}}$ : -10.2 ‰) and nitrification reference values were adjusted to atmospheric O<sub>2</sub> ( $\delta^{18}\text{O}_{\text{O}_2}$ : 23.5 ‰). The adjusted ranges are indicated by the dashed-line boxes within the grey-shaded areas. We used common endmember values for the process groups nitrifier denitrification / heterotrophic denitrification (ND&HD) and nitrification / fungal denitrification (NI&FD), respectively (mean values indicated by green diamonds within grey boxes). Depending on assumptions regarding the sequential order of N<sub>2</sub>O mixing versus reduction, observational isotope data yield different estimates on the contribution of the ND&HD process group ( $f_{\text{ND\&HD}}$ ) and the residual N<sub>2</sub>O ( $f_{\text{N}_2\text{O}}$ ): a) N<sub>2</sub>O reduction first followed by mixing b) mixing first followed by N<sub>2</sub>O reduction (see main text for details).

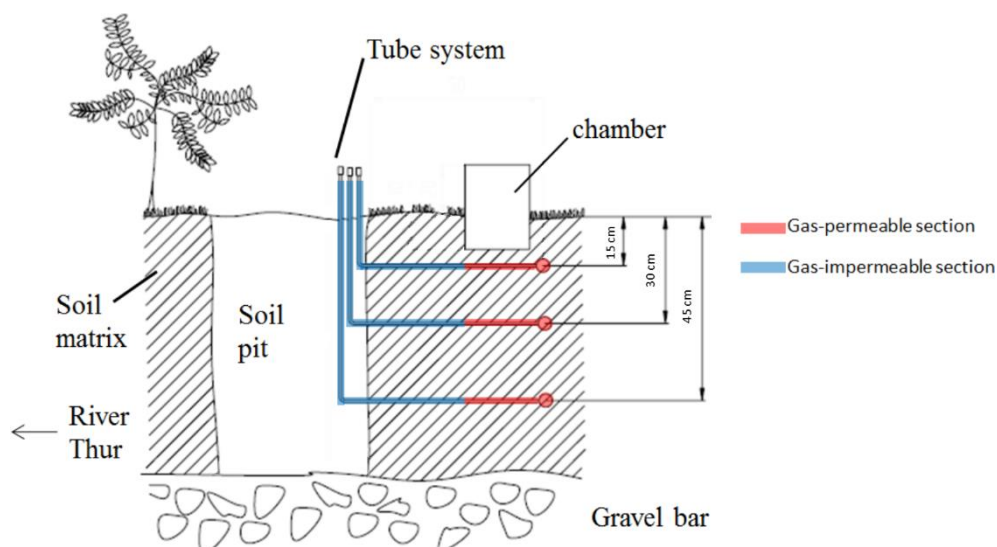


**Figure S4.2.** Schematic representation of the tube system alignment in a vertical soil profile. Tubes were installed by pushing a guiding rod with the tubing attached horizontally from the working pit through the plot. After installation the working pits were closed again (modified after Bruderer 2012).

**Table S4.1:** Isotopic signatures of the  $N_2O$  standards and standards used in the denitrifier method.

N <sub>2</sub> O gas standards					
	$\delta^{15}N^{bulk}$ (‰)	$\delta^{18}O_{N_2O}$ (‰)	$\delta^{15}N^{\alpha}$ (‰)	$\delta^{15}N^{\beta}$ (‰)	$^{15}N$ SP (‰)
Standard 1	-35.74	26.94	-22.21	-49.28	27.07
Standard 2	48.09	36.01	1.71	94.44	-92.73
Standard 3	6.84	35.39	17.11	-3.43	20.54
Standards used in denitrifier method					
	$\delta^{15}N$ (‰ vs. AIR-N <sub>2</sub> )	$\delta^{18}O$ (‰ vs. VSMOW)			
IAEA-NO-3	4.7	25.6			
USGS32	180	25.7			
USGS34	-1.8	-27.9			
UBN-NO3	14.15	25.6			
Deep Pacific Nitrate	~5.1	~2.1			

**Table S4.2:** Ranges of  $^{15}\text{N}$  SP and  $\delta^{18}\text{O}_{\text{N}_2\text{O}}$  (unadjusted literature values in parentheses) used in the dual-isotope maps and the isotopic fractionation factors for the reduction of  $\text{N}_2\text{O}$  to  $\text{N}_2$  used in the model calculations.

Process	$^{15}\text{N}$ SP (‰)		$\delta^{18}\text{O}_{\text{N}_2\text{O}}$ (‰)		Reference
	min	max	min	max	
Nitrification (NI)	32	38.7	20.5	26.5	Frame and Casciotti, 2010; Sutka et al., 2006
Fungal denitrification (FD)	27.2	39.9	30.16 (42)	43.26 (55.1)	Maeda et al., 2015; Rohe et al., 2017, 2014; Sutka et al., 2008
Heterotrophic bacterial denitrification (HD)	-7.5	3.7	4.86 (16.7)	11.46 (23.3)	Sutka et al., 2006; Toyoda et al., 2005
Nitrifier denitrification (ND)	-13.6	1.9	0.56 (12.4)	7.56 (19.4)	Frame and Casciotti, 2010; Sutka et al., 2006
ND&HD endmember	-4.95			6.01	This study
NI&FD endmember	33.55			31.88	This study
Fractionation factors of $\text{N}_2\text{O}$ reduction					
$\epsilon^{15}\text{N}$ SP	-3.7				Jinuntuya-Nortman et al., 2008
$\epsilon^{18}\text{O}$				-15.8	

**Table S4.3:** Primer List and applied Thermal profiles for different target genes.

Target gene	Primers	Primer Sequence (5'-3')	Primers Reference	Thermal profile	Number of Cycles
16S rRNA gene (bacterial and archeal)	341F	CCTAYGGGDBGCWSCAG	Frey et al., 2016	95 °C/2 min	1
	806R	GGACTACNVGGGTHCTAAT	Frey et al., 2016	94 °C/40 sec - 58 °C/40 sec - 72 °C/1 min 72 °C/10 min	35 1
ITS2 (fungal)	ITS3	CAHCGATGAACGYRG	Tedersoo et al., 2014	95 °C/2 min	1
	ITS4	TCCTSCGCTTATTGATATGC	Tedersoo et al., 2014	94 °C/40 sec - 58 °C/40 sec - 72 °C/1 min 72 °C/10 min	38 1
bacterial amoA	amoA-1F	GGGGHTTYTACTGGTGGT	Rotthauwe et al., 1997	95 °C/15 min	1
	amoA-2R	CCCCTCKGSAAAGCCTTCTTC	Rotthauwe et al., 1997	95 °C/45 sec - 55 °C/45 sec - 72 °C/45 sec 95 °C/15 sec - 60 °C/15 sec - 95 °C/15 sec	40 1
archaeal amoA	Arch-amoA-for	CTGAYTGGGCTGGACATC	Wuchter et al., 2006	95 °C/15 min	1
	Arch-amoA-rev	TTCTTCTTTGTTGCCAGTA	Wuchter et al., 2006	95 °C/45 sec - 53 °C/45 sec - 72 °C/45 sec 95 °C/15 sec - 60 °C/15 sec - 95 °C/15 sec	40 1
nxB	nxB169f	TACATGTGGTGGAACA	Pester et al., 2014	95 °C/15 min	1
	nxB638r	CGGTTCTGGTCRATCA	Pester et al., 2014	95 °C/45 sec - 57 °C/45 sec - 72 °C/45 sec 95 °C/15 sec - 60 °C/15 sec - 95 °C/15 sec	40 1
nirS	cd3AF	G TSAACG TSAAGGARACSGG	Throbäck et al., 2004	95 °C/15 min	1
	R3cd	GASTTCGGRTGSGTCTTGA	Throbäck et al., 2004	95 °C/45 sec - 58 °C/45 sec - 72 °C/45 sec 95 °C/15 sec - 60 °C/15 sec - 95 °C/15 sec	35 1
nosZ	nosZ-1F	WCSYTGTTTCMTCGACAGCCAG	Henry et al., 2006	95 °C/15 min	1
	nosZ-R	ATGTCGATCARCTGVKCRTTYTC	Henry et al., 2006	95 °C/15 sec - 67 °C/30 sec - 72 °C/30 sec 95 °C/15 sec - 62 °C/15 sec - 72 °C/30 sec	(Touchdown) 6 40
				95 °C/15 sec - 60 °C/15 sec - 95 °C/15 sec	1



---

## References

- Bruderer, Ch., 2012. Nitrous oxide Emissions and Production in a Floodplain of the River Thur. University of Zurich, GEO 511
- Frame, C.H., Casciotti, K.L., 2010. Biogeochemical controls and isotopic signatures of nitrous oxide production by a marine ammonia-oxidizing bacterium. *Biogeosciences* 7, 2695–2709. doi:10.5194/bg-7-2695-2010
- Frey, B., Rime, T., Phillips, M., Stierli, B., Hajdas, I., Widmer, F., Hartmann, M., 2016. Microbial diversity in European alpine permafrost and active layers. *FEMS Microbiology Ecology* 92, fiw018. doi:10.1093/femsec/fiw018
- Henry, S., Bru, D., Stes, B., Hallet, S., Philippot, L., 2006. Quantitative detection of the *nosZ* gene, encoding nitrous oxide reductase, and comparison of the abundances of 16S rRNA, *narG*, *nirK*, and *nosZ* genes in soils. *Applied and Environmental Microbiology* 72, 5181–5189. doi:10.1128/AEM.00231-06
- Jinuntuya-Nortman, M., Sutka, R.L., Ostrom, P.H., Gandhi, H., Ostrom, N.E., 2008. Isotopologue fractionation during microbial reduction of N<sub>2</sub>O within soil mesocosms as a function of water-filled pore space. *Soil Biology and Biochemistry* 40, 2273–2280. doi:10.1016/j.soilbio.2008.05.016
- Maeda, K., Spor, A., Edel-Hermann, V., Heraud, C., Breuil, M.C., Bizouard, F., Toyoda, S., Yoshida, N., Steinberg, C., Philippot, L., 2015. N<sub>2</sub>O production, a widespread trait in fungi. *Scientific Reports* 5, 9697. doi:10.1038/srep09697
- Pester, M., Maixner, F., Berry, D., Rattei, T., Koch, H., Lückner, S., Nowka, B., Richter, A., Spieck, E., Lebedeva, E., Loy, A., Wagner, M., Daims, H., 2014. *NxrB* encoding the beta subunit of nitrite oxidoreductase as functional and phylogenetic marker for nitrite-oxidizing Nitrospira. *Environmental Microbiology* 16, 3055–3071. doi:10.1111/1462-2920.12300
- Rohe, L., Anderson, T.H., Braker, G., Flessa, H., Giesemann, A., Lewicka-Szczebak, D., Wrage-Mönnig, N., Well, R., 2014. Dual isotope and isotopomer signatures of nitrous oxide from fungal denitrification - A pure culture study. *Rapid Communications in Mass Spectrometry* 28, 1893–1903. doi:10.1002/rcm.6975
- Rohe, L., Well, R., Lewicka-Szczebak, D., 2017. Use of oxygen isotopes to differentiate between nitrous oxide produced by fungi or bacteria during denitrification. *Rapid Communications in Mass Spectrometry* 31, 1297–1312. doi:10.1002/rcm.7909
- Rotthauwe, J.H., Witzel, K.P., Liesack, W., 1997. The ammonia monooxygenase structural gene *amoA* as a functional marker: Molecular fine-scale analysis of natural ammonia-oxidizing populations. *Applied and Environmental Microbiology* 63, 4704–4712. doi:10.1128/aem.63.12.4704-4712.1997
- Sutka, R.L., Adams, G.C., Ostrom, N.E., Ostrom, P.H., 2008. Isotopologue fractionation during N<sub>2</sub>O production by fungal denitrification. *Rapid Communications in Mass Spectrometry* 22, 3989–3996. doi:10.1002/rcm.3820
- Sutka, R.L., Ostrom, N.E., Ostrom, P.H., Breznak, J.A., Gandhi, H., Pitt, A.J., Li, F., 2006. Distinguishing nitrous oxide production from nitrification and denitrification on the basis of isotopomer abundances. *Applied and Environmental Microbiology* 72, 638–644. doi:10.1128/AEM.72.1.638-644.2006
- Tedersoo, L., Bahram, M., Pölme, S., Kõljalg, U., Yorou, N.S., Wijesundera, R., Ruiz, L.V., Vasco-Palacios, A.M., Thu, P.Q., Suija, A., Smith, M.E., Sharp, C., Saluveer, E., Saitta, A., Rosas, M., Riit, T., Ratkowsky, D., Pritsch, K., Põldmaa, K., Piepenbring, M., Phosri, C., Peterson, M., Parts, K., Pärtel, K., Otsing, E., Nouhra, E., Njouonkou, A.L., Nilsson, R.H., Morgado, L.N., Mayor, J., May, T.W., Majuakim, L., Lodge, D.J., Lee, S.S., Larsson, K.-H., Kohout, P., Hosaka, K., Hiiesalu, I., Henkel, T.W.,

- Harend, H., Guo, L., Greslebin, A., Grelet, G., Geml, J., Gates, G., Dunstan, W., Dunk, C., Drenkhan, R., Dearnaley, J., de Kesel, A., Dang, T., Chen, X., Buegger, F., Brearley, F.Q., Bonito, G., Anslan, S., Abell, S., Abarenkov, K., 2014. Global diversity and geography of soil fungi. *Science* 346, 1256688. doi:10.1126/science.1256688
- Throbäck, I.N., Enwall, K., Jarvis, Å., Hallin, S., 2004. Reassessing PCR primers targeting *nirS*, *nirK* and *nosZ* genes for community surveys of denitrifying bacteria with DGGE. *FEMS Microbiology Ecology* 49, 401–417. doi:10.1016/j.femsec.2004.04.011
- Toyoda, S., Mutobe, H., Yamagishi, H., Yoshida, N., Tanji, Y., 2005. Fractionation of N<sub>2</sub>O isotopomers during production by denitrifier. *Soil Biology and Biochemistry* 37, 1535–1545. doi:10.1016/j.soilbio.2005.01.009
- Wuchter, C., Abbas, B., Coolen, M.J.L., Herfort, L., van Bleijswijk, J., Timmers, P., Strous, M., Teira, E., Herndl, G.J., Middelburg, J.J., Schouten, S., Damsté, J.S.S., 2006. Archaeal nitrification in the ocean. *Proceedings of the National Academy of Sciences of the United States of America* 103, 12317–12322. doi:10.1073/pnas.0600756103

# CURRICULUM VITAE

**Martin Ley**

July 23, 1979

Basel, Switzerland

## EDUCATION

- 02.2014 – 12.2021 **Doctoral Studies**  
University of Basel and  
Swiss Federal Institute for Forest, Snow and Landscape Research  
WSL  
Thesis: *Microhabitat Effects on Nitrous Oxide Emissions,  
Production Pathways, and Reduction in Floodplain Soils*
- 09.2011 – 08.2013 **Master of Science in Geosciences (MSc)**  
University of Basel  
Thesis: *In vitro simulation of microbial biomass dynamics during  
organic matter degradation in lake sediments*
- 09.2007 – 08.2011 **Bachelor of Science in Geosciences (BSc)**  
University of Basel  
Thesis: *GIS-based Analysis of Vegetation Patterns in Arid  
Ecosystems - An Example from the Nizzana Dune Field, Israel*
- 11.1999 – 04.2003 **Operating Room Assistant HF (Red Cross Certified)**  
School for technical operating room assistance Zurich

## WORK EXPERIENCE

- 11.2019 – 02.2022 **Technical Assistant**  
University of Basel, Switzerland
- 04.2019 – 01.2021 **Lecturer**  
Medtest GmbH, Switzerland
- 02.2018 – 02.2022 **Visiting Scientist**  
Swiss Federal Institute for Forest, Snow and Landscape Research  
WSL, Switzerland
- 02.2014 – 12.2021 **Teaching Assistant**  
University of Basel, Switzerland
- 06.2010 – 08.2010 **Student Intern**  
Department of Environment and Energy, Switzerland
- 08.2003 – 08.2007 **Operating Room Assistant HF**  
Merian Iselin Hospital, Switzerland

## **PUBLICATIONS**

**Ley, M.,** Lehmann, M. F., Niklaus, P. A., and Luster, J.: Alteration of nitrous oxide emissions from floodplain soils by aggregate size, litter accumulation and plant-soil interactions, *Biogeosciences*, 15, 7043-7057, <https://doi.org/10.5194/bg-15-7043-2018>, 2018

**Ley, M.,** Luster, J., Niklaus, P. A., Hartmann, M., Kuhn, Th., Frey, B., and Lehmann, M. F.: Microhabitat effects on source partitioning and reduction of nitrous oxide during flood-induced emissions from floodplain soils (Manuscript in revision with *Soil Biology and Biogeochemistry*)

**Ley, M.,** Lehmann, M. F., Hartmann, M., Ley, S., Niklaus, P. A., Riaz, M., Frey, B., and Luster, J.: Pioneer plant *Phalaris arundinacea* modifies temporal patterns of enhanced N<sub>2</sub>O emissions, source partitioning and N<sub>2</sub>O reduction from floodplain soils after a short-term flood event (Manuscript in preparation for *Science of the Total Environment*)

## **PRESENTATIONS**

### **TALKS**

- 08.2021           EUROSOIL 2021 Virtual Congress
- 09.2017           Annual meeting of the German Soil Science Society 2017, Georg-August-University, Göttingen, Germany

### **POSTERS**

- 10.2019           International N<sub>2</sub>O Workshop, EMPA, Dübendorf, Switzerland
- 04.2016           European Geosciences Union, General Assembly 2016, Vienna, Austria
- 11.2015           13<sup>th</sup> Swiss Geoscience Meeting, University of Basel, Basel, Switzerland
- 09.2015           Annual meeting of the German Soil Science Society 2015, Ludwig-Maximilians-University, Munich, Germany
- 04.2015           European Geosciences Union, General Assembly 2015, Vienna, Austria